Synthetic, Structural and Molecular Modelling Studies of Organoiron Complexes of Catalytic Importance

Robert Oliver Hill

Thesis Presented for the Degree of

DOCTOR OF PHILOSOPHY

in the Department of Chemistry

UNIVERSITY OF CAPE TOWN

March 1999

Abstract

The synthesis and characterization of a series of new alkyl dicarbonyl pentamethylcyclopentadienyl iron compounds, $[(\eta^5\text{-}C_5(CH_3)_5)Fe(CO)_2R]$, is the starting point for an investigation of these compounds and their relevance as models for catalytic reactions. The compounds have been synthesized by the reaction of $Na[(\eta^5\text{-}C_5(CH_3)_5)Fe(CO)_2]$ with the appropriate n-alkyl chloride or bromide (R = n-C_3H_7 to n-$C_{12}H_{25}$). The majority of the compounds are new and have been fully characterized by microanalysis, IR, ^1H, and ^{13}C NMR and mass spectrometry. The data are discussed and some properties and reactions of the compounds are described. The X-ray crystal and molecular structure of $[(\eta^5\text{-}C_5(CH_3)_5)Fe(CO)_2(n\text{-}C_5H_{11})]$ has been determined. The compound forms monoclinic crystals in the space group $P2_1/c$ and has a Fe-C(alkyl) bond length of 2.07Å with the alkyl in an extended conformation. The structure is compared with similar structures retrieved from the Cambridge Crystallographic Database (CSD). The structure, conformation, and β-hydride elimination of $[(\eta^5\text{-}C_5H_5)Fe(CO)_2(CH_2CH_3)]$ are investigated by ab initio Molecular Orbital (MO) and Density Functional (DFT) calculations. The ethyl group is predicted to exist in two different conformations that have relative energy differences of less than 0.5 kcal.mol^{-1}. This finding is verified by the existence of both conformations in structures retrieved from the Cambridge Crystallographic Database. β-hydride elimination is predicted to occur spontaneously following the loss of one CO ligand, and the overall reaction is found to be endothermic by +35.3 kcal.mol^{-1} (DFT) and +38.8 kcal.mol^{-1} (MP2). The β-hydride abstraction reaction of $[(\eta^5\text{-}C_5H_5)Fe(CO)_2(CH_2CH_3)]$ by CH_3^+ is investigated by DFT calculations and found to be exothermic by -117.4 kcal.mol^{-1}.

The X-ray crystal and molecular structure of $[(\eta^5\text{-}C_5H_5)Fe(CO)_2(C(O)CH_3)]$ has been determined. The compound forms triclinic crystals in the space group $P\bar{1}$ and has a Fe-C(acetyl) bond length of 1.98Å with the acetyl ligand in a conformation with the C-C=O plane of the acetyl orientated to minimise interaction with the cyclopentadienyl ligand. Comparison of the structure with iron acyl structures retrieved from the CSD is made. Intermolecular C-H···O hydrogen bonding is observed in the crystal and influences the crystal packing. The rotational barrier of the acetyl ligand is investigated by DFT and MP2 calculation and compared to crystal structure data and previous calculations. The methyl migration reaction of $[(\eta^5\text{-}C_5H_5)Fe(CO)_2CH_3]$ is predicted by DFT to occur with a barrier of +19.9 kcal.mol^{-1} and the overall reaction is exothermic with a reaction energy of -17.9 kcal.mol^{-1}. The effects on the reaction of the alkyl chain, ligand substitution, metal substitution, and the functional employed in the calculation are presented.

Acknowledgements

I am indebted to many people and organisations who have helped and supported me throughout the work for this thesis in many many different ways. I am deeply thankful to each and every one of them.

I would like especially to thank my supervisors. John Moss for his unfailing enthusiasm, encouragement and support in all areas of my work, and for letting me loose on computational chemistry and crystallography. This thesis could not have been done without his interest and guidance. I throughly enjoyed being part of his organometallic group. Charles Marais for introducing me to theoretical chemistry and encouraging me to go for it. I enjoyed our many philosophical discussions. Kevin Naidoo for 'taking me' on at such a late stage and focussing my investigations and teaching me how computational results should be written up!

Research would have been difficult without the support services of the UCT Chemistry Department. In particular I'd like to thank Noel Hendricks and Dr Krassi Dimitrova for running NMR spectra, and Piero Benincasa for the many microanalyses and mass spectra. I'd like to thank Prof. Mino Caira for teaching me the art and science of crystallography and to Leonard Barber and Anita Coetzee for collecting my data and fielding my many questions. Thank you also to John Bacsa for setting me up to use the Cambridge Structural Database from a distance.

My colleagues in the organometallic research group provided a wonderful environment in which to work, and I'd like to acknowledge them all for their assistance and thoughts on a range of topics: Yi-Hsien Liao, Holger Friedrich, Morgan Naidoo, Mansoor Gafoor, Jo-Ann Andersen, Meredith Hearshaw, Earl Star, Jacques Maré, Robyn George, Paul Galatalo, and Ipe Mavunkal.

Much of the computational work in this thesis could not have been done without the generosity of several people and organizations, who had nothing at all to gain from my using their computers. I'd like to acknowledge Rob Waldeck and Silicon Graphics (South Africa) for the use of their *Challenge XL* machine and loan of a large disk, Henk Goosen for the giving me almost complete freedom on his systems, especially the *Onyx*, to Prof. Richard Catlow at the

Royal Institution for accommodating me so kindly on his system and to Rob Bell and Phillip Sinclair for setting up my account there, and finally to Shyam Vyas and Jeremy Wendt at Molecular Simulations for facilitating the use of their software on various systems, and in transferring my data.

Financial assistance over the course of this work is gratefully acknowledged from the Foundation of Research and Development and the University of Cape Town. Funding for conference attendance was generously given by the University of Cape Town, the Roberts Bequest Fund and the North Atlantic Treaty Organisation (NATO) - Advanced Study Institute.

I'd like to thank my parents for all their love and support, and the rest of my family for all their encouragement. Thanks to my brother, Andrew, for often donating his computer to the cause of chemistry at short notice. My friends have been unfailing in their support over the course of this work, and I grateful to them all.

Lastly I'd like to thank my wife with all my heart. Without her love, support, and patience this thesis would never have been completed. She has endured and suffered it all!

Scope of the Thesis

Catalysis involving transition metals is of great importance in modern industrial chemistry. Many of the reactions may involve transition metal alkyl species as intermediates. The study of transition metal alkyls and their transformations are thus fundamental to understanding these reactions. Iron is an active catalyst in the Fischer-Tropsch reaction, which is employed on a large scale in South Africa for the conversion of coal and natural gas to liquid fuels and chemicals. The Fischer-Tropsch process remains one of the only commercialized routes from coal and gas to liquid fuels, and the plants in South Africa are the largest of their kind in the world. Iron alkyl intermediates are proposed intermediates in the reaction, presenting a rationale for investigation of such species in the present study. Transition metal alkyl species are also involved in many other important reactions

The work presented here explores the chemistry of a particular class of iron complex, which may be a model for alkyl species in a catalytic reaction. Organometallic complexes are useful in such investigations as they are well defined and more easily characterized than species on a catalyst surface. A new series of model iron alkyl complexes are thus synthesised and characterized. Structural studies were employed to give information on bond lengths and bond angles, as well as information on the conformational preferences of the organic ligands. New structures were determined for representatives of the model complexes. Although it is easier to study organometallic complexes than species on a catalyst surface, there is nevertheless information which cannot be obtained purely by experiment. For this reason molecular modelling was employed to yield more information on possible intermediates in two important reactions of iron alkyls, and to give values for the relative energies of some of the species. Conformations within the structures are investigated and compared with X-ray crystal structure data, and previous predictions. This multi-faceted approach (i.e. synthetic, structural, and molecular modelling) was employed to obtain more complete information of the system under investigation.

Chapter 1 introduces the Fischer-Tropsch reaction and the quantum mechanical methods employed later in the thesis. Chapter 2 presents an overview of iron alkyl compounds and the synthesis, characterization, and reactions of a new series of iron complexes. Chapter 3 examines

the structures of iron alkyl and acyl compounds and reports two new structures, one in each of these classes. Chapter 4 examines theoretically the formation of alkenes via β-hydride elimination from the alkyl. Chapter 5 examines the formation of acyl complexes from the migratory insertion of CO into the alkyl bond. Chapter 6 presents a summary and conclusions of all these investigations.

Presentations of Research

The following presentations of this work have been made:

- S. A. Chemical Institute 31st Convention, Rhodes University, 24-27 June 1991. A poster and talk titled: *Modelling of metal alkyl intermediates in catalytic reactions.* Authors: *R. O. Hill and J. R.. Moss.*

- Catalysis Society of SA Conference, Highlands National Park Golden Gate, 27-30 October 1991. A poster titled: *Modelling termination reactions of metal alkyl intermediates in catalytic reactions, a two sided approach.*
  Authors: *R. O. Hill, C. F. Marais and J. R. Moss.*

- S. A. Chemical Institute Young Chemists Meeting, Fine Chemicals, August 1993. A talk by R. O. Hill titled: *Organometallic molecular modelling.*

- Catalysis Society of SA International Conference on Catalysis and Catalytic Processing, Breakwater Prison, Victoria & Alfred Waterfront, Cape Town, 24-27 October 1993. A poster titled: *Molecular Modelling of the β-Elimination reaction - A preliminary study in the Rational Design of Catalytic Systems.*
  Authors: *R. O. Hill, C. F. Marais and J. R. Moss.*

- International Symposium on Molecular Reaction Mechanisms involving Transition Metals: Experimental and Theoretical Aspects, Florence, Italy, 25-30 October 1994, ***and*** NATO-ASI on Metal Ligand Interactions, Cetraro, Italy, 4-16 September 1994. A poster titled: *β-elimination of $CpFe(CO)_2(CH_2)_2CH_3$ - a theoretical study of the reaction pathway.*
  Authors: *R. O. Hill, C. F. Marais and J. R. Moss.*

- South African Chemical Institute, Inorganic '95, Pietermaritzburg, 22-25 January 1995. A poster titled: *Molecular modelling of organometallic reactions - β-elimination of $CpFe(CO)_2CH_2CH_3$.*
  Authors: *R. Oliver Hill, Charles F. Marais and John R. Moss.*

- South African Chemical Institute, 33rd Convention, University of Cape Town, Cape Town, January 1996. Presented a lecture titled: *Molecular Modelling of reactions of iron alkyl compounds.*
  Authors: *R. Oliver Hill, Charles F. Marais and John R. Moss.*

- The synthesis, characterization and properties of alkyl complexes of the type $[Cp^*Fe(CO)_2R]$ ($Cp^* = \eta^5\text{-}C_5(CH_3)_5$; R = n-$C_3H_7$ to n-$C_{12}H_{25}$); the X-ray crystal and molecular structure of $[Cp^*Fe(CO)_2(n\text{-}C_5H_{11})]$ and Molecular Orbital and Density Functional calculations on the β-hydride elimination of $[CpFe(CO)_2(CH_2CH_3)]$. Reference: *R. O. Hill, J. R. Moss, C. F. Marais, and K. J. Naidoo, J. Organomet. Chem., Accepted for publication.*

Abbreviations

BSSE	Basis Set Superposition Error
bbl	barrel
CI	Configuration Interaction
CO	Carbon Monoxide
Cp	Cyclopentadienyl
Cp^*	Pentamethylcyclopentadienyl
CSD	Cambridge Structural Database
DFT	Density Functional Theory
DMSO	Dimethylsulfoxide
ECP	Effective Core Potential
EHT	Extended Hückel Theory
GTO	Gaussian Type Orbital
HMPA	Hexamethylphosphoric Acid
IR	Infrared
LCAO	Linear Combination of Atomic Orbitals
MFLOPS	Million Floating Point Operations Per Second
MIPS	Million Instructions Per Second
MO	Molecular Orbital theory
MP2	Møller-Plesset second order correction
NMR	Nuclear Magnetic Resonance
PES	Potential Energy Surface
PPh_3	Triphenylphosphine
RHF	Restricted Hartree-Fock
SCF	Self-Consistent Field
STO	Slater Type Orbital
THF	Tetrahydrofuran
UHF	Unrestricted Hartree-Fock

Contents

Chapter 1

Introduction

Chapter 1

If I have seen farther it is by standing on the shoulders of giants
- Isaac Newton

Introduction

Transition metal alkyl compounds are important as catalytic intermediates in many industrially significant reactions. Iron is an active catalyst in the Fischer-Tropsch reaction, which is employed on a large scale in South Africa for the conversion of coal and natural gas to liquid fuels and chemicals. The work presented here explores the chemistry of a particular class of iron complex, which may be a model for alkyl species in a catalytic reaction, from a synthetic, structural, and molecular modelling perspective. This Chapter introduces the Fischer-Tropsch reaction and the quantum mechanical methods employed later in the thesis. Chapter 2 presents an overview of iron alkyl compounds and the synthesis, characterization, and reaction of a new series of iron complexes. Chapter 3 examines the structures of iron alkyl and acyl compounds and reports two new structures, one in each of these classes. Chapter 4 examines theoretically the formation of alkenes via β-hydride elimination from the alkyl. Chapter 5 examines the formation of acyl complexes from the migratory insertion of CO into the alkyl bond. Chapter 6 presents a summary and conclusions of all these investigations.

1.1. The Fischer-Tropsch Synthesis

1.1.1. History

The hydrogenation of oxides of carbon (usually carbon monoxide) over a catalyst to form hydrocarbons and/or alcohols, the chains of the molecules being predominantly straight in the range C_4-C_{10} has come to be called the Fischer-Tropsch synthesis [1]. The reaction of carbon monoxide and hydrogen over a catalyst was first observed by P. Sabatier and J. D. Senderens in 1902 when they formed methane from the hydrogenation of carbon monoxide over a nickel catalyst. This reaction is now referred to as methanation.

It was not until 1913 that Badische Anilin und Soda Fabrik (BASF) in Germany showed that a mixture of hydrocarbons and oxygenates could be synthesised by reacting a mixture of hydrogen

and carbon monoxide (synthesis gas) over a cobalt catalyst [2]. Later in 1923 Frans Fischer and Hans Tropsch observed that alkalized iron turnings at 100-150 atm of hydrogen and carbon monoxide and 400°-450° C catalysed the production of "synthol" - chiefly oxygenated compounds with a small amount of hydrocarbons [3]. BASF had obtained a patent for this reaction at high pressure causing Fischer and Tropsch to work at atmospheric pressure. In 1925 they announced the synthesis of higher hydrocarbons at atmospheric pressure. Cobalt and nickel seemed to be the best catalysts; iron catalysts were mistakenly thought to be active at higher pressures for the production of oxygenated compounds only, and at atmospheric pressure for the production of hydrocarbons. This delayed the development of useful iron catalysts for many years.

By the 1930s Fischer had refined his catalyst enough for construction of a pilot plant, and by 1935 a commercial plant had been built using a cobalt catalyst. This was the same year that Hans Tropsch died. Commercialization of the process was driven by the need for Germany, which lacked its own petroleum reserves, to be self sufficient in fuels. The history of the process since then has similarly been driven by the political and economic fortunes of nations. To understand the reasons behind the building of the few commercial Fischer-Tropsch plants that have been built and the considerable research efforts that have been expended to understand and improve the process, it is necessary to view it in the context of the oil and chemical industry as a whole and its development through the twentieth century.

Crude oil was first exploited on a large scale in Pennsylvania, USA, after discoveries of oil wells there in the 1859. Commercial use of the oil was initially driven by the increased need for oil for lighting and heating, driven by the industrial revolution. Petroleum thus replaced whale oil, which was the main source of oil at the time. Shale oil was also being used, and a refining process was patented by a Scottsman, James Young, in 1851. It was not until the early twentieth century that petroleum found use as a fuel for transport (gasoline). The refining of crude oil to produce gasoline resulted in various by-products being produced. These included ethylene and propylene. The petrochemical industry was thus born in the 1920s when chemicals such as ethanol and isopropanol were first prepared from these by-products [4]. The petrochemical industry based on the seven basic chemicals: ethylene, propylene, benzene, toluene, methanol, butadiene, and xylene soon grew to an enormous industry in its own right [4]. Today products

from paints to pharmaceuticals are all derived from petroleum. Nevertheless the usage of petroleum in the petrochemical industry amounts to less than 10% of the total worldwide petroleum usage [5]. The main usage is for energy as a liquid fuel (e.g. gasoline, diesel, fuel oil).

Against this background of the increasing importance of petroleum, it was essential that Germany in the 1930s have an alternative source of liquid fuels and chemicals if it were to enter a war and keep its armies supplied with fuel. The Fischer-Tropsch process provided the solution and by the beginning of World War II nine plants had been built in Germany, producing 16 000 barrels/day (1 barrel = 0.159 m^3), using a cobalt based catalyst [6]. So important was this self sufficiency in fuels, that when the synthetic petroleum plant at Leuna was heavily bombed in 1944 it contributed substantially to ending the war [7]. Japan also used Fischer-Tropsch technology during World War II, operating three plants with a combined capacity of about 2 500 bbl/day [8].

After World War II the vast oil reserves of the middle east began to be fully exploited and the Fischer-Tropsch process became uneconomic in Germany and Japan. Interest in the process

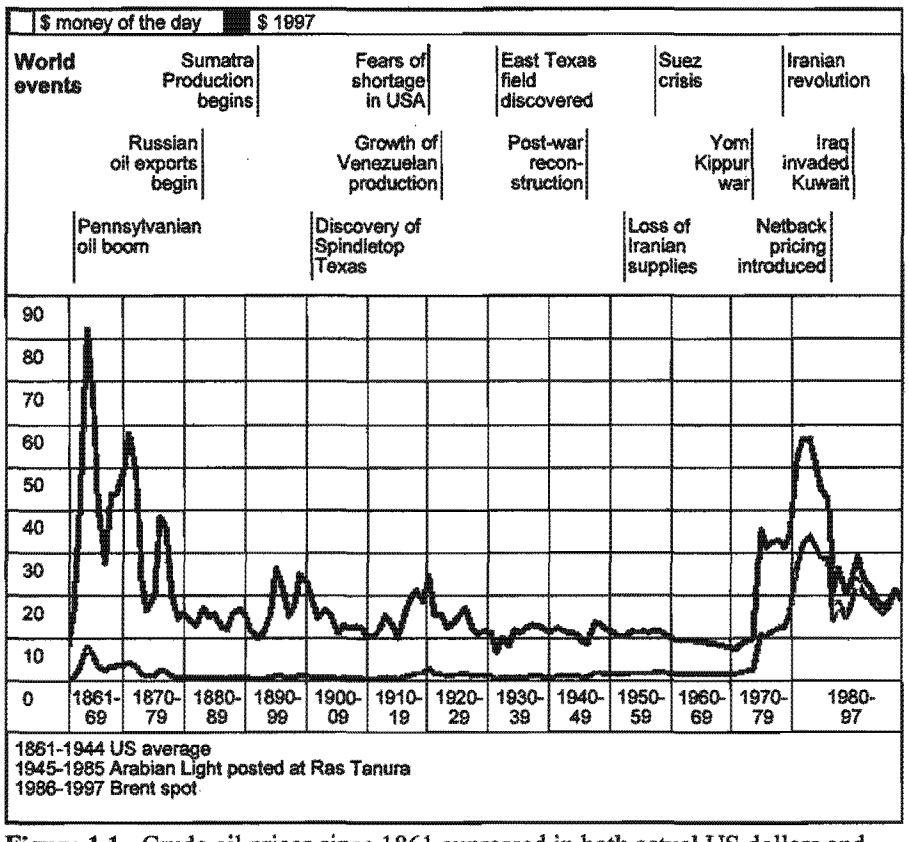

Figure 1.1 Crude oil prices since 1861 expressed in both actual US dollars and equivalent 1997 US dollars. Major events which influenced price are also displayed [50].

remained however, particularly in the United States of America and South Africa. South Africa has no oil of its own but has extensive coal deposits which could be utilized to produce liquid fuels. The United States on the other hand had both oil and coal reserves. The oil reserves were finite though and the large reserves of the Alaskan North Slope had yet to be discovered. Predictions of decreasing production on the continent, and ever increasing demand led to searches for alternative sources of liquid fuels. In 1950 a Fischer-Tropsch plant (8 600 bbl/day) was built in Texas, USA based on natural gas and using an iron catalyst [8]. Increasing gas prices forced the plant to close after only a brief period of operation.

In South Africa a mining company obtained rights to two processes: one developed in Germany by Ruhrchemie and Lurgi, and the other in the United States of America by M. W. Kellogg Corporation. The project was not able to be financed privately, so a government backed company was formed in 1950, the South African Coal, Oil and Gas Corporation . This company, later renamed South African Synthetic Oil Limited (SASOL), built two reactors, one based on the German technology, the other on the American technology. At the time of the formation of SASOL the cost of South African coal was U$0.60/ton compared to U$1.50/barrel (i.e. U$10.87/ton) for oil. These plants became operational in 1955 [9]. Problems with the iron catalyst in the American process and the stability of world oil prices prevented any further Fischer-Tropsch plants being built. Attempts were made around this time to build a Fischer-Tropsch plant in the United States of America based on natural gas. These however proved uneconomic at the time.

In 1973 the world price of crude oil increased substantially, in the wake of the Yom Kippur war and the Arab oil embargo, reaching U$11/barrel. The SASOL plant was at this stage producing a wide range of chemicals in addition to liquid fuels and was showing a profit albeit under protective government tariffs. It was decided to build a second much larger plant (ten times bigger than the original plant) based on the SASOL Synthol process (See Figure 1.3) which was developed out of the original American process. Before this second (SASOL II) plant was completed the Iranian revolution, in 1979, sparked another world oil crisis and crude oil prices increased further (See Figure 1.2). South Africa was at this time subject to increasing international isolation and sanctions due to the policies of Apartheid. It was thus decided to built a third plant (SASOL III), identical to the second on an adjacent site. This approach enabled

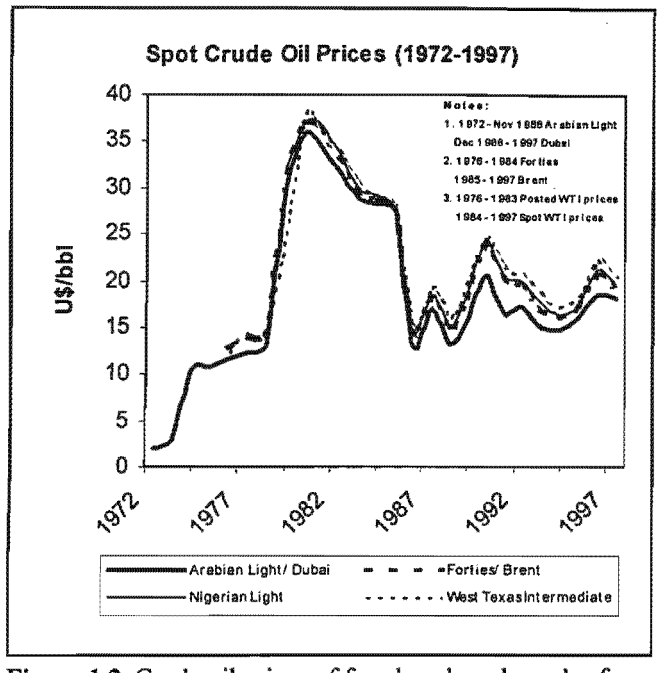

Figure 1.2 Crude oil prices of four benchmark crudes from 1972 to 1979 [50].

SASOL III to be built in only three years and at a reduced cost. SASOL II went into production in 1980 and SASOL III in 1982. At the time of construction it was one of the largest industrial projects ever undertaken at a cost of U$7 billion [10].The price of crude oil had by now past its peak of U$ 37.96 bbl (1980, West Texas Intermediate) and by 1986 had declined to U$ 12.97 bbl (Arabian Light) in the wake of the introduction of net-back[a] pricing by Saudi Arabia. This decline in crude oil prices led Sasol to move in the direction of increased chemicals production from the Fischer-Tropsch process as these could be sold for much higher prices [11]. Expansion into Fischer-Tropsch based chemicals production is today a major aim of Sasol [12]. At present Sasol produces 150 000 bbl/day of fuels and over 120 other chemical products including α-olefins [13], paraffins, methyl isobutyl ketone (MIBK), acrylonitrile, alkylamines, and specialty waxes.

In 1989 Sasol introduced a new advanced reactor (Advanced Synthol Reactor) [14]which is based on a Fixed Fluidized Bed (FFB) configuration. This reactor costs less than half what the original Synthol Circulating Fluidized Bed (CFB) cost, uses less catalyst, and operational costs are about a quarter of those for the CFB [12].

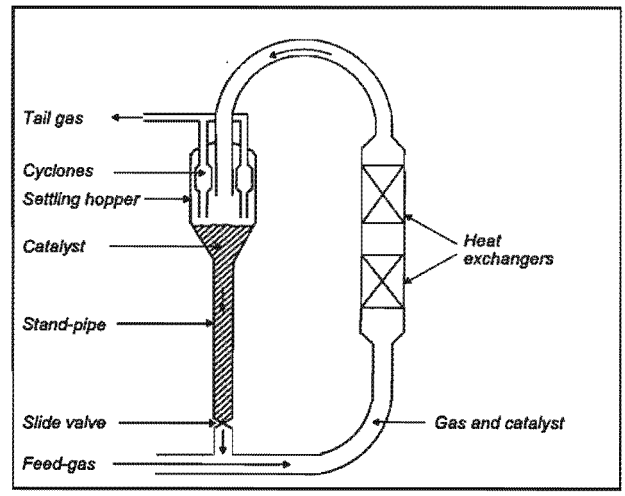

Figure 1.3 The SASOL Synthol Circulating Fluidized Bed (S-CFB) reactor which was employed in the SASOL I, II & III plants [2].

[a]Net-back pricing effectively ended the era of fixed crude oil prices introduced by OPEC. It gave the refiners a fixed profit no matter what the selling price of oil and was introduced by the Saudis to regain lost market share.

Although South Africa has no commercially exploitable oil, off-shore natural gas fields have been found. In 1992 the South African government built a new Fischer-Tropsch plant (Mossgas) based on the off-shore gas fields located in the Indian Ocean off the south coast of the country. The technology for this plant was provided by SASOL and was oriented to the production of gasoline (petrol) and diesel fuels. Total capacity of the plant is 21 600 bbl/day of product [8]. Production of chemicals from the process is limited by the licensing agreement with SASOL [15].

Other companies around the world, notably the Royal Dutch/Shell group and Exxon have been active in Fischer-Tropsch research. This research was driven by the desire to find alternatives to crude oil and to realize value for remotely situated natural gas reserves. Shell completed a Fischer-Tropsch plant based on natural gas in Sarawak in 1992. The plant is built on Shell's Middle Distillate Process (SMDS) and has a capacity of 12 000 bbl/day of mainly gasoline and fuel oil [16]. Shell's approach is somewhat different to the Sasol approach. In order to minimize the limitations of the Anderson-Shultz-Flory distribution of products, the process is optimized to produce longer chain hydrocarbons in the wax range. These products are then catalytically "cracked" to produce the desired products. Shell's production costs on commissioning were approximately U$ 5/bbl for the natural gas and U$ 4/bbl for production costs. This excludes the cost of the plant which was U$660 million. The plant suffered an explosion in December 1997 [17] and is expected to resume production in the year 2000 [18].

There are currently a number of companies pursuing Fischer-Tropsch technology either through research, pilot plants, or planned large scale plants. The companies include Syntroleum, Rentech, Exxon, Texaco, ARCO and Enron. Some of these developments and prospects for future Fischer-Tropsch plants are discussed in section 1.1.7.

1.1.2. Synthesis Gas (Syngas) Formation

Synthesis gas (syngas), a mixture of carbon monoxide and hydrogen, is the feedstock for all Fischer-Tropsch processes. It is also used in the production of a wide variety of chemicals. Its use in chemicals production in fact far exceeds its use in Fischer-Tropsch processes. Syngas is used in the production of ammonia, methanol, and in the Oxo synthesis as well as many others

(See Figure 1.4) [19]. The reaction is thus of fundamental importance to the chemical industry and has been well studied and optimized. As a basic building block for the production of chemicals and fuels, syngas is often in competition with petroleum based processes. It remains

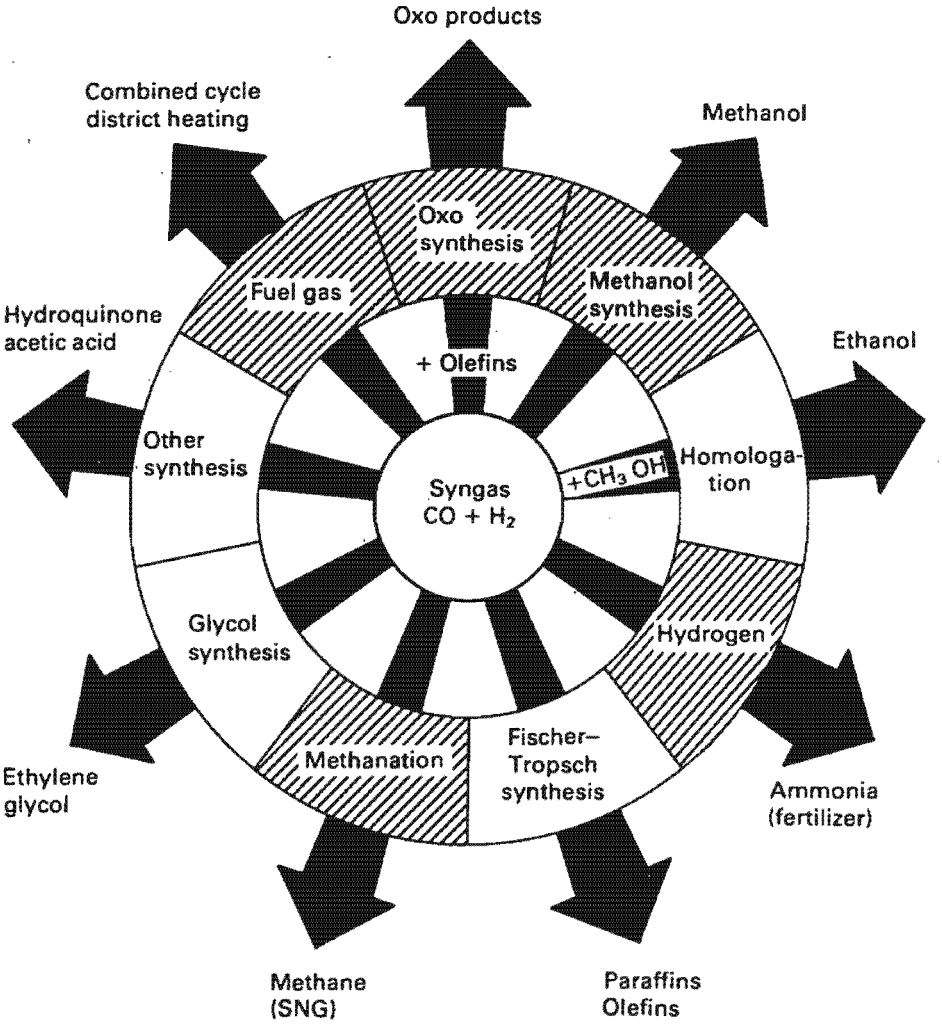

Figure 1.4 Syngas as a building block for the chemical industry [19].

the best alternative for the conversion of fossil fuels (i.e. coal and natural gas) to fuels and petrochemicals. With the decline in world oil prices (See Figure 1.2) over the last 20 years however, many efforts in this area have been scaled back to research stage. Despite this several arguments can be but forward for continued research into this area of syngas conversion:

- Given that there are plentiful low cost coal and natural gas reserves in the earth, they will be necessarily utilized as raw materials. As processes can take 10-20

years from bench to commercial scale, the need for research in this area is obvious.

- Oil reserves will eventually be exhausted and will become more expensive as the most economic reserves are utilized first.
- Alternative feedstocks will ease monopoly positions of crude oil suppliers.
- Countries without oil may choose to utilize coal or natural gas in order to ease shortages of foreign currency.
- Research may lead to cost effective production of chemicals which can compete with petroleum derived products (eg. acetic acid, esters, and Fischer-Tropsch derived α-olefins).

Syngas is obtained by reforming coal (coal gasification) or natural gas with steam. Syngas formation from coal may be endothermic or exothermic depending on whether oxygen is added to the reaction (Equations 1and 2). The reformation of natural gas (essentially methane) is given in Equations 3 and 4. For chemicals production the CO/H_2 ratio may be adjusted as required by employing the water gas shift reaction (Equation 5) which converts CO and H_2O to H_2 and CO_2. In syntheses such as the reaction of H_2 with N_2 to produce NH_3 (Haber process) all the CO may be converted to H_2 and CO_2.

$$C + H_2O \rightarrow CO + H_2 \qquad (\Delta H = +131\ kJ/mol) \qquad (1)$$

$$5C + 3H_2O + O_2 \rightarrow 3CO + CO_2 + H_2 + CH_4 \qquad (2)$$

$$CH_4 + H_2O \rightarrow CO + 3H_2 \qquad (\Delta H = +205 kJ/mol) \qquad (3)$$

$$CH_4 + \tfrac{1}{2}O_2 \rightarrow CO + 2H_2 \qquad (\Delta H = -35 kJ/mol) \qquad (4)$$

$$CO + H_2O \rightarrow H_2 + CO_2 \qquad (5)$$

From the above reactions it can be seen that the endothermic conversion of coal and natural gas, and the exothermic conversion of natural gas with added oxygen all produce the desired syngas only. The exothermic conversion of coal however results in a 25% loss of carbon. It should be noted however that carbon loss can occur in all four types of conversion through the water gas shift reaction.

1.1.3. Fischer-Tropsch reactions

In the Fischer-Tropsch reaction syngas reacts over a catalyst to produce a number of different products. The proportion of these products depends on the CO/H_2 ratio, the catalyst employed and the reaction conditions. The reactions to form some of these products are given below:

$$n\mathrm{CO} + 2n\mathrm{H_2} \rightarrow \mathrm{C}_n\mathrm{H}_{2n} + n\mathrm{H_2O} \quad (6)$$

$$n\mathrm{CO} + (2n+1)\mathrm{H_2} \rightarrow \mathrm{C}_n\mathrm{H}_{2n+2} + n\mathrm{H_2O} \quad (7)$$

$$n\mathrm{CO} + 2n\mathrm{H_2} \rightarrow \mathrm{C}_n\mathrm{H}_{2n+1}\mathrm{OH} + (n\text{-}1)\mathrm{H_2O} \quad (8)$$

The reactions given are for the formation of olefins, paraffins and alcohols respectively. Significant quantities of methane are often formed in the Fischer-Tropsch synthesis and this is ordinarily reformed to produce syngas which is then recycled. The Fischer-Tropsch reactions are all highly exothermic, with product formation being accompanied by a substantial fall in standard free energy.

1.1.4. Mechanisms

The Fischer-Tropsch reaction yields predominantly straight chain hydrocarbons and has been termed a methylene polymerization reaction where the monomer unit ($-CH_2-$) is not initially present. The overall reaction consists of monomer generation, chain propagation, and chain termination. Analyses of the product distributions show that they obey what has become known as Anderson-Schultz-Flory chain-length statistics:

$$\log(w_i/i) = A + B_i \quad (9)$$

where

w_i is the weight fraction of product,
i is the length of the hydrocarbon chain,
A and B are constants depending on temperature, catalyst, CO/H_2 ratio and pressure.

The mechanism for the Fischer-Tropsch reaction must therefore be consistent with the Anderson-Schultz-Flory distribution, although modifications may be necessary to take account of the nature

of the catalyst particles [20,21]. Many proposals for the reaction mechanisms for the formation of the various product types (i.e. hydrocarbons, 1-alkenes, alcohols, etc.) have been made [22], and there is still some debate as to which mechanism is correct [6]. The task of elucidating the mechanism is made more difficult by a number of factors:

- The reaction produces a large number of different products, making the study of the formation of a single compound more difficult.
- Direct observation of the species reacting on the catalyst surface is often not possible. Most observation techniques require low temperature and/or pressure conditions which are far removed from actual reaction conditions.
- A wide variety of catalysts are active for the reaction, including iron, cobalt, ruthenium, and rhodium. It is not always clear whether a proposed mechanism on one type of catalyst is necessarily applicable to other catalysts. This is made more complex by the effects of catalyst supports and promoter effects.

One way of overcoming the difficulties of observing intermediates directly on the catalyst surface is to synthesize and study well defined organometallic species which resemble the proposed intermediates. The validity of this relationship between organometallic chemistry and chemistry occurring on metal surfaces is now widely recognised [23-26].This method has been extensively employed by researchers and many of the results are referred to in the following discussion.

The majority of the products of the Fischer-Tropsch synthesis are linear hydrocarbons, and it is the mechanism for their formation that we shall discuss first. As stated above the Fischer-Tropsch reaction may be viewed as a polymerization of methylene units. This implies three distinctive mechanistic steps: initiation to form the methylene units, chain growth, and chain termination to form the hydrocarbon product. Several mechanisms have been proposed, including mechanisms involving hydroxymethylene species, carbonyl insertion [27], carbide/methylene species, and alkenyl species [26,28-30]. The hydroxymethylene and carbonyl insertion mechanisms have largely been discredited due to the fact that hydroxymethylene surface intermediates have not been detected. The CO insertion mechanism has lost favour due to the observation that all catalysts active for the Fischer-Tropsch reaction also dissociate CO when it

is absorbed on the surface. In addition studies have confirmed that the species C, CH, and CH_2 can exist; for example see [31].

The presence of C, CH, and CH_2 species supports the carbide (or methylene) mechanism. This mechanism (See Figure 1.6) involves both the CO molecule and H_2 molecule becoming absorbed onto the surface and dissociating into their constituent elements on the surface. This is supported by both experimental evidence and theoretical study [32]. Reaction of surface hydrogen atoms with surface carbon (carbide) atoms leads to the formation of surface methylene. There is ample evidence for the existence of methylene species from both experiments on catalysts [33], and a number of model compounds which have been made and characterized [34-38]. The methylene units thus formed are the monomer units of the overall polymerization reaction. Surface hydrogen can react further with the methylene to form a surface methyl group. This step has been demonstrated for a ruthenium complex [39], and alkyl complexes containing metals used in Fischer-Tropsch catalysis have been known for some time [40]. The formation of a surface methyl group completes the initiation step of the mechanism.

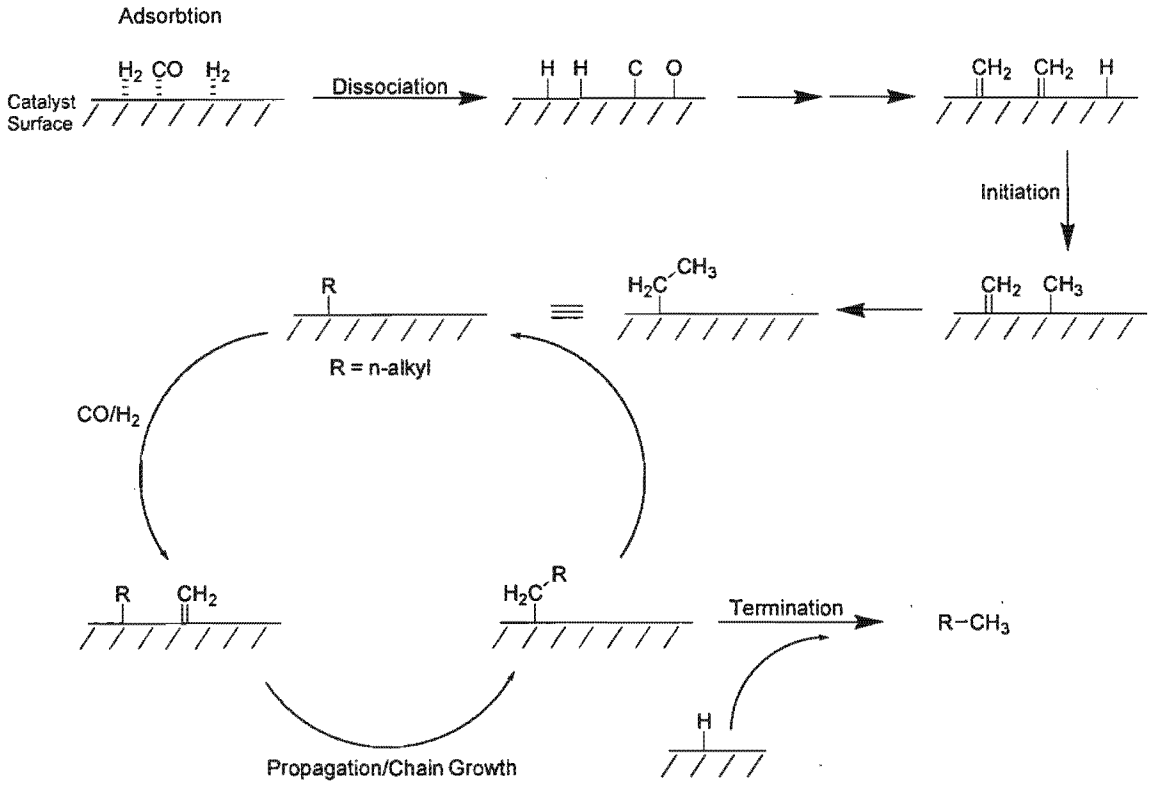

Figure 1.5 The Carbide/Methylene mechanism for chain growth in the Fischer-Tropsch synthesis is the currently preferred mechanism.

The propagation, or chain growth, step of the mechanism involves the 'insertion' of surface methylene species into the metal-methyl bond of the surface methyl group to form a surface ethyl group [39]. This in turn can react with further methylene units sequentially, thus effecting chain growth. Experiments have been devised to isolate these surface alkyl intermediates [41], and complexes with alkyl groups extending to more than six carbon atoms in the chain have been synthesized and characterized [42,43].

Termination of the chain growth occurs when surface hydrogen reacts with the alkyl species to form an alkane. Other products may be formed through different termination reactions. 1-Alkenes (α-olefins) may be formed through a β-elimination reaction, in which a hydrogen on the β-carbon transfers to the surface, forming a double bond between the α and β carbons [6,22,33,44] (See Figure 1.6). The weakly coordinated alkene leaves the surface yielding the product. Support for the mechanism has been shown from the thermal decomposition of iron alkyl complexes. These yield α-olefins [45-47], however the alkene hydride intermediate has not been isolated.

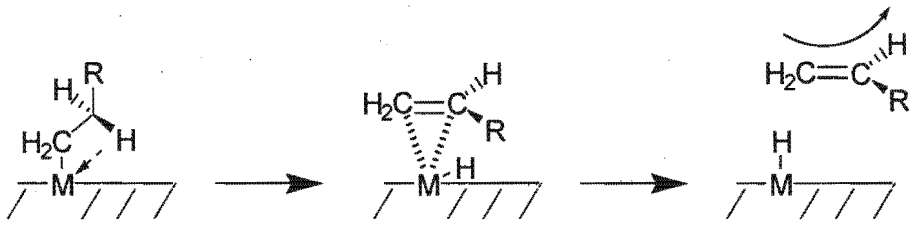

Figure 1.6 Possible mechanism of chain termination via β-elimination to form α-olefins.

Ethylene can also be formed through the coupling of two surface methylene species, followed by desorption from the surface.

Oxygenates in the Fischer-Tropsch reaction may be formed through a CO insertion reaction with a surface alkyl species to form a surface acyl species. Acyl compounds of Fischer-Tropsch active metals have been synthesised [40], and characteristic acyl bands have been identified by in-situ IR studies [6].

An alternative to the carbide/methylene mechanism, which has been proposed by Maitlis and is based on work involving a rhodium catalyst, is the alkenyl mechanism [26,28-30]. This mechanism, shown in Figure 1.7, is initiated in the same way as carbide/methylene mechanism

described above by the formation of surface methylene groups. The chain growth is proposed to occur through the reaction of a surface vinyl group with a surface methylene to form an allyl species which undergoes isomerization to yield a vinyl species which may react further (i.e. chain growth). Termination occurs when the surface vinyl species reacts with surface hydride to form the free alkene.

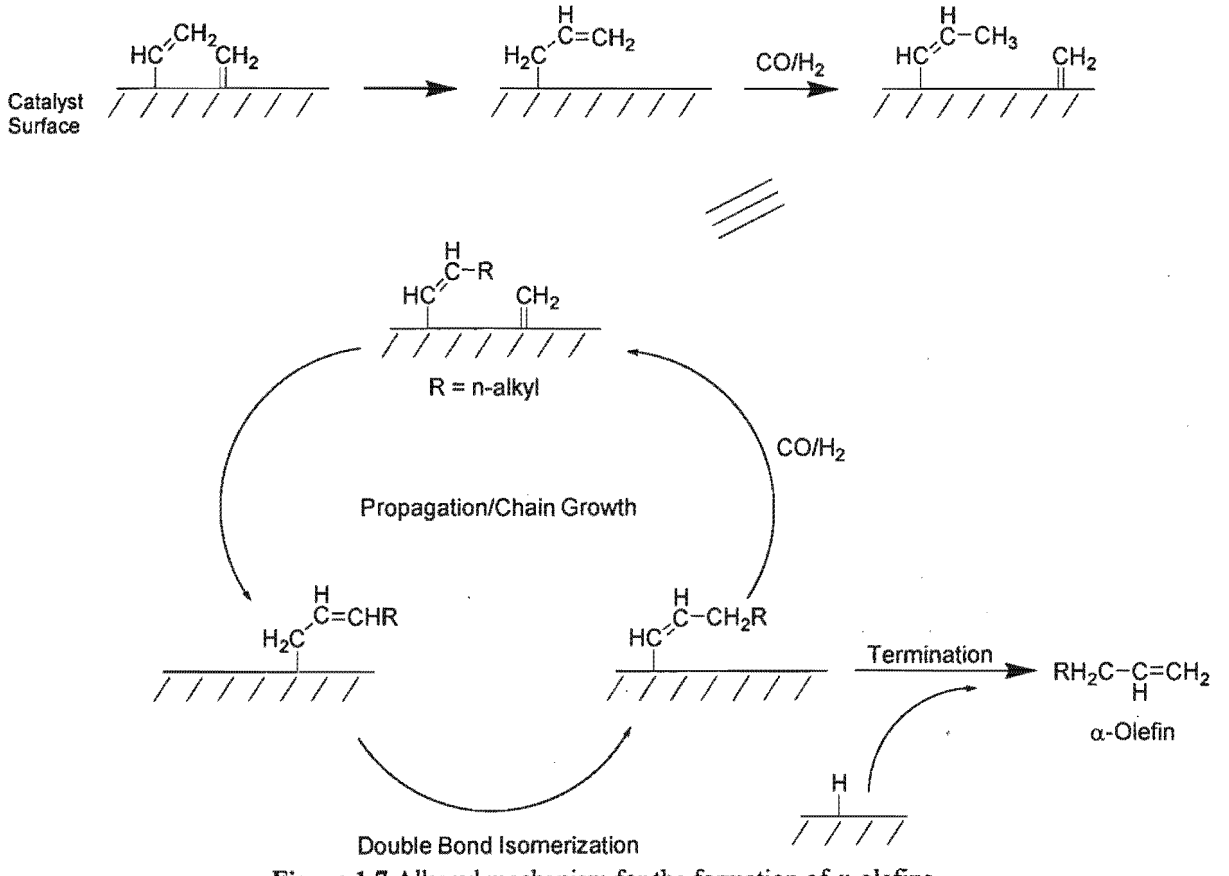

Figure 1.7 Alkenyl mechanism for the formation of α-olefins.

Both the alkenyl and β-elimination mechanisms are plausible and both are supported by studies on the catalyst and on model compounds. Further research is clearly necessary to gain more information on each of these mechanisms and how they may be effected by the use of different metals. The work presented later in this thesis is directed towards providing more information on one of these mechanisms, namely β-elimination.

1.1.5. Product Distributions

The many hydrocarbon products produced in the Fischer-Tropsch reaction obey approximately the Anderson-Shultz-Flory distribution (See page 1-9). This distribution is dependent on the probability of chain growth and chain termination, which in turn are determined by the catalyst and operating conditions such as temperature and pressure. A theoretical depiction of this is given in Figure 1.8. A clear consequence of the Anderson-Shultz-Flory distribution is the wide

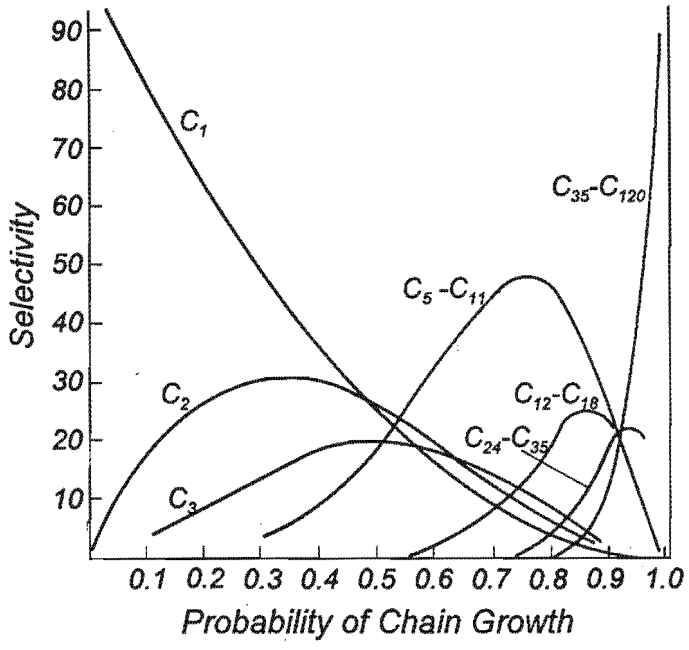

Figure 1.8 Theoretical Anderson-Shultz-Flory distribution for hydrocarbons in the Fischer-Tropsch reaction.

spectrum of products obtained in the reaction. This is not usually desirable, as all products may not be wanted in the proportion they are produced, or at all. Both SASOL and Shell have had to address this limitation but have done so in different ways.

SASOL predominantly use their Synthol or advanced Synthol reactors which produce mainly light products as illustrated in the following table.

Table 1.1	
Selectivities obtained in the SASOL Synthol reactor, 325°C [2].	
Product	**% (C atom basis)**
CH_4	10
C_2H_4	4
C_2H_6	4
C_3H_6	12
C_3H_8	2
C_4H_8	9
C_4H_{10}	2
C_5 to C_{11} (gasoline)	40
C_{12} to C_{18} (diesel)	7
C_{19} to C_{23} C_{24} to C_{35} (medium wax) > C_{35} (hard wax)	4
Water soluble chemicals	6

Some of the lighter products are oligomerized to produce hydrocarbons in the gasoline range, however SASOL have found it advantageous to use certain products such as ethylene and propene as feedstocks for polymerization production and other downstream processes. SASOL also operates low temperature reactors for the production of waxes which are marketed internationally.

The Shell Middle Distillate Synthesis is based on a fixed bed reactor and uses a cobalt catalyst. The reaction produces mainly heavy hydrocarbons and waxes. Roughly half of these products are selectively "cracked" to yield middle distillates. In addition to fuels, Shell also markets waxes obtained in the synthesis.

1.1.6. Fischer-Tropsch as a Source of Fuels and Chemicals

1.1.6.1. Introduction

Historically the Fischer-Tropsch process has been used for the production of transportation fuels (See section 1.1.1). The reaction products obtained in the process also include compounds such

as alcohols, ethylene, propylene, α-olefins, and waxes. These products are worth significantly more as building blocks for the chemical industry than as fuels (See Table 1.2 for comparison).

Table 1.2

Selected fuel and chemical prices (1990) [48].

Product	Comment	Quoted Price	U$/Metric Ton	Source
Crude Oil	Average World FOB	17.39 $/bbl	**126**	a
Gasoline	NY, 87 octane	21.63 $/bbl	**194**	a
Heating Oil	No. 2 (Diesel proxy)	24.51 $/bbl	**186**	a
LCO	High aromatic	19.30 $/bbl	**128**	c
Fuel Oil	No. 6	17.75 $/bbl	**124**	a
Benzene	Baytown, Tex.	1.25 $/gal	**373**	b
Toluene	Baytown, Tex.	0.77 $/gal	**223**	b
Xylenes	Baytown, Tex.	0.85 $/gal	**259**	b
Ethylene	Contract, delivered	0.25 $/lb	**551**	b
Propylene	Gulf Coast	0.16 $/lb	**353**	b
1-octene	α-olefin	0.40 $/lb	**882**	c
1-octanol	Tanks, FOB	0.92 $/lb	**2,028**	b
FT wax	Vestowax FT-300*	1.23 $/lb	**2,712**	d

Notes:
a. Oil and Gas Journal (November 27, 1989)
b. Chemical and Marketing Reporter (November 27, 1989)
c. UOP estimate
d. Price quote from Durachem, Harrison, NY, Jan. 16, 1990
*Vestowax is a trademark of Chemische Werke Huels.

1.1.6.2. α-Olefins

α-Olefins are used in a variety of processes in the petrochemical industry such as the manufacture of soaps. The usual method of producing these compounds is through the oligermerization of ethylene such as in the Shell Higher Olefin Process (SHOP). The process begins by using a nickel catalyst to produce higher alkenes. The double bond is then isomerized to the α position with a manganese catalyst to produce the α-olefins; it should be noted that only even carbon numbered oligomers result. The whole process involves three steps: the formation of ethylene from crude oil (naphtha cracking), oligmerization, and isomerization. α-Olefins produced in the Fischer-Tropsch process require only two steps: syngas formation, and synthesis. Although there is still some debate over the exact mechanism of formation (See section 1.1.4), these products are being produced commercially by SASOL [13] with plans for further expansion [49].

1.1.6.3. Oxygenated compounds

Oxygenated compounds produced in the Fischer-Tropsch reaction include alcohols, aldehydes, acids, and ketones. The majority of the products are linear with terminal functionality. Ethanol is the principle oxygenate formed followed by methanol, n-propanol, and acetic acid[b].

1.1.6.4. Waxes

Waxes are one of the highest value products obtained from the Fischer-Tropsch reaction (See Table 1.2). Waxes are used in coatings for fruit, vegetables, and a variety of packaging. They can also be used as hot-melt adhesives, and for candles. Both SASOL and Shell produce waxes from their respective plants, and market these worldwide.

Chemically the waxes are long polymethylene chains, identical to polyethylene but with shorter chain lengths.

1.1.7. Future of the Fischer-Tropsch Process

The future of Fischer-Tropsch is inextricably linked to the future of the oil industry. In particular the use of Fischer-Tropsch technology for the production of synthetic fuels is dependent largely on the prevailing price of crude oil. The price of crude oil is in turn dependent on remaining oil reserves and their economic exploitablity. It is also dependent on political factors, and the economics of supply and demand. These factors taken together would seem to make a long term prediction for oil prices, nothing more than guess work. Indeed history bears the marks of this unpredictability. The decline or rise in Fischer-Tropsch technology and its widespread use however, is dependent upon this very price, as it has been in the past (See section 1.1.1). It is thus necessary to examine some of these factors more closely so that Fischer-Tropsch can be seen in context and research appropriately directed.

---

[b]This depends on the catalyst and operating conditions (figures given for an iron catalyst at 220° C [8]).

World oil reserves and consumption

In 1997 seventy two million barrels per day of oil were consumed (i.e. 26.13 billion barrels for the year). The total reported proven oil reserves[c] in existence are 1 037.6 billion barrels [50], or nearly 40 years supply at current consumption levels. There is an estimated 550 billion barrels of oil still to be discovered on earth [51], bringing the total exploitable oil available to 1 587 billion barrels, which adds another 21 years supply. On the surface therefore it appears there will be oil available well into the next century. Barring other factors, oil prices might be expected to remain at or near their current levels. Recent research however, suggests that matters are not that simple for the following reasons [51,52]:

- Current reserves may be overestimated due to revisions by OPEC[d] countries which may be motivated by countries desire to increase their quotas.
- Production of oil will begin to decline long before reserves are exhausted, perhaps within twenty years. This will drive up prices of oil as supply struggles to keep up with demand.
- Over sixty five percent of current world oil reserves (as stated) are located in the Middle East and over seventy five percent of world oil reserves are controlled by OPEC [50]. This control of a large segment of the world's oil reserves by a few countries may lead to a manipulation of oil prices in future.

Against these potentially negative factors relating to world oil reserves, must be balanced the following positive influences:

- New techniques for oil recovery such as directional drilling, and off-shore oil platforms operating in increasingly deeper water may increase the amount of recoverable oil [53]. These effects are already noticeable, and have helped reduce oil prices [54].
- There exist substantial alternative oil sources, such as the tar sands located in Canada, which are already being exploited [55], and the heavy oil sludges located in Venezuela [52]. Recovery of these may be more costly than conventional oil, but could serve as a ceiling for prices.
- Although the Middle East has the majority of the stated world oil reserves, the region enjoys only thirty percent of current production. New discoveries in countries such as Angola [56] and West Africa [57,58], and further exploration in places such as Alaska

[c]Proven reserves are those amounts that may reasonable be expected to be recovered from a well. Most wells currently yield approximately 50% of their oil.

[d]Organisation of Petroleum Exporting Countries which account for over 75% of world reserves.

[59] may prevent future oil production being controlled by a few countries for the foreseeable future. The effects of a diversified production base for oil on prices can readily be seen today by the historically low oil prices (currently U$10-12/bbl [60-62]) and the inability of OPEC to influence price through production quotas [63-69].

Can Fischer-Tropsch compete with crude oil?

Considering the above it seems unlikely that oil prices will return to the levels reached during the period 1973 to 1980. It could be expected that oil prices will remain in the region of U$10-20/bbl for the foreseeable future, although some predictions are that it may decline to as low as U$5/bbl [70]. Where then does this place Fischer-Tropsch technology? During the oil crises of the 1970s prices rose to a level where SASOL could produce fuels via the Fischer-Tropsch process that were competitive with crude oil derived fuels. In 1997 dollars however the price of oil in 1979 was in excess of U$55/bbl! Improvements in the Fischer-Tropsch process and catalysts [71] since then however, have helped make it more competitive. Several companies have developed processes which are capable of competing with oil priced as low as U$19/bbl [72], and SASOL aim to achieve a production cost of U$10/bbl [73]. Production of chemicals can enhance the competitiveness of Fischer-Tropsch further as chemicals have an intrinsically higher value than fuels [11].

Fischer-Tropsch technology may also find applications in specific circumstances. It is well known that much of the world's natural gas is located in remote corners of the globe. Pipelines to transport the gas to market are too expensive and transport via sea requires the gas to be liquified and transported in specialized carriers requiring specialized handling facilities. In these cases Fischer-Tropsch may be more attractive as the products can be transported in conventional tankers and handled at existing facilities. Natural gas often occurs with oil. Conversion of this

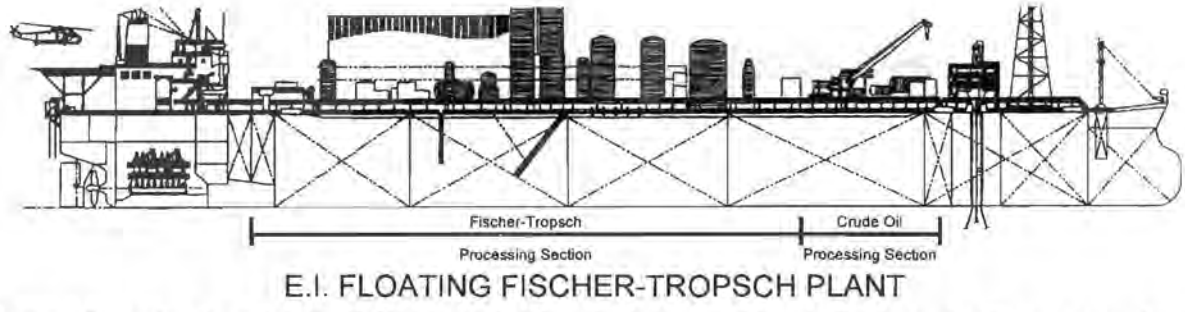

Figure 1.9 A plan for a floating Fisher-Tropsch plant, designed to make use of associated off-shore natural gas [75].

associated gas can often improve the economics of crude oil projects. A recent study has concluded that a Fischer-Tropsch plant located on the declining oil fields of Alaska's North Slope would have a positive impact on the economics of these oil fields [74]. Similarly a study of off-shore associated gas in the Gulf of Mexico concluded that a floating Fischer-Tropsch plant (See Figure 1.9) could increase the viability of wells further than 200 miles off-shore [75]. This arrangement has the added flexibility of being able to be moved to other locations once the gas has been exhausted.

The Fischer-Tropsch process produces very clean fuels. The fuels are free of sulphur and nitrogen containing compounds, as well as low in aromatics. This property is highly desirable in areas of high vehicle pollution such as southern California, which uses diesel from Shell's Fischer-Tropsch plant in Malaysia [71].

In the long term supplies of crude oil will eventually be exhausted. The reserves of natural gas and the very large coal reserves (See Figure 1.10) will then become more widely utilized. Unless a major breakthrough is made in direct methods of conversion of these fossil fuels, the Fischer-

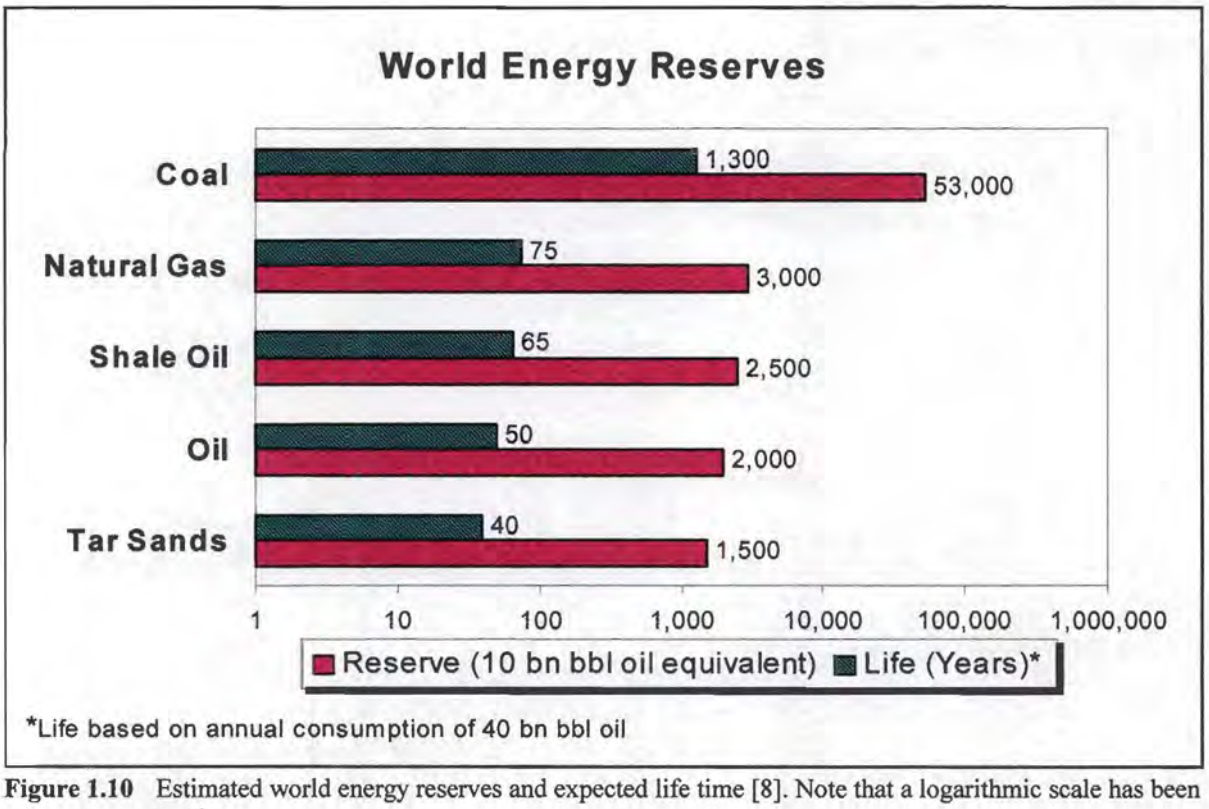

Figure 1.10 Estimated world energy reserves and expected life time [8]. Note that a logarithmic scale has been used.

Tropsch process could remain one of the best methods for the future production of liquid fuels. This alone is compelling enough to warrant further research into the process and its reaction mechanisms.

1.2. Quantum mechanical calculations on transition metal systems

1.2.1. Introduction to molecular modelling

Molecular structure lies at the very heart of chemistry. With the advent of X-ray crystallography, chemists were able to "see" molecules and their structure for the first time. Indeed today it remains a technique central to the structural study of molecules and materials. These studies give a detailed picture of a molecule in terms of bond lengths, bond angles and torsion angles. The shape of a molecule may be viewed and compared with other molecules giving insights into the reactivity of molecules and perhaps how this may be tuned or controlled to suit a particular purpose. Diffraction studies (X-ray and neutron) for the most part are limited to studies of molecules *within* crystals. This fact imposes certain limitations on the structures that are obtained. Firstly the structures of flexible molecules as observed in a crystal structure will most likely be very different from those in solution or the liquid and gas phases. Secondly the structure must represent a minimum energy structure both conformationally and chemically (i.e. structures of unstable species and transition states cannot be obtained).

Molecular modelling does not suffer from the above limitations that X-ray and neutron diffraction techniques do, however it also does not enjoy the conclusive results that are obtained from a diffraction experiment. Molecular Modelling should not therefore be viewed as a replacement for diffraction studies, but as an extension, enabling a wider variety of systems to be studied structurally. It is as easy to study a species stable for only a few nanoseconds (or even compounds that cannot be made) as it is to study a substance that is stable for years.

Structural information, although central to molecular modelling, is only one piece of information that can be obtained from a calculation. In theory it is possible to obtain the heat of formation, dipole moment, ionization potentials, charge densities, bond orders and spin densities (to name just a few) of a compound in one experiment/calculation [76]. Computing this information to a degree of accuracy useful to the chemist is no small task, indeed such calculations rank with the most complex problems ever to be undertaken on computers. This single fact has perhaps been the biggest hindrance to molecular modelling in the past. The huge increase in the power of computers over the last two decades combined with the reduction in the price/performance ratio

has significantly reduced this problem and has opened up areas of chemistry to theoretical studies that were previously unaccessible. This is not to say that any imaginable chemical system is now treatable by the most advanced quantum mechanical method, but merely that many chemical problems, previously too computationally demanding, can now be tackled using an appropriate molecular modelling technique. There are in fact a bewildering array of techniques which are implemented in an even larger array of programs. It is thus important that the prospective modeller has at least a qualitative understanding of the theory underlying any one particular computational method to be applied to a problem, and its strengths and weaknesses. This is because, unlike experimental chemistry, there is no physical measurement to be made so the results obtained are completely determined by the quality of the theory being employed. All molecular modelling techniques make use of approximations to a greater or lesser extent. These approximations should be understood so that the method be employed appropriately to give useful and meaningful results.

Molecular modelling may be used in a number of ways (see Figure 1.11). At the simplest level a particular method may be employed on a system in an attempt to reproduce an experimental result or property. This result may then be used to verify the theory underlying the method. At a higher level a molecular modelling method may be employed which can reproduce certain experimentally observed properties and provide, by analysis of the calculation, the reason or rationale for the particular observation. Other different properties (not obtained by experiment) may also be obtained in the calculation. At its highest level, molecular modelling seeks to predict properties of molecules and substances which have yet to be synthesised or subjected to

Figure 1.11 Diagram showing the types of information we may like from molecular modelling studies and their associated difficulties.

experimentation. This is at best an extremely difficult task and at worst impossible. Although in theory it *is* possible to obtain detailed and accurate results from a solution of the Schrödinger

equation, in practice many assumptions and simplifications must be made to reduce the complexity of the calculation. These can affect the results, sometimes in an unpredictable manner.

Molecular modelling generally falls into two disciplines. One is based on the classical theory of atoms and molecules, Molecular Mechanics, and the second is based on quantum mechanical theory. As the calculations in this thesis fall into the second category, only the briefest overview of Molecular Mechanics will be presented here. The interested reader is referred to several well-known texts on the subject [76,77].

Molecular Mechanics

Molecular mechanics or force field calculations are generally used in the study of molecules which are not undergoing chemical reaction. This is due to the fact that molecular mechanics is based on a classical view of molecules; that is, a model where bonds exist between atoms in a molecule and remain intact. Parameters are obtained experimentally (largely from vibrational spectroscopy and X-ray crystallography) or from quantum mechanical calculations for different

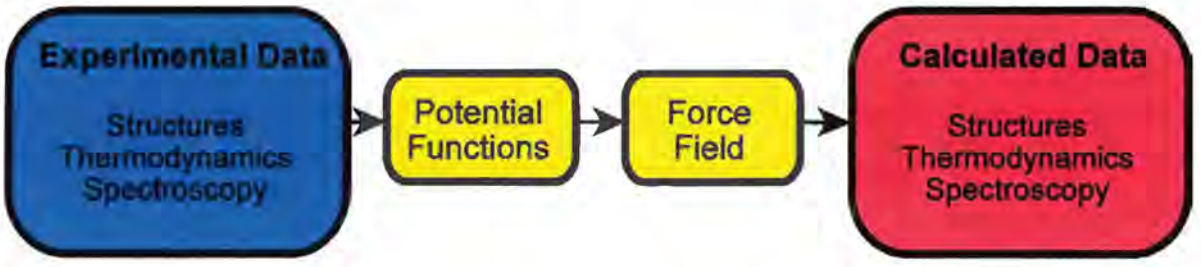

Figure 1.12 The process of molecular mechanics calculation.

types of bonds between different elements. Added to this are parameters for bond stretching, angle bending, non-bonded interactions etc. Each type of interaction is described by a potential energy function. For example the bonding interaction, E_b, of two atoms may be described by:

$$E_b = \frac{1}{2} k_b (r_{ij} - r_0)^2 \qquad (1.1)$$

Where r_{ij} is the bond distance between atoms i and j,
r_0 is the ideal bond length for this bond type, and
k_b is a constant for this type of bond.

The total strain energy for a molecule(s) can thus be described by the sum of these component energies:

$$E_{total} = \sum_{molecule} (E_b + E_\theta + E_\phi + E_{nb} + E_\varepsilon + E_{hb} + E_\delta + ...) \qquad (1.2)$$

Where E_b, E_θ, E_ϕ, E_{nb}, E_ε, E_{hb} and E_δ are the bonding, valence, torsional angle, non-bonded, electrostatic, hydrogen bonding, and out-of-plane bending interactions respectively.

This expression is often termed a *Force Field*, and can be used to calculate properties of a molecule (See Figure 1.2). This calculation is simple for modern computers and is extremely fast for systems containing hundreds or even thousands of atoms. A minimisation of the energy described by the force field will yield a predicted equilibrium geometry of the system. Any correctly paramerterised force field should predict the correct structure and properties of the molecule(s) that were used to obtain the parameters. The utility of the method lies then, in its applicability to other molecular systems. The number of elements and types of bonds found in organic chemistry are relatively small and are well understood. Molecular mechanics is thus ideally suited for the study of organic molecules. Furthermore, many organic molecules of interest are composed of simple monomers which can be easily parameterised and the polymer molecule (eg. carbohydrates, proteins, synthetic polymers, etc.) then studied. The size of these molecules is often very large and thus precludes their study by more sophisticated (and hence more costly) quantum chemical methods.

Inorganic and organometallic compounds contain many different types of bonds and can involve many different elements. The behaviour of these compounds, particularly of the transition metals, are often dominated by electronic effects, and it is these effects which are of primary interest to the researcher. For these reasons the development of force fields and parameters that are generally applicable to inorganic and organometallic compounds has been difficult. Several force fields have been derived, but these have not met with the widespread success enjoyed by ones derived for their organic counterparts. Significant advances are being made however in the groups of Clark Landis [78-81], Robert Deeth [82,83], and Peter Comba [84-89].

The modelling of isolated molecules, by both molecular mechanics and quantum chemical approaches, can yield important information and chemical insights. An isolated molecule however, represents a molecule in a vacuum or in the gas phase. Much chemistry of interest occurs in the liquid phase or in solution. Further problems arise in the treatment of large molecules, especially flexible molecules, where many different conformations are possible, and the location of the global minimum energy conformation may not be found by conventional minimization techniques. Methods to overcome these problems have been developed. These include *Monte-Carlo* methods, and *Molecular Dynamics*.

1.2.2. Qualitative molecular orbital theory

Molecular orbital (MO) theory is well established in chemistry and is taught in some form to all chemistry students in the undergraduate curriculum. As with any theory of bonding, the aim of molecular orbital theory is to successfully explain why atoms form the bonds that they do in molecules, and why these molecules exhibit particular properties (eg. paramagnetism). Molecular orbital theory addresses these problems by considering the electrons in a molecule to be found in molecular orbitals. These orbitals are composed of a linear combination of the atomic orbitals of the constituent atoms. If there are N atomic orbitals there will be N corresponding molecular orbitals. A molecular orbital calculation involves finding the combinations of atomic orbitals with the proper symmetry that yield the lowest electronic energy. This is termed the Linear Combination of Atomic Orbitals (LCAO) formalism. Each molecular orbital is expressed as follows:

$$\psi_i = \sum_{\mu=1}^{N} c_{\mu i}\phi_\mu \qquad (1.3)$$

Where ψ_i is the i'th molecular orbital
$c_{\mu i}$ is the coefficient of the μ'th atomic orbital in the i'th molecular orbital, and
ϕ_μ is the μ'th atomic orbital.

By examining the composition and shape of the orbitals, type and strength of bonds may be assessed, and sites of reactivity identified. Properties, such as polarity and magnetism may be predicted or explained. The various methods for calculating molecular properties within the molecular orbital framework are discussed below.

1.2.3. *Approximate molecular orbital methods*

1.2.3.1. *Extended Hückel method*

The Extended Hückel method is an extension of the simple Hückel method which was proposed by E. Hückel in the early 1930s. The simple Hückel method considers only the π electrons and is used in the study of the reactivity of unsaturated organic systems. It assumes that it is possible to separate out the π and σ contributions to the wavefunction, ψ, and hence the total energy in the following way:

$$E_{\text{total}} = E_{\sigma} + E_{\pi} \tag{1.4}$$

i.e. the π electrons are moving in a field due to the nuclei and a σ core. This, of course, is not a valid assumption, but since the π-orbital energies, E_i are ultimately obtained via parameters that include experimental numbers, the interaction is implicitly included to some extent.

The extended Hückel method was developed and applied systematically to a wide range of problems in chemistry by Roald Hoffmann. This work incorporating his symmetry rules for reactions and his isolobal theory earned Hoffmann the 1982 Nobel prize for chemistry. As the name implies, the method of Hückel was *extended* by Hoffmann [90] (amongst others) to include all the valence electrons of the atoms, instead of just the π electrons. This addition complicated the construction of the molecular orbitals making the method impractical unless carried out using a digital computer.

Both the simple Hückel method and the extended Hückel method are *one electron* methods. That is, the molecular orbitals and their energies are calculated before populating the orbitals with electrons. This means that no account is taken of electron-electron repulsion. Furthermore neither method takes account explicitly of nuclear-nuclear repulsion. The total energy of the system is thus calculated by adding up the energies for each electron in the molecule, hence the term one electron energy. This is done by solving the *secular equations*:

$$Hc_i = e_i S c_i \qquad i = 1, 2, \ldots, N \tag{1.5}$$

Where H is the effective one electron Hamiltonian matrix,
S is the overlap matrix of atomic orbitals,
c_i is the vector of atomic orbital coefficients for molecular orbital i,
e_i is the energy of molecular orbital i, and
N is the total number of valence atomic orbitals in the molecule.

The extended Hückel calculation is thus performed as follows:

- A set of coordinates defining the positions of the nuclei for the molecular system are defined. These will usually be derived from values of bond lengths, bond angles, and torsion angles of known compounds.

- Next the atomic orbitals to be used in construction of the molecular orbitals must be defined in terms of some mathematical function, and centred on the appropriate nucleus. The functions used to describe the orbitals are called *Slater Type Functions* and the orbitals are termed *Slater Type Orbitals* (STOs). These have the form:

$$\phi_i(\varsigma, n, l, m; r, \theta, \phi) = Nr^{(n-1)}e^{-\varsigma}Y_{lm}(\theta, \phi) \qquad (1.6)$$

Where N is the normalization constant,
ς is called the exponent,
r, θ, and ϕ are spherical coordinates,
Y_{lm} is the angular momentum part which describes shape, and
n, l, and m are the principle, angular momentum, and magnetic quantum numbers respectively.

- Having defined the atomic orbitals of the molecule and their location, it is now possible to calculate the extent to which the orbitals overlap with each other. Note that different orbitals on the same atom are orthogonal and hence do not overlap. The result of this calculation is the overlap matrix, S. The diagonal elements of the matrix all have the value 1, as each orbital overlaps exactly with itself. The matrix is also symmetrical about the diagonal as the overlap of orbital i with orbital j is exactly equivalent to the overlap of orbital j with orbital i. The extended Hückel method considers only the valence orbitals explicitly in the calculation.

- Next the elements of the *Hamiltonian* matrix must be defined. The diagonal elements (H_{ii}) are taken to be the valence state ionization potential (VSIP) of an electron in its

atomic orbital. The off diagonal elements are calculated according to the *Wolfsberg-Helmhotz* formula:

$$H_{ij} = KS_{ij}(H_{ii} + H_{jj})/2 \tag{1.7}$$

Where H_{ii} and H_{jj} are the valence state ionization potentials of atomic orbitals i and j respectively,
S_{ij} is the overlap between orbitals i and j, and
K is an adjustable parameter.

- The secular equations can now be solved to yield the molecular orbitals and the one electron energy calculated by summing the energy of the electrons occupying the molecular orbitals.

$$E_{elec} = \sum_{i=1}^{NOCC} n_i e_i \tag{1.8}$$

Where $NOCC$ is the number of occupied molecular orbitals,
n_i is the occupation number of molecular orbital i, and
e_i is the energy of molecular orbital i.

The results obtained by extended Hückel calculation, have been used to rationalize many conformational and reactivity problems in chemistry. The method is not very useful in obtaining optimized molecular structures, so geometry optimization routines are not usually found in extended Hückel programs. The method is nevertheless a useful tool for obtaining a qualitative description of molecular systems.

Several modifications of the method have been proposed. These include the charge iteration method for obtaining H_{ii} values in polarized bonds, especially metals; *double zeta* basis sets for metals; modified Wolfsberg-Helmhotz formula for H_{ij} values; and schemes to optimize molecular geometries.

1.2.3.2. Fenske-Hall method

The Fenske-Hall method [91,92] is more sophisticated than the Extended Hückel method in its treatment of the energies of the molecular orbitals. The method is derived from the more complex Hartree-Fock ab initio method which is described in Section 1.2.4. The Fenske-Hall method differs from the Hartree-Fock method in two important ways. Firstly the types of mathematical

functions used to describe the atomic orbitals (See Section 1.2.4.3) is different. Slater type orbitals (STOs) are employed, as in the Extended Hückel method, rather than Gaussian type orbitals (GTOs), and the number of functions used to describe each atoms is a minimum or slightly extended. The second difference is the treatment of orbital overlap (the overlap matrix). Certain elements are created with mathematically evaluated integrals which approximate the real Hartree-Fock elements. This approximation leads to a very large reduction in computational effort. The method is parameter free meaning it relies only on the basis set and inter-nuclear distances for its results. The method has not been used for any of the work presented in this thesis, however it was used for some preliminary calculations. It is mentioned here due to its use in the organometallic literature, particularly with regards to interpretation of photoelectron spectra [92-94].

1.2.3.3. Semi-empirical calculations

Semi-empirical calculations are based on a more complete model of the electronic structure of molecules. Like the ab initio methods described in section 1.2.4 account is taken of electron-electron repulsion. The calculation of this interaction is very time consuming and so approximations are made here based on experimentally determined parameters. The core electrons are also not included in the calculation explicitly, but are absorbed into the nuclear core, on the premise that it is only the valence electrons that are involved in bonding. The main differences between the various semi-empirical schemes is in which parts of the electron-electron interactions are to be explicitly calculated and which are to be replaced by parameters, and what values these parameters should take. The different methods are commonly referred to by their acronyms. Some of the more popular methods are listed in the following table.

Table 1.3	
Semi-empirical molecular orbital methods	
Acronym	**Method**
ZDO	Zero Differential Overlap
CNDO	Complete Neglect of Differential Overlap [95]
INDO	Intermediate Neglect of Differential Overlap [96]
NDDO	Neglect of Diatomic Differential Overlap
MINDO/3	Modified INDO [97]
MNDO	Modified Neglect of Diatomic Overlap [98]
AM1	Austin Model 1 (2nd MNDO) [99]
PM3	3rd MNDO [100]
SAM1	Semi-Ab Initio Model 1 [101]
ZINDO	Zerner's INDO [102]
MNDO/d	MNDO with Transition Metals [103,104]
PM3(tm)	PM3 Transition Metals [105]

The methods listed in Table 1.3 are in approximate order of increasing sophistication. Semi-empirical methods were developed out of a need to handle larger molecular systems than could be handled by ab initio calculations. However many of the parameters were calculated using ab initio methods on small systems. Even so the accuracy of these parameters was limited by the computers of the day [106]. One consequence of this is that parameters for transition metals, with their partially filled d-orbitals, were rarely derived. One of the first methods to include parameters for transition metals was ZINDO [102]. This method was developed by Zerner, principally for the study of the electronic spectra of metal porphyrins. Trial calculations by this author however gave unsatisfactory results, with predicted geometries that did not make chemical sense. Newer methods which include parameterization for some transition metals are the MINDO/d method, the PM3(tm) method and the SAM1 (in AMPAC 5.0) methods.

1.2.4. Ab initio molecular orbital calculations

Ab initio molecular orbital calculations are so named because they do not make use of parameters obtained from experiment except for a few fundamental constants such as Plank's constant and the speed of light. This leads to extremely complex calculations which are impossible to calculate in a reasonable amount of time for all but the simplest of systems. Many approximations have been proposed in order to speed up the calculation and enable the study of larger systems. Indeed the Linear Combination of Atomic Orbitals - Molecular Orbital theory (LCAO-MO) is itself an approximation. The approximations made can lead to inaccurate descriptions of the systems being studied, and it does not therefore follow that because a calculation is ab initio, it will yield the correct answer to a particular problem. It is thus important that results be carefully scrutinised and where possible compared with any available experimental data. Transition metals, with their large number of electrons and d-orbitals are particularly sensitive to these approximations. *Hartree-Fock* theory forms the basis of most ab initio molecular orbital techniques, and is described below.

1.2.4.1. Hartree-Fock calculations

In Hartree-Fock theory, electrons are assumed to move independently and full allowance is not made for electron correlation (i.e. the electron's ability to avoid each other).

To begin we consider the Schrödinger equation for the total energy of a molecule which is given by the expression:

$$[T_{nuc}(R) + T_{el}(r) + V_{nn}(R) + V_{ne}(R,r) + V_{ee}(r)]\Psi(R,r) = E_{tot}\Psi(R,r) \quad (1.9)$$

where $T_{nuc}(R)$ is the operator for the kinetic energy of the nuclei,
$V_{nn}(R)$ is the operator for the *nucleus-nucleus* potential energy,
$T_{el}(r)$ is the operator for the kinetic energy of the electrons,
$V_{ne}(R,r)$ is the operator for the *nuclear-electron* potential energy, and
$V_{ee}(r)$ is the operator for the *electron-electron* potential energy.

$T_{nuc}(R)$ and $V_{nn}(R)$ are purely nuclear terms and can be handled separately from the electronic terms. This is because $T_{nuc}(R)$ can be separated out due to the Born-Oppenheimer approximation. This approximation states that because the mass of the nuclei is very great compared to that of

the electrons, the electrons move much faster than the nuclei, and hence can be considered to be moving in a static potential created by the nuclei[c]. The term $T_{nuc}(R)$ is thus ignored in the calculation. $V_{nn}(R)$ is just the classical expression for the repulsion of the nuclei for each other, and is a trivial calculation. The term is added to the electronic energy once this has been calculated. This sum is usually referred to as the *potential energy surface* of the system and is expressed with respect to the nuclear coordinates of the constituent atoms (i.e. 3n-6 (linear = 3n-5) dimensional space).

The major effort in the calculation involves solving the electronic Schrödinger equation which is given by:

$$[T_{el}(r) + V_{ne}(R,r) + V_{ee}(r)]\Phi(R,r) = E(R)\Phi(R,r) \qquad (1.10)$$

where $T_{el}(r)$ is the operator for the kinetic energy of the electrons
$V_{ne}(R,r)$ is the operator for the *nuclear-electron* potential energy
$V_{ee}(r)$ is the operator for the *electron-electron* potential energy, and
R and r are positions of the nuclei and electrons respectively..

When using atomic units this becomes :

$$\left(\sum_{i=1}^{n} -\frac{1}{2}\nabla_i^2 - \sum_{i=1}^{n}\sum_{\alpha=1}^{N} \frac{Z_\alpha}{r_{i\alpha}} + \sum_{i<j}\sum \frac{1}{r_{ij}} \right) \Phi(R,r) = E(R)\Phi(R,r) \qquad (1.11)$$

Where i and α are summation indices over electrons and nuclei respectively, and
Z is the nuclear charge on atom α.

Now the interelectronic (*electron-electron*) repulsion term (third term) cannot be solved directly. An approximate solution is found using the *SCF (Self Consistent Field)* method, which makes use of the *variational principle*. This considers each electron to be moving in the average field of all the other electrons. We start by omitting the interelectronic (*electron-electron*) repulsion term, giving the n-electron Schrödinger equation:

---

[c]Note that the positions of the nuclei can and do change for geometry optimizations or molecular dynamics calculations. These changes amount to an exploration of the potential energy surface, but do not influence the nature of the surface (i.e. they are separated out).

$$\left(\sum_{i=1}^{n} \hat{h}(i) \right) \Phi(R,r_1,...,r_n) = E(R)\Phi(R,r_1,...,r_n) \tag{1.12}$$

where ĥ(i) is the one-electron operator given by

$$\hat{h}(i) = -\frac{1}{2}\nabla_i^2 - \sum_{\alpha=1}^{N} \frac{Z_\alpha}{r_{i\alpha}} \tag{1.13}$$

The n-electron equation may be separated into *n* one-electron equations of the form:

$$\hat{h}(i)\phi_i(r_i) = e_i\phi_i(r_i) \tag{1.14}$$

where $\phi_i(r_i)$ is a one electron wavefunction and e_i is the orbital energy for electron *i*. The n-electron wavefunction $\Phi(R,r_1,...,r_n)$ will be a product of *n* one-electron wavefunctions $\phi_i(r_i)$:

$$\Phi(R,r_1,\cdots,r_n) = \phi_1(r_1)\phi_2(r_2)\cdots\phi_n(r_n) \tag{1.15}$$

Taking into account the electron spin and satisfying the Pauli principle the wavefunction becomes:

$$\Phi(r_1,\cdots,r_n) = \phi_1(r_1)\,\alpha(1)\,\phi_1(r_2)\,\beta(2)\cdots\phi_{\frac{1}{2}n}(r_n)\,\beta(n) \tag{1.16}$$

Now electrons are indistinguishable so all n! permutations of the electrons must be considered. Electrons also belong to a class of particles known as fermions. This type of particle is anti-symmetric with respect to the interchanging of any two particles. Accounting for this leads to:

$$\Phi(r_1,\cdots,r_n) = M\sum_P \varepsilon_P P\phi_1(r_1)\alpha(1)\phi_1(r_2)\beta(2)\cdots\phi_{\frac{1}{2}n}(r_n)\beta(n) \qquad (1.17)$$

where M is the normalization factor ε_P is +1 for an even and -1 for an odd number of exchanges, and P is a permutation operator. This sum can be written easily as a *Slater determinant*

$$\Phi(R,r) = \frac{1}{\sqrt{n!}}\begin{vmatrix} \phi_1(r_1)\alpha & \phi_1(r_1)\beta & \cdots & \phi_{\frac{1}{2}n}(r_1)\beta \\ \phi_1(r_2)\alpha & \phi_1(r_2)\beta & \cdots & \phi_{\frac{1}{2}n}(r_2)\beta \\ \cdots & \cdots & \cdots & \cdots \\ \phi_1(r_n)\alpha & \phi_1(r_n)\beta & \cdots & \phi_{\frac{1}{2}n}(r_n)\beta \end{vmatrix} \qquad (1.18)$$

Solving this determinant forms the basis for the Hartree-Fock calculation. The electron-electron repulsion energy has not yet been accounted for in this scheme however, and this energy is not inconsequential. It can be partially accounted for in the Hartree-Fock formalism by the variation method. This requires the minimization of the electronic energy E, given by the expectation value:

$$E = \frac{\int \Phi^* \hat{H} \Phi d\tau}{\int \Phi^* \Phi d\tau} \qquad (1.19)$$

Where the Hamiltonian operator, $\hat{H}$ is given by the terms in parentheses in equation 1.11:

$$\hat{H} = \sum_{i=1}^{n} -\frac{1}{2}\nabla_i^2 - \sum_{i=1}^{n}\sum_{\alpha=1}^{N}\frac{Z_\alpha}{r_{i\alpha}} + \sum\sum_{i<j}\frac{1}{r_{ij}} \qquad (1.20)$$

Solving equation 1.19 involves finding the molecular orbital coefficients which give the minimum energy. The energy given is always an upper bound of the true energy, and the variational principle ensures that full minimization of the energy yields the true ground state wavefunction. Using this method a set of equations called the Hartree-Fock equations may be

derived. The derivation of these equations involves lengthy algebraic manipulation and may be found elsewhere [107]. The form of the equations derived are as follows:

$$\hat{F}_i(1)\phi_i(1) = \varepsilon_i\phi_i(1) \qquad i = 1,2,...,n \tag{1.21}$$

where ε_i is the energy of orbital i and $\hat{F}_i$ is the Fock operator which is given by:

$$\hat{F}_i(1) = \hat{h}(1) + \sum_j \left[2\hat{J}_j(1) - \hat{K}_j(1)\right] \tag{1.22}$$

The first term, $\hat{h}(1)$ corresponds to the one-electron part, and includes terms for the average kinetic energy and the nuclear-electronic attraction energy of an electron in orbital ϕ_i. The summation term, which represents the electronic interactions, is made up of two operators, $\hat{J}_j$ and $\hat{K}_j$ which are termed the *coulomb* and *exchange* operators respectively. The coulomb operator, $\hat{J}_j$ is defined as the classical electrostatic interaction between an electron in ϕ_i and the two electrons in ϕ_j, and is given by the integral:

$$J_{ij} = \int \phi_i(1)\phi_j(2)\frac{1}{r_{12}}\phi_i(1)\phi_j(2)d\tau_{12} \tag{1.23}$$

Where $d\tau_{12}$ is the integration with respect to the coordinates of electrons 1 and 2.

The exchange operator, $\hat{K}_j$ arises from the anti-symmetric nature of the electrons (see page 1-34) and does not have a classical interpretation. It is given by the integral:

$$K_{ij} = \int \phi_i(1)\phi_j(2)\frac{1}{r_{12}}\phi_i(2)\phi_j(1)d\tau_{12} \tag{1.24}$$

Inspection of equations 1.21, 1.22, 1.23, and 1.24, 25, 26, 27 reveals that in order to set up the Fock equations for a particular problem we need to know the answer because the operators $\hat{J}_j$ and $\hat{K}_j$ are defined in terms of the molecular orbitals, ϕ_i. The goal of the calculation is to obtain the coefficients of the ϕ_i expansion (i.e. the coefficients of the LCAO), but to do this we need the coefficients! To solve this problem the coefficients are guessed (usually by a Extended

Hückel calculation) and the determinant solved resulting in a new set of coefficients. This is the SCF cycle. The cycle continues until coefficients (or density matrix or energy) do not change from cycle to cycle (i.e. the change in energy (or electron density) between cycles is below some threshold value). We then say that SCF has been achieved.

Now the total energy of the system may be obtained. In the SCF process we have included the inter-electronic interactions twice (i.e. we have counted the interaction of electron *a* with electron *b* ***and*** electron *b* with electron *a*) so this extra contribution must be subtracted from the electronic energy. This leads to the following expression for the electronic energy:

$$E_{elec} = \sum_{i=1}^{n}\left[2H_{ii} + \sum_{j=1}^{n}\left(2J_{ij} - K_{ij}\right)\right] \tag{1.25}$$

Where H_{ii} is the average kinetic plus nuclear-electronic attraction energy

Finally the total energy of the system is given by:

$$E_{total} = E_{elec} + V_{nn} \tag{1.26}$$

where V_{nn} is the nuclear-nuclear repulsion energy given by:

$$V_{nn} = \sum_{\mu=1}^{N-1}\sum_{\nu=\mu+1}^{N}\frac{Z_\mu Z\nu}{r_{\mu\nu}} \tag{1.27}$$

Having calculated the total energy of the system it is now possible to obtain useful information from the solution. For example the orbitals may be inspected to see what the degree and type of bonding exists between elements in the system. A plot of the electron density, or electrostatic potential around the molecule may be produced to gain insight into the properties and reactivity of the molecule. It is also possible to calculate the first and second derivatives of the energy with respect to the positions of the atoms in the molecule. Such a calculation allows us to search for structures which represent minima on the potential energy surface (PES) or transition state structures. These aspects are discussed further in Section 1.2.5.4 on page 1-49.

Up until now we have considered the molecular orbitals to be of the closed-shell type (i.e. doubly occupied or spin paired). This is not always so, for example in doublet or triplet states where

there is an excess of electrons with α spin. There are two methods commonly used to deal with open-shell systems. The first method extends the closed shell method described so far. This situation is known as the *Restricted Hartree-Fock (RHF)* formalism.

The second method considers electrons with α and β spin to occupy different sets of orbitals. These two sets of orbitals are then solved independently. This treatment is referred to as the *Unrestricted Hartree-Fock (UHF)* formalism. It should be noted that UHF wavefunctions are not true eigenfunctions of the total spin operator and may lead to spin contamination of a state by states with higher multiplicity.

1.2.4.2. Post Hartree-Fock calculations

The energy obtained from the Hartree-Fock SCF calculation does not fully account for electron-electron repulsion. Account is taken in the SCF procedure of the average repulsion experienced by an electron due to all the other electrons in the system. Electrons can, to a certain extent, avoid each other, thus reducing the electron-electron repulsion energy further than what is given by the Hartree-Fock calculation. The difference between the true energy and the Hartree-Fock SCF calculated energy is called the *correlation energy*. The true energy of the system may now be expressed as:

$$E_{true} = E_{Hartree-Fock} - E_{correlation} \tag{1.28}$$

Note that this expression is only true if $E_{Hartree-Fock}$ represents the Hartree-Fock limit (see section 1.1.4.3).

The correlation energy is important not just because it gives a better absolute value of the total energy of a system, but because the magnitude of this contribution can differ from system to system, and for different geometries of the same system. Properties such as bond lengths in the molecule may also be effected. Chemical processes such as the making and breaking of bonds may also be better described by including electron correlation in the calculation. Hartree-Fock methods are based on a single determinant which imposes certain restraints on the calculation. This is most easily demonstrated in the calculation of the dissociation of the hydrogen H_2 molecule into two hydrogen atoms. The Hartree-Fock wavefunction leads to a solution where,

even at infinite separation the electrons spend half their time both on one hydrogen (either a or b) and half their time with one electron on each hydrogen (as they should be). This problem can only be solved by resorting to a *Multi-determinantal* wavefunction. Two general methods exist to calculate the correlation energy, *Configuration Interaction (CI)* and *Møller-Plesset perturbation theory*. These methods are computationally *very* expensive and complex, typically scaling as the 5^{th} - 7^{th} power of the number of basis functions. These types of calculation are usually only used for single point calculations, although with fast modern computers it has become possible to perform geometry optimizations on systems composed of about twenty atoms or more.

Configuration interaction (CI) calculations consider the wavefunction to be composed of a linear combination of different electronic configurations.

$$\Psi = c_0\Psi_0 + c_1\Psi_1 + c_2\Psi_2 + \ldots \tag{1.29}$$

Where Ψ_0 is the single determinant wavefunction obtained by solving the Hartree-Fock equations,
Ψ_1, Ψ_2, etc., are wavefunctions that represent different electron configurations, and
c_0, c_1, c_2, etc., are coefficients which are optimized.

The number of possible different configurations in a system with N electrons and K orbitals is given by (2K!)/[N!(2K-N)!]. For a system of even moderate size the number of configurations quickly becomes very large (eg. Water (7 orbitals and 10 electrons) has 1001 configurations, whereas methane (9 orbitals and 10 electrons) has 43 758 configurations!). The very large numbers of possible configurations renders even moderately sized systems impractical to calculate. To overcome this, the number of different configurations being considered as part of the CI calculation (i.e. Equation 1.29) is reduced. Some of the techniques used are to consider single excitations only (CIS), or single and double excitations (CISD), etc. These methods all use the determinant obtained from the Hartree-Fock equations. Clearly a better, lower energy, solution could be obtained by optimizing the determinants for each configuration as well. This technique is referred to as the multi-configurational self consistent field (MCSCF) method. A popular MCSCF technique is the complete active space SCF method (CASSCF). This method splits the molecular orbitals into three sets: orbitals that are doubly occupied in all configurations,

orbitals that are unoccupied in all configurations, and the remaining 'active' orbitals. The configurations of the active orbitals are then considered in the calculation.

The second method of accounting for electron correlation in a system after Hartree-Fock calculation is through the use of *Møller-Plesset perturbation theory*. Møller and Plesset based their method on Rayleigh-Schrödinger perturbation theory. The 'true' Hamiltonian operator $\hat{H}$ is expressed as the zeroth order Hamiltonian, $\hat{H}_0$ (i.e. Hartree-Fock derived) and a perturbation, $\lambda\hat{V}$, where λ is a scalar parameter.

$$\hat{H} = \hat{H}_0 + \lambda\hat{V} \tag{1.30}$$

The eigenfunctions, Ψ_i and eigenvalues, E_i of the 'true' Hamiltonian, $\hat{H}$ are expressed in powers of λ:

$$\Psi_i = \Psi_i^{(0)} + \lambda\Psi_i^{(1)} + \lambda^2\Psi_i^{(2)} + \ldots \tag{1.31}$$

and

$$E_i = E_i^{(0)} + \lambda E_i^{(1)} + \lambda^2 E_i^{(2)} + \ldots \tag{1.32}$$

A correction to the Hamiltonian can be made up to a certain order. The second order correction, termed MP2, would be made to the energy by including terms up to $E_i^{(2)}$, and the third order correction (MP3) by including terms up to $E_i^{(3)}$. The form of the perturbation will not be discussed here, however it should be stated that the first order correction is equivalent to the Hartree-Fock energy (with nuclear-nuclear repulsion), and it is therefore necessary to include second order corrections to gain any improvement. It can be seen from the above equations that a systematic way of improving the wavefunction of a system is provided. The *Møller-Plesset* method is also size consistent, while the *Configuration Interaction (CI)* method is not (See Section 1.2.4.5). It is however, not variational.

1.2.4.3. Basis sets

In describing the ab initio methods discussed so far, the molecular orbitals have been assumed to have been built up of atomic orbitals. A mathematical description of these orbitals however is required in order for them to be treated computationally. In the extended Hückel and Fenske-Hall methods (Section 1.2.3.1 and 1.2.3.2) the atomic orbitals were described by exponential functions called Slater type orbitals. These functions give a very good description of atomic orbitals, however calculation of their interactions (i.e. calculation of integrals) is difficult and time consuming. A faster method is to approximate each Slater type orbital by sets of Cartesian gaussian functions which have exponential terms of the form $exp(-\alpha r^2)$. Although many gaussian type functions may be necessary to approximate the original Slater type orbital, it is nevertheless computationally more efficient. Two problems that arise however are that (1) gaussian type functions do not have cusps at $r=0$, i.e. the nucleus, and (2) they decay faster at large r than do actual hydrogen like orbitals. To overcome these deficiencies each orbital is constructed by a linear combination of gaussian functions with several values of α (i.e. some very compact and some very diffuse). Multiplication by standard θ and ϕ dependencies gives the p, d, etc orbitals. The coefficients of this linear combination are now fixed in what is termed a contracted gaussian function. These contracted gaussians may now be used in an orbital scheme. Notation to describe these basis sets has been developed. From the Pople school we have the following basis set descriptions:

STO-3G	Each Slater Type Orbital (STO) is approximated by three gaussian functions.
6-31G	Each inner shell STO is approximated by six gaussians, and each valence shell STO is approximated by a split inner and outer set of three and one gaussian functions respectively.
6-31G*	6-31G basis set with six *d*-type gaussians for each atom with $Z>2$, to allow polarization.
6-31G**	6-31G* basis set with a set of *p*-type gaussians on H and He.
6-31+G*	6-31G* basis set with a set of diffuse s- and p-type gaussians to help model diffuse electron distributions.

An alternative notation, which is better suited to more complex basis sets, explicitly specifies the number of primitives and contractions. For example (12s,9p,1d) → [5s,4p,1d] means that 12 *s*-type gaussian functions were contracted to form 5 *s*-type contractions, 9 *p*-type gaussians were

contracted to form 4basis functions and a *d*-type gaussian was used without contraction. Note that the *p* contractions actually results in 12 basis functions, 4 for each of p_x, p_y, and p_z. The *d*-, *f*-, and higher angular momentum functions behave similarly. This notation does not show explicitly how many gaussians are in each of the contractions. More elaborate notation can be used for this. Using the previous example, specified as (63111/4311/1), means that there are 5 s-type contractions made up of 6, 3, 1, 1, and 1 gaussian functions respectively. There are 4 p-type basis functions made up of 4, 3, 1, and 1 gaussian functions respectively, and 1 gaussian function for the d-type basis function. Many variations of this notation exist, so the same basis function may appear as (6s,3s,1s,1s,1s/4p,1p,1p,1p/1d).

It usually follows that the greater number of primitive gaussian functions and contractions the basis set contains, the better (lower energy) the results of the calculation will be. Eventually the improvement gained by adding more gaussians will reach a limiting value. This is called the Hartree-Fock limit (i.e. it is impossible to improve the result further within the Hartree-Fock framework). The basis set in this case may be termed 'saturated'.

1.2.4.4. Effective core potentials (ECPs)

Atoms which have a large number of electrons are difficult to deal with computationally because as the number of electrons increase, the time taken for a calculation increases. The computational effort scales with the 4^{th} power for Hartree-Fock calculations, and with 5^{th} - 7^{th} power for MP2/4 and CI calculations. One way of overcoming this problem is to replace the core non-valence electrons in each atom with a pseudopotential which represents the effect of the core electrons along with the equivalent number of protons. The assumption made here is that it is only the valence electrons that take part in bonding with other atoms. The result is a decrease in the number of basis functions in the system and therefore reduced computational expense. The potentials derived are sometimes termed effective core potentials and depending on the implementation may result in accompanying nodeless valence "pseudo-orbitals." Pseudopotentials may also account for relativistic effects which become important in the heavier elements. Effective core potentials and their accompanying basis sets were used in MP2 calculations presented later in this thesis [108].

1.2.4.5. *Errors and corrections*

A number of errors can arise in ab initio molecular orbital calculations. Many of these such as correlation energy have been dealt with elsewhere. This section presents other potential sources of error in calculations.

Basis set superposition error (BSSE) is the error that arrises when the energy of molecular fragments are compared with the union of the fragments (i.e. a dissociation reaction or interaction energy). BSSE occurs because the description of each isolated fragment in terms of its own basis set is more restricted than the whole, leading to a higher energy. This is due to the fact that the fragment as part of a larger system is able to gain greater flexibility (i.e. lower energy) because there are more basis functions in the calculation. The error is not a quantum mechanical one, but is based more on 'intuition'. BSSE can be corrected for by the use of the Boys-Bernardi counterpoise correction method [109], or derivatives thereof [110]. Essentially the calculation of each fragment on its own is performed with the orbitals (i.e. basis sets) of the remaining fragment(s) included as ghost orbitals. Generally the larger the basis set employed in a calculation the smaller the BSSE will be.

Configuration Interaction (CI) and Møller-Plesset perturbation theory provide ways of accounting for correlation energy in a molecular system. Both methods however introduce potential errors. Configuration Interaction (CI) methods are not size consistent unless full CI is performed. This means that a calculation performed on N non-interacting atoms or molecules will not yield the same energy as N times the energy calculated for one atom or molecule. The Møller-Plesset perturbation method is size consistent, however it is not variational. This means that the energy obtained from such a calculation may be *less* than the 'true' energy of the system. Despite these drawbacks both methods are widely used.

1.2.5. *Density functional theory*

Density functional[f] theory (DFT) has emerged as an alternative to the traditional *ab initio* molecular orbital methods. Recent recognition of the growing importance of the method was given by the award of the 1998 Nobel Prize in Chemistry to Walter Kohn (together with John Pople). The roots of Density functional theory go back to the late 1920s and solid state physics when Thomas and Fermi had the idea that statistical considerations may be used to approximate the electron density distribution in an atom. In essence the electron density was assumed to vary slowly within a molecular system, so that each region takes the form of a homogeneous electron gas. The total energy of the system and its ground state properties could then be obtained from the electron density, ρ. The electron density is an attractive quantity to work with as it depends only on x, y, z and the spin of the electrons. Conventional Hartree-Fock theory relies on a many particle wavefunction which depends on all the coordinates of the particles (electrons) which leads to 3n variables.

The notion that the energy of a system and its ground state properties could be obtained from the electron density of the system was, before 1964, without proof. The model however yielded useful results and was extended to systems with more than one atom in the Hartree-Fock-Slater or Xα method in 1951. This method is the predecessor to modern density functional methods. In 1964 Hohenberg and Kohn published two theorems [111]. The first of these proved that every ground state property of a quantum mechanical system is a functional of the electron density. The proof however is an existence proof so does not provide the form of the functional needed to obtain the ground state properties. That is, the density functional theory *is* a rigorous theory, but the functionals used to obtain the ground state properties are approximations. The various functionals proposed in the literature and implemented in a number of density functional computer codes are all attempts to approximate the true functionals of the electron density to yield the kinetic energy, and the correlation and exchange energy.

[f] A functional is a function which operates on another function to yield a value, i.e. $F[f(x)] = a$. For example the integral from 1 to 2 of $f(x)$ is a functional.

To perform DFT calculations of the electronic energy the energy must optimized with respect to variations in the electron density, and in a similar way to the variational principle in Hartree-Fock theory it can be shown that for an approximate density $\tilde{\rho}$,

$$E[\tilde{\rho}] \geq E[\rho] \tag{1.33}$$

that is , a variational principle based on the electron density exists. This was the second theorem proved by Hoenberg and Kohn. The total energy E may be expressed in terms of the electron density by the following equation:

$$E[\rho] = T[\rho] + V_{ee}[\rho] + \int \rho(r) v(r) dr \tag{1.34}$$

Where ρ is the electron density,
E is the total energy,
$T[\rho]$ is the kinetic energy of the system,
$V_{ee}[\rho]$ is the electron-electron interaction energy, and
$\int \rho(r)\, v(r) dr$ is the interaction with the external potential (normally arises from the nucleii)

The ground state electron density is the density that minimizes $E[\rho]$ and hence satisfies the Euler equation:

$$\mu = v(r) + \frac{\delta F[\rho]}{\delta \rho(r)} \tag{1.35}$$

Where $F[\rho] = T[\rho] + V_{ee}[\rho]$,
μ is the Lagrange multiplier associated with the constraint, and
$v(r)$ is the external potential.

Equation 1.34 as expressed in the Thomas-Fermi and related models is a direct approach where approximations of $T[\rho]$ and $V_{ee}[\rho]$ are explicitly constructed. Thus far only crude approximations have emerged although efforts in this area are continuing. An alternative idea to solving this problem was proposed by Kohn and Sham in 1965 [112]. Trading the simplicity of an electron density only approach for an indirect approach, they were able to substantially improve the accuracy, thereby making DFT calculations feasible and practical. Kohn and Sham started with the idea that an electron density may be represented by the sum of squares of N orbital densities (see equation below), with the orbitals themselves defining a single Slater determinant.

$$\rho = \sum_{i}^{N} |\phi_i|^2 \tag{1.36}$$

The problem with equation 1.34 is that it contains two unknown pieces, $T[\rho]$ and the non-classical part of $V_{ee}[\rho]$. Instead of approximating these contributions separately, Kohn and Sham introduced a non-interacting reference system corresponding to each real system. This system had no electron-electron repulsion terms in the Hamiltonian, but had the same electron density as the real system (with a different external potential), i.e. equation 1.36 must be satisfied. The kinetic energy of this non-interacting system, can be written $T_s[\rho]$ and has been found to differ from $T[\rho]$ by less than the Hartree-Fock (HF) correlation energy. This difference as well as the non-classical part of $V_{ee}[\rho]$ are incorporated into a new functional $E_{XC}[\rho]$, which is defined as:

$$E_{XC}[\rho] = \{V_{ee}[\rho] - J[\rho]\} + \{T[\rho] - T_s[\rho]\} \tag{1.37}$$

Where $J[\rho]$ is the classical part of $V_{ee}[\rho]$ defined by:

$$J[\rho] = \frac{1}{2}\iint \frac{\rho(r_1)\rho(r_2)}{|r_2 - r_1|} dr_1 dr_2 \tag{1.38}$$

The total energy of the system may now be defined, without approximation[g], by the following equation:

$$E[\rho] = T_s[\rho] + U[\rho] + E_{XC}[\rho] \tag{1.39}$$

Where ρ is the electron density,
E is the total energy,
$T_s[\rho]$ is the kinetic energy of a system of non-interacting particles with density ρ,
$U[\rho]$ is the classical electrostatic energy due to coulombic interactions, and
$E_{xc}[\rho]$ includes all many body contributions to the total energy, in particular the exchange and correlation energies.

and equation 1.35 now becomes:

$$\mu = v_{KS}(r) + \frac{\delta T_s[\rho(r)]}{\delta \rho(r)} \tag{1.40}$$

[g]Other than the Born-Oppenheimer separation of nuclear and electronic motion.

where

$$v_{KS}(r) = v(r) + v_J(r) + v_{XC}(r) \tag{1.41}$$

with v_J the classical potential due to $\rho(r)$, and
$v_{XC} = \delta E_{XC}[\rho(r)]/\delta\rho(r)$

The solution to equation 1.40 is a single determinant of spin orbitals that are solutions of what are called the Kohn-Sham equation:

$$\left[-\tfrac{1}{2}\Delta^2 + v_{KS}\right]\phi_i = \varepsilon_i\phi_i \tag{1.42}$$

These equations are solved via a SCF procedure with the constraint that equation 1.36 is satisfied. The procedure is illustrated in Figure 1.13 below.

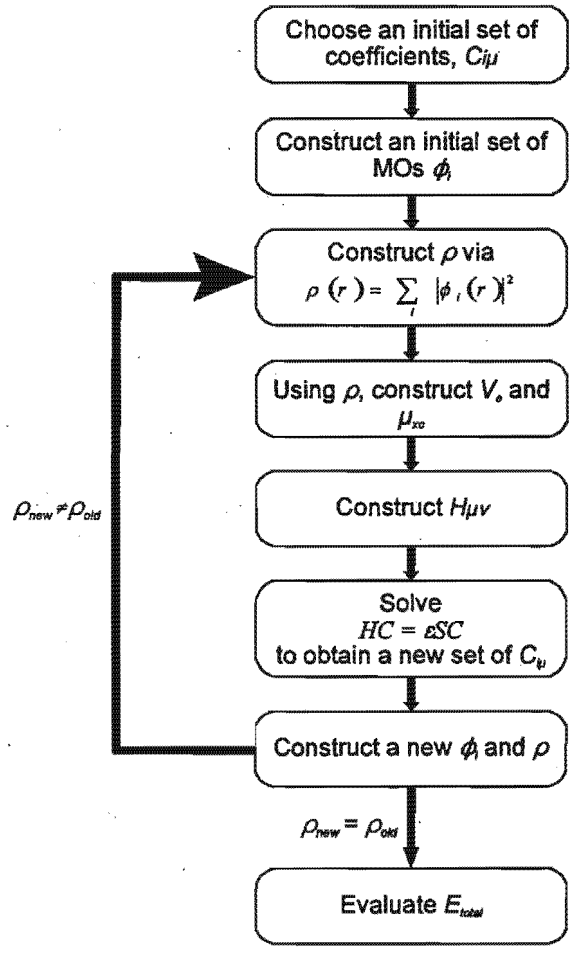

Figure 1.13 Diagram showing the steps in a Density Functional Theory (DFT) energy calculation by the Kohn-Sham method.

1.2.5.1. *Local density approximation*

The local density approximation (LDA) makes the assumption that the electron density within a molecular system varies slowly and so each region behaves like a uniform electron gas. This allows the exchange-correlation energy to be calculated from the known exchange-correlation energy of a uniform electron gas. Despite the apparent crudeness of this approximation it has produced surprisingly good results [113]. However it does tend to cause an over estimation of molecular binding energies.

1.2.5.2. *Non-local corrections*

To correct for the simplified assumptions of the local density approximation (LDA) approach (i.e. the homogeneous electron gas model), nonlocal density functionals have been derived. The commonly used nonlocal functionals are formulated so that $\varepsilon_{XC}\left[\rho(r)\right]$ is a function of $\rho(r)$ and its gradients, i.e. a correction is made to the LDA. This approach is termed the generalized gradient approximation (GGA). Other approaches to the problem are the weighted density approximation (WDA), which is a genuinely nonlocal functional. The exchange and correlation contributions to the energy are often separated out into different functionals (see section 1.2.5.3 for examples).

Application of non-local gradient corrected functionals have been found to give values for molecular energies and properties at the HF + MP2 level or better [114,115]. The gradient corrections may be applied during the SCF cycles (full SCF gradient corrected nonlocal DFT), however it has been found that application of the gradient correction after the SCF cycle has completed leads to a decrease in computing time while retaining comparable accuracy.

1.2.5.3. *Functionals*

The exchange and correlation term, E_{xc} of equation 1.39 has to be approximated. A number of different functionals for this purpose have been described in the literature and incorporated in various DFT computer codes. The following table details some of the better known functionals:

Table 1.4

Some common functionals in Density Functional Theory (DFT).

Abbreviation	Author(s)	Type	Reference
LYP	Lee, Yang, and Parr	Correlation (gradient corrected)	[116]
B88	Becke	Exchange (gradient corrected)	[117]
BLYP	Used to describe the use of B88 in conjunction with LYP.		
PW	Perdew and Wang	Correlation (gradient corrected)	[118]
BWP or BP	Used to describe the use of B88 in conjunction with PW.		
VWN	Vosko, Wilk and Nusair	Correlation	[119]
BH	Von Barth and Hedin	Exchange-Correlation	[120]
B3LYP	Becke, Lee, Yang, and Parr	Hybrid functional using Hartree-Fock for exchange	[121,122]

1.2.5.4. *Frozen core approximation*

In a similar manner to effective core potentials in Hartree-Fock theory, computational time may be reduced by using a frozen core approximation. In this approximation the core functions are frozen at the values of the free atoms. The valence orbitals are then orthogonalized to them. This method has been implemented in the DMol program [123] which allows all the non-valence electrons to be frozen, or the inner core electrons only to be frozen.

1.2.6. Structure optimizations

Computing properties of a molecular system described by a set of coordinates can yield valuable information. As chemists, we are often very interested in knowing the molecular arrangement or

structure which yields the lowest energy (i.e. the most stable structure). It is also of interest to know how this energy (and properties) change as the structure changes; whether it leads to a new structure(s), i.e. a reaction, and what the barrier to this reaction is. Obtaining this information involves the exploration of a potential energy surface (PES) which is defined by the coordinates of the atoms and the calculated energy of the structure. This means that the PES is in $3n+1$ dimensional space[h], where n is number of atoms in the system. Even a relatively small molecule leads to a surface of high dimensionality. Such surfaces are conceptually unimaginable and impossible to represent graphically without reducing to two or three dimensions. Fortunately the familiar concepts of gradients and curvatures of surfaces in two and three dimensions extends naturally to higher dimensions and can be used to explore and characterise the PES. The optimization of structures by exploration of the PES represents a subject in its own right. The various mathematical techniques used are described below in Section 1.2.6.4, but this is not intended to be a comprehensive treatment of the subject, merely an introduction to the more commonly used methods.

Points on the potential energy surface (PES) at which the gradient of the energy with respect to the coordinates of the atoms, is zero are called stationary points. Two types of stationary points are of particular interest to chemists. Points of minimum energy which describe stable structures of a molecular system, and saddle points which describe transition states. These are described below.

1.2.6.1. Structural minima (reactants and products)

Structural minima are stationary points (i.e. gradient of the energy equals zero) where the second derivative describing the curvature of the surface is positive in every direction. This corresponds to a "bowl" shaped surface in a three dimensional system. In terms of the structure it means that for any change in the structure, the energy of the system must increase. This minimum structure represents a structure that theoretically can exist. The stability of the structure will depend on how large the energy barrier is when the structure changes before the energy begins to decrease. There is no way of calculating this with absolute certainty, but the problem may be tackled by

[h]Note that this includes translations and rotations of the system which can be projected out, or eliminated through the use of internal coordinates.

the use of molecular dynamics, where this is computationally feasible. In a chemical reaction, the structures defined by the minima on the PES would be the reactant(s) and product(s) of the reaction. The relative energies of the reactant(s) and product(s) gives information about the thermodynamics of the reaction[i].

1.2.6.2. Transition state structures

The transition state of a reaction is of great importance in understanding the reaction as a whole. The energy of the transition state is directly related to the rate of the reaction (kinetics), and the structure of the transition state can yield useful insights into the selectivity of the reaction and important bond breaking and bond formations.

The transition state of a reaction is the lowest point of highest energy on the PES when going from reactant(s) to product(s) structures. The point is a stationary point, i.e. the gradient of the energy is zero, and the curvature is positive in every direction but one. Performing a vibrational analysis at a transition state yields exactly one imaginary frequency (mode) of vibration. This mode is not just a convenient property of the transition state, but corresponds to an actual physical process. The imaginary vibration is nothing more than a vibration to which there is no restoring force, and corresponds to the system moving in the direction of the reactant(s) and product(s) structures.

Transition state structures are notoriously difficult to find. It is usually necessary to have a good initial structure, however this is not always easy as there are no standard bond lengths or angles which can be used. Techniques employed include the linear synchronous transit (LST) method which can provide reasonable guesses providing the reaction path is not too complex. More often than not the initial transition states structure is constructed from chemical intuition followed by optimization (See Section 1.2.6.4).

---

[i]This does not include contributions to the entropy.

1.2.6.3. Reaction coordinates

The reaction coordinate in terms of the geometry of the molecular system, is just the simultaneous change of atomic coordinates which lead from the reactant(s) through the transition state to the product(s) via the lowest energy pathway. When examining a reaction computationally by the methods described previously in this chapter, the structures sought are the minima representing the reactant(s) and product(s) structures and the structure of the transition state. Finding these points however does not necessarily constitute a rigorous description of the reaction. The transition state identified may not be *the* transition state for the reactant(s) and product(s) identified. It is necessary to calculate the reaction coordinate to be certain that the correct transition state has been found. This can be done by following the imaginary vibration at the transition state (in both directions) which should lead to the reactant(s) and product(s) structures.

1.2.6.4. Optimization methods

A number of different mathematical techniques are employed to find energy minima and transition states. These all involve exploration of the potential energy surface (PES) for the structure being studied. Some of the more common methods are described here, without a full development of the underlying mathematics.

Modern optimization methods usually make use of derivatives of the total energy with respect to the molecular coordinates. One of the simplest methods is the *steepest descent* method, which uses the first derivative of the energy (i.e. gradient) to move 'downhill' along the PES in the direction of the steepest gradient. This method is reasonably robust, even when starting far from a minimum energy structure. It does have some drawbacks however: it does not take account of the rate of change of the gradient (i.e. second derivative of the energy) and may not always choose the appropriate sized step to take. In certain situations it may not choose the most 'direct' path to the minimum, and when close to the minimum it may converge slowly.

The *conjugate gradient* method is similar to the steepest descent method, except that the directions of each step are conjugate, not orthogonal. Each step is taken based on the gradient at

that point and the direction of the previous step. Several variations of the method exist, the most common being Fletcher-Reeves and Polak-Ribiere which differ by the value of the scaling factor used for incorporation of the direction of the previous optimization step into the new step.

A more complex method based on first and second derivatives of the energy is the *Newton-Raphson* method. The method is capable of finding the minimum on a quadratic surface in one step. The potential energy surface of a molecule is not usually quadratic however, and more steps are therefore necessary. The drawbacks of the method are that it is not robust when far from a minimum on the PES, and it requires the second derivative of the energy (hessian), which must be positive definite (i.e. all eigenvalues positive). Variation of the method include *quasi-Newton-Raphson* which builds the hessian during optimization, and *block diagonal Newton-Raphson*, which optimizes one atom at a time.

Optimization of transition state structures requires that the structure be minimized in the direction of all second derivatives (i.e. hessian) and maximized in the direction of one negative hessian entry (i.e imaginary vibrational mode). It is also possible to move from a minimum energy structure to a transition state by following one of the lower vibrational modes (real) for the molecule.

1.2.7. Environmental effects

The vast majority of molecules and reactions that are of interest occur in some sort of medium (eg. solution), which may effect the structure or reactivity of the molecule(s). It is therefore desirable to include in some way any effects the medium or environment may have on the system. Methods that are used to include these effects are:

- Continuum Solvation Model (CSD).
- Explicit Solvation (i.e. solvent molecules explicitly included in system).

The continuum solvation model considers the solute molecule to exist in a cavity within a dielectric continuum of permittivity ε that represent the solvent [124,125]. The charge

distribution of the solute molecule induces a polarization of the dielectric medium which is described by screening charges on the cavity surface.

The explicit model of solvation involves nothing more than the generation of solvent molecules in a box around the solute molecule. The calculation performed therefore includes all the generated solvent molecules, which can be computationally very expensive.

Solvation effects were not considered in the computational work presented later in this thesis.

1.3. References

1. Anderson, R. B. *The Fischer-Tropsch Synthesis*; First ed.; Academic Press, Inc.: Orlando, 1984.
2. Dry, M. E., *The Fischer-Tropsch synthesis as a source of raw materials for the chemical industry*, in *Chemicals from Coal: New Processes*; Payne, K. R., Ed.; Critical Reports on Applied Chemistry, Finch, C. A., John Wiley & Sons: Chichester, 1987; Vol. 14, pp 73.
3. Storch, H. H.; Golumbic, N.; Anderson, R. B. *The Fischer-Tropsch and Related Syntheses*; First ed.; John Wiley & Sons, Inc.: New York, 1951.
4. Sheldon, R. A. *Chemicals from Synthesis Gas*; D. Reidel Publishing Company: Dordrecht, 1983.
5. Keim, W. *Synthesis Gas: Feedstock for Chemicals*; Fahey, D. R., Ed.; American Chemical Society: New York, USA, 1986; Vol. 328, pp 1.
6. Thomas, J. M.; Thomas, W. J., *Fischer-Tropsch Catalysis*, in *Principles and Practice of Heterogeneous Catalysis*, First ed., VCH Verlagsgesellschaft mbH: Weinheim, 1996, pp 524.
7. Birkett, D. *Chem. Brit.* **1997**, *33*, 37.
8. Dry, M. E. *App. Cat. A* **1996**, *138*, 319.
9. Dry, M. E.; Erasmus, H. B. d. W. *Ann. Rev. Energy* **1987**, *12*, 1.
10. Heylin, M. *Chem. Eng. News* **1979**, 13.
11. *Adapt, Die or Make Chemicals (Sasol)*, in *The Economist*, 4 November, **1995**.
12. Jager, B. *La Chimica e l'Industria* **1996**, *78*, 451.
13. Waddacor, M. *Chem. Proc. SA* **1994**, 2.
14. Dry, M. E.; Jager, B.; Shingles, T.; Steynberg, A. P. *Cat. Let.* **1990**, 293.
15. Ensor, L., *Mossgas CEO Requests R2,4bn More for Exploration of New Oil Field*, in *Business Day*: Johannesburg, 30 July, **1998**.
16. Eilers, J.; Posthuma, S. A.; Sie, S. T. *Cat. Let.* **1990**, 253.
17. Morse, P. M. *Chem. Eng. News* **1998**, 17.
18. *Chem. Eng. News* **1998**, 18.
19. Cornils, B., *Syngas via coal gasification*, in *Chemicals from Coal: New Processes*; Payne, K. R., Ed., John Wiley & Sons: Chichester, 1987; Vol. 14, pp 1.
20. Jacobs, P. A.; Nijs, H. H. *J. Catalysis* **1980**, *65*, 328.

21. Yang, Y.; Pen, S.; Zhong, B. *Cat. Let.* **1992**, 351.
22. Rofer-DePoorter, C. K. *Chem. Rev.* **1981**, *81*, 447.
23. Hoffmann, R.; Wijeyesekera, S. D.; Sung, S. *Pure & Appl. Chem* **1986**, *58*, 481.
24. Marks, T. J. *Acc. Chem. Res.* **1992**, *25*, 57.
25. Gates, B. C. *Angew. Chem. Int. Ed. Engl.* **1993**, *32*, 228.
26. Maitlis, P. M.; Long, H. C.; Quyoum, R.; Turner, M. L.; Wang, Z.-Q. *J. Chem. Soc., Chem. Commun.* **1996**, 1.
27. Henrici-Olive, G.; Olive, S. *Angew. Chem. Int. Ed. Engl.* **1976**, *15*, 136.
28. Maitlis, P. M.; Ma, F.; Sunley, G. J.; Saez, I. M. *J. Chem. Soc., Chem. Commun.* **1990**, 1279.
29. Maitlis, P. M.; Byers, P. K.; Long, H. C.; Turner, M. L. *J. Am. Chem. Soc.* **1993**, *115*, 4417.
30. Maitlis, P. M.; Long, H. C.; Shenton, A.; Byers, P. K. *Chem. Eur. J.* **1995**, *1*, 549.
31. Muetterties, E. L. *J. Organomet. Chem.* **1980**, *200*, 177.
32. Hoffmann, R.; Sung, S.-S. *J. Am. Chem. Soc.* **1985**, *107*, 578.
33. Brady, R. C.; Pettit, R. *J. Am. Chem. Soc.* **1980**, *102*, 6181.
34. Schrock, R. R.; Guggenberger, L. J. *J. Am. Chem. Soc.* **1975**, *97*, 6578.
35. Schrock, R. R. *J. Am. Chem. Soc.* **1975**, *97*, 6577.
36. Herrmann, W. A. *Angew. Chem. Int. Ed. Engl.* **1978**, *17*, 800.
37. Lin, Y. C.; Calabrese, J. C.; Wreford, S. S. *J. Am. Chem. Soc.* **1983**, *105*, 1679.
38. Moss, J. R.; Gafoor, M. A.; Hutton, A. T. *J. Organomet. Chem.* **1996**, *510*, 233.
39. Carter, E. A.; Goddard, W. A. *Organometallics* **1988**, *7*, 675.
40. Piper, T. S.; Wilkinson, G. *J. Inorg. Nucl. Chem.* **1956**, *3*, 104.
41. Ekerdt, J. G.; Wang, C. J. *J. Catalysis* **1984**, *86*, 239.
42. Emeran, A.; Gafoor, M. A.; Goslett, J. K. I.; Liao, Y.; Moss, J. R.; Pimble, L. *J. Organomet. Chem.* **1991**, *405*, 237.
43. Moss, J. R. *J. Mol. Cat. A* **1996**, *107*, 169.
44. Herrmann, W. A. *Angew. Chem. Int. Ed. Engl.* **1982**, *21*, 117.
45. Sterling, G. P.; Wegner, P. A. *J. Organomet. Chem.* **1978**, *162*, c31.
46. Barnhart, T. M.; Bartz, J. A.; Crim, F. F.; Galloway, D. B.; Glenewinkel-Meyer, T.; Huey, L. G.; McMahon, R. J. *J. Am. Chem. Soc.* **1993**, *115*, 8389.
47. Culbertson, E. C.; Reger, D. L. *J. Am. Chem. Soc.* **1976**, *98*, 2789.

48. Gregor, J. H. *Cat. Let.* **1990**, 317.
49. "SASOL Annual Report," Sasol Limited, **1997**.
50. "BP Statistical Review of World Energy," British Petroleum Company plc, **1998**.
51. Hatfield, C. B. *Nature* **1997**, *387*, 121.
52. Campbell, C. J.; Laherrere, J. H. *Sci. Am.* **1998**, 60.
53. Anderson, R. N. *Sci. Am.* **1998**, 68.
54. *Cheap production costs keep lid on crude prices*, in *Gulf News*: Dubai, Thursday 9 April, **1998**.
55. George, R. L. *Sci. Am.* **1998**, 66.
56. Shaxson, N., *Angola: Peace brings its dividend*, in *Financial Times*: London, 9 June, **1998**, pp VII.
57. Bearman, J., *Nigeria: Squandered Inheritance*, in *Financial Times*: London, 9 June, **1998**, pp VIII.
58. Corzine, R., *Regional Focus: West Africa. Deep Pockets Full of Riches*, in *Financial Times*: London, 9 June, **1998**, pp VII.
59. *Alaska. More Oil, Anyone?*, in *The Economist*, 9 May, **1998**.
60. Corzine, R., *OIL: Troubled Waters for the Industry*, in *Financial Times*: London, 16 February, **1999**.
61. Solman, P., *WORLD BANK: Doubts over prices recovery*, in *Financial Times*: London, 3 February, **1999**.
62. *Drowning in oil*, in *The Economist*, 6 March, **1999**, pp 19.
63. *Oil Shocked*, in *The Economist*, March 28, **1998**, pp 79.
64. Corzine, R., *Saudis signal new informal alliance of oil exporters*, in *Financial Times*: London, 26 June, **1998**, pp 1.
65. Corzine, R., *Opec tries to convince oil market that cuts will stick*, in *Financial Times*: London, 26 June, **1998**, pp 3.
66. McDonald, P. *Middle East Energy* **1998**, 10.
67. *At last, a market for energy.*, in *The Economist*, March 28, **1998**, pp 17.
68. *OPEC, Lying Low*, in *The Economist*, 4 July, **1998**.
69. Corzine, R.; O'Connor, G.; Solman, P., *Oil jumps on News of Opec Talks*, in *Financial Times*: London, 9 March, **1999**.
70. *Cheap Oil - The Next Shock?*, in *The Economist*, 6 March, **1999**, pp 27.

71. Fouda, S. A. *Sci. Am.* **1998**, 74.

72. Parkinson, G. *Chem. Eng.* **1997**, 39.

73. "SASOL Annual Report," Sasol Limited, **1998**.

74. Robertson, E. P.; Thomas, C. P. *Economics of Alaska North Slope Gas Utilization Options*; U. S. Department of Energy: Houston, Texas, 1997.

75. Singleton, A. H.; Cooper, P. G. *Conversion of Associated Natural Gas to Liquid Hydrocarbons*; U. S. Department of Energy: Houston, Texas, 1997.

76. Clark, T. *A Handbook of Computational Chemistry*; John Wiley & Sons: USA, 1985.

77. Allinger, N. L.; Burket, U. *Molecular Mechanics*; American Chemical Society: Washington, D. C., 1982; Vol. 177.

78. Landis, C. R.; Doman, T. N.; Bosnich, B. *J. Am. Chem. Soc.* **1992**, *114*, 7264.

79. Landis, C. R.; Kelly, C. M.; Giovannetti, J. S. *J. Am. Chem. Soc.* **1993**, *115*, 4040.

80. Landis, C. R.; Root, D. M.; Cleveland, T. *Rev. Comput. Chem* **1995**, 73.

81. Landis, C.; Cleveland, T.; Casey, C. P. *Inorg. Chem.* **1995**, *34*, 1285.

82. Deeth, R. J. *Struct. Bond.* **1995**, *82*, 1.

83. Deeth, R. J.; Burton, V. J.; Kemp, C. M.; Gilbert, P. J. *J. Am. Chem. Soc.* **1995**, *117*, 8407.

84. Comba, P. *Modeling of Structural and Spectroscopic Properties of Transition Metal Compounds*; Gans, W., Amann, A. and Boeyens, J. C. A., Ed.; Plenum: Kruger National Park, South Africa, 1995, pp 167.

85. Comba, P.; Zimmer, M. *J. Chem. Educ.* **1996**, *73*, 108.

86. Comba, P.; Hambley, T. W.; Stoehle, M. *Helv. Chim. Acta* **1995**, *78*, 2042.

87. Comba, P.; Zimmer, M. *Inorg. Chem.* **1994**, *33*, 5368.

88. Comba, P.; Bernhardt, P. V. *Inorg. Chem.* **1993**, *32*, 2798.

89. Comba, P.; Bernhardt, P. V. *Inorg. Chem.* **1992**, *31*, 2638.

90. Hoffmann, R. *J. Chem. Phys.* **1963**, *39*, 1397.

91. Fenske, R. F. *Pure & Appl. Chem* **1971**, *27*, 61.

92. Fenske, R. F.; Hall, M. B. *Inorg. Chem.* **1972**, *11*, 768.

93. Fenske, R. F.; Lichtenberger, D. L. *J. Am. Chem. Soc.* **1976**, *98*, 50.

94. Fenske, R. F. *Prog. Inorg. Chem.* **1976**, *21*, 179.

95. Pople, J. A.; Segal, G. A. *J. Chem. Phys.* **1965**, *43*, S136.

96. Pople, J. A.; Beveridge, D. L.; Dobosh, P. A. *J. Chem. Phys.* **1967**, *47*, 2026.

97. Dewar, M. J. S.; Bingham, R. C.; Lo, D. H. *J. Am. Chem. Soc.* **1975**, *97*, 1285.

98. Dewar, M. J. S.; Thiel, W. *J. Am. Chem. Soc.* **1977**, *99*, 4899.

99. Dewar, M. J. S.; Zoebisch, E. G.; Healy, E. F.; Stewart, J. J. P. *J. Am. Chem. Soc.* **1985**, *107*, 3902.

100. Stewart, J. J. P. *J. Computational Chem.* **1989**, *10*, 209.

101. Dewar, M. J. S.; Jie, C.; Yu, J. *Tetrahedron* **1993**, *49*, 5003.

102. Zerner, M. C., *Semiempirical Molecular Orbital Methods*, in *Reviews in Computational Chemistry*; Boyd, D. B. and Lipkowitz, K. B., Ed., VCH Publishers: New York, 1991; Vol. 2, pp 313.

103. Thiel, W.; Voityuk, A. *Theo. Chim. Acta.* **1992**, *81*, 391.

104. Thiel, W.; Voityuk, A. *Int. J. Quantum Chem.* **1992**, *44*, 807.

105. Hehre, W. J.; Yu, J. *J. Computational Chem. , to be submitted.*

106. Leach, A. R., *Semi-Empirical Methods*, in *Molecular Modelling - Principles and Applications*, Addison Wesley Longman: Singapore, 1996, pp 90.

107. Lowe, J. P., *Appendix 7 - Derivation of the Hartree-Fock Equation*, in *Quantum Chemistry*, Second ed., Academic Press, Inc.: San Diego, 1993, pp 627.

108. Basch, H.; Jasien, P. G.; Krauss, M.; Stevens, W. J. *Can. J. Chem.* **1992**, *70*, 612.

109. Boys, S. F.; Bernardi, F. *Mol. Phys.* **1970**, *19*, 553.

110. Cammi, R.; Bonaccorsi, R.; Tomasi, J. *Theo. Chim. Acta.* **1985**, *68*, 271.

111. Kohn, W.; Hohenberg, P. *Phys. Rev. A* **1964**, *136*, B864.

112. Kohn, W.; Sham, L. J. *Phys. Rev. A* **1965**, *140*, 1133.

113. Ziegler, T. *Chem. Rev.* **1991**, *91*, 651.

114. Perdew, J. P.; Burke, K.; Ernzerhof, M. *Local and Gradient-Corrected Density Functionals*; Laird, B. B., Ross, R. B. and Ziegler, T., Ed.; American Chemical Society: Anaheim, California, 1995; Vol. 629, pp 453.

115. Parr, R. G.; Yang, W. *Annu. Rev. Phys. Chem.* **1995**, *46*, 701.

116. Lee, C.; Yang, W.; Parr, R. G. *Physical Review B* **1988**, *37*, 785.

117. Becke, A. D. *J. Chem. Phys.* **1988**, *88*, 2547.

118. Perdew, J. P.; Wang, Y. *Phys. Rev. B* **1992**, *45*, 13244.

119. Vosko, S. J.; Wilk, L.; Nusair, M. *Can. J. Phys.* **1980**, *58*, 1200.

120. von Barth, U.; Hedin, L. *J. Phys. C* **1972**, *5*, 1629.

121. Becke, A. D. *J. Chem. Phys.* **1993**, *98*, 1372.

122. Becke, A. D. *J. Chem. Phys.* **1993**, *98*, 5648.

123. *DMol*; *V. 4.0.0*; Molecular Simulations Inc.: San Diego, **1996**.

124. Klamt, A.; Schuurmann, G. *J. Chem. Soc., Perkin Trans. 2* **1993**, *2*, 799.

125. Andzelm, J.; Klamt, A.; Kolmel, C. *J. Chem. Phys.* **1995**, *103*, 9312.

Chapter 2

The Synthesis, Characterization and Reactions of Alkyl and Acyl compounds of the type $[(\eta^5\text{-}C_5R_5)Fe(CO)_2R']$ and $[(\eta^5\text{-}C_5R_5)Fe(CO)_2(COR')]$

Chapter 2

The Synthesis, Characterization and Reactions of Alkyl and Acyl compounds of the type $[(\eta^5\text{-}C_5R_5)Fe(CO)_2R']$ and $[(\eta^5\text{-}C_5R_5)Fe(CO)_2(COR')]$

2.1. Introduction to Transition Metal Alkyl Compounds

Transition metal alkyl intermediates are involved in many industrially important catalytic reactions (See Chapter 1 for a discussion of the Fischer-Tropsch Synthesis). Early transition metals such as Ti, Zr, Hf, V are extremely active in olefin polymerization, involving insertion of olefins into metal-alkyl bonds [1]. Late transition metals are active in hydroformylation [2] and carbonylation [3] (Co,Rh), olefin oligimerization (Shell Higher Olefin Process - SHOP) (Ni) [4-7], co-polymerization of CO and olefins (Pd, Ni) [8] and olefin hydrogenation [9] (Pt - heterogenous, Rh - homogenous). Many of these important catalytic reactions involve transition metal alkyl intermediates.

Transition metals in the middle of the d-block (Mn and Fe triads) are not nearly as widely used in catalysis and consequently have been less studied. However, they are active catalysts for a number of important reactions including olefin metathesis(SHOP) [4], epoxidation (Re) [10], and the Fischer-Tropsch reaction (Fe) [11] (See Chapter 1). Implicit in these reactions are the existence of metal alkyl species. These species are often difficult observe and study due to the high temperatures and pressures employed in many of the processes. This has led to the use of organometallic alkyl complexes as models for the alkyl species proposed in catalytic reactions [12]. The focus of the work in this thesis is the study of compounds of the type $[(\eta^5\text{-}C_5R_5)Fe(CO)_2R']$, where R = H, CH_3 and R′ = simple alkyl. This introduction will therefore concentrate on simple alkyl compounds of the type $[(\eta^5\text{-}C_5R_5)Fe(L)(L')\ R']$, where L,L′ = CO, tertiary phosphine, and their reactions. Attention will also be given to acyl compounds as they relate to alkyl migration reactions, and to alkene compounds as they relate to β-elimination reactions. These two transformations are of general importance in industrial reactions, and are the subject of further investigation in this thesis. For further information on other reactions of cyclopentadienyl iron derivatives, the reader is referred to several reviews [13-16].

2.1.1. Compounds of the Type (η^5-C_5R_5)Fe(L)(L')Alkyl

Compounds of the type [(η^5-C_5R_5)Fe(L)(L')Alkyl], where R = H or alkyl, L = CO or tertiary phosphine, and L' = CO or tertiary phosphine are commonplace in modern organometallic chemistry. The first reported synthesis of a [(η^5-C_5R_5)Fe(CO)$_2$R'] type alkyl complex was that by Piper and Wilkinson in 1956 [17]. These authors synthesized a range of complexes with iron to carbon σ bonds, including the methyl cyclopentadienyl iron dicarbonyl, and ethyl cyclopentadienyl iron dicarbonyl complexes.

2.1.1.1. Synthesis and Properties

Piper and Wilkinson first prepared [(η^5-C_5H_5)Fe(CO)$_2$R] type compounds by allowing the strong nucleophile Na[(η^5-C_5H_5)Fe(CO)$_2$] to react with the appropriate alkyl halide. Na[(η^5-C_5H_5)Fe(CO)$_2$] is typically formed by the reduction of the [(η^5-C_5H_5)Fe(CO)$_2$]$_2$ dimer by sodium metal. The methyl compound was found to be a yellow solid melting at 78-82°C [17], however the ethyl compound was an oil at room temperature. It was reported that these compounds were unstable both thermally and in air, especially the ethyl compound which showed decomposition after only 15 minutes exposure to air. The compounds were found to be stable towards water. Piper and Wilkinson also synthesized the compounds by the reaction of [(η^5-C_5H_5)Fe(CO)$_2$X], where X = Cl, Br, or I, with a Grignard reagent, RMgX, or an alkyl lithium reagent, to form the iron alkyl [(η^5-C_5H_5)Fe(CO)$_2$R]. Other preparations have been reported [18,19], but have not found widespread use. The analogous pentamethylcyclopentadienyl compound was first prepared by King by allowing Na[(η^5-$C_5(CH_3)_5$)Fe(CO)$_2$] to react with CH_3I [20]. The compound was isolated as a yellow solid, m.p. 72 - 74°C.

The alkyls [(η^5-C_5H_5)Fe(CO)$_2$R] are eighteen electron compounds with iron in a formally +2 oxidation state, and a single bond between the iron and the alkyl carbon. The compounds are diamagnetic making them amenable to investigation by standard NMR techniques [17,21-23], and the infrared spectra exhibit two very strong, easily identifiable, bands due to the two carbonyl ligands [17,21]. The compounds are generally yellow/orange in colour, and are either soft, brittle crystals or oils at room temperature.

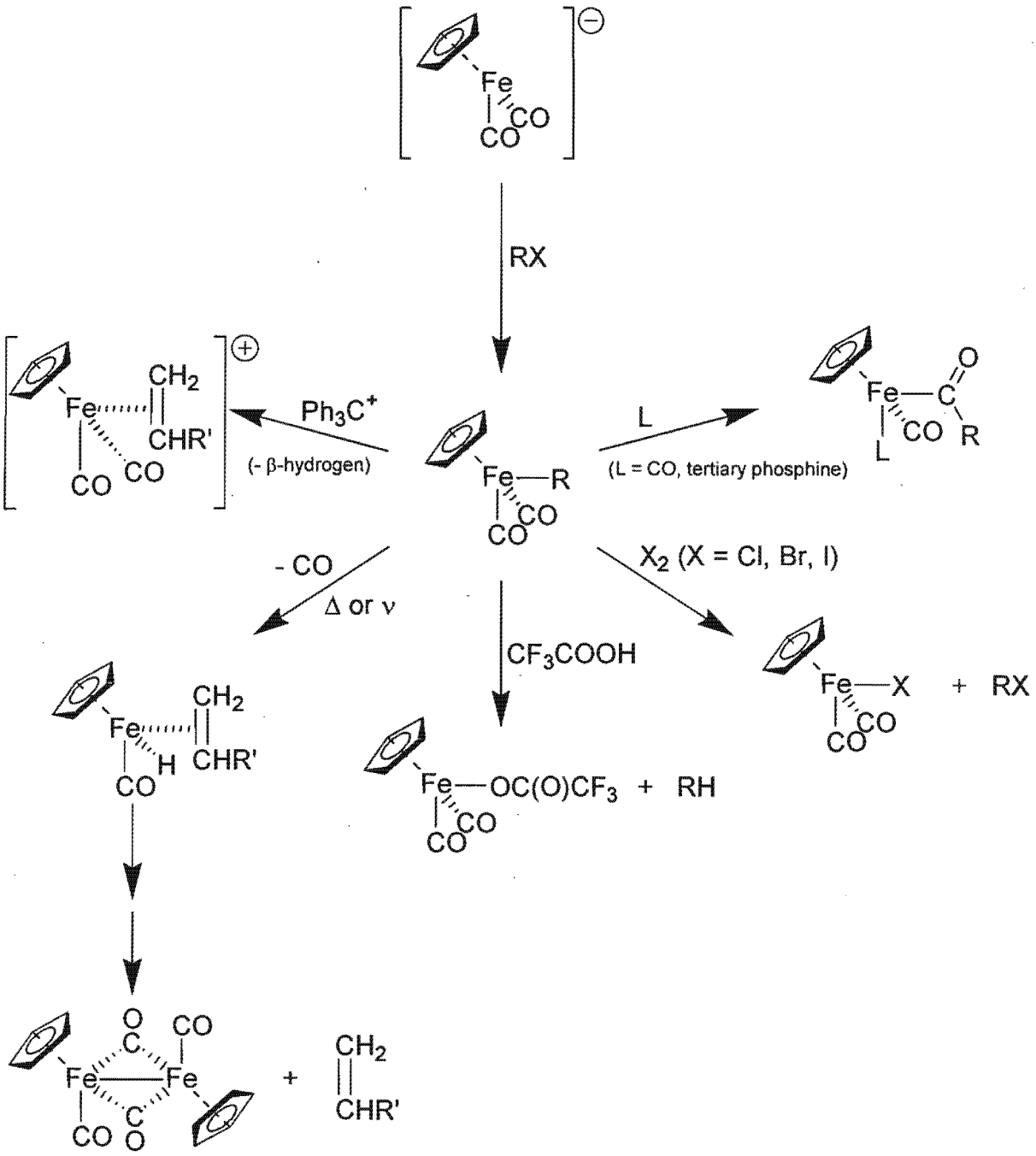

Figure 2.1 Synthesis and some reaction pathways of $[(\eta^5\text{-}C_5H_5)Fe(CO)_2R]$ compounds.

The tertiary phosphine compounds, $[(\eta^5\text{-}C_5H_5)Fe(PR_3)(CO)R']$, which are chiral, and $[(\eta^5\text{-}C_5H_5)Fe(PR_3)_2R']$ have similar properties to their dicarbonyl analogues. The compound $[(\eta^5\text{-}C_5H_5)Fe(PPh_3)(CO)CH_3]$ was first prepared by Treichel *et al* [24] by the substitution reaction of $[(\eta^5\text{-}C_5H_5)Fe(CO)_2CH_3]$ with PPh_3 under ultraviolet irradiation at 90-100°C to form a red crystalline compound. These alkyl compounds may also be prepared indirectly by the reaction of RLi with $[(\eta^5\text{-}C_5H_5)Fe(PR_3)(CO)X]$, X = halide. The compounds are thermally more stable

and have higher melting points than their dicarbonyl analogues (e.g. M.p. for $[(\eta^5\text{-}C_5H_5)Fe(PPh_3)(CO)CH_3]$ is 152°C compared to 78-82°C for $[(\eta^5\text{-}C_5H_5)Fe(CO)_2CH_3]$) [24]. The corresponding trimethylphosphine compound, $[(\eta^5\text{-}C_5H_5)Fe(PMe_3)(CO)CH_3]$, however has a melting point of 45°C [25,26].

The bis-tertiary phosphine compound $[(\eta^5\text{-}C_5H_5)Fe(PMe_3)_2CH_3]$ was first prepared in 1981 by the photochemical reaction of $[(\eta^5\text{-}C_5H_5)Fe(CO)_2CH_3]$ with trimethylphosphine in petroleum ether [26]. The compound is a highly air sensitive deep red crystalline solid which melts at 93-100°C. Pentamethylcyclopentadienyl and ethyl analogues have been synthesized by reaction of $[(\eta^5\text{-}C_5H_5)Fe(PMe_3)_2Cl]$ with a Grignard reagent, EtMgBr, to give red crystals [27,28].

2.1.1.2. Structure and Bonding

The compounds $[(\eta^5\text{-}C_5R_5)Fe(L)(L'')R']$ adopt a pseudo octahedral structure where the $(\eta^5\text{-}C_5R_5)$ ligand occupies three coordination sites and the L, L″ and alkyl occupy the other three coordination sites. The bond angles between the L, L″ ligands and the alkyl group approximate 90°. A full examination of the structures of $[(\eta^5\text{-}C_5R_5)Fe(L)(L'')R']$ type compounds is given in Chapter 3.

The bonding in compounds of the type $[(\eta^5\text{-}C_5R_5)Fe(L)(L'')R']$, where L, L″ = CO, tertiary phosphine; and R, R′ = alkyl, obeys the eighteen electron rule for transition metal complexes [29]. The iron atom is formally in a +2 oxidation state, and the cyclopentadienyl and alkyl ligands each in a -1 oxidation state. The iron atom has nine orbitals in its valence shell with which to bond (5 x 3d, 1 x 4s, 3 x 4p) and eight electrons (neutral atom). To satisfy the eighteen electron rule it requires ten electrons from the ligand system. The cyclopentadienyl ligand has five π-electrons and five π- and π^* orbitals to interact with orbitals on the iron to form π-type bonds. The carbonyl or tertiary phosphine ligands each have a lone pair of electrons which can interact with orbitals on the metal. In addition these ligands have anti-bonding orbitals (π^* in the case of the carbonyls and σ^* in the case of the tertiary phosphines) into which the metal can donate electrons (back donation). The alkyl ligand can be viewed as having a lone pair of electrons in a σ-type orbital which can interact with an empty orbital on the metal to form a single σ-type bond. The cyclopentadienyl ligand rotates freely at room temperature as evidenced by the single

signal for the cyclopentadienyl hydrogens in the ^{1}H NMR spectrum. The electronic structure of the compound $[(\eta^5\text{-}C_5H_5)Fe(CO)_2CH_3]$ has been investigated by Extended Hückel [30] and Fenske-Hall [31] calculations, and by photoelectron spectroscopy [31-33] and is described more fully in Chapter 4.

2.1.1.3. Reactivity

The reactivity of $[(\eta^5\text{-}C_5R_5)Fe(L)(L'')R']$, where L, L'' = CO, tertiary phosphine; and R = H, alkyl, and R' = alkyl, has been well studied, especially the compound $[(\eta^5\text{-}C_5H_5)Fe(CO)_2CH_3]$, and the chiral compounds, $[(\eta^5\text{-}C_5H_5)Fe(PR_3)(CO)R']$, which have utility in organic syntheses [34-36]. The cyclopentadienyl ligand is strongly bound to the iron atom and is thus often not involved in the reactions of these compounds. Presented here are transformations which primarily effect the iron to carbon bond of the alkyl group, and which have relevance to catalytic processes.

2.1.1.3.1. Alkyl Migration Reactions

The alkyl migration reaction is a fundamental organometallic transformation, and is involved in the carbonylation and hydroformylation reactions of many transition metals. The reaction is often reversible giving rise to a decarbonylation reaction. Initially the reaction was believed to be the result of insertion of CO into a metal-alkyl bond, however it has been established that the reaction occurs through the migration of the alkyl group onto a co-ordinated CO ligand [37].

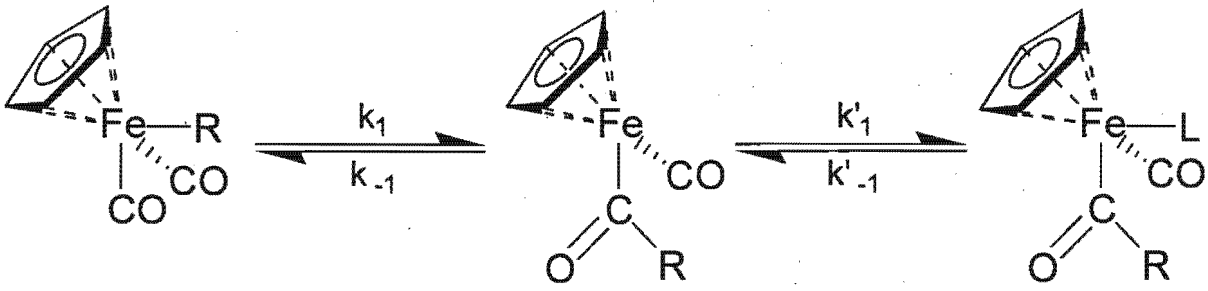

Figure 2.2 The alkyl migration reaction proceeds via an intermediate, which may be stabilized by the solvent.

The first alkyl migration reaction observed for $[(\eta^5\text{-}C_5R_5)Fe(L)(L'')R']$ type compounds was the reaction in THF, under CO pressure (2000 PSI) at 125°C of $[(\eta^5\text{-}C_5H_5)Fe(CO)_2CH_3]$ by Coffield

et al [38] to give $[(\eta^5\text{-}C_5H_5)Fe(CO)_2C(O)CH_3]$. This was followed by reactions with a range of tertiary phosphines and phosphites (PPh_3, $P(C_4H_9)_3$, $P(OC_6H_5)_3$, $P(OC_4H_9)_3$) in refluxing THF to give the acetyl compound (i.e. $[(\eta^5\text{-}C_5H_5)Fe(CO)(PPh_3)C(O)CH_3]$ in the case of PPh_3) [39]. It has been found that the rate of reaction increases with increasing tertiary phosphine concentration up to a limiting value [40,41], implying that the reaction proceeds via a tertiary phosphine (ligand) independent alkyl migration step (fast). This is followed by co-ordination of the tertiary phosphine ligand to the iron in the vacant co-ordination site left by the alkyl group (slow). Co-ordinating solvents such as acetonitrile, trifluoroethanol, and DMSO assist the reaction by helping to stabilize the unsaturated acyl intermediate. The reaction is promoted by Lewis acids and also by the substitution of one of the carbonyl ligands with a tertiary phosphine. Oxidation of the alkenyl complex with one electron oxidants such as the ferrocenium cation or Ce(IV) in catalytic amounts have been shown to increase the rate of migration [42], with similar results being obtained for the alkyl compound [43,44]. Electrochemical (Cyclic Voltametry) one electron oxidation of the alkyl $[(\eta^5\text{-}C_5H_5)Fe(CO)(PPh_3)CH_3]$ induces a dramatic increase in reactivity for the 17 electron species, with the rate being increased 10^7 - 10^8 times compared to the 18 electron species [43].

The nature of alkyl ligand affects the rate of migration, which is generally rationalized on the basis that the rate is enhanced by electron donating groups that increase the electron density on the α-carbon and hence its attraction to the carbonyl carbon which is δ+. Conversely an electron withdrawing group will slow the rate of migration (See Figure 2.3).

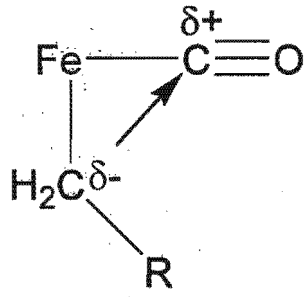

Figure 2.3 Illustration of charge distribution on the alkyl and carbonyl carbon atoms.

A large number of compounds with many different substituents on the alkyl chain have been studied. Exhaustive analysis of these compounds is beyond the scope of this introduction and these derivatives will not be presented here in detail. Simple linear alkyl groups have been shown

to exhibit different rates of migration depending on the length of the alkyl chain [45]. It was found that the rate for the forward reaction, assisted by DMSO, followed the following order: Et > ^{n}Pr ≈ ^{n}Butyl ≈ ^{n}Hexyl ≈ ^{n}Octyl > Me. This rate dependence on alkyl chain length has been reported by co-workers in systematic studies of manganese [46], iron and ruthenium [47] conducted with triphenylphosphine as the incoming ligand. In these studies however the rate of migration was found to be fastest for the ^{n}Pr compounds, and then slows down for the longer chain alkyls.

Modifications to the cyclopentadienyl ligand can have an effect on the alkyl migration reaction, but this is generally more measured than modifications to the alkyl group itself. Replacement of cyclopentadienyl ligand by indenyl (C_9H_7) increases the rate of reaction; the suggested reason being the indenyl ligand's ability to change from η^5 to $\dot{\eta}^3$ co-ordination, thus decreasing the electron density on the carbonyl carbon (through decreased back-bonding) and by allowing the reaction to proceed through a more associative (S_N2) reaction mechanism [48]. The use of a pentamethylcyclopentadienyl ligand appeared to have little effect on the rate of alkyl migration in simple alkyls [48], the expectation being that this replacement would lead to a decrease in the migration rate through increased electron density being donated onto the iron, and hence into the π^* orbital on the CO. The resulting decrease in the δ+ charge on the carbonyl carbon would result in a reduced rate of reaction. This expected effect has, however, been observed for a derivative of an alkyl compound. The compound $[(\eta^5\text{-}C_5R_5)Fe(CO)_2CH_2CH_2CH_2Si(OCH_3)_3]$, R = H or CH_3, underwent alkyl migration using PPh_3 as the incoming ligand for the cyclopentadienyl (i.e. R = H) compound, but only very slowly and not to completion for the pentamethylcyclopentadienyl analogue (i.e. R = CH_3) [49]. The reaction did proceed however for both compounds when electrooxidized in the presence of PPh_3. The rate was found to be dependent on the nature of the incoming ligand, suggesting that the mechanism does not involve a 15 electron intermediate.

Compounds of the type $[(\eta^5\text{-}C_5R_5)Fe(CO)(PR'_3)CH_3]$ are chiral and thus have potential use in asymmetric syntheses. For this reason the stereochemistry of the alkyl migration reaction of these compounds has attracted attention. It has been found that the stereochemical course of the reaction is dependent on the choice of solvent and whether the migration is oxidatively induced [44]. Nitromethane was found to be highly stereoselective with MeCN and HMPA less so.

Solvents such as Me_2SO, DMF and propylene carbonate gave low stereoselectivities [50,51]. Promoters such as BF_3 have been found to increase stereoselectivity [52], while oxidatively promoted migration procceds with low stereoselectivity, owing to the configurational instability of the $[(\eta^5\text{-}C_5H_5)Fe(CO)(PPh_3)CH_3]^+$ cation [44]. The stereoselective nature of this reaction and the $[(\eta^5\text{-}C_5R_5)Fe(CO)(PR'_3)]$ auxiliary has been exploited in asymmetric organic syntheses [36,53-55].

Compounds of the type $[(\eta^5\text{-}C_5R_5)Fe(CO)_2R]$ are not chiral. This means that the product of alkyl migration, where the incoming ligand is not CO, is a racemic mixture of enantiomers. Recent attempts have been made to overcome this limitation through complexation of the metal compound in chiral cyclodextrins. The approach has thus far failed with no, or very little, enantiomeric excess being observed [56].

The alkyl migration reaction to form acyl compounds, as described above, provides a method of increasing the number of carbon atoms in the alkyl fragment by one, using an inorganic source, CO. Insertion of further CO molecules does not occur owing to the electron withdrawing effects of the acyl oxygen on the carbon bonded to the metal. Insertion can take place however under oxidizing ($[(\eta^5\text{-}C_5H_5)_2Fe][PF_6]$) conditions at -78°C using NO as the incoming ligand for the second migration step [57]. A different strategy for forming carbon chains is to reduce the alkyl migration product (i.e. the acyl ligand), thereby allowing it to undergo further migration in the normal way. Pentanoic acid has been derived in this way entirely form carbon monoxide [58].

2.1.1.3.2. Alkyl Cleavage Reactions

Reactions in which the alkyl group is cleaved from the metal are of interest because of their relevance as termination steps in catalytic reactions, and as steps in organic transformations. The simplest method of cleaving the alkyl from the metal is through treatment of the complex with acid. The mechanism of the reaction has been investigated kinetically [59], and stereochemically [60]. A mechanism is proposed where the metal is initially protonated, followed by reductive elimination of the hydrogen and alkyl ligand, and finally the coordination of the anion to the metal (See Figure 2.4). It has been found in heteronuclear alkanediyl compounds containing iron

and tungsten that treatment with acid cleaved the tungsten-alkyl bond specifically and not the iron-alkyl bond [61].

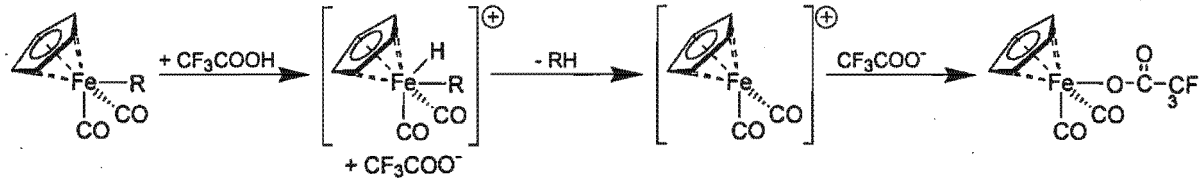

Figure 2.4 Reaction scheme showing the cleavage of the iron-carbon bond with trifluoro acetic acid.

An alternative method of cleaving the metal-alkyl bond is through treatment of the alkyl complex with a halogen. This results in the formation of a terminally halogenated alkyl and the halogenated metal complex $[(\eta^5\text{-}C_5R_5)Fe(L)(L')X]$, were X = halogen, R = H or alkyl, L = CO or tertiary phosphine, and L' = CO or tertiary phosphine.

2.1.1.3.3. Rearrangement of the Alkyl Ligand to form an η^2-Alkene

The mechanism of formation of 1-alkenes (α-olefins) in the Fischer-Tropsch reaction is not yet agreed on [62] (See also Chapter 1), yet 1-alkenes remain one of the highest value chemicals obtained from the process [63]. The complexes of the type $[(\eta^5\text{-}C_5R_5)Fe(L)(L'')R']$, where L, L'' = CO, tertiary phosphine; and R = H, alkyl, and R' = alkyl undergo reactions to form co-ordinated 1-alkenes. These reactions may be models for the reactions occurring on the surface of the catalyst and may therefore yield useful information on the catalytic system.

The first route to co-ordinated 1-alkenes from $[(\eta^5\text{-}C_5R_5)Fe(L)(L'')R']$ is by reaction with a hydride abstraction agent such as $[Ph_3C]^+[BF_4]^-$. It has been found that this agent abstracts a

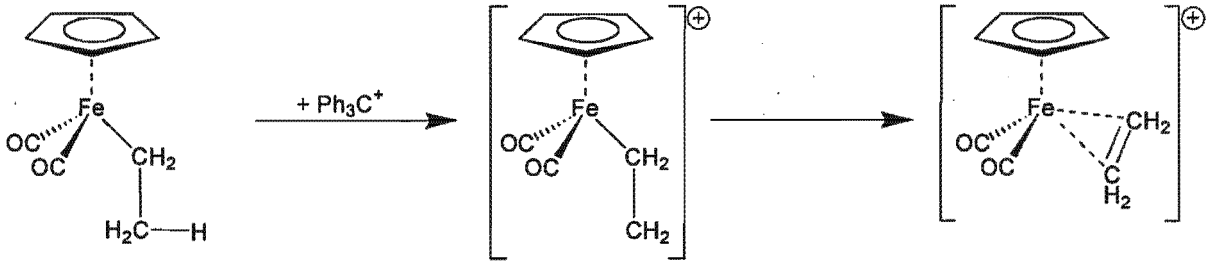

Figure 2.5 Abstraction of a hydride from the β-carbon, followed by rearrangement to give a co-ordinated alkene.

hydride specifically from the β-carbon of the alkyl chain [64]. The result of this abstraction is a rearrangement of the alkyl chain to form a co-ordinated 1-alkene. The resultant complex is positively charged, and can be isolated as a salt which is reasonably stable in air and to light. It was also found that on the addition of a hydride source (eg. sodium borohydride) to the alkene complex, the alkene reverted to the alkyl. Starting with the n-propyl complex resulted in the formation of the iso-propyl complex (i.e. the net result was the isomerization of the alkyl chain).

The second route by which co-ordinated 1-alkenes may be formed is via a β-hydride elimination reaction. In this reaction a hydride from the β-carbon migrates onto the metal. The resulting unsaturation at the β-carbon causes the formation of a double bond between the α- and β-carbon atoms. This coincides with a rearrangement of the η^1 co-ordination of the alkyl to an η^2 co-ordinated alkene. The reaction (and its reverse, alkene insertion) occurs readily in unsaturated

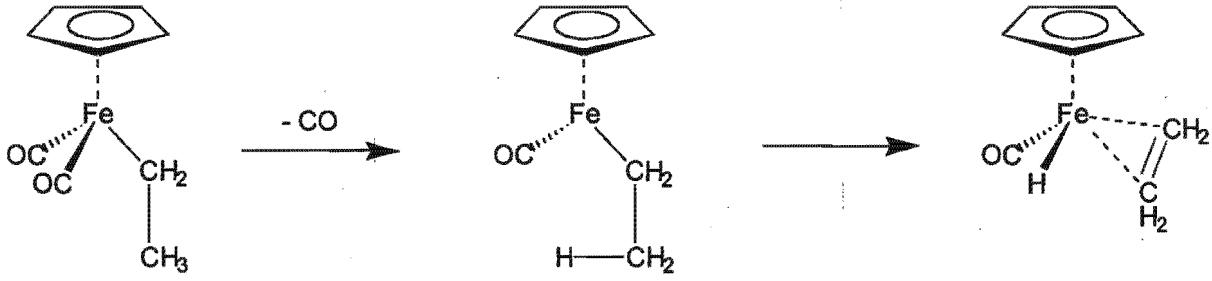

Figure 2.6 Decomposition of $[(\eta^5\text{-}C_5H_5)Fe(CO)_2CH_2CH_3]$ by loss of CO followed by β-elimination.

alkyl compounds of the late transition metals [65-70], however in 18 electron compounds of the type $[(\eta^5\text{-}C_5R_5)Fe(L)(L'')R']$ the reaction is believed to occur following loss of a ligand from the metal. This would create a reactive, co-ordinatively unsaturated 16 electron species, which could rearrange to give the 18 electron alkene hydride complex. There is evidence to support this type of reaction for dicarbonyl compounds, $[(\eta^5\text{-}C_5H_5)Fe(CO)_2R]$ [71-73], mono-carbonyl mono-tertiary phosphine compounds, $[(\eta^5\text{-}C_5H_5)Fe(CO)(PPh_3)R]$ [74,75], and the bis-tertiary phosphine compounds $[(\eta^5\text{-}C_5R_5)Fe(PMe_3)_2R']$ [27,28]. The the β-elimination mechanism, and the existence of the alkene hydride complex, in the case of the dicarbonyl and mono-carbonyl mono-tertiary phosphine compounds is inferred from the isolation of alkenes and hydride species from the reaction [71,74,75], or from spectroscopic observations of these species [72,73]. The key alkene hydride intermediate has, however not been observed directly or isolated. In the case of the bis-tertiary phosphine compounds $[(\eta^5\text{-}C_5R_5)Fe(PMe_3)_2R']$, the alkene hydride compound

has been isolated and characterized, and the reaction found to be reversible [27,28]. The reaction in all compounds is believed to occur following the loss of a carbonyl or tertiary phosphine ligand either thermally of photochemically. Both 1- and 2-alkenes (*cis* and *trans*) have been isolated as products of the reaction, suggesting that the mono- and di-carbonyl compounds also undergo a reversible reaction. Deuterium labelling of the alkyl chain supports this conclusion, and also reveals that unreacted alkyl compound recovered from the reaction has scrambled hydrogens on the alkyl chain (i.e. the scrambling occurs owing to the reversibility of the reaction).

2.1.2. Other Iron Alkyl Compounds

Iron can form alkyl complexes with other ligand systems apart form cyclopentadienyl type ligands. Examples of these types of complexes include complexes with only alkyl ligands, complexes with chelating nitrogen or tertiary phosphine ligands, and complexes with carbonyl ligands (See Figure 2.7) [76]. The compounds listed also include iron in various oxidation states. When considering complexes as models for species in catalytic reactions, the di-alkyl complexes derived from $[Fe(CO)_4]^{2-}$ (Collman's reagent) [77] are potentially interesting, as they contain only hydrocarbons, carbon monoxide, and the metal (i.e. all species which may be present in the Fischer-Tropsch reaction for example). Many of the di-alkyl compounds however are extremely unstable and tend to reductively eliminate the alkyl groups as an alkane. This often occurs with an alkyl migration step included, leading to the formation of aldehydes and ketones [78]. Formyl and acyl compounds have been found to be more stable [79], as have fluorocarbon derivatives [80]. $Na_2[Fe(CO)_4]$ (Collman's reagent) is prepared by reduction of $Fe(CO)_5$ with sodium metal [77] or reduction of $FeCl_3$ with sodium naphthalenide under a CO atmosphere [81]. This supernucleophile is a transition metal analogue of a Grignard Reagent [77] and reacts with alkyl and acyl halides, leading to the formation of alkyls, aldehydes, ketones, acids, etc. It is thus more useful as a reagent for organic couplings and transformations, than as a model complex for iron alkyl species.

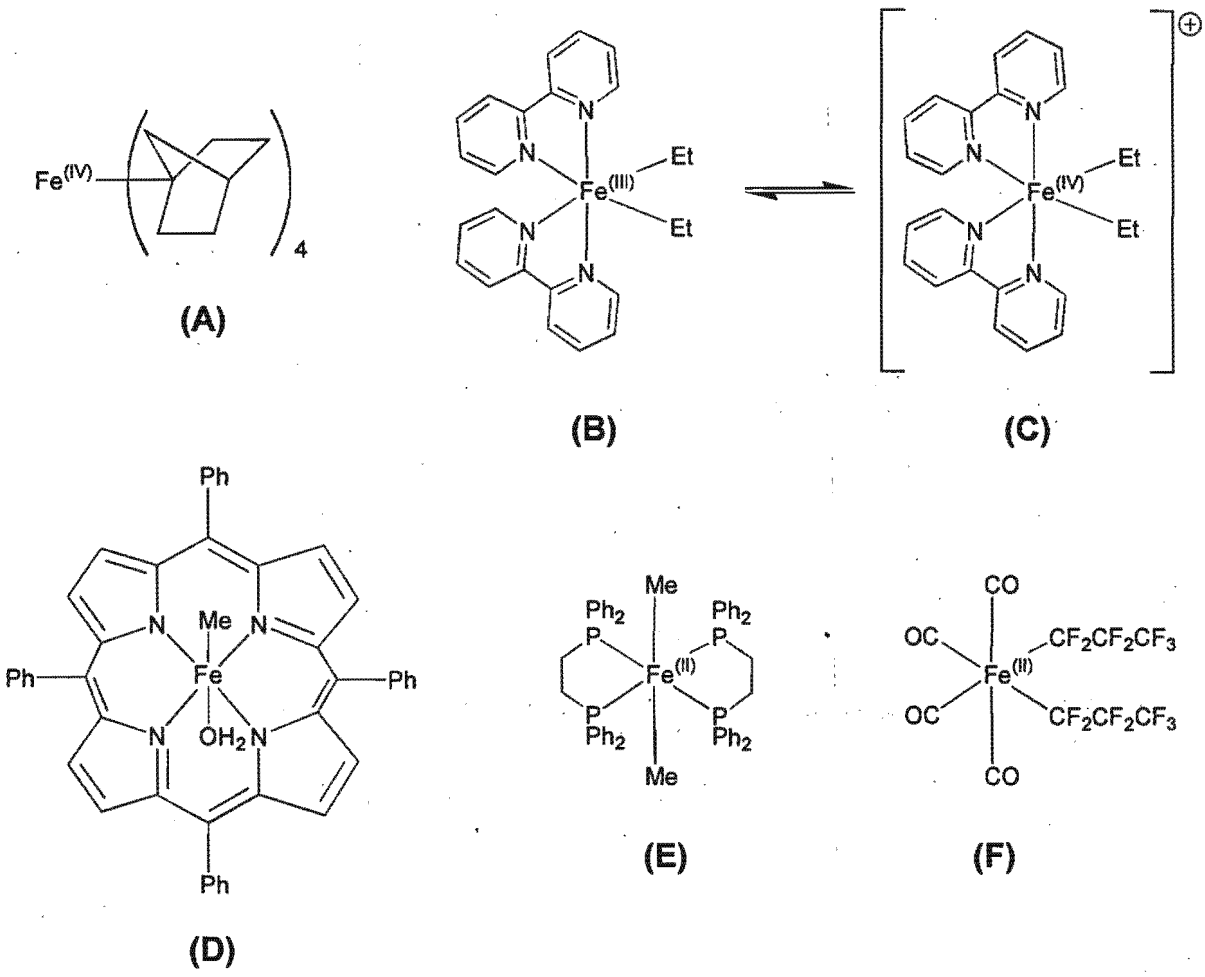

Figure 2.7 Some examples of stable non-cyclopentadienyl iron alkyl complexes, with iron occurring in a range of oxidation states.

2.1.3. Iron Acyl Compounds

Iron acyl compounds are the direct product of an alkyl migration reaction of the corresponding alkyl compound with CO as the incoming ligand. The compounds are generally more stable than their alkyl analogues, presumably owing to the blocking of further migration to a CO by a decreased charge on the acyl carbon, and by the hindrance to β-elimination owing to an increased metal-hydrogen distance, caused by the sp^2 centre, and decreased electron density on the β-hydrogens owing to the electron withdrawing effects of the acyl group.

2.1.3.1. Synthesis

The mononuclear acyl compounds $[(\eta^5\text{-}C_5H_5)Fe(CO)_2(C(O)CH_3)]$ and $[(\eta^5\text{-}C_5H_5)Fe(CO)_2(C(O)CH_2CH_3)]$ we first synthesized by Coffield *et al* in 1959 [38], and later by King [82]. The syntheses were first carried out utilizing the alkyl migration reaction (See Section 2.1.1.3.1) with CO as the incoming ligand (See Equation 2.2).

$$[(C_5H_5)Fe(CO)_2CH_3] \xrightarrow{CO,\ 2000PSI,\ 125\ ^\circ C} [(C_5H_5)Fe(CO)_2C(O)CH_3] \qquad (2.2)$$

It is also possible to synthesize acyl compounds by reaction of the nucleophile $Na[(\eta^5\text{-}C_5H_5)Fe(CO)_2]$ with the appropriate acid halide [82] in a reaction analogous to that used to form alkyl compounds (See Section 2.1.1.1).

The acyl derivatives, $[(\eta^5\text{-}C_5R_5)Fe(CO)_2C(O)R]$ have been well characterized by infrared spectroscopy [82-84], mass spectrometry [85], ^1H [84] and ^{13}C NMR [86], and Mössbauer spectroscopy [83].

2.1.3.2. Decarbonylation

The decarbonylation reaction of acyl compounds is the reverse of the alkyl migration reaction (See Section 2.1.1.3.1). Dicarbonyl acyl complexes of the type $[(\eta^5\text{-}C_5R_5)Fe(CO)_2C(O)CH_3]$ only undergo decarbonylation when irradiated with ultraviolet light, although the forward reaction occurs thermally [21]. The first step of the decarbonylation is the photochemically induced loss of a CO ligand. This is followed by the migration of the R group from the acyl carbon to the iron. The photochemical decarbonylation has been found to be thermally reversible [87]. In experiments in the presence of $P(OCH_3)_3$ the decarbonylation reaction was found to be in competition with the ligand substitution reaction which was pressure dependent. The results were interpreted on the basis of the solvated intermediate $[(\eta^5\text{-}C_5R_5)Fe(CO)(Sol)C(O)CH_3]$, where Sol = solvent molecule, which may react with the tertiary phosphine ligand in an associative manner to form the substitution product $[(\eta^5\text{-}C_5R_5)Fe(CO)(P(OCH_3)_3)C(O)CH_3]$, and through a dissociation of the solvent molecule for the migratory step of the decarbonylation to occur [88].

The carbonyl tertiary phosphine compounds, $[(\eta^5\text{-}C_5H_5)Fe(CO)(PR_3)C(O)R']$, also undergo photochemical decarbonylation, although first attempts at the reaction failed [24]. The reaction is found to proceed with a high degree of stereospecificity and with retention of configuration at the α-carbon [89]. It has been found that when a pentamethylcyclopentadienyl ligand is substituted for the cyclopentadienyl ligand in $[(\eta^5\text{-}C_5H_5)Fe(CO)(PPh_3)_3C(O)R]$, that the tertiary phosphine ligand is lost exclusively leading to the decarbonylation product $[(\eta^5\text{-}C_5(CH_3)_5)Fe(CO)_2R]$, whereas the cyclopentadienyl complex results in $[(\eta^5\text{-}C_5H_5)Fe(CO)(PPh_3)_3R]$ being formed [90].

2.2. Synthesis and Characterization

2.2.1. Mononuclear alkyl compounds $[(\eta^5\text{-}C_5(CH_3)_5)Fe(CO)_2R]$ (R = n-C_3H_7 to n-$C_{12}H_{25}$)

The pentamethylcyclopentadienyl iron dicarbonyl methyl, **1** (R = CH_3), and ethyl, **2** (R = C_2H_5) compounds have been reported previously [91,92]. These compounds (**1** and **2**) were prepared in good yield by the reaction of the sodium salt of the pentamethylcyclopentadienyl iron dicarbonyl anion with the appropriate alkyl halide (Equation 2.2).

$$Na[(\eta^5\text{-}C_5(CH_3)_5)Fe(CO)_2] + RX \longrightarrow [(\eta^5\text{-}C_5(CH_3)_5)Fe(CO)_2R] + NaX \qquad (2.2)$$

The syntheses of the new alkyl compounds, $[(\eta^5\text{-}C_5(CH_3)_5)Fe(CO)_2R]$ (R = n-C_3H_7, **3**; n-C_4H_9; **4**; n-C_5H_{11}, **5**; n-C_6H_{13}, **6**; n-C_7H_{15}, **7**; n-C_9H_{19}, **9**; n-$C_{10}H_{21}$, **10**; n-$C_{12}H_{25}$, **12**) are now reported for the first time in this thesis. These compounds were all prepared as shown in equation 2.2. Compounds **8** and **11** had already been prepared in our laboratory but were not fully characterized and have not been reported [93]. They are included here for completeness.

The compounds (**3-5** and **8**) were isolated as yellow solids and the remaining compounds (**6,7,9-12**) were isolated as yellow oils. The compounds are more stable than their cyclopentadienyl analogues [94], both thermally, and in air. They are also moderately stable in solution under nitrogen, and to light. The compounds have been fully characterized by IR, ^1H and ^{13}C NMR, elemental analysis and mass spectrometry. The data are presented in Tables 2.1-2.4.

IR data

The IR spectra in the υ(CO) region for compounds **3-12** (see Table 2.1) are in good agreement with the values reported for other $[(\eta^5\text{-}C_5(CH_3)_5)Fe(CO)_2R]$ compounds [91,92] and show two strong bands, at 1987 cm^{-1} and 1933 cm^{-1} in hexane solution. In the analogous $[(\eta^5\text{-}C_5H_5)Fe(CO)_2R]$ compounds [94] the two υ(CO) bands occur at 2008 and 1954 cm^{-1}, indicating that the C≡O bond is weaker in the $[(\eta^5\text{-}C_5(CH_3)_5)Fe(CO)_2R]$ compounds than in the $[(\eta^5\text{-}C_5H_5)Fe(CO)_2R]$ compounds; conversely, the Fe-CO bond is stronger in the $[(\eta^5\text{-}C_5(CH_3)_5)Fe(CO)_2R]$ compounds than in the $[(\eta^5\text{-}C_5H_5)Fe(CO)_2R]$ compounds. This effect is owing to the increased electron density on the iron atom, from the $\eta^5\text{-}C_5(CH_3)_5$ (i.e. Cp^*) ligand, which is donated into the π^* orbital of the carbonyl, thus weakening the C≡O bond. There is no significant change in υ(CO) on changing the length of the alkyl chain in either the Cp or Cp^* series.

Table 2.1
Data for $[(\eta^5\text{-}C_5(CH_3)_5)Fe(CO)_2R]$

Compound	R	Yield (%)	m.p. (°C)	Elemental analysis[a] (%) C	H
3	n-C_3H_7	83	76-82	62.38 (62.07)	7.68 (7.66)
4	n-C_4H_9	82	57-60	63.32 (63.16)	8.09 (7.95)
5	n-C_5H_{11}	93	31-32	64.49 (64.16)	8.34 (8.23)
6	n-C_6H_{13}	60	oil	65.22 (65.07)	8.70 (8.50)
7	n-C_7H_{15}	81	oil	65.90 (65.90)	8.05 (8.73)
8	n-C_8H_{17}	60	30-33	66.95 (66.65)	9.01 (8.97)
9	n-C_9H_{19}	88	oil	67.50 (67.36)	9.42 (9.17)
10	n-$C_{10}H_{21}$	31	oil	67.1 (68.02)	9.0 (9.36)
11	n-$C_{11}H_{23}$	90	oil	68.25 (68.64)	9.20 (9.54)
12	n-$C_{12}H_{24}$	75	oil	69.77 (69.21)	9.93 (9.70)

[a]Calculated values in parentheses.

^{1}H and ^{13}C NMR data for compounds 1-12

Separate ^{1}H resonances were observed for the methyls of the pentamethylcyclopentadienyl ligand and the methyl protons of the alkyl chain; the pentamethylcyclopentadienyl methyl protons showed no variation in chemical shift with varying alkyl chain length. The α-methylene protons appear separate from the other methylene protons, owing to the electron density from the metal, and are further upfield than in the corresponding cyclopentadienyl compounds [94], owing to the increased electron density on the metal from the pentamethylcyclopentadienyl ligand. The other methylene protons appear as a broad singlet, the integration being the only way to distinguish between compounds of differing alkyl chain length. Data for the ^{1}H NMR are given in Table 2.2.

Table 2.2

^{1}H NMR data for $[(\eta^{5}\text{-}C_5(CH_3)_5)Fe(CO)_2R]$[a]

R	$C_5(CH_3)_5$	$Fe\text{-}CH_2$	$(CH_2)_x$	CH_3
CH_3[b,c]	1.45	---	---	0.08
C_2H_5[c]	1.72	1.03	---	1.25
n-C_3H_7	1.71	0.95	1.48	0.92
n-C_4H_9	1.71	0.94	1.36	0.87
n-C_5H_{11}	1.72	0.94	1.26	0.86
n-C_6H_{13}	1.71	0.94	1.27	0.87
n-C_7H_{15}	1.71	0.94	1.26	0.86
n-C_8H_{17}	1.71	0.93	1.25	0.86
n-C_9H_{19}	1.71	0.94	1.25	0.86
n-$C_{10}H_{21}$	1.72	0.95	1.26	0.88
n-$C_{11}H_{23}$	1.70	0.94	1.24	0.86
n-$C_{12}H_{25}$	1.71	0.94	1.24	0.86

[a]Measured in $CDCl_3$ relative to TMS (δ 0.00 ppm); the methyl protons are triplets (J = 6.6 Hz); the α-methylene protons are triplets (J = 8.3 Hz).
[b]Measured in C_6D_6 relative to TMS (δ 0.00 ppm).
[c]Data from reference [91,92].

The ^{13}C NMR data for the compounds are given in Table 2.3. Assignments were made by comparison with data reported for the short chain compounds [91,92], and related long chain

compounds $[(\eta^5\text{-}C_5H_5)Fe(CO)_2R]$ [94]. The resonances for the Cp^* carbons and methyl carbons, and the CO appear at the expected positions and are independent of the alkyl chain length. The resonance of the α-methylene carbon varies from -13.1 in the methyl complex to a maximum of 17.00 in the n-propyl complex and then decreases to 14.11 in the hexyl complex, after which it remains constant. This effect is a property of the alkyl chain and has been shown to correlate with the alkyl migration rate in related manganese compounds [46,95,96].

An example of the ^{13}C NMR spectrum of $[(\eta^5\text{-}C_5H_5)Fe(CO)_2R]$ type compounds is shown in Figure 2.8 for compound **5**.

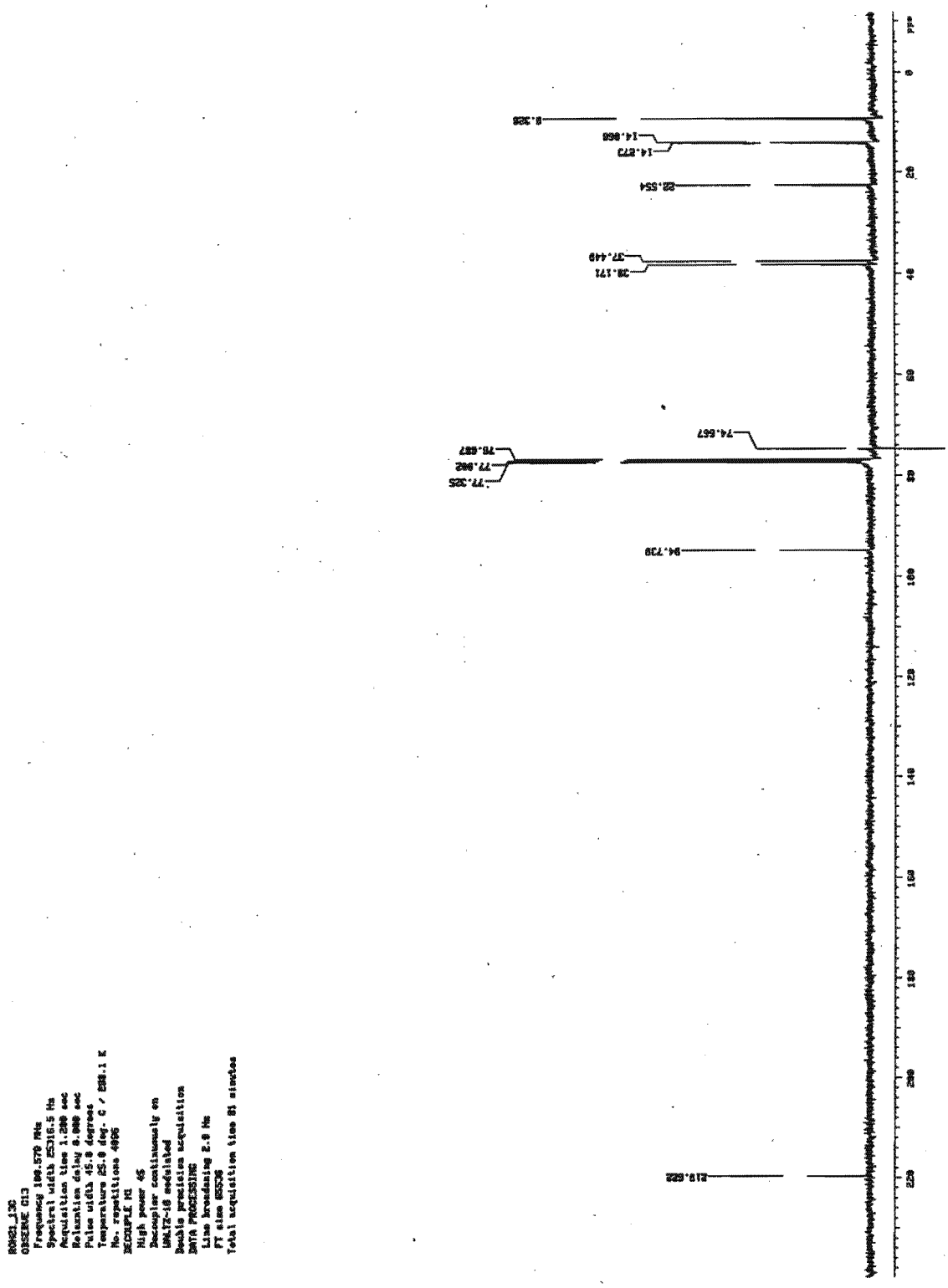

Figure 2.8 ^{13}C NMR spectrum of $[(\eta^5\text{-}C_5(CH_3)_5)Fe(CO)_2CH_2)_4CH_3]$, **5**, in $CDCl_3$.

Table 2.3
^{13}C NMR of $[(\eta^5\text{-}C_5(CH_3)_5)Fe(CO)_2R]$ in $CDCl_3$ relative to TMS (δ 0.0 ppm)

R	Compound	CO	C_{Cp}	$C(CH_3)$	$FeCH_2$ (α)	C_2 (β)	C_3 (γ)	C_4 (δ)	C_5 (ϵ)	C_6	C_7	C_8	C_9	C_{10}	C_{11}	C_{12}
methyl	**1**	219.5	105.2	9.2	-13.1											
ethyl	**2**	219.5	94.8	9.3	6.72	21.6										
n-propyl	**3**	---	94.79	9.34	17.00	30.28	20.16									
n-butyl	**4**	---	94.66	9.23	13.60	40.02	28.58	13.86								
n-pentyl	**5**	219.62	94.74	9.23	14.07	38.17	37.45	22.55	14.27							
n-hexyl	**6**	219.61	94.74	9.31	14.11	37.79	35.61	31.83	22.84	14.16						
n-heptyl	**7**	219.63	94.74	9.33	14.13	37.86	35.92	29.27	32.10	22.76	14.13					
n-octyl	**8**	219.62	94.74	9.33	14.14	37.84	35.96	29.54	29.51	31.99	22.72	14.14				
n-nonyl	**9**	219.61	94.74	9.32	14.12	37.84	35.94	29.80	29.56	29.41	31.96	22.71	14.12			
n-decyl	**10**	219.61	94.72	9.31	14.12	37.84	35.95	29.84	29.73	29.57	29.36	31.93	22.69	14.12		
n-undecyl	**11**	219.59	94.72	9.30	14.11	37.83	35.94	29.83	29.73	29.67	29.56	29.37	31.92	22.68	14.11	
n-dodecyl	**12**	219.63	94.75	9.33	14.14	37.86	35.97	29.86	29.74	29.74	29.69	29.59	29.38	31.95	22.71	14.14

Mass Spectra

The mass spectra of **3-12** are reported in Table 2.4 and are all similar. All the compounds prepared showed parent molecular ions in their mass spectra. The main fragmentation pathways begin as follows for the compounds: *M*, *M* - CO, *M* - 2CO - 2H.

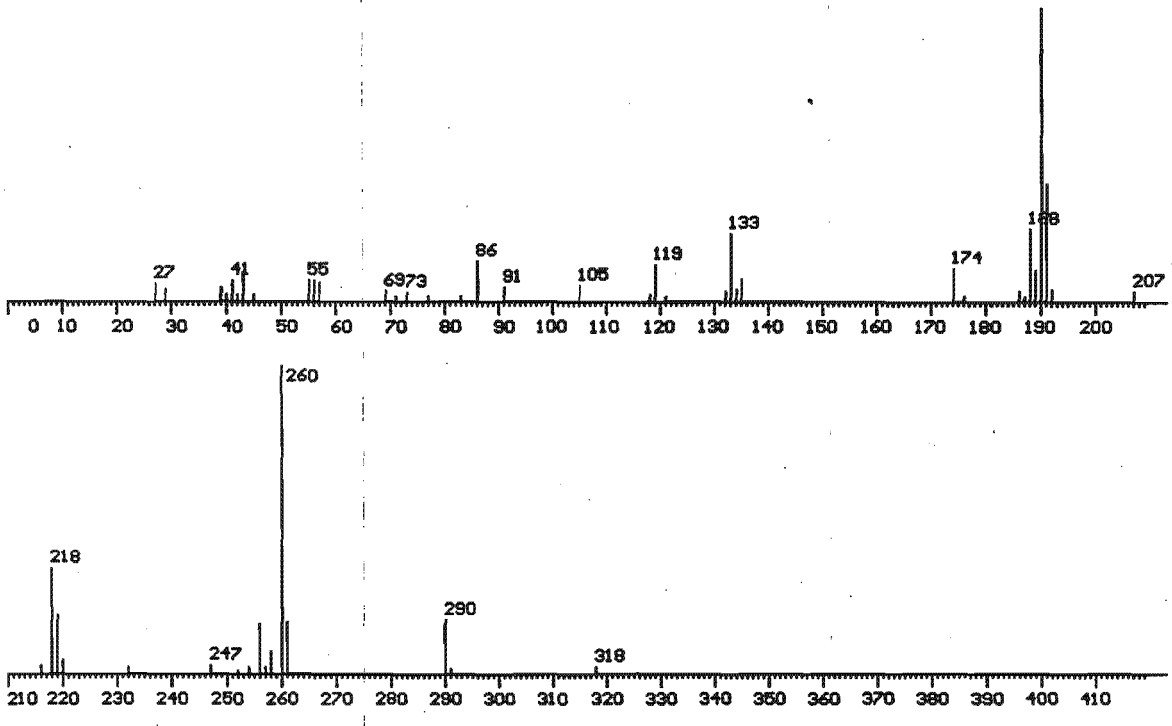

Figure 2.9 Mass spectrum of $[(\eta^5\text{-}C_5(CH_3)_5)Fe(CO)_2(CH_2)_4CH_3]$ **5**, showing the molecular ion peak at m/e=318.

Table 2.4

Mass spectral data for $[(\eta^5\text{-}C_5(CH_3)_5)Fe(CO)_2R]$

Assignments	Relative peak intensities for compounds **3** to **12**									
	3	**4**	**5**	**6**	**7**	**8**	**9**	**10**	**11**	**12**
Parent, *M*	63	7	2	15	5	19	8	7	9	5
M - CO	---	17	17	20	18	---	30	19	18	8
M - 2CO	---	2	---	3	---	---	24	---	---	---
M - 2CO - H	---	22	17	20	21	---	---	24	37	27
M - 2CO - 2H	---	92	100	100	100	---	100	100	100	100
M - 2CO - 4H	---	8	7	17	22	---	---	---	---	25
M - 2CO - 6H	---	---	16	28	40	---	---	---	---	27
$Cp^*Fe(CO)H$	---	5	4	6	7	---	13	---	9	8
Cp^*FeH	---	7	4	5	6	---	---	---	5	4
Cp^*Fe - H	---	100	96	50	66	---	32	48	50	39
Cp^* - 2H	100	26	22	23	27	100	25	25	8	17
C_3H_7	---	---	9	5	45	54	---	25	14	18
CO	100	---	---	21	9	---	7	100	100	9

2.2.2. Mononuclear alkyl compounds $[(\eta^5\text{-}C_5H_5)Fe(CO)_2(CH_2)_{17}CH_3]$, $[(\eta^5\text{-}C_5H_5)Fe(CO)_2CH_3]$, $[(\eta^5\text{-}C_5H_5)Fe(CO)_2CH_2CH_3]$ and $[(\eta^5\text{-}C_5H_5)Fe(CO)_2(CH_2)_5CH_3]$

$[(\eta^5\text{-}C_5H_5)Fe(CO)_2(CH_2)_{17}CH_3]$, **13**, is an extension of a series of long chain alkyl compounds prepared previously in our laboratory [94]. It was prepared by the reaction of $Br(CH_2)_{17}CH_3$ with the $[(\eta^5\text{-}C_5H_5)Fe(CO)_2]^-$ anion (Equation 2.2). The compound was obtained as a waxy yellow solid which, in contrast to the other members of the series ($-CH_3$ to $n\text{-}C_{12}H_{25}$), is stable in air in the dark for several months with only surface decomposition. This stability may be due to the solid waxy nature of the compound protecting it from oxidation by the air, although the role of oxidation as a decomposition pathway seems unclear (See Section 2.3.2). The IR spectra in the υ(CO) region, taken in hexane solution, is in excellent agreement with the values reported for

$[(\eta^5\text{-}C_5H_5)Fe(CO)_2R]$ compounds [94]. The two υ(CO) bands occur at 2008 and 1954 cm^{-1} respectively and are very strong. The ^1H NMR spectrum shows peaks at δ = 0.89 (s, CH_3), 1.26 (bs, $(\text{-}CH_2\text{-})_{16}$), 1.44 (t, J = 6.5 Hz, Fe-CH_2-) and corresponds well with values reported for $[(\eta^5\text{-}C_5H_5)Fe(CO)_2R]$ compounds [94]. The mass spectrum showed a peak for the molecular ion at m/e = 430, and the elemental analysis gave the results consistent with the calculated values, which are given in parentheses: C 69.5 (69.76), H 9.6 (9.83).

$[(\eta^5\text{-}C_5H_5)Fe(CO)_2CH_3]$, **14**, $[(\eta^5\text{-}C_5H_5)Fe(CO)_2CH_2CH_3]$, **15**, and $[(\eta^5\text{-}C_5H_5)Fe(CO)_2(CH_2)_5CH_3]$, **16**, have been prepared previously [17,94]. They were prepared here in the same way as **13** (Equation 2.2). The compound **14**, is a yellow/orange solid, and compounds **15** and **16** are yellow oils which decompose easily in air and when exposed to light. They are moderately stable in solution in the dark, under nitrogen.

2.2.3. Mononuclear acyl compound $[(\eta^5\text{-}C_5H_5)Fe(CO)_2(C(O)CH_2R)]$, R = H, CH_3

The mononuclear acyl compounds $[(\eta^5\text{-}C_5R_5)Fe(CO)_2C(O)R]$ are the direct products of alkyl migration reaction in the presence of CO. $[(\eta^5\text{-}C_5H_5)Fe(CO)_2(C(O)CH_3)]$, **17**, was prepared previously [38] by reaction of $[(\eta^5\text{-}C_5H_5)Fe(CO)_2(CH_3)]$ with CO, as shown in Equation 2.3.

$$[(C_5H_5)Fe(CO)_2CH_3] \xrightarrow{CO,\ 2000PSI,\ 125\ ^oC} [(C_5H_5)Fe(CO)_2C(O)CH_3] \qquad (2.3)$$

An alternative to this synthesis is reaction of the strong nucleophile $Na[(\eta^5\text{-}C_5R_5)Fe(CO)_2]$ with the appropriate acid halide (RC(O)X, X=Cl, Br or I), as shown in Equation 2.4.

$$Na[(\eta^5\text{-}C_5H_5)Fe(CO)_2] + RC(O)X \longrightarrow [(\eta^5\text{-}C_5H_5)Fe(CO)_2C(O)R] + NaX \qquad (2.4)$$

$[(\eta^5\text{-}C_5H_5)Fe(CO)_2(COCH_3)]$, **17**, was prepared by allowing $Na[(\eta^5\text{-}C_5H_5)Fe(CO)_2]$ to react with CH_3COCl (Equation 2.4) and $[(\eta^5\text{-}C_5H_5)Fe(CO)_2(COCH_2CH_3)]$, **18**, was prepared by reaction

of $[(\eta^5\text{-}C_5H_5)Fe(CO)_2(CH_2CH_3)]$, **15**, with CO (500 PSI[a], 80°C) (Equation 2.3). There was no decomposition of the starting material, $[(\eta_5\text{-}C_5H_5)Fe(CO)_2(CH_2CH_3)]$, **15**, detected in the reaction. It is interesting to note that attempts to carry out this reaction at atmospheric pressure and 90-100°C failed [24].

Compound **17** was obtained as a yellow/orange solid and compound **18** as a yellow/orange oil. The compounds are reasonably stable thermally, in air, and to light (more so than their alkyl analogues). In solution they are stable under nitrogen, but decompose within hours on exposure of the solution to air.

2.3. Reactions

A number of reactions were carried out on the alkyl compounds synthesised. These reactions on the long chain alkyl compounds were intended to test reactions of catalytic significance, which were already known for short chain alkyl compounds, $[(\eta^5\text{-}C_5H_5)Fe(CO)_2R]$. The products of the reactions were thus not all fully characterized. The reactions chosen are all reactions which involve the metal alkyl bond and thus could be of relevance as model reactions involving metal alkyl species.

2.3.1. Reaction of $[(\eta^5\text{-}C_5(CH_3)_5)Fe(CO)_2(CH_2)_6CH_3]$ with $[Ph_3C]^+[PF_6]^-$

Reaction of the alkyl compound, $[(\eta^5\text{-}C_5H_5)Fe(CO)_2(CH_2)_6CH_3]$ with trityl salt $[Ph_3C]^+[PF_6]^-$ results in the abstraction of H^- from the β-carbon of the alkyl chain. The alkyl rearranges to form a co-ordinated alkene salt, $[(\eta^5\text{-}C_5H_5)Fe(CO)_2(CH_2{=}CH(CH_2)_3CH_3]^+[PF_6]^-$, **19**. It is possible that the formation of α-olefins in the Fischer-Tropsch reaction may occur through reaction of a gas phase species, such as $[CH_3]^+$, which abstracts $[H]^-$ causing formation a co-ordinated alkene which can desorb from the surface of the catalyst giving the α-olefin. Molecular modelling calculations for this reaction are presented in Chapter 4.

---

[a]1 kPa = 6.895 Pounds per Square Inch (PSI).

2.3.2. *Reaction of $[(\eta^5\text{-}C_5H_5)Fe(CO)_2CH_2CH_3]$ with air in the presence of PPh_3*

The instability of $[(\eta^5\text{-}C_5H_5)Fe(CO)_2R]$ compounds, especially in solution, has been recognized since these type of compounds were first synthesized [17]. The reason for this instability however has not been fully explained. The compound $[(\eta^5\text{-}C_5H_5)Fe(CO)_2CH_2CH_3]$ is particularly unstable, and if not handled with great care in solution will quickly show signs of decomposition and the formation of $[(\eta^5\text{-}C_5H_5)Fe(CO)_2]_2$. The purpose of this experiment was to expose the compound $[(\eta^5\text{-}C_5H_5)Fe(CO)_2CH_2CH_3]$ in solution to oxygen, by bubbling air through the solution, in the presence of an excess of PPh_3. The PPh_3, as a coordinating ligand, could occupy any vacant co-ordination site created through the dissociation of a CO ligand.

The exposure of $[(\eta^5\text{-}C_5H_5)Fe(CO)_2CH_2CH_3]$, **15**, in a THF solution in the presence of PPh_3 to air did not result in decomposition to the iron dimer $[(\eta^5\text{-}C_5H_5)Fe(CO)_2]_2$ even after 24 hours. A small amount of $[(\eta^5\text{-}C_5H_5)Fe(CO)(PPh_3)(C(O)CH_2CH_3)]$, **20**, was detected, but most of the starting material remained unreacted. This seems to suggest that the CO ligands and the vacant co-ordination site created by dissociation of one of these ligands plays a significant role in the stability of these compounds. This is further indicated by the observation in Section 2.2.3 that no decomposition of **15** was observed during reaction in THF solution with CO at elevated temperatures and pressures. THF is a co-ordinating solvent which increases the rate of carbonylation [39], and may also play a role in stabilizing an unsaturated species formed through the dissociation of CO. The formation of **20** through a carbonylation reaction is expected as this reaction is known to occur in refluxing THF or acetonitrile, and is a common method of synthesis of **20** [39-41].

2.3.3. *Reaction of $[(\eta^5\text{-}C_5H_5)Fe(CO)_2(CH_2)_{17}CH_3]$ with Sulfur*

In the Fischer-Tropsch reaction the presence of even small quantities of sulfur is known to quickly deactivate the catalyst, and is the reason for its thorough removal from the carbon monoxide and hydrogen (syngas) feedstock. The cause of deactivation is believed to be the blocking of the active sites on the catalyst by the sulfur. A further mode of deactivation may be owing to the reaction of sulfur with alkyl species on the catalyst surface to form stable species which then block the active site on the catalyst. Sulfur has been shown to inset into short chain

alkyl species [97]. The reaction of $[(\eta^5\text{-}C_5H_5)Fe(CO)_2(CH_2)_{17}CH_3]$, **13**, with sulfur confirms that this insertion does occur, resulting in the formation of a new compound $[(\eta^5\text{-}C_5H_5)Fe(CO)_2(SC(O)(CH_2)_{17}CH_3)]$, **21** which is a blackish crystalline compound (mp. 48-50 °C) that is stable in air. The mechanism proposed for this reaction is the migratory insertion of a carbonyl with the alkyl ligand, followed by insertion of sulfur into the iron-carbon bond. Disproportionation results in replacement of the carbonyl ligand.

The infrared spectrum of **21** reveals two carbonyl bands at ν(CO) 2042 and 1995 cm^{-1} and a band for the SC(O) group at ν(C(O)) 1620 cm^{-1} in dichloromethane. This compares well with the bands observed for $[(\eta^5\text{-}C_5H_5)Fe(CO)_2(SC(O)CH_3)]$ which occur at 2044, 1996, and 1629 in $CDCl_3$ [97]. The ^1H and ^{13}C NMR spectra showed resonances which were assigned by comparison to the short chain compound [97]. ^1H NMR ($CDCl_3$) 4.98 (s, 5H (Cp)), 2.67 (t, J=7.6 Hz, 2H (-C(O)CH_2-)), 1.24 (m, 32H (-$(CH_2)_{16}$-)), 0.88 (t, J=6.8Hz, 3H (-CH_3)). ^{13}C NMR ($CDCl_3$) 212.06 (2 x CO), 85.00 (Cp), 47.09 (C(O)$\underline{C}H_2$-), 31.93, 29.67, 29.66, 29.622, 29.50, 29.42, 29.36, 29.05, 26.96 (15 x -CH_2-), 22.69 (-$\underline{C}H_2$Me), 14.11 (-CH_3). No ^{13}C NMR resonance was observed for C(O) expected at 205ppm. The 15 'middle' carbons of the alkyl chain could not be distinguished from each other from this spectrum.

2.4. Experimental

Unless otherwise stated, all reactions were carried out under nitrogen using standard Schlenk tube techniques. Tetrahydrofuran (THF) was distilled from sodium before use. The alkyl halides were obtained from the suppliers shown, with % purity in parentheses: n-C_3H_5Br (99), n-$C_5H_{11}Cl$ (99), n-$C_6H_{13}Cl$ (99), n-$C_7H_{15}Cl$ (99), n-$C_8H_{17}Br$ (99), n-$C_9H_{19}Br$ (98), n-$C_{11}H_{23}Br$ (99) from Aldrich; n-C_4H_9Br (99) from Riedel-de Haën; n-$C_{10}H_{21}Br$ (98) from Merck and n-$C_{12}H_{25}Br$ from Sigma. $[CpFe(CO)_2]_2$ and $[Cp^*Fe(CO)_2]_2$ were obtained from Strem.

Alumina (BDH, active neutral, Brockman grade 1) was deactivated before use. Melting points were recorded on a Kofler hot-stage microscope (Reichert Thermovar) and are uncorrected. Microanalyses were performed by the University of Cape Town Microanalytical Laboratory. Infrared spectra were recorded on a Perkin-Elmer 983 spectrophotometer. ^1H NMR and ^{13}C NMR

spectra were recorded either on a Varian XR 200 or a Varian Unity-400 spectrometer. Low resolution mass spectra were recorded with a VG Micromass 16F spectrometer, operating at 70 eV ionising voltage. The source temperature was raised from room temperature until the spectrum was observed.

2.4.1. Synthesis of $[(\eta^5\text{-}C_5(CH_3)_5)Fe(CO)_2R]$ Compounds

The synthesis of all $[(\eta^5\text{-}C_5(CH_3)_5)Fe(CO)_2R]$ compounds, R = $\text{-}C_3H_7$ to $\text{-}C_{12}H_{23}$, was conducted by the same method. This method is described below for the compound $[(\eta^5\text{-}C_5(CH_3)_5)Fe(CO)_2(CH_2)_4CH_3]$ of the series.

A Na/Hg amalgam was prepared using 0.2g Na in 2ml Hg in a Schlenk tube under nitrogen. After the amalgam had cooled to room temperature 5ml of dry tetrahydrofuran (THF) was added. A sample of 0.512g (1.036 mmol) $[(\eta^5\text{-}C_5(CH_3)_5)Fe(CO)_2]_2$ was added followed by 10 ml of dry THF, washing any remaining $[(\eta^5\text{-}C_5(CH_3)_5)Fe(CO)_2]_2$ down the side of the tube into the solution. The red/black mixture was left stirring under nitrogen for 24 hours.

The solution was allowed to stand under nitrogen for a few minutes to allow the mercury amalgam to settle. The $[Na][(\eta^5\text{-}C_5(CH_3)_5)Fe(CO)_2]$ salt formed was syringed across slowly over ten minutes to a Schlenk tube containing 0.20 ml (0.177g, 1.66 mmol) $Cl(CH_2)_4CH_3$ under nitrogen at 0° C (ice bath). The $[Na][(\eta^5\text{-}C_5(CH_3)_5)Fe(CO)_2]$ salt was added in excess (1.67 mmol at 80% conversion of the $[(\eta^5\text{-}C_5(CH_3)_5)Fe(CO)_2]_2$ dimer) to avoid separation of alkyl halide from the product at the end of the reaction. The solution was stirred for four hours, during which time the solution was allowed to attain room temperature. The solvent, THF, was then removed under reduced pressure. The compound was loaded onto a column of deactivated alumina (Al_2O_3), 7cm in length and eluted with hexane. The yellow fraction was collected and the infrared spectrum recorded between 2200 cm^{-1} and 1500 cm^{-1} (ν(CO) = 1987 cm^{-1} (vs), 1933 cm^{-1} (vs)). The solvent, hexane, was removed under reduced pressure and the compound dried for 1 hour under high vacuum (<0.5 mm Hg). The compound, $[(\eta^5\text{-}C_5(CH_3)_5)Fe(CO)_2(CH_2)_4CH_3]$, was weighed giving a yield of 0.487g (1.54 mmol, 93%) of pure product. Samples were taken of the product in order to measure the ^1H and ^{13}C NMR, the mass spectrum, and the C, H, O percentages by microanalysis. The compound was stored in the dark at -10° C under nitrogen.

2.4.2. *Synthesis of $[(\eta^5\text{-}C_5H_5)Fe(CO)_2(CH_2)_{17}CH_3]$ and $[(\eta^5\text{-}C_5H_5)Fe(CO)_2CH_2CH_3]$*

The synthesis of $[(\eta^5\text{-}C_5H_5)Fe(CO)_2(CH_2)_{17}CH_3]$ and $[(\eta^5\text{-}C_5H_5)Fe(CO)_2CH_2CH_3]$ were by the same method, using the same reaction times and conditions. Thus only the experimental procedure for one of the compounds is given below.

A Na/Hg amalgam was prepared using 0.35g Na in 3.5 ml Hg in a Schlenk tube under nitrogen. After the amalgam had cooled to room temperature 5ml of dry tetrahydrofuran (THF) was added. A sample of 1.136g (3.21 mmol) $[(\eta^5\text{-}C_5H_5)Fe(CO)_2]_2$ was added followed by 10 ml of dry THF, washing any remaining $[(\eta^5\text{-}C_5H_5)Fe(CO)_2]_2$ down the side of the tube into the solution. The red/black mixture was left stirring under nitrogen for 12 hours.

The solution was allowed to stand under nitrogen for a few minutes to allow the mercury amalgam to settle. The $[Na][(\eta^5\text{-}C_5H_5)Fe(CO)_2]$ salt formed was syringed across slowly over ten minutes to a Schlenk tube containing1.709g (5.13 mmol) $Br(CH_2)_{17}CH_3$ under nitrogen at 0° C (ice bath). The $[Na][(\eta^5\text{-}C_5H_5)Fe(CO)_2]$ salt was added in excess (5.14 mmol at 80% conversion of the $[(\eta^5\text{-}C_5H_5)Fe(CO)_2]_2$ dimer) to ensure complete reaction of alkyl halide, and thus avoid separation of the alkyl halide from the product at the end of the reaction. The solution was stirred for four hours, during which time the solution was allowed to attain room temperature. The solvent, THF, was then removed under reduced pressure. The compound was loaded onto a column of deactivated alumina (Al_2O_3), 7cm in length and eluted with hexane. The yellow fraction was collected and the infrared spectrum recorded between 2200 cm^{-1} and 1500 cm^{-1} (ν(CO) = 2008 cm^{-1} (vs), 1954 cm^{-1} (vs)). The solvent, hexane, was removed under reduced pressure and the compound (a waxy solid) dried for 1 hour under high vacuum (<0.5 mm Hg). The compound, $[(\eta^5\text{-}C_5H_5)Fe(CO)_2(CH_2)_{17}CH_3]$, was weighed giving a yield of 1.859g (4.32 mmol, 84%) of pure product. Samples were taken of the product in order to measure the ^1H and ^{13}C NMR, the mass spectrum, and the C, H, O percentages by microanalysis. The compound was stored in the dark at -10° C under nitrogen, although it appeared to be stable in air at room temperature.

2.4.3. *Synthesis of* $[(\eta^5\text{-}C_5H_5)Fe(CO)_2(C(O)CH_3)]$

A Na/Hg amalgam was prepared using Na (0.65g) in Hg (5 ml) in a Schlenk tube under nitrogen. After the amalgam had cooled to room temperature 10ml of dry tetrahydrofuran (THF) was added. A sample of $[(\eta^5\text{-}C_5H_5)Fe(CO)_2]_2$ (2.048g, 5.78 mmol) was added followed by 10 ml of dry THF, washing any remaining $[(\eta^5\text{-}C_5H_5)Fe(CO)_2]_2$ down the side of the tube into the solution. The red/black mixture was left stirring under nitrogen for 4 hours.

The solution was allowed to stand under nitrogen for a few minutes to allow the mercury amalgam to settle. The $[(\eta^5\text{-}C_5H_5)Fe(CO)_2]^-$ anion formed was syringed across slowly over ten minutes to a Schlenk tube containing 0.86 ml (0.91g, 12 mmol) $CH_3C(O)Cl$ under nitrogen at 0° C (ice bath). The acetyl chloride was added in slight excess. The solution was stirred for 3 hours 15 minutes, during which time the solution was allowed to attain room temperature. The solvent, THF, was then removed under reduced pressure. The compound was dissolved in a small amount of dichloromethane (CH_2Cl_2) and filtered and the IR spectrum recorded between 2200 cm^{-1} and 1500 cm^{-1} (ν(CO) = 2019 cm^{-1} (vs), 195 cm^{-1} (vs), ν(C(O)) = 1647 cm^{-1} (s)). The solvent was removed and the coumpound loaded onto a column of silica (SiO_2), 11cm in length and eluted with 1:1 hexane:diethyl ether. The orange/yellow fraction was collected and the solvent was removed under reduced pressure. The compound, $[(\eta^5\text{-}C_5H_5)Fe(CO)_2(C(O)CH_3)]$,(a brittle solid) was dried for 1 hour under high vacuum (<0.5 mm Hg). The pure compound was weighed giving a yield of 1.859g (8.45 mmol, 73%) of product. Samples were taken of the product in order to measure the ^1H and ^{13}C NMR, the mass spectrum, and the C, H, O percentages by microanalysis. The compound was stored in the dark at -10° C under nitrogen, although it is stable in air at room temperature for a number of days.

2.4.4. *Synthesis of* $[(\eta^5\text{-}C_5H_5)Fe(CO)_2(C(O)CH_2CH_3)]$

A sample of $[(\eta^5\text{-}C_5H_5)Fe(CO)_2CH_2CH_3]$, 1.014g (4.92 mmol), was weighed out and placed in a small beaker and dissolved in 15ml of dry THF. The beaker was placed in an autoclave which was flushed three times with carbon monoxide (CO) before being charged to pressure. The temperature was raised to 80°C with the pressure reaching 500 PSI. The reaction mixture was stirred for 7 hours, after which the autoclave was allowed to cool to room temperature over two

hours. The solvent was removed under reduced pressure, and the crude product loaded on to a silica (SiO_2) column 10cm in length. The column was eluted with 1:1 hexane : diethyl ether, and the yellow/orange fraction collected. An infrared (IR) spectrum was recorded between 2200 cm^{-1} and 1500 cm^{-1} (ν(CO) = 2019 cm^{-1} (vs), 1959 cm^{-1} (vs), ν(C(O)) = 1646 cm^{-1} (s)). The pure compound, $[(\eta^5\text{-}C_5H_5)Fe(CO)_2(C(O)CH_2CH_3)]$,(an oil) was dried for 2.5 hours under high vacuum (<0.5 mm Hg) and weighed, 1.002g, 4.28 mmol, 87% yield. The compound was stored in the dark at -10° C under nitrogen.

2.4.5. Reaction of $[(\eta^5\text{-}C_5(CH_3)_5)Fe(CO)_2(CH_2)_6CH_3]$ with $[Ph_3C]^+[PF_6]^-$

A sample of $[(\eta^5\text{-}C_5(CH_3)_5)Fe(CO)_2(CH_2)_6CH_3]$ (0.090g , 0.26 mmol) was placed in a Schlenk tube under nitrogen. To this was added 15ml of dry THF, and 0.18g (0.46 mmol), a 1.5 times excess, of $[Ph_3C]^+[PF_6]^-$ and the reaction mixture stirred for three hours. An infrared spectrum was recorded between 1500 and 2200 cm^{-1}, and the solvent removed leaving a greeny residue. The residue was dissolved in dry acetone, filtered and the solution concentrated by blowing off some of the solvent with nitrogen. A small amount of diethyl ether was added to the solution causing a yellow precipitate to form. The solution was cooled in ice and the precipitate filtered on a Hirsh funnel and washed with cold dry acetone. The precipitate was dried under high vacuum (<0.5mm Hg) and weighed, 0.091g, 0.19 mmol, giving a yield of 72%.

2.4.6. Reaction of $[(\eta^5\text{-}C_5H_5)Fe(CO)_2CH_2CH_3]$ with air in the presence of PPh_3

A sample of $[(\eta^5\text{-}C_5H_5)Fe(CO)_2CH_2CH_3]$ (0.1g, 0.5 mmol) was placed in a Schlenk tube under nitrogen and light excluded from the tube with aluminium foil. A five times excess of PPh_3 (0.6g, 2.3 mmol) was dissolved in dry THF and added to the Schlenk tube containing the $[(\eta^5\text{-}C_5H_5)Fe(CO)_2CH_2CH_3]$. Air was bubbled through the solution which was monitored by infrared spectroscopy. After several hours there was no sign of reaction occurring or of decomposition of $[(\eta^5\text{-}C_5H_5)Fe(CO)_2CH_2CH_3]$. After 24 hours there was still no sign of a reaction or of decomposition. The solvent was removed by reduced pressure from the reaction mixture and the mixture extracted with hexane. The hexane solution was concentrated on a rotary evaporator and the residue placed on a column (7 cm) of deactivated alumina (Al_2O_3) and eluted with hexane. Two bands were observed consisting of a major yellow band identified by infrared

spectroscopy as the starting material [$(\eta^5$-$C_5H_5)Fe(CO)_2CH_2CH_3$], and a very minor band (<10%) which exhibited an infrared spectrum consistent with the compound [$(\eta^5$-$C_5H_5)Fe(CO)(PPh_3)C(O)CH_2CH_3$].

2.4.7. Reaction of [$(\eta^5$-$C_5H_5)Fe(CO)_2(CH_2)_{17}CH_3$] with Sulfur

A sample of [$(\eta^5$-$C_5H_5)Fe(CO)_2(CH_2)_{17}CH_3$] (0.201g, 0.47 mmol) was placed in a Schlenk tube under nitrogen. An slight excess of sulfur (0.022g, 0.69 mmol) was added to the Schlenk tube and mixed with the [$(\eta^5$-$C_5H_5)Fe(CO)_2(CH_2)_{17}CH_3$]. The mixture was heated in a paraffin bath to 100°C for one hour. After five minutes of heating the melt turned black. The mixture was allowed to cool and was extracted with dry acetone, filtered and the acetone removed under reduced pressure. The residue was loaded onto a 8 cm column of deactivated alumina (Al_2O_3) and eluted with 1:1 petroleum ether: diethyl ether. Two fractions were collected. The first fraction was identified by infrared spectroscopy as being the starting compound [$(\eta^5$-$C_5H_5)Fe(CO)_2(CH_2)_{17}CH_3$] (ν(CO) 2000 and 1939 cm^{-1} in $CHCl_3$). The second fraction was identified as [$(\eta^5$-$C_5H_5)Fe(CO)_2(SC(O)(CH_2)_{17}CH_3)$] (ν(CO) 2042 and 1995 cm^{-1} and ν(C(O)) 1620 cm^{-1} in CH_2Cl_2). The solvent was removed from this fraction, and the compound placed under high vacuum (<0.5 mm Hg) for 2.5 hours. The compound was weighed (0.050g, 0.10 mmol) giving a yield of 22%. The compound was submitted for ^1H and ^{13}C NMR, mass spectrometry, and determination of the C, H, O percentages by microanalysis. However, the mass spectrum did not yield an identifiable spectrum and the microanalysis was inconclusive. The melting point of the compound was determined to be 48-50 °C, with decomposition following at 132 °C.

2.5. References

1. Ewen, J. *J. Am. Chem. Soc.* **1984**, *106*, 6355.
2. Wilkinson, G.; Brown, C. K. *J. Chem. Soc. A* **1970**, *1392*, 2753.
3. Busby, D. C.; Wegman, R. W. *J. Chem. Soc., Chem. Commun.* **1986**, 332.
4. Parshall, G. W.; Ittel, S. D. *Homogeneous Catalysis*; 2nd ed.; John Wiley & Sons:, 1992.
5. Keim, W.; Hirose, K. *J. Mol. Cat.* **1992**, *73*, 271.
6. Keim, W.; Schulz, R. P. *J. Mol. Cat.* **1994**, *92*, 21.
7. Raubenheimer, H. G.; Meyer, W. H.; Brull, R. *S. Afr. J. Chem.* **1998**, *51*, 73.
8. Vrieze, K.; Elsevier, C. J.; Dekker, G. P. C. M.; Van Leeuwen, P. W. N. M.; Roobeek, C. F. *J. Organomet. Chem.* **1992**, *430*, 357.
9. Daniel, C.; Fu, X. Y.; Han, J.; Koga, N.; Morokuma, K. *J. Am. Chem. Soc.* **1988**, *110*, 3773.
10. Herrmann, W. A.; Fischer, R. W.; Rauch, M. U.; Scherer, W. *J. Mol. Cat.* **1994**, *86*, 243.
11. Rofer-DePoorter, C. K. *Chem. Rev.* **1981**, *81*, 447.
12. Moss, J. R. *J. Mol. Cat. A* **1996**, *107*, 169.
13. Johnson, M. D., *Mononuclear Iron Compounds with η^1-Hydrocarbon Ligands*, in *Comprehensive Organometallic Chemistry - Synthesis Reactions and Structures of Organometallic Compounds*; Wilkinson, G., Stone, F. G. A. and Abel, E. W., Ed.; Comprehensive Organometallic Chemistry, Pergamon Press: Oxford, 1982; Vol. 4, pp 331.
14. Yamamoto, A. *J. Organomet. Chem.* **1986**, *300*, 347.
15. Rosenblum, M. *J. Organomet. Chem.* **1986**, *300*, 191.
16. Kerber, R. C., *Mononuclear Iron Compounds with η^1-η^6 Hydrocarbon Ligands*, in *Comprehensive Organometallic Chemistry II - A Review of the Literature 1982 - 1995*; Shriver, P. F. and Bruce, M. I., Ed.; Comprehensive Organometallic Chemistry II, Abel, E. W., Stone, F. G. A. and Wilkinson, G., Pergamon Press - Elsevier Science Ltd: Oxford, 1995; Vol. 7, pp 101.
17. Piper, T. S.; Wilkinson, G. *J. Inorg. Nucl. Chem.* **1956**, *3*, 104.
18. Clifford, A. F.; Mukherjee, A. K. *J. Inorg. Nucl. Chem.* **1963**, *25*, 1065.
19. Florio, S. M.; Nicholas, K. M. *J. Organomet. Chem.* **1976**, *112*, C17.
20. King, R. B.; Douglas, W. M.; Efraty, A. *J. Organomet. Chem.* **1974**, *69*, 131.
21. King, R. B.; Bisnette, M. B. *J. Organomet. Chem.* **1964**, *2*, 15.
22. Marks, T. J.; Kristoff, J. S.; Alich, A.; Shriver, D. F. *J. Organomet. Chem.* **1971**, *33*, C35.

23. Norton, J. R.; Jordan, R. F. *J. Am. Chem. Soc.* **1979**, *101*, 4853.
24. Treichel, P. M.; Shubkin, R. L.; Barnett, K. W.; Reichard, D. *Inorg. Chem.* **1966**, *5*, 1177.
25. Alt, H. G.; Herberhold, M.; Rausch, M. D.; Edwards, B. H. *Z. Naturforsch* **1979**, *34B*, 1070.
26. Treichel, P. M.; Komar, D. A. *J. Organomet. Chem.* **1981**, *206*, 77.
27. Green, M. L. H.; Wong, L.-L. *J. Chem. Soc., Chem. Commun.* **1984**, 1442.
28. Green, M. L. H.; Wong, L.-L. *J. Chem. Soc., Dalton Trans.* **1987**, 411.
29. Crabtree, R. H., *General Properties of Organometallic Complexes*, in *The Organometallic Chemistry of the Transition Metals*, 1st ed., John Wiley & Sons, Inc.: Singapore, 1988, pp 20.
30. Hoffmann, R.; Lichtenberger, D. L.; Schilling, B. E. R. *J. Am. Chem. Soc.* **1979**, *101*, 585.
31. Fenske, R. F.; Lichtenberger, D. L. *J. Am. Chem. Soc.* **1976**, *98*, 50.
32. Symon, D. A.; Waddington, T. C. *J. Chem. Soc., Dalton Trans.* **1975**, 2140.
33. Green, J. C.; Jackson, S. E. *J. Chem. Soc., Dalton Trans.* **1976**, 1698.
34. Davies, S. G.; Seeman, J. I. *J. Chem. Soc., Chem. Commun.* **1984**, 1019.
35. Davies, S. G.; Seeman, J. I. *J. Am. Chem. Soc.* **1985**, *107*, 6522.
36. Brown, S. L.; Davies, S. G.; Foster, D. F.; Seeman, J. I.; Warner, P. *Tetrahedron Let.* **1986**, *27*, 623.
37. Calderazzo, F.; Noack, K. *J. Organomet. Chem.* **1967**, *10*, 101.
38. Coffield, T. H.; Kozikowski, J.; Closson, R. D. *Alkyl, Aryl, and Acyl Metal Carbonyl Compounds*; Chemical Society: London, 1959; Vol. Special Publication 13, pp 126.
39. Bibler, J. P.; Wojcicki, A. *Inorg. Chem.* **1966**, *5*, 889.
40. Basolo, F.; Butleere, I. S.; Pearson, R. G. *Inorg. Chem.* **1967**, *6*, 2074.
41. Green, M.; Westlake, D. J. *J. Chem. Soc. A* **1971**, 367.
42. Reger, D. L.; Mintz, E.; Lebioda, L. *J. Am. Chem. Soc.* **1986**, *108*, 1940.
43. Giering, W. P.; Magnuson, R. H.; Meirowitz, R.; Zulu, S. J. *Organometallics* **1983**, *2*, 460.
44. Chang, R.; Chen, J.; Eriks, K.; Giering, W. P.; Greene, J. E.; Hoffman, S. L.; Magnuson, R. H.; Meirowitz, R. E.; Prock, A.; Wilson, M.; Woska, D. C. *Organometallics* **1991**, *10*, 3479.
45. Cotton, J. D.; Crisp, G. T.; Latif, L. *Inorg. Chim. Acta* **1981**, *47*, 171.
46. Moss, J. R.; Andersen, J.-A. M. *Organometallics* **1994**, *13*, 5013.
47. Moss, J. R.; Andersen, J.-A. M.; George, R. *J. Organomet. Chem.* **1995**, *505*, 131.
48. Cutler, A. R.; Forschner, T. C. *Organometallics* **1985**, *4*, 1247.

49. Moran, M.; Pascual, C.; Cuadrado, I.; Masaguer, J. R.; Losada, J. *J. Organomet. Chem.* **1989**, *363*, 157.
50. Flood, T. C.; Campbell, K. D.; Downs, H. H.; Nakanishi, S. *Organometallics* **1983**, *2*, 1590.
51. Campbell, K. D.; Flood, T. C. *J. Am. Chem. Soc.* **1984**, *106*, 2853.
52. Bernal, I.; Brunner, H.; Hammer, B.; Draux, M. *Organometallics* **1983**, *2*, 1595.
53. Davies, S. G.; Cooke, J. W. B.; Naylor, A. *Tetrahedron* **1993**, *49*, 7955.
54. Davies, S. G.; Baker, T. M.; Bodwell, G. J.; Edwards, A. J.; Metzler, M. R. *Tetrahedron* **1993**, *49*, 5635.
55. Davies, S. G.; Beckett, R. P.; Mortlock, A. A. *Tet. Asym.* **1992**, *3*, 123.
56. Patel, P. P.; Welker, M. E. *J. Organomet. Chem.* **1997**, *547*, 103.
57. Geoffroy, G. L.; Han, S. H.; Sheridan, J. B. *J. Am. Chem. Soc.* **1987**, *109*, 8097.
58. Brown, S. L.; Davies, S. G. *J. Chem. Soc., Chem. Commun.* **1986**, 84.
59. De Luca, N.; Wojcicki, A. *J. Organomet. Chem.* **1980**, *193*, 359.
60. Flood, T. C.; Miles, D. L. *J. Organomet. Chem.* **1977**, *127*, 33.
61. Mapolie, S. F.; Moss, J. R. *J. Chem. Soc., Dalton Trans.* **1990**, 299.
62. Thomas, J. M.; Thomas, W. J., *Fischer-Tropsch Catalysis*, in *Principles and Practice of Heterogeneous Catalysis*, 1st ed., VCH Verlagsgesellschaft mbH: Weinheim, 1996, pp 524.
63. Waddacor, M. *Chem. Proc. SA* **1994**, 2.
64. Green, M. L. H.; Nagy, P. L. I. *J. Organomet. Chem.* **1963**, *1*, 58.
65. Ikariya, T.; Yamamoto, A. *J. Organomet. Chem.* **1976**, *120*, 257.
66. Brainard, R. L.; Whitesides, G. M. *Organometallics* **1985**, *4*, 1550.
67. Brookhart, M.; Lincoln, D. M. *J. Am. Chem. Soc.* **1988**, *110*, 8719.
68. Alibrandi, G.; Minniti, D.; Romeo, R.; Scolaro, L. M. *Inorg. Chem.* **1990**, *29*, 3467.
69. Kakyaki, Y.; Kawataka, F.; Shimizu, I.; Yamamoto, A. *Organometallics* **1994**, *13*, 3517.
70. Keister, J. W.; Parsons, E. J. *J. Organomet. Chem.* **1995**, *487*, 23.
71. Sterling, G. P.; Wegner, P. A. *J. Organomet. Chem.* **1978**, *162*, c31.
72. Mahmoud, K. A.; Rest, A. J.; Alt, H. G. *J. Chem. Soc., Dalton Trans.* **1985**, 1365.
73. Barnhart, T. M.; Bartz, J. A.; Crim, F. F.; Galloway, D. B.; Glenewinkel-Meyer, T.; Huey, L. G.; McMahon, R. J. *J. Am. Chem. Soc.* **1993**, *115*, 8389.
74. Culbertson, E. C.; Reger, D. L. *J. Am. Chem. Soc.* **1976**, *98*, 2789.
75. Culbertson, E. C.; Reger, D. L. *Inorg. Chem.* **1977**, *16*, 3104.

76. Paulson, P. L., *Organo-iron Compounds*, in *Chemistry of Iron*; Silver, J., Ed., Blackie Academic & Professional: London, 1993, pp 106.
77. Collman, J. P. *Acc. Chem. Res.* **1975**, 342.
78. Collman, J. P.; Siegl, W. O. *J. Am. Chem. Soc.* **1972**, *94*, 2516.
79. Collman, J. P.; Winter, S. R. *J. Am. Chem. Soc.* **1973**, *95*, 4089.
80. King, R. B.; Stafford, S. L.; Stone, F. G. A.; Treichel, P. M. *J. Am. Chem. Soc.* **1961**, *83*, 3604.
81. Devasagayaraj, A.; Periasamy, M. *Trans. Met. Chem.* **1991**, *16*, 503.
82. King, R. B. *J. Am. Chem. Soc.* **1963**, *85*, 1918.
83. Ingletto, G.; Tondello, E.; Di Sipio, L.; Carturan, G.; Graziani, M. *J. Organomet. Chem.* **1973**, *56*, 335.
84. Weber, L. *J. Organomet. Chem.* **1976**, *122*, 69.
85. King, R. B. *J. Am. Chem. Soc.* **1968**, *90*, 1417.
86. Kuhlmann, E. J.; Alexander, J. J. *Inorg. Chim. Acta* **1979**, *34*, L193.
87. Hooker, R. H.; Rest, A. J.; Whitwell, I. *J. Organomet. Chem.* **1984**, *266*, C27.
88. Ford, P. C.; Van Eldik, R.; Ryba, D. W. *Organometallics* **1993**, *12*, 104.
89. Davison, A.; Martinez, N. *J. Organomet. Chem.* **1974**, *74*, C17.
90. Davies, S. G.; Watkins, W. C. *J. Chem. Soc., Chem. Commun.* **1994**, 491.
91. Astruc, D.; Catheline, D. *J. Organomet. Chem.* **1982**, *226*, c52.
92. Guerchais, V.; Lapinte, C.; M.; Roger, C.; Tudoret *J. Organomet. Chem.* **1989**, *365*, 347.
93. Moss, J. R.; Goslett, J. K. I.; Scott, L., Unpublished Results.
94. Emeran, A.; Gafoor, M. A.; Goslett, J. K. I.; Liao, Y.; Moss, J. R.; Pimble, L. *J. Organomet. Chem.* **1991**, *405*, 237.
95. Andersen, J.-A. *Synthesis and Reactivity of Alkyl and Acyl Complexes of Manganese and Rhenium, PhD Thesis*; University of Cape Town: Cape Town, 1994.
96. Andersen, J.; Moss, J. R. *Adv. Oragnomet. Chem.* **1995**, *37*, 169.
97. Welker, M. E.; Powell, K. R.; Elias, W. J. *J. Organomet. Chem.* **1991**, *407*, 81.

Chapter 3

X-ray crystal and molecular structures of $[(\eta^5\text{-}C_5(CH_3)_5)Fe(CO)_2(CH_2)_4CH_3]$ and $[(\eta^5\text{-}C_5H_5)Fe(CO)_2(C(O)CH_3)]$

Chapter 3

The real voyage of discovery consists not in seeking new landscapes but in having new eyes. **Proust**

Research is to see what everybody sees, and to think what nobody else has thought. **Albert Szent-Györgyi**

X-ray crystal and molecular structures of $[(\eta^5\text{-}C_5(CH_3)_5)Fe(CO)_2(CH_2)_4CH_3]$ and $[(\eta^5\text{-}C_5H_5)Fe(CO)_2(C(O)CH_3)]$

3.1. X-ray crystal and molecular structure of $[(\eta^5\text{-}C_5(CH_3)_5)Fe(CO)_2(CH_2)_4CH_3]$

3.1.1. Introduction

Alkyl compounds are central to organometallic chemistry. In particular, in transition metal chemistry, alkyl species have been proposed as intermediates in many important catalytic reactions. These include alkene polymerisation, hydroformylation, carbonylation reactions, hydrogenation of alkenes, and Fischer-Tropsch syntheses (See Chapter 1 and 2). X-ray crystallographic studies are important tools in the investigation of transition metal alkyls as they can provide information on bond distances, which give an indication of the nature and strength of the bond, as well as information concerning the conformation of the alkyl at the metal centre. This information may be useful in understanding the reactivity and selectivity of alkyl species involved in important catalytic reactions.

3.1.2. Structures of transition metal alkyl compounds

3.1.2.1. Structures of iron and ruthenium alkyl compounds

The Cambridge Structural Database (CSD) contains a wealth of structural information (the October 1998 release has over 190 000 structures) which can be utilized both to understand different types of bonding between elements and to predict what structures other compounds (for which structures have not been obtained) may adopt. The data has also been used to understand the structural changes occurring in reactions and isomerizations of molecules [1-5].

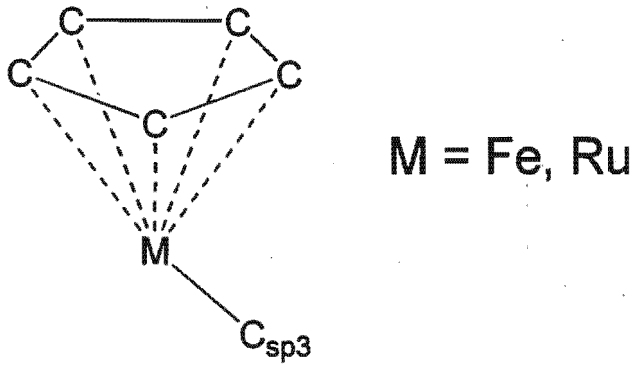

Figure 3.1.1 Alkyl fragment searched for in the Cambridge Structural Database.

A search was performed on the CSD for structures of alkyl compounds of iron and ruthenium. The purpose of the study was to elucidate structural features of these compounds (eg. bond lengths and preferred conformations), and to compare these with structures obtained from high level theoretical calculations (Chapters 4 and 5). The main focus of the study was on compounds of the type [CpM(L)L'R], these being the subject of synthetic and theoretical work elsewhere in this thesis. These types of compounds have a pseudo-octahedral structure, with the cyclopentadienyl ligand occupying three coordination sites. The metal generally has a formal oxidation state of +2 although a few compounds were located with an oxidation state of +3. A search for fragments of the type shown in Figure 3.1.1 found a total of 76 structures of distinctive compounds (64 iron and 12 ruthenium).

The majority of structures found were iron compounds and these will be discussed first. All of the iron structures found in the database have a pseudo-octahedral structure where the cyclopentadienyl or substituted cyclopentadienyl ligand occupies three coordination sites, and the alkyl and other two remaining ligands occupy three coordination sites. The compounds may be classified in a number of different ways according to the nature of the attached ligands. The compounds found in the database can be classified as follows:

A. Structures with two carbonyl ligands bonded to the iron atom. There were fifty six fragments of this type found, making it the largest sub group of structures (i.e. structures with the general formula $[CpFe(CO)_2R]$).

B. Structures with one carbonyl ligand and one phosphine ligand bonded to the iron atom. There were thirteen fragments of this type found (i.e. structures with the general formula [CpFe(CO)(PR′$_3$)R]).

C. Structures with two phosphines ligands bonded to the iron atom. The phosphines may be the same or different, and may be bidentate. There were two fragments of this type found (i.e. structures with the general formula [CpFe(PR′$_3$)$_2$R]).

D. Structures which have non-carbonyl or non-phosphine ligands bonded to the iron atom. There were five fragments of this type found (i.e. structures with the general formula [CpFe(L)(L′)R], where L is CO, or tertiary phosphine and L′ is another ligand such as a carbene).

The above groups of structures may be further classified in the following way:

E. Structures with long, or bulky alkyl groups, which may bridge the iron atom and a second metal. There were fifty eight fragments in this group.

F. Structures where the alkyl group is bonded to the cyclopentadienyl ligand (i.e. forming a metallocycle). There were five fragments in this group.

G. Structures where the alkyl group is a methyl group (i.e. primary). There were seven fragments in this group.

H. Structures where the alkyl group has a single substituent (other than hydrogen) at the α-carbon (i.e. secondary). There were forty four fragments in this group.

I. Structures where the alkyl group has two substituents at the α-carbon (i.e. tertiary). There were eighteen fragments in this group.

J. Structures where the alkyl group has three substituents at the α-carbon (i.e. quaternary). There were nine fragments in this group.

K. Structures with substituted cyclopentadienyl ligands (eg. pentamethylcyclopentadienyl). There were sixteen fragments in this group.

Note that any one structure may belong to more than one of the above groups. The structures found, together with their groups and key bond distances and angles are given in the following table.

Table 3.1.1

Cyclopentadienyl iron alkyl compounds located in the Cambridge Crystallographic Database

Structure	Fragment	Refcode	Cp-Fe	Fe-C	Cp-Fe-C	Group	Ref
1	1	BEFCAQ	1.732	2.112	124.925	A, J	[6]
2	2	BEYREC	1.723	2.036	123.806	A, H	[7]
3	3	BIRLAP	1.740	2.097	120.302	A, E, F, H, K	[8]
4	4	BIRLET	1.743	2.111	120.685	A, E, F, I, K	[8]
5	5	BUCFEC	1.736	2.083	122.557	A, E, H	[9]
5	6	BUCFEC	1.736	2.078	122.724	A, E, H	[9]
6	7	BUPZUH10	1.742	2.088	122.178	A, E, I	[10]
7	8	BUWDAY	1.726	2.101	122.223	A, E, H	[11]
7	9	BUWDAY	1.721	2.094	123.134	A, E, H	[11]
8	10	BUWDEC	1.726	2.081	120.417	A, E, H	[11]
9	11	CAGKEA	1.734	2.060	119.920	A, E, I	[12]
10	12	CAJREK	1.747	2.201	115.599	A, E, H	[13]
11	13	CAKSUC	1.732	2.085	125.766	A, E, I	[14]
12	14	CEDMON	1.746	2.065	119.051	B, G	[15]
12	15	CEDMON10	1.741	2.055	118.899	B, G	[16]
13	16	CFEALL	1.730	2.125	124.094	A, E, H	[17]
13	17	CFEALL	1.729	2.135	125.606	A, E, H	[17]
14	18	CPCMFE10	1.814	2.065	123.070	A, H	[18]
15	19	CPICCP	1.701	2.110	122.513	A, I	[19]
16	20	CYMPFE	1.737	2.096	123.731	A, E, J	[20]
16	21	CYMPFE	1.732	2.099	123.229	A, E, J	[20]
17	22	DIDDOJ	1.711	2.074	123.035	A, E, J	[21]
18	23	DULSAE	1.744	2.075	119.963	A, E, I	[22]
18	23	DULSAE10[a]				A, E, I	[23]
19	24	FADJAV	1.731	2.166	124.415	B, I	[24]
20	25	FADJUP	1.727	2.060	127.967	A, J	[25]
21	26	FAWGOZ	1.723	2.069	119.462	A, E, F, H, K	[26]
22	27	FEWNAW	1.732	2.070	122.952	A, G, K	[27]
23	28	FICSAL10	1.737	2.079	120.509	B, E, H	[28]
24	29	FOBWUO	1.742	2.065	118.717	B, H	[28]
24	29	FOBWUO10[a]				B, H	[29]
25	30	FOXDAX	1.746	2.044	120.949	D, E, H	[30]
26	31	FOYHIK	1.734	2.063	119.991	A, E, H	[31]
27	32	GAKCIE	1.724	2.046	125.975	D, E, J	[32]
28	33	GAVXAC	1.803	2.003	120.384	C, H, K	[33]
29	34	GAXROM	1.720	2.061	123.149	A, E, H	[34]
30	35	GAXRUS	1.727	2.067	122.312	A, E, H	[34]
31	36	GAXSAZ	1.745	2.075	121.722	A, E, H	[34]
32	37	HEJFOR	1.719	2.154	124.229	C, E, H	[35]
33	38	HEZHOJ	1.730	2.077	118.532	A, E, H	[36]
34	39	JUDDUH	1.737	2.091	119.017	A, E, H, K	[37]
34	40	JUDDUH	1.736	2.099	122.615	A, E, H, K	[37]

Structure	Fragment	Refcode	Cp-Fe	Fe-C	Cp-Fe-C	Group	Ref
35	41	KALTIA	1.725	2.056	120.597	A, G, K	[38]
36	42	KAPLIW	1.729	2.088	122.216	A, E, H	[39]
37	43	KAPLOC	1.726	2.082	118.940	A, E, H	[39]
38	44	KESBIT	1.745	2.109	119.314	A, E, H	[40]
39	45	MECPFF	1.712	2.146	122.522	A, E, H	[41]
39	46	MECPFF	1.721	2.158	122.731	A, E, H	[41]
40	47	MPFCFE10	1.738	2.150	123.344	A, E, F, J ,K	[42]
41	48	PCPRFE	1.738	2.079	120.678	A, E, J	[43]
42	49	POHTUB	1.724	2.074	121.267	A, E, H	[44]
43	50	PRCFEC	1.737	2.082	122.445	A, E, H	[9]
44	51	RCMXFE	1.720	2.107	120.670	B, E, H	[45]
44	52	RCMXFE	1.765	2.105	118.189	B, E, H	[45]
45	53	REBJAJ	1.723	2.091	122.594	A, E, H	[46]
45	54	REBJAJ	1.722	2.076	122.400	A, E, H	[46]
45	55	REBJAJ	1.723	2.075	121.182	A, E, H	[46]
46	56	SANMID	1.713	2.159	124.025	A, E, I	[47]
47	57	SATVUE	1.732	2.073	118.450	A, E, H	[48]
48	58	SATWAL	1.739	2.068	120.251	A, E, H, K	[48]
49	59	SATWEP	1.732	2.070	121.277	A, E, H	[48]
50	60	SECHEN	1.738	2.061	121.576	B, E, H	[49]
51	61	SECHIR	1.733	2.016	120.426	B, H	[49]
52	62	SEPPEI	1.721	2.039	121.733	A, G, K	[50]
53	63	SIRVUK	1.735	2.026	123.101	A, E, I	[51]
54	64	SIRVUK	1.728	2.033	123.765	A, E, I	[51]
54	65	SIRWAR	1.730	2.037	124.103	A, E, I	[51]
55	66	SOFYAN	1.746	2.118	122.337	A, E, H, K	[52]
56	67	SOSVUR	1.727	2.022	125.671	D, E, I	[53]
56	68	SOSVUR	1.760	2.038	125.345	D, E, I	[53]
57	69	SOSWAY	1.688	2.043	119.063	A, E, I	[53]
58	70	SOSWEC	1.738	2.080	121.005	B, E, I	[53]
59	71	TEDGIS	1.727	2.064	121.467	B, E, F, G, K	[54]
60	72	TEXWIC	1.735	2.060	121.332	B, G, K	[55]
61	73	VACCOR	1.745	2.086	120.388	A, H, K	[56]
62	74	VAYCIH	1.761	2.080	125.505	D, E, I	[57]
63	75	WAMBUH	1.752	2.079	121.215	A, E, J	[58]
64	76	ZISSID	1.736	2.072	121.316	B, E, H	[59]
Number of Values			76	76	76		
Mean			1.734	2.082	121.878		
Standard Deviation (Sample)			0.017	0.036	2.201		
Standard Deviation (Population)			0.017	0.036	2.187		
Minimum			1.688	2.003	115.599		
Maximum			1.814	2.201	127.967		

[a]Structure reported twice in the literature.

Structures of type A are of particular interest as they are the subject of synthetic, structural, and theoretical study elsewhere in this thesis. There were forty eight compounds of this type in the database which comprised fifty six fragments. This was the largest single group structures of cyclopentadienyl iron compounds found (i.e. $[CpFe(CO)_2R]$, where Cp is cyclopentadienyl or substituted cyclopentadienyl, and R is an alkyl), providing a good set of data for the examination of the structural features of these types of compounds. The average iron to alkyl-carbon bond length is 2.086 ± 0.033 Å. The values ranged from a minimum of 2.026 Å to a maximum of 2.201 Å. Only three of the structures in this class (i.e. type A) are methyl compounds (i.e. type G). The alkyl group in the majority of the structures in class A have the α-carbon singly substituted (i.e. $-CH_2R$, type H). This feature of the alkyl (i.e. type A and H) gives a definite conformation of the alkyl with respect to the cyclopentadienyl and CO ligands, and is discussed in detail later in this section. Structures where the α-carbon of the alkyl group has two substituents other than hydrogen bonded to it (i.e. -CRR'H, type I) predominantly adopt a conformation with the hydrogen positioned between the two carbonyl ligands. This observation would be expected on geometrical ground as illustrated in the figure below which shows two possible conformations. Note that a plane of symmetry exists in the $[CpFe(CO)_2]$ fragment which reduces the number of possible conformations.

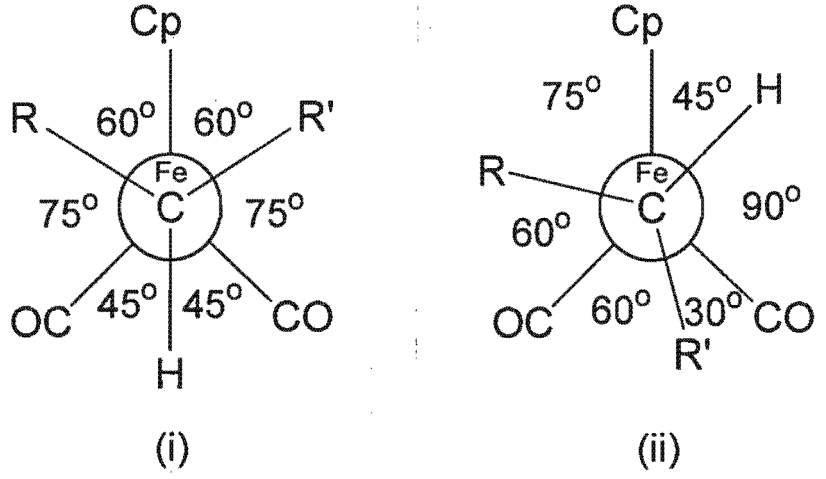

Figure 3.1.2 Diagram showing the two possible conformations of the alkyl group for type A, I (i.e. $[CpFe(CO)_2CHRR']$ structures.

From Figure 3.1.2 it can be seen that an idealised fragment adopting the conformation illustrated in (i) is preferable to the conformation illustrated in (ii) because the torsion angles between the groups are maximised and the smallest torsion angles (45°) are between the carbonyls and the hydrogen which is sterically less demanding than the other groups. Seven of the eleven fragments

of this type (i.e. type A, I) adopt the predicted conformation (i.e. (i) in Figure 3.1.2). Only one of the fragments, out of the eleven found, has two distinct R and R′ fragments [14], the remainder all have ring systems incorporating both R and R′. The presence of this ring and groups bonded to the ring and/or intermolecular interactions may be the cause of the alternate conformation observed in four of the eleven fragments. The different conformations observed are illustrated in Figure 3.1.3.

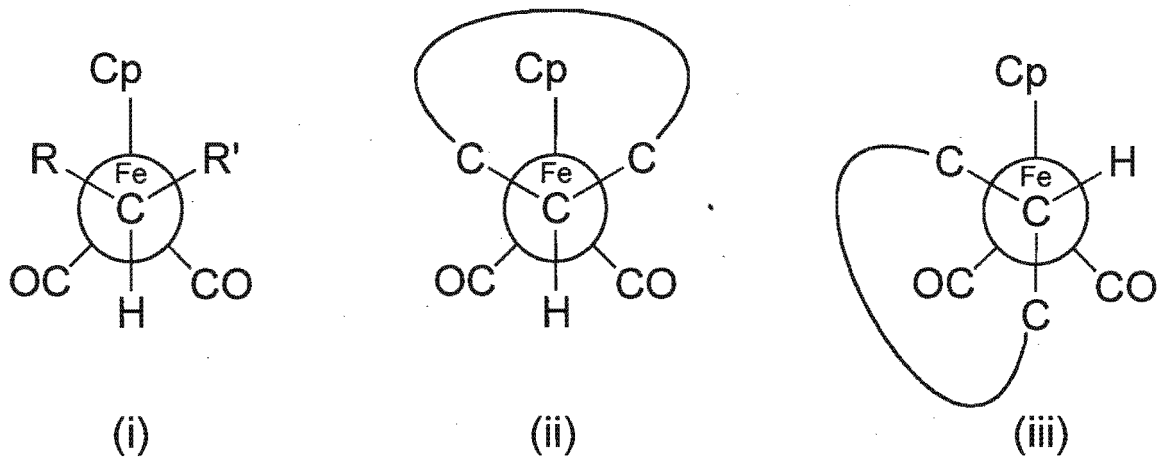

Figure 3.1.3 Diagram showing conformations adopted by [$CpFe(CO)_2CHRR'$], type A, I, compounds.

Fragments of the type [$CpFe(CO)_2CRR'R''$], i.e. type A, J, all adopted a conformation as illustrated in Figure 3.1.4. There were eight fragments of this type found, comprising seven compounds.

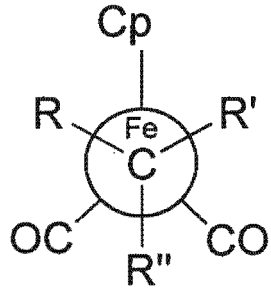

Figure 3.1.4 Diagram showing conformation adopted by type A, J (i.e. [$CpFe(CO)_2CRR'R''$]) compounds.

The largest group of fragments of type A, $[CpFe(CO)_2R]$, found were compounds where the α-carbon atom had a single R group and two hydrogen atoms bonded to it. From a conformational perspective it also proved the most interesting. There were thirty four fragments of this type, i.e. type A, H, $[CpFe(CO)_2CH_2R]$. The fragments include simple alkyls, bridging alkyls, as well as fragments with complex bulky alkyl groups. Many of the fragments contain substituted cyclopentadienyl ligands including two fragments containing a pentamethylcyclopentadienyl ligand. The alkyl group can adopt two different conformations as illustrated in Figure 3.1.5. Examples of both these conformations exist in the CSD. Twenty three of the thirty four fragments found adopted a syn type conformation as in Figure 3.1.5 (i) and

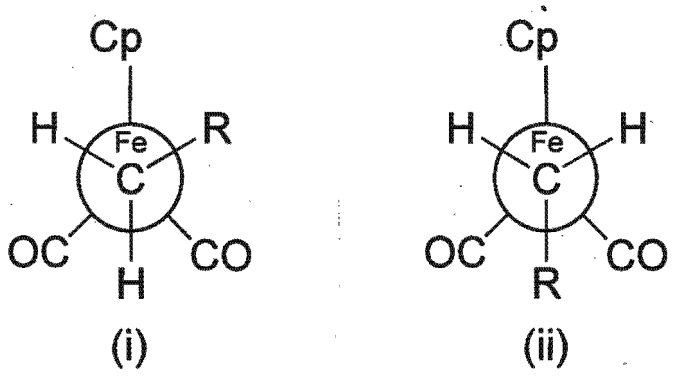

Figure 3.1.5 The two possible conformations of $[(\eta^5\text{-}C_5R'_5)Fe(CO)_2CH_2R]$.

eleven adopted an anti type conformation as in Figure 3.1.5 (ii). Examination of the molecular structures of the fragments does not reveal any compelling evidence to suggest the reason for adopting one conformation in preference to the other. Intermolecular interactions (i.e. hydrogen bonds) between C-H groups (i.e. the alkyl) and lone pair donors (eg. C=O) do occur but do not seem to play a role in this case.

Steric bulk of the alkyl group (i.e. Type E) does not seem to be a factor as bulky alkyl groups are found in structures of each conformation. Substitution of the cyclopentadienyl ligand (i.e. Type K) does not appear to be a factor where the cyclopentadienyl is singly substituted. It may be a factor where there is greater substitution. There were however only two examples of this type of fragment (i.e. Type A, H, K) both of which contained pentamethylcyclopentadienyl ligands [40,48]. The conformation adopted by both fragments was the anti conformation (i.e. Figure 3.1.5 (ii)), suggesting that the steric bulk of the pentamethylcyclopentadienyl forced the

alkyl to adopt an anti conformation. One of the structures, however has a formal oxidation state of +3 for the iron, although this does not change the metal ligand bond distances significantly. The second structure was reported together with its cyclopentadienyl analogue [48], which adopts the same conformation as the pentamethylcyclopentadienyl structure. It is therefore not possible from this data to draw a definite conclusion concerning the influence of substitution in the cyclopentadienyl ring on the conformation of the alkyl group (See Section 3.1.5 for further discussion).

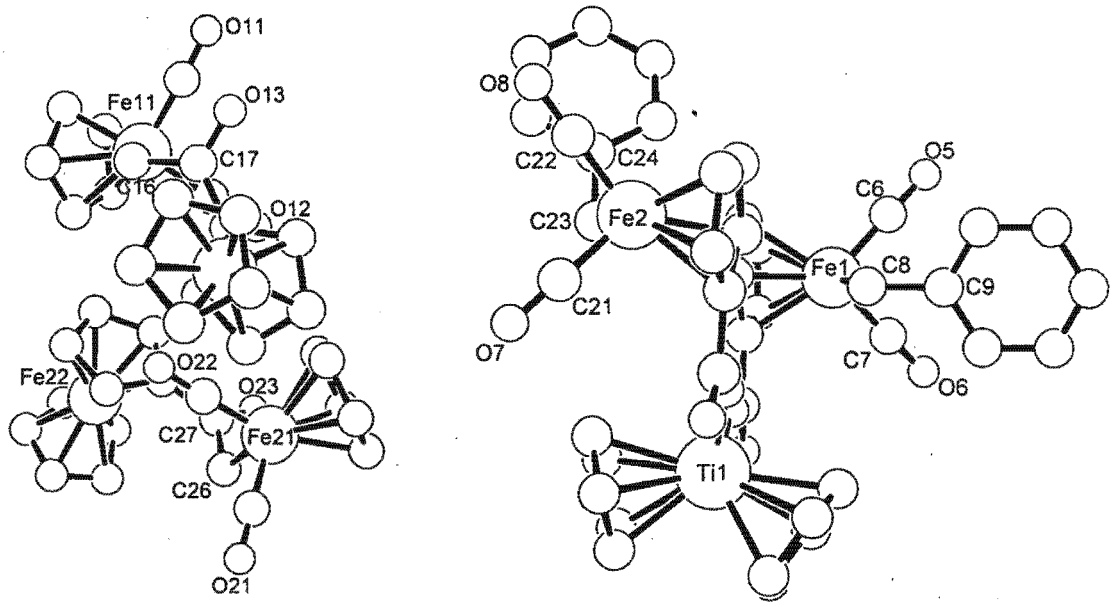

Figure 3.1.6 Diagram showing two structures containing four fragments of type A, H (i.e. $CpFe(CO)_2CH_2R$) where the alkyl group adopts two different conformations although the two fragments in each structure are identical.

Two structures involving four fragments out of the total of thirty four fragments found are remarkable as both structures have two chemically identical fragments which adopt different conformations (See Figure 3.1.6) [11,37]. Furthermore the alkyl group is not involved in any inter- or intramolecular hydrogen bonding. This suggests that the different conformations adopted by the identical fragments are due to packing effects within the crystal structure. Less research has been conducted on crystal structures (as opposed to molecular structures) in the past, and many factors influencing the structure (eg. space group selection) are not well understood. Efforts

to predict space group (i.e. packing) of the crystal structure from a molecular structure have been partially successful for organic compounds and there is much current interest in this field [60]. Recent X-ray crystallographic work on a rhenium complex found that a solid state transformation which altered the crystal structure, resulted in a conformational change of the substituted cyclopentadienyl ligand [61]. In the two structures shown in Figure 3.1.6, the authors of the paper describing the second structure (Figure 3.1.6, JUDDUH) [37] note the conformational differences of the two alkyl groups but do not discuss it further or suggest the cause of this difference. The authors of the first paper (Figure 3.1.6, BUWDAY) [11,62] do not note or discuss the difference in the conformation between the two fragments. If the conformational differences are due to packing effects in the crystal structure then the energy difference between the two conformations would be expected to be relatively small (~1 Kcal/mol). Conformational studies of the alkyl group in $[CpFe(CO)_2CH_2CH_3]$ in solution using infrared spectroscopy confirm that the energy difference is small [63], as does a similar study using infrared spectroscopy and molecular mechanics calculations on $[CpFe(CO)_2CH_2C(O)CH_3]$ [64]. Ab Initio calculations on the rotational barrier for $[CpFe(CO)_2CH_2CH_3]$ presented later in this thesis (Chapter 4) further confirm the existence of a small barrier to rotation and energy difference.

Structures of type B (i.e. $[CpFe(CO)(PR_3)R]$) are chiral and are of interest in asymmetric syntheses. There were thirteen fragments of this type in the CSD, four were methyl compounds (i.e. type G), seven fragments were of type H (i.e. $[CpFe(CO)(PR_3)CH_2R']$, see Figure 3.1.7), two fragments were of type I (i.e. $[CpFe(CO)(PR_3)CHR'R'']$), and there were no fragments of type J. The conformation of the alkyl chain in fragments of type H was found to be such that the alkyl chain is positioned between the cyclopentadienyl and CO ligands, thus minimising steric interactions with the tertiary phosphine ligand. Two exceptions to this were found where the alkyl group is positioned between the cyclopentadienyl ligand and the tertiary phosphine ligand. This is a sterically demanding conformation and it is unclear what the cause is, however it may be due to interactions between the tertiary phosphine and groups on the alkyl ligand (See Figure 3.1.7, Refcodes SECHEN [49], SECHIR [49]).

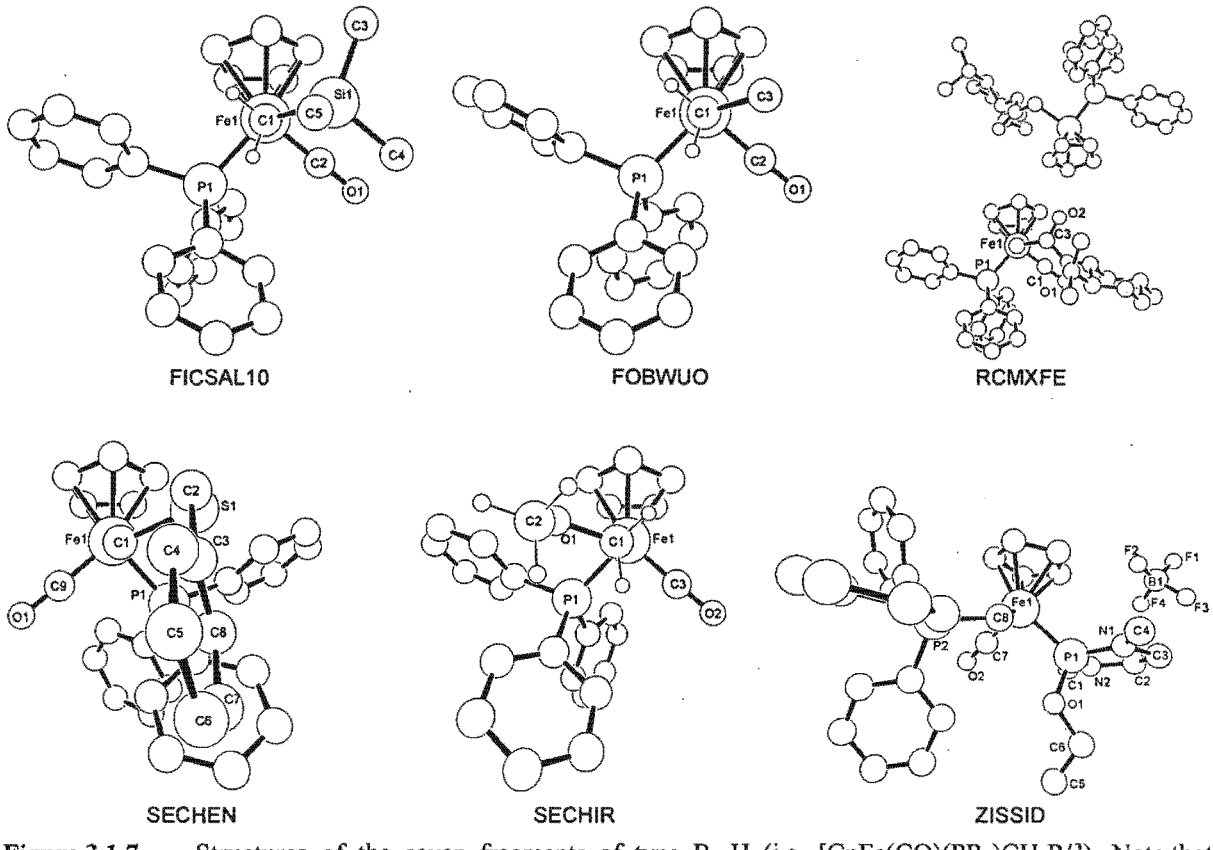

Figure 3.1.7 Structures of the seven fragments of type B, H (i.e. [CpFe(CO)(PR_3)CH_2R']). Note that RCMXFE contains two fragments. Structure labels correspond to CSD Refcodes.

The two fragments of type B, I (i.e. [CpFe(CO)(PR_3)CHR′R″]) found [24,53], adopt a conformation of the alkyl group that places the non-hydrogen atoms bonded to the α-carbon

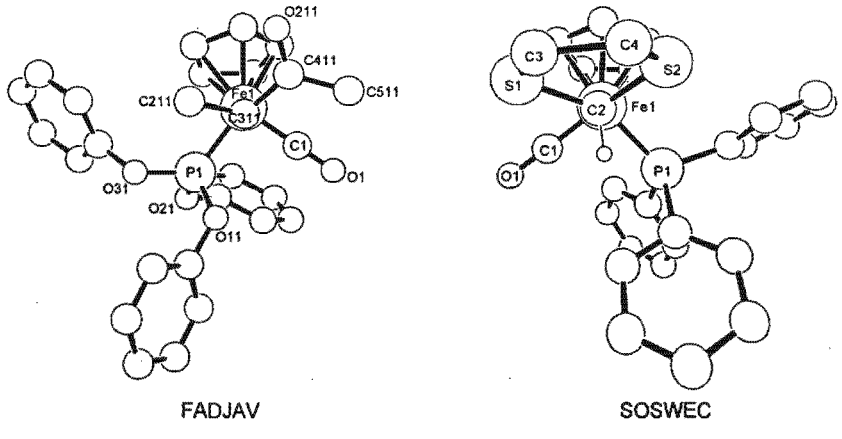

Figure 3.1.8 Structures of type B, I (i.e. [CpFe(CO)(PR_3)CHR′R″]) showing the conformation of the alkyl ligand. Structure labels correspond to CSD Refcodes.

between the cyclopentadienyl ligand and the carbonyl and tertiary phosphine ligand respectively (See Figure 3.1.8). This conformation provides the least steric hindrances and places the hydrogen atom between the carbonyl and phosphine ligands.

Two fragments of type C (i.e. [CpFe(PR_3)R′] were found . Both structures contained bidentate phosphine ligands with the alkyl group of type I (i.e. -CH_2R) [33,35] (See Figure 3.1.9). The alkyl group in the first structure (Refcode: GAVXAC [33]) adopts a conformation placing it between the two phosphines, despite the P-Fe-P angle being reduced from an ideal 90° to around 85°. The iron to alkyl-carbon bond distance is shorter, at 2.003 Å, than the mean for all the structures found of 2.08 ± 0.04 (See Table 3.1.1). This shortening of the bond may be due to the formal oxidation state of +3 on the iron atom. The second structure (Refcode: HEJFOR [35]) has a conformation which eclipses the cyclopentadienyl ligand. The iron to alkyl-carbon bond distance of 2.154 Å is longer than the mean distance for all structures found of 2.08 ± 0.04 (See Table 3.1.1). This may be due, in part, to the presence of two bis-tertiary phosphine ligands, however the lack of further data renders it impossible to drawn any definite conclusion from structural observations alone.

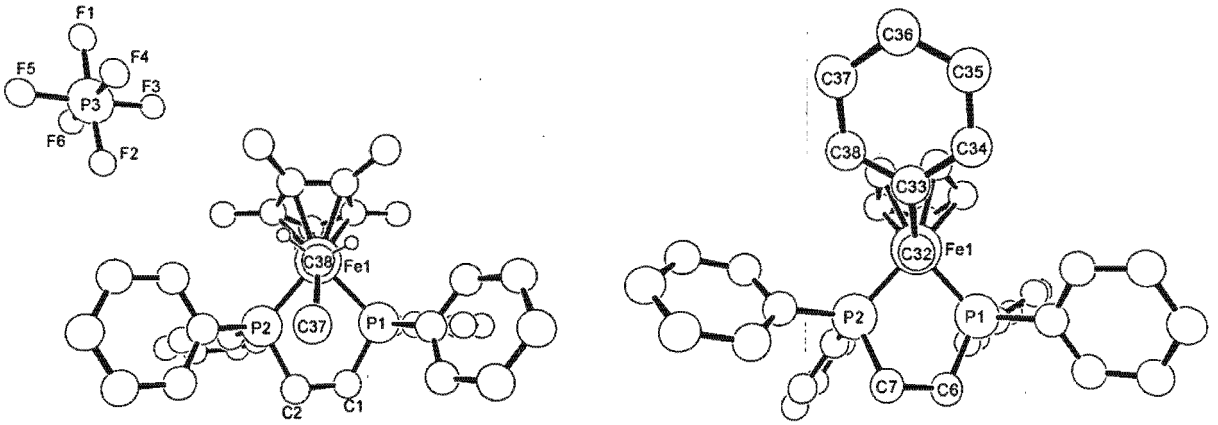

GAVXAC HEJFOR

Figure 3.1.9 Structures of type C (i.e. [CpFe(PR_3)$_2$R′]) showing the conformation adopted by the alkyl ligand. Note that structure labels correspond to CSD Refcodes.

Structures in which on of the carbonyl or phosphine ligands is replaced by another type of ligand such as a carbene (i.e. type D) are shown in Figure 3.1.10. All five fragments found in this class had a single carbonyl ligand and either a carbene or a sulphur ligand. In all cases the alkyl group

and the carbene or sulphur ligand formed part of a metallocycle which fixed the conformation of the alkyl ligand.

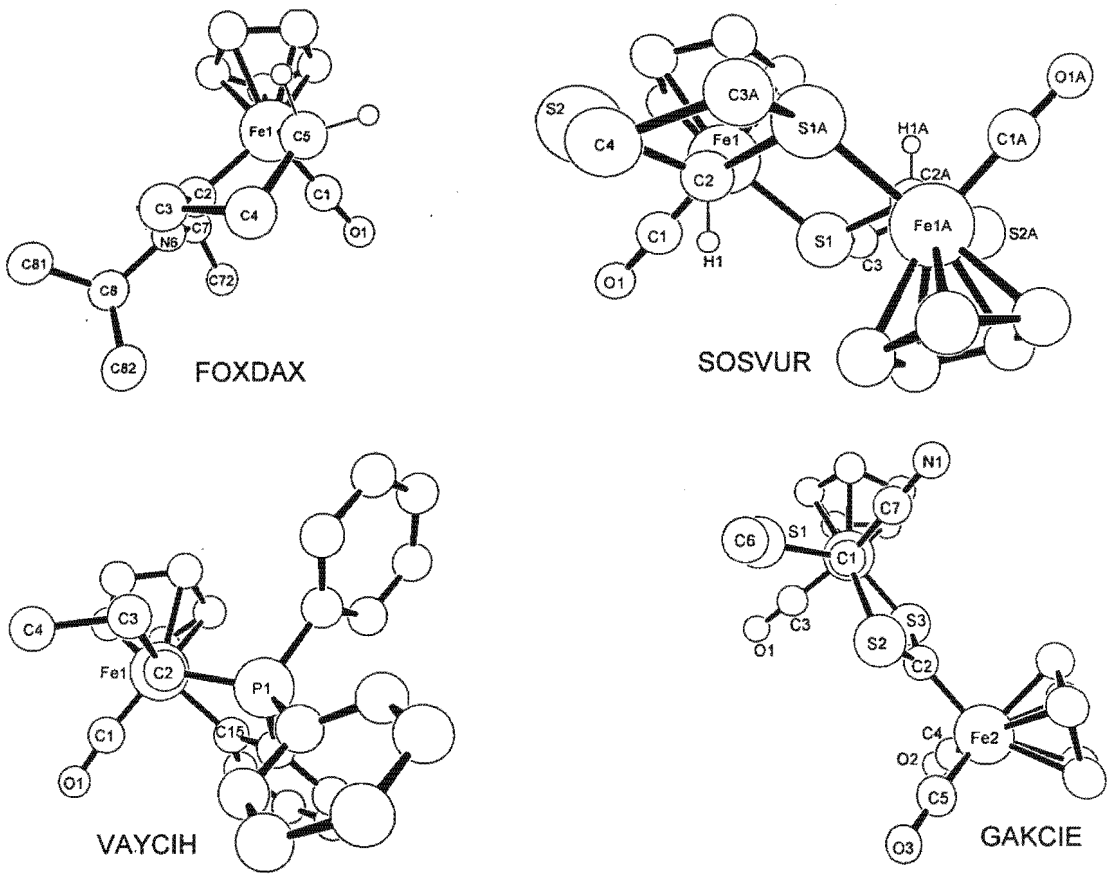

Figure 3.1.10 Structures of type D (i.e. [CpFe(L)(L')R] where L = CO or PR'$_3$ and L' = any other ligand) showing the conformation adopted by the alkyl ligand. Note that structure labels correspond to CSD Refcodes.

The twelve ruthenium structures found in the Cambridge Crystallographic Database consisted of five dicarbonyl structures [65-69], two mono-carbonyl, mono-tertiary phosphine structures [70,71], one bis-tertiary phosphine structure [72], two mono-carbonyl structures [73,74] and two dialkyl structures [75]. The average ruthenium alkyl carbon bond length was 2.14 ± 0.07 Å. Three of the structures have pentamethylcyclopentadienyl ligands, and three structures have an alkyl chain which consists of a metallocycle. The alkyl chain in all structures lies between the cyclopentadienyl ligand and one of the other ligands (i.e. CO), except in the case of the bis-tertiary phosphine structure were it lies between the tertiary phosphines.

3.1.3. *Growing crystals of $[(\eta^5\text{-}C_5(CH_3)_5)Fe(CO)_2(CH_2)_4CH_3]$*

Yellow/orange crystals were grown from a concentrated hexane solution kept in the dark at -10°C for one month. The crystals thus formed were rhombohedral plates of a soft brittle nature. Crystals were also grown from an acetone solution which was kept in the dark at -10°C. The acetone solution was open to water vapour which caused the compound to slowly precipitate out of solution and form crystals.

3.1.4. *X-ray photography of $[(\eta^5\text{-}C_5(CH_3)_5)Fe(CO)_2(CH_2)_4CH_3]$*

A number of crystals were used in the preliminary investigations of the structure of $[(\eta^5\text{-}C_5(CH_3)_5)Fe(CO)_2(CH_2)_4CH_3]$ by X-ray photography. The crystals used were of approximate dimensions 0.5mm x 0.4mm x 0.2mm. The crystals were found to decompose somewhat in air over 24 hrs during photography. The crystal changed colour from yellow to reddish orange which is most likely due to the presence of the iron dimer $[(\eta^5\text{-}C_5(CH_3)_5)Fe(CO)_2]_2$. Embedding of a crystal in an acrylonitrile (super-glue) matrix stabilised the compound enough for the necessary photography.

From oscillation photography it was determined that the crystal was monoclinic and the number of molecules per unit cell was estimated to be four. The crystals proved too unstable and weakly diffracting to enable complete determination of the space group by this method.

3.1.5. *Structure of $[(\eta^5\text{-}C_5(CH_3)_5)Fe(CO)_2(CH_2)_4CH_3]$*

The crystals are monoclinic, $P2_1/c$, a = 8.304, b = 16.345, c = 12.568Å, β = 91.43°, V = 1705.3218Å^3, Z = 4, D_{xo} = 1.24Mg.m^{-3}, $F(000)$ = 679.96, λ(Mo, Kα) = 0.71069 Å, μ = 8.29 mm^{-1}, Temperature = -35°C.

A crystal with dimensions 0.3 x 0.3 x 0.2 mm was used for the data collection. Lattice parameters were determined by least-squares fitting of the setting angles of 25 reflections $1° \geq \theta \geq 25°$ automatically centred on a CAD4 diffractometer. Intensities were collected with graphite-monochromated Mo Kα radiation, $\omega/2\theta$ scan mode, scan width $(0.80+0.35 \tan \theta)°$, aperture

setting (1.12 + 1.05 tan θ)mm and 4mm length, range of reflections 25 ≥ θ ≥ 1°. 3260 reflections were measured of which 2676 were unique, and 2108 of these were used in the refinement, index range h -9/9, k 0/19, l 0/14. Three intensity control reflections (-5 -2 7, 2 -12 2, -3 2 9) monitored every 120 reflections showed a 8.6% loss in intensity; attempts to apply a linear absorption correction failed so the data were used uncorrected. This may have been the cause of the high R factor. Data were corrected for background, scan speed, Lorentz and polarization effects. The iron atom was located using the Patterson function. The remainder of the structure was solved using SHELX76 [76] and refined by difference Fourier methods using SHELX86 [77]. The final model included anisotropic refinement of all non-hydrogen atoms and isotropic refinement of hydrogens constrained to idealized positions with C-H = 1.00 Å which gave final R = 0.095, wR = 0.095, W = 30.213/[$\sigma^2(F_0)$], S = 36.57, residual electron density + 0.33 ≥ Δρ ≥ -0.38 e Å^{-3}. The observed and calculated structure factors are given in Appendix A.

Final atomic coordinates, equivalent isotropic temperature factors, bond lengths and angles are given in Tables 3.1.2 and 3.1.3 The structure of the molecule and crystal are shown in Figures 3.1.11, 3.1.12 and 3.1.14.

Table 3.1.2
Fractional atomic coordinates (X10^4) and thermal parameters (Å^2 X 10^3) with esd's in parentheses for [Cp*Fe(CO)$_2$(n-C$_5$H$_{11}$)].

Atom	x	y	z	U_{eq} [a]
Fe(1)	1608(2)	2130(1)	1109(1)	35(1)
C(1)	4002(12)	2483(6)	1146(9)	42(4)
C(2)	4412(15)	3380(6)	1110(9)	51(4)
C(3)	6241(14)	3545(6)	1142(8)	45(4)
C(4)	6633(14)	4448(6)	1137(8)	45(4)
C(5)	8455(15)	4605(7)	1130(10)	58(4)
C(6)	-104(12)	1289(6)	1650(8)	37(3)
C(7)	1474(13)	1082(6)	2073(8)	40(4)
C(8)	2443(15)	904(6)	1210(8)	47(4)
C(9)	1477(17)	1028(6)	266(8)	53(5)
C(10)	-59(17)	1254(6)	524(9)	53(4)

C(11)	-1555(14)	1474(8)	2290(10)	58(5)
C(12)	1922(20)	996(8)	3225(8)	68(5)
C(13)	4137(15)	570(7)	1294(10)	62(5)
C(14)	2121(20)	883(8)	-862(9)	69(5)
C(15)	-1471(16)	1388(8)	-230(11)	65(5)
C(16)	1247(14)	2782(6)	36(9)	48(4)
C(17)	1199(12)	2824(7)	2129(8)	39(3)
O(1)	927(11)	3179(5)	-697(6)	64(3)
O(2)	960(12)	3280(5)	2791(7)	71(4)

[a]Equivalent isotropic U calculated from anisotropic U: $U_{eq} = \frac{1}{3}\sum_i\sum_j U_{ij}\mathbf{a}_i^*\mathbf{a}_j^*\mathbf{a}_i\cdot\mathbf{a}_j$.

Table 3.1.3
Bond lengths (Å) and angles(°) for $[Cp^*Fe(CO)_2(n\text{-}C_5H_{11})]$.

Fe(1)-C(1)	2.069(10)	C(6)-C(7)	1.442(15)
Fe(1)-C(6)	2.102(10)	C(6)-C(10)	1.418(15)
Fe(1)-C(7)	2.103(10)	C(6)-C(11)	1.496(16)
Fe(1)-C(8)	2.123(10)	C(7)-C(8)	1.397(15)
Fe(1)-C(9)	2.091(10)	C(7)-C(12)	1.492(15)
Fe(1)-C(10)	2.110(12)	C(8)-C(9)	1.430(16)
Fe(1)-C(16)	1.739(11)	C(8)-C(13)	1.510(17)
Fe(1)-C(17)	1.751(11)	C(9)-C(10)	1.375(19)
C(1)-C(2)	1.508(14)	C(9)-C(14)	1.546(16)
C(2)-C(3)	1.542(17)	C(10)-C(15)	1.505(19)
C(3)-C(4)	1.512(14)	C(16)-O(1)	1.153(13)
C(4)-C(5)	1.535(17)	C(17)-O(2)	1.139(14)
C(16)-Fe(1)-C(17)	97.93(51)	Fe(1)-C(6)-C(11)	127.03(77)
C(10)-Fe(1)-C(17)	123.82(49)	Fe(1)-C(6)-C(10)	70.64(62)
C(10)-Fe(1)-C(16)	92.65(49)	Fe(1)-C(6)-C(7)	69.98(58)
C(9)-Fe(1)-C(17)	156.95(47)	C(10)-C(6)-C(11)	125.90(101)
C(9)-Fe(1)-C(16)	97.42(47)	C(7)-C(6)-C(11)	125.86(94)
C(9)-Fe(1)-C(10)	38.20(48)	C(7)-C(6)-C(10)	108.18(93)
C(8)-Fe(1)-C(17)	129.53(44)	Fe(1)-C(7)-C(6)	69.90(57)
C(8)-Fe(1)-C(16)	132.41(46)	C(6)-C(7)-C(12)	125.57(98)
C(8)-Fe(1)-C(10)	65.89(42)	C(6)-C(7)-C(8)	107.37(90)
C(8)-Fe(1)-C(9)	39.66(39)	Fe(1)-C(7)-C(12)	128.27(76)
C(7)-Fe(1)-C(17)	95.27(43)	Fe(1)-C(7)-C(8)	71.49(58)
C(7)-Fe(1)-C(16)	159.31(47)	C(8)-C(7)-C(12)	126.82(107)
C(7)-Fe(1)-C(10)	66.73(40)	Fe(1)-C(8)-C(7)	69.90(58)
C(7)-Fe(1)-C(9)	65.63(39)	C(7)-C(8)-C(13)	125.07(95)
C(7)-Fe(1)-C(8)	38.61(39)	C(7)-C(8)-C(9)	107.01(102)
C(6)-Fe(1)-C(17)	92.36(44)	Fe(1)-C(8)-C(13)	130.36(75)
C(6)-Fe(1)-C(16)	123.12(49)	Fe(1)-C(8)-C(9)	68.96(57)

C(6)-Fe(1)-C(10)	39.34(42)	C(9)-C(8)-C(13)	127.70(97)
C(6)-Fe(1)-C(9)	64.79(40)	Fe(1)-C(9)-C(8)	71.38(57)
C(6)-Fe(1)-C(8)	65.58(39)	C(8)-C(9)-C(14)	122.64(115)
C(6)-Fe(1)-C(7)	40.13(39)	C(8)-C(9)-C(10)	110.31(95)
C(1)-Fe(1)-C(17)	90.38(47)	Fe(1)-C(9)-C(14)	125.58(76)
C(1)-Fe(1)-C(16)	89.63(48)	Fe(1)-C(9)-C(10)	71.63(62)
C(1)-Fe(1)-C(10)	144.92(43)	C(10)-C(9)-C(14)	127.00(113)
C(1)-Fe(1)-C(9)	106.82(45)	C(6)-C(10)-C(9)	107.10(99)
C(1)-Fe(1)-C(9)	106.82(45)	Fe(1)-C(10)-C(9)	70.16(68)
C(1)-Fe(1)-C(8)	87.12(43)	Fe(1)-C(10)-C(6)	70.01(61)
C(1)-Fe(1)-C(7)	106.19(42)	C(9)-C(10)-C(15)	127.11(109)
C(1)-Fe(1)-C(6)	146.31(41)	C(6)-C(10)-C(15)	125.68(107)
Fe(1)-C(1)-C(2)	119.23(72)	Fe(1)-C(10)-C(15)	128.00(77)
C(1)-C(2)-C(3)	113.05(83)	Fe(1)-C(16)-O(1)	175.41(99)
C(2)-C(3)-C(4)	112.44(91)	Fe(1)-C(17)-O(2)	178.81(99)
C(3)-C(4)-C(5)	112.07(88)		

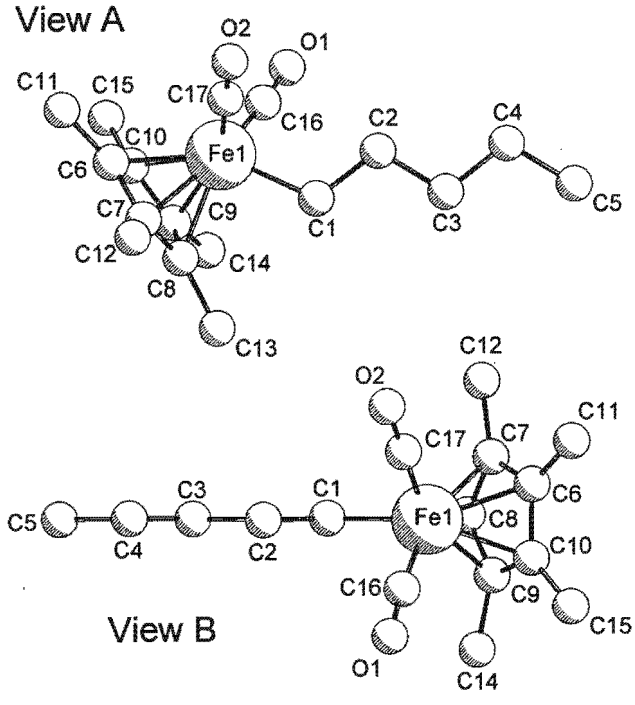

Figure 3.1.11 Two views of the molecular structure of $[(\eta^5\text{-}C_5(CH_3)_5)Fe(CO)_2(CH_2)_4CH_3]$ showing the extended alkyl chain.

The iron atom is octahedrally coordinated to two carbonyls, the alkyl chain and with the pentamethylcyclopentadienyl ligand occupying three coordination sites. The alkyl chain lies in

an extended, staggered conformation (Figure 3.1.11, view A) oriented between the two CO ligands giving the molecule approximate C_s symmetry (Figure 3.1.11, view B). This is in contrast to several compounds where the alkyl group is located between the Cp ligand and the CO ligand (See Section 3.1.2). The pentamethylcyclopentadienyl structures discussed in Section 3.1.2 however both have a conformation which places the alkyl group between the two CO ligands. Based on those two structures it was not possible to ascribe the alkyl group conformation to the presence of the pentamethylcyclopentadienyl group. This structure gives further evidence that this may be caused by the presence of the pentamethylcyclopentadienyl ligand. Additional evidence is provided by the structure of $[(\eta^5\text{-}C_5(CH_3)_5Fe(CO)_2]_2[\mu\text{-}(CH_2)_4]$ which has been determined recently by co-researchers [78] (See Figure 3.1.13). This structure also adopts a conformation with the alkyl

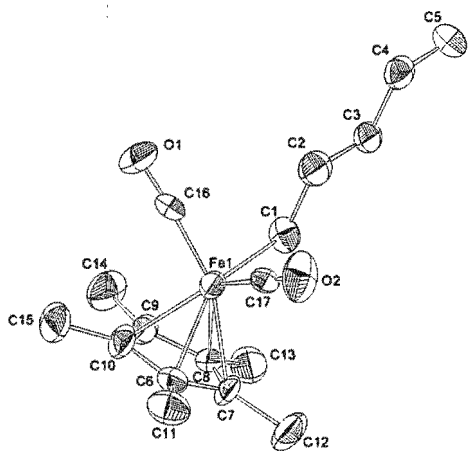

Figure 3.1.12 ORTEP drawing of $[(\eta^5\text{-}C_5(CH_3)_5)Fe(CO)_2(CH_2)_4CH_3]$ showing atom numbering.

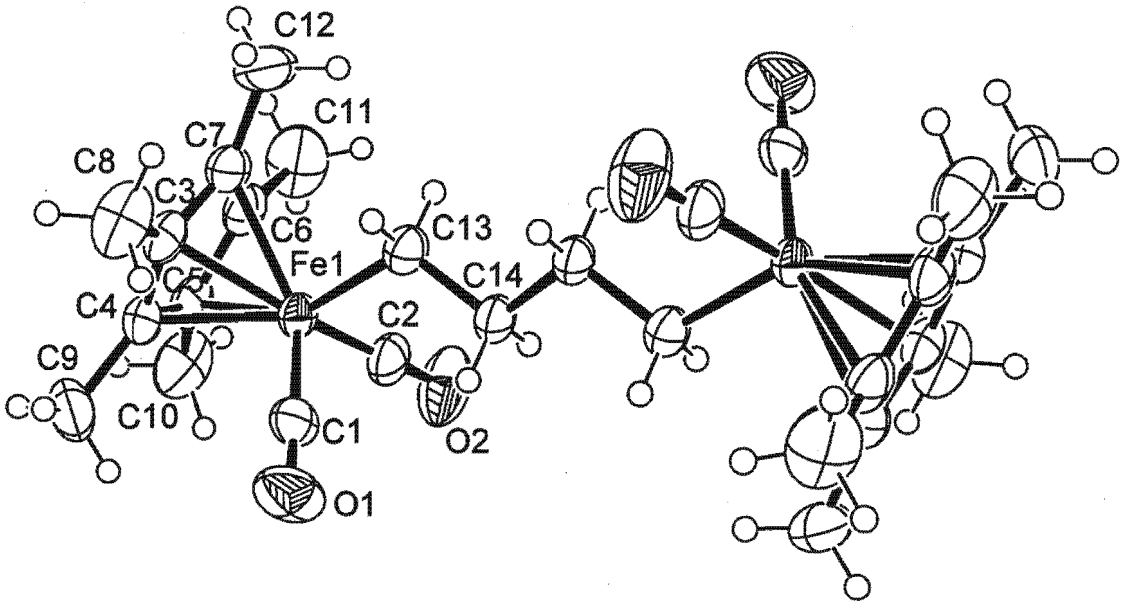

Figure 3.1.13 ORTEP drawing of the structure of $[(\eta^5\text{-}C_5(CH_3)_5Fe(CO)_2]_2[\mu\text{-}(CH_2)_4]$. The conformation of the alkyl bridge between the two metals is such that alkyl chain is placed between the two carbonyl ligands.

ligand placed between the two carbonyl ligands. The structure of the analogous cyclopentadienyl compound, which has been determined previously [9], exhibits a conformation of the alkyl chain with the chain positioned between the cyclopentadienyl ligand and a carbonyl ligand. This evidence suggests that the conformation of the alkyl group may be controlled by the presence of the pentamethylcyclopentadienyl ligand. The positions of the carbon atoms were easily located, and no evidence of disorder could be found. The five carbons and iron are coplanar to within ± 0.02Å, and the ten carbons of the pentamethylcyclopentadienyl ligand are coplanar to within ± 0.01Å. No evidence for rotational disorder of the Cp^* ligand could be found.

The alkyl chain in $[Cp^*Fe(CO)_2(n\text{-}C_5H_{11})]$ is in an extended, staggered conformation, and the iron carbon bond (2.07Å) shows remarkable insensitivity to the increased electron density going from the cyclopentadienyl compounds to the pentamethylcyclopentadienyl compound (i.e. the bond is of similar strength). This suggests that the greater instability of the cyclopentadienyl compounds has more to do with the bonding of the ancillary ligands than with the strength of the Fe-C(alkyl) bond. Indeed recent photochemical studies of iron acyl compounds have shown that on exposure to UV radiation the CO ligand is lost in the cyclopentadienyl compound, $[(\eta^5\text{-}C_5H_5)Fe(CO)(PPh_3)COMe]$, and the PPh_3 ligand is lost in the analogous pentamethylcyclopentadienyl compound, $[(\eta^5\text{-}C_5(CH_3)_5)Fe(CO)(PPh_3)COMe]$[79].

$[Cp^*Fe(CO)_2(n\text{-}C_5H_{11})]$, crystallizes in the monoclinic space group $P2_1/c$. There are 4 molecules per unit cell. The molecules are arranged in layers with the alkyl chains of the molecule oriented in opposite directions in alternate layers. Within each layer the alkyl chains are directed alternately upwards and downwards in the direction of the alkyl chain (See fig. 3.1.4). There are no significant intermolecular interactions within the crystal.

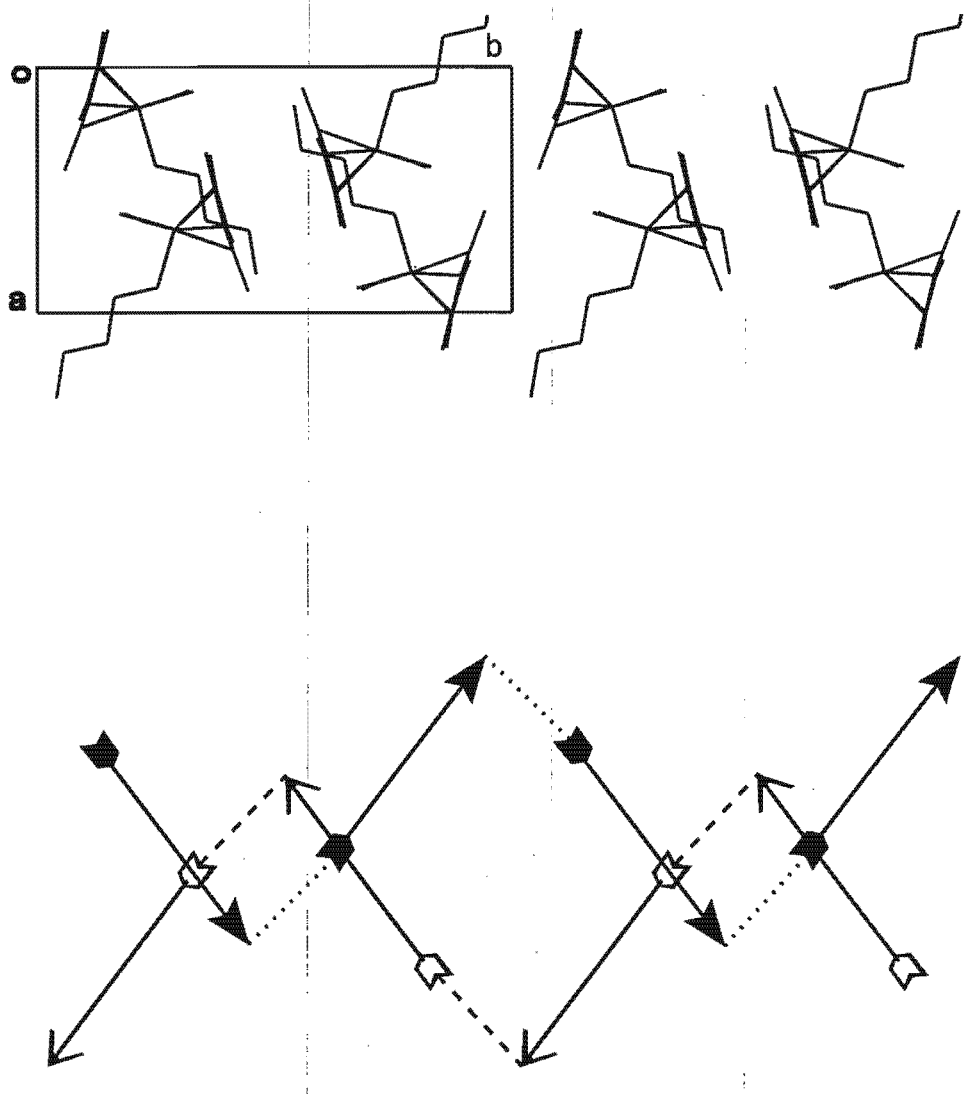

Figure 3.1.14 Crystal packing of $[(\eta^5\text{-}C_5(CH_3)_5)Fe(CO)_2(CH_2)_4CH_3]$ showing the orientation of the alkyl chains.

3.2. X-ray crystal and molecular structure of $[(\eta^5\text{-}C_5H_5)Fe(CO)_2C(O)CH_3]$

3.2.1. Introduction

Acyl compounds are important as intermediates in a number of catalytic reactions including the hydroformylation reaction for the synthesis of aldehydes from alkenes, carbon monoxide and hydrogen, co-polymerization of carbon monoxide and alkenes, acetic acid synthesis, and other carbonylation reactions. These reactions often involve migratory insertion of an alkyl ligand onto a carbonyl ligand to form an acyl ligand [80]. The aldehyde is formed by the reaction of the acyl ligand with hydrogen. Acyl species have also been proposed as intermediates in the Fischer-Tropsch reaction [81] (See Chapter 1).

The compound $[(\eta^5\text{-}C_5H_5)Fe(CO)_2(C(O)CH_3)]$ was first synthesized and characterized in 1956 by Piper and Wilkinson [82] and was one of the first transition metal acyl compounds to be synthesized. Since then, it has been the subject of numerous investigations [83-88], but no X-ray crystallographic study has ever been undertaken on this compound, or compounds of the general type $[(\eta^5\text{-}C_5H_5)Fe(CO)_2(C(O)R)]$ where R is a simple alkyl. This surprising fact may in part be due to the low melting point of most of these compounds and the difficulties in growing suitable single crystals. Extensive work has been done on the mono-substituted tertiary phosphine compounds of the type $[(\eta^5\text{-}C_5H_5)Fe(CO)(PR'_3)(C(O)R)]$, which are chiral [89-92].

3.2.2. Structures of iron acyl compounds

An analysis of structures of iron acyl compounds, as described by the fragments in Figure 3.2.1, stored in the Cambridge Structural Database (CSD) was carried out. In cases where there were multiple determinations of the same structure, the determination with the best solution was used.

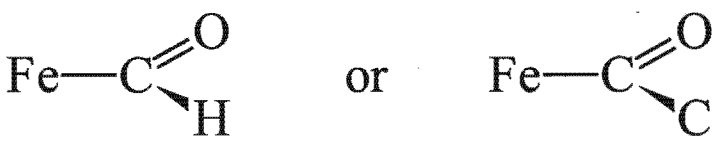

Figure 3.2.1. Fragments searched for in the Cambridge Structural Database.

Where there were multiple fragments reported (within the same molecule or enantiomers in the crystal structure) in a determination they are indicated by multiple entries of the same CSD refcode[a]. For example the compound $[(CpFe(CO)_2)_2(\mu\text{-}C(O)C_3F_6(O)C)]$ is a di-metallic bridged compound with each metal having an acyl group bonded to it. This is one compound, which contains two acyl fragments.

The analysis revealed a total of 161 different iron acyl compounds[b], involving 195 fragments of which 3 entries (4 fragments) were formyl compounds. The non-formyl compounds may be classified as follows:

A. **Compounds containing a cyclopentadienyl or substituted cyclopentadienyl (eg. pentamethylcyclopentadienyl) ligand coordinated to the iron.** 77 compounds were found involving 93 fragments.

B. **Compounds without a cyclopentadienyl or substituted cyclopentadienyl (eg pentamethylcyclopentadienyl) ligand coordinated to the iron.** 80 compounds were found involving 114 fragments.

C. **Compounds where the acyl ligand is part of a metallocycle.** 69 compounds were found involving 95 fragments.

D. **Compounds where the acyl ligand exhibits π-bonding to a metal (same or different metal from the acyl σ-bond).** 30 compounds were found involving 44 fragments. Of these only 4 were of the type where the π-coordination occurred

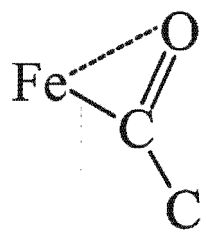

Figure 3.2.2 A π-bonded iron acyl fragment.

[a] Refcode is the unique alpha-numeric code given to each structure in the Cambridge Structural Database.

[b] This analysis was performed on an earlier release of the CSD, however a search of the latest release, although revealing structures which have since been added, did not produce any data to alter the conclusions reached in this thesis.

between the same metal to which the acyl ligand was bonded to (See Figure 3.2.2). This is clearly seen in Figure 3.2.3 where the O..Fe distance is reduced to between 1.9 and 2.2 Å (from a mean value of 2.9 Å), and the Fe-C=O angle reduced to below 93° from an ideal 120° (Sample mean: 126.5°). None of these four compounds were of type A (i.e. cyclopentadienyl compounds).

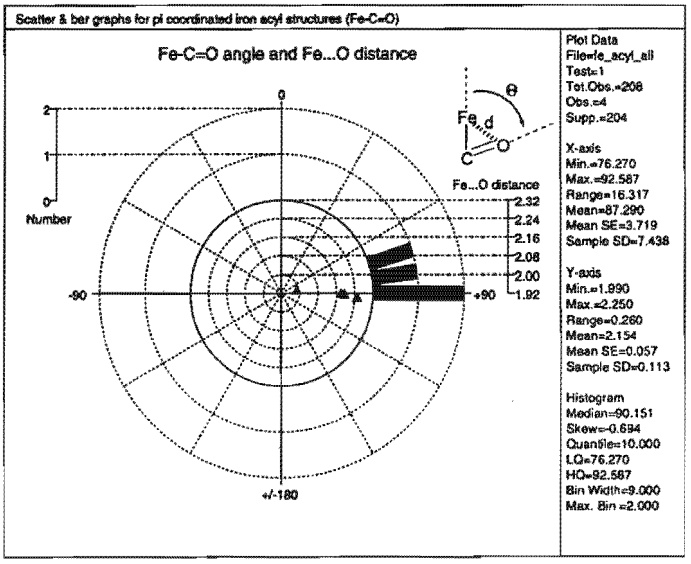

Figure 3.2.3 The Fe...O distance and the Fe-C=O bond angle in π-bonded iron acyl structures.

Note that some compounds were members of more than one of the above groups. A complete list of the entries, along with some of the key structural features, is given in Table 3.2.1. References for these structures may be found in Appendix C.

Table 3.2.1

Iron acyl compounds located in the Cambridge Crystallographic Database.

Cmpd	Frag	Refcode	Group(s)	Angles (degrees)			Distances (Å)			
				Fe-C=O	Fe-C-C	C-C=O	Fe-C	C=O	C-C	Fe...O
1	1	ACFENA	B	128.15	122.60	109.24	1.919	1.267	1.494	2.879
2	2	ACMPFE	A	123.73	119.65	116.44	1.964	1.228	1.531	2.836
3	3	APZBFE	B	124.30	118.99	116.69	1.967	1.193	1.521	2.818
4	4	BAPYEW	A	124.58	118.26	117.03	1.975	1.209	1.544	2.841
5	5	BIRBIN	B, C	124.31	115.19	120.50	2.026	1.202	1.546	2.880
6	6	BITYEI	A	126.04	123.75	110.21	1.878	1.287	1.515	2.833
7	7	BOPPAX10	B, D	117.91	127.08	115.00	1.962	1.244	1.494	2.771
	8	BOPPAX10	B, D	117.48	125.63	116.75	1.952	1.250	1.508	2.761
8	9	BOWBUK	B, D	114.81	130.62	113.90	1.910	1.325	1.499	2.744
9	10	BYFELI	B	123.86	119.74	116.37	1.988	1.227	1.534	2.859

Cmpd	Frag	Refcode	Group(s)	Angles (degrees)			Distances (Å)			
				Fe-C=O	Fe-C-C	C-C=O	Fe-C	C=O	C-C	Fe...O
10	11	BZPEFE	A	126.18	120.83	112.92	1.934	1.237	1.514	2.845
11	12	CALWAN	A	122.91	119.99	117.11	1.965	1.206	1.536	2.809
12	13	CECBUH	B, D	123.82	122.05	112.90	1.925	1.254	1.483	2.823
	14	CECBUH	B, D	122.59	122.26	114.79	1.917	1.245	1.475	2.792
13	15	CEZYIP	B, D	113.66	130.58	115.75	1.943	1.256	1.536	2.705
	16	CEZYIP	B, D	115.61	128.85	115.54	1.931	1.248	1.559	2.715
14	17	CFMTPI	A, C	126.91	115.19	117.89	1.954	1.215	1.522	2.854
15	18	CIYPIJ	A, D	125.63	121.98	112.25	1.920	1.261	1.517	2.846
	19	CIYPIJ	A, D	126.42	121.24	112.30	1.922	1.249	1.522	2.847
16	20	CORTAE10	A, C	123.95	114.36	121.57	1.984	1.218	1.495	2.849
17	21	CUBGIP	B	125.67	118.50	115.82	2.006	1.226	1.518	2.897
18	22	CUXBIG	A	123.57	119.19	117.07	1.952	1.217	1.540	2.814
19	23	CYPFEP	B, C	122.99	113.66	123.33	2.042	1.206	1.500	2.883
20	24	DAJNAD10	B, D	112.90	130.03	111.70	1.913	1.432	1.550	2.800
21	25	DAJNEH	B, D	117.49	126.58	115.44	1.936	1.256	1.512	2.751
22	26	DAWDUA	A	121.65	120.45	117.74	1.956	1.215	1.514	2.792
23	27	DCHPFE10	B, C	127.27	113.20	119.54	1.976	1.194	1.496	2.861
24	28	DEFCPO	B, C	124.64	113.88	121.45	2.014	1.210	1.483	2.880
	29	DEFCPO	B, C	124.97	113.58	121.45	2.003	1.205	1.489	2.869
25	30	DFMCFE10	A, C	133.33	109.89	116.78	1.989	1.214	1.543	2.957
26	31	DIWSUX	A, D	127.37	121.10	111.37	1.901	1.252	1.517	2.841
27	32	DOKHOA	A	121.81	120.18	117.98	1.967	1.211	1.517	2.801
28	33	DOKHUG	A	122.37	119.16	118.39	1.968	1.208	1.535	2.807
	34	DOKHUG	A	122.61	121.06	116.03	1.955	1.220	1.515	2.807
29	35	DOKXIK	A	125.08	116.64	118.14	1.976	1.185	1.539	2.829
30	36	DORBUH10	A, D	121.49	128.09	110.42	1.888	1.291	1.545	2.789
	37	DORBUH10	A, D	125.44	123.88	110.67	1.857	1.294	1.500	2.812
31	38	DORCAO10	A, D	127.08	124.68	108.25	1.862	1.290	1.500	2.834
	39	DORCAO10	A, D	126.69	124.69	108.57	1.867	1.289	1.516	2.833
32	40	DORHAT	B	122.79	123.84	113.23	2.000	1.211	1.533	2.845
33	41	DUHFUH	A, C	129.15	115.62	115.22	1.907	1.223	1.542	2.842
34	42	DUHXOT	A	122.84	118.87	118.28	1.958	1.223	1.488	2.816
35	43	DUZBIJ	B, D	90.37	145.01	124.26	1.805	1.236	1.486	2.194
	44	DUZBIJ	B, D	89.94	148.33	121.48	1.804	1.229	1.432	2.181
36	45	EMOPFC	B, C	144.41	75.84	138.96	1.960	1.194	1.449	3.013
37	46	FAMNAI	A	123.10	120.59	116.21	1.950	1.228	1.523	2.815
38	47	FCPENO	B, C	126.09	112.99	120.91	2.016	1.210	1.477	2.898
39	48	FEBNAB	A, D	118.90	126.22	114.82	1.923	1.289	1.482	2.785
40	49	FEBNEF	A, D	117.78	127.83	114.09	1.919	1.286	1.496	2.763
41	50	FECPCC10	B, C	125.88	113.28	120.83	2.005	1.213	1.511	2.889
42	51	FEHTUH	A	123.08	118.30	118.50	1.956	1.208	1.520	2.805
43	52	FELFOR	A	124.77	115.85	119.36	1.962	1.211	1.497	2.832
44	53	FEYBAM	B, C	148.25	75.63	135.31	1.913	1.213	1.450	3.013
45	54	FICBOI	B	124.94	119.77	115.30	2.006	1.183	1.506	2.853
46	55	FISBIS10	B, C	124.16	112.44	123.39	2.044	1.200	1.456	2.894
47	56	FIZMIK	A, C	127.79	115.53	116.60	1.951	1.204	1.554	2.852
48	57	FIZPOT	A, C	126.63	116.60	116.77	1.957	1.207	1.540	2.846
49	58	FOBDOP	B, C	124.12	113.49	122.15	2.024	1.201	1.524	2.875
50	59	FOCTUM	B, D	115.00	130.22	114.68	1.929	1.248	1.504	2.705
51	60	FOHGIS	A, C	124.86	116.05	119.08	1.970	1.217	1.499	2.846

Cmpd	Frag	Refcode	Group(s)	Angles (degrees)			Distances (Å)			
				Fe-C=O	Fe-C-C	C-C=O	Fe-C	C=O	C-C	Fe...O
52	61	FORTOV	B, C	146.78	78.47	133.82	1.857	1.213	1.479	2.949
53	62	FUWMEP	B	126.40	115.69	117.90	1.991	1.218	1.522	2.885
54	63	FUXGUA	B, D	92.59	142.01	125.40	1.827	1.233	1.508	2.250
55	64	FUXHUB	A	123.69	117.70	118.44	1.967	1.220	1.519	2.832
56	65	GACWIQ	B, C	144.63	75.88	138.33	1.928	1.200	1.448	2.988
	66	GACWIQ	B, C	145.14	76.19	137.48	1.922	1.208	1.442	2.994
	67	GADWEN01	A	124.55	121.14	114.27	1.939	1.215	1.462	2.812
57	68	GADWEN02	A	123.09	122.83	114.01	1.917	1.234	1.490	2.789
58	69	GAKJEH	A	123.08	122.14	114.70	1.952	1.228	1.546	2.817
59	70	GARHOW	B, D	76.27	162.91	120.79	1.856	1.283	1.490	1.990
60	71	GATZAC	B, C	124.40	118.61	116.89	2.010	1.230	1.504	2.889
61	72	GEGHEF	A	123.19	120.93	115.76	1.945	1.220	1.508	2.805
62	73	GEJFAC	B, C	147.98	66.73	144.77	2.054	0.998	1.391	2.948
63	74	GIBTUG	A	122.54	118.70	118.60	1.964	1.215	1.509	2.811
64	75	GIKDIN	B, C	126.27	117.48	115.73	2.018	1.223	1.516	2.914
	76	GIKDIN	B, C	126.96	114.41	118.63	1.974	1.241	1.468	2.895
65	77	HAPSIA	A	121.64	121.58	116.45	1.973	1.213	1.547	2.807
66	78	HEMCOR	B, D	121.70	126.79	111.33	1.996	1.203	1.542	2.821
	79	HEMCOR	B, D	120.59	125.39	114.02	1.993	1.247	1.541	2.838
67	80	HXCPFE10	A, C	126.94	115.68	117.38	1.960	1.206	1.554	2.852
68	81	JALKEM	B, D	143.80	75.15	139.80	1.936	1.208	1.442	2.996
69	82	JAWKOH	A	124.32	122.65	112.81	1.920	1.219	1.512	2.794
70	83	JUCJEW	A	123.62	119.09	117.09	1.943	1.210	1.526	2.801
	84	JUCJEW	A	121.50	121.06	117.34	1.950	1.210	1.500	2.781
71	85	JUDNEB	A	123.35	121.47	114.85	1.952	1.217	1.556	2.811
	86	JUDNEB01	A	125.78	118.58	115.41	1.928	1.213	1.593	2.815
72	87	JUZHIV	A, C	143.82	75.07	139.31	1.889	1.196	1.437	2.940
73	88	KAJLOW	B, C	137.62	71.09	126.88	2.138	1.220	1.463	3.149
	89	KAJLOW	B, C	120.56	110.65	126.88	2.179	1.220	1.463	2.990
74	90	KAJLOW10	B, C	137.62	71.09	126.88	2.138	1.220	1.463	3.149
	91	KAJLOW10	B, C	120.56	110.65	126.88	2.179	1.220	1.463	2.990
75	92	KAJNAK	A	124.15	118.88	116.79	1.972	1.217	1.520	2.840
76	93	KAJYID	B, C	122.05	114.38	123.37	2.067	1.229	1.473	2.912
77	94	KALTOG	A	131.93	115.50	112.56	1.907	1.147	1.591	2.806
78	95	KAVVOS	A	128.04	119.79	112.14	1.926	1.213	1.498	2.839
79	96	KAXFOE	A, C	128.83	113.73	117.42	1.955	1.208	1.530	2.871
80	97	KAXYAJ	B, C	140.64	76.38	142.65	1.965	1.161	1.450	2.956
81	98	KEDSER	B, D	121.68	117.26	120.78	1.913	1.313	1.451	2.832
82	99	KEDSIV	B, D	120.89	116.83	122.12	1.938	1.295	1.452	2.831
83	100	KEDSOB	B, D	122.60	114.69	122.56	1.935	1.286	1.466	2.842
84	101	KETFEA	B, C	143.89	79.90	135.07	1.871	1.229	1.379	2.954
	102	KETFEA	B, C	143.75	77.48	138.11	1.883	1.218	1.439	2.954
	103	KETFEA11	B, C	145.55	76.90	135.81	1.914	1.203	1.470	2.984
	104	KETFEA11	B, C	145.29	77.31	136.00	1.900	1.206	1.463	2.972
85	105	KEWSEK	A	124.33	115.86	119.75	1.962	1.212	1.538	2.828
86	106	KEWSIO	A, D	122.21	122.04	115.45	1.925	1.261	1.532	2.808
87	107	KINFOC	B, C	131.50	61.58	166.90	2.315	1.179	1.317	3.220
88	108	KISZAN	A, C	134.55	74.35	150.59	1.981	1.236	1.343	2.981
89	109	KITVAK	A	118.28	126.01	115.71	1.982	1.232	1.471	2.786
90	110	KITVEO	A	121.29	123.33	115.35	1.959	1.219	1.514	2.794

Cmpd	Frag	Refcode	Group(s)	Angles (degrees)			Distances (Å)			
				Fe-C=O	Fe-C-C	C-C=O	Fe-C	C=O	C-C	Fe...O
91	111	KOJDES	B, C	126.72	114.31	118.63	2.018	1.204	1.558	2.903
92	112	KUCGIY	B, C	149.04	79.13	131.05	1.833	1.229	1.493	2.955
93	113	KUCTEH	B, C	113.14	120.91	125.95	2.114	1.274	1.580	2.865
	114	KUCTEH	B, C	133.01	118.44	107.89	1.923	1.179	1.554	2.861
94	115	KUWSIE	A	127.90	119.39	112.66	1.953	1.213	1.556	2.863
	116	KUWSIE	A	127.41	122.03	109.64	1.919	1.185	1.543	2.801
95	117	LAGHAC	B, C	144.10	75.23	140.21	1.976	1.189	1.442	3.021
96	118	LAGHEG	B, C	144.26	75.14	140.18	1.973	1.196	1.442	3.026
97	119	LAJPUH	A, D	120.93	128.39	110.66	1.946	1.319	1.431	2.857
98	120	LEXYUI	B	118.50	118.95	122.46	1.965	1.205	1.477	2.751
99	121	LEZVAN	A	120.91	118.85	120.16	1.992	1.220	1.502	2.821
100	122	MAFOTR	B, C	126.14	112.76	120.96	1.957	1.194	1.522	2.830
101	123	MPYMYF10	B, C	125.72	113.64	120.63	2.011	1.201	1.504	2.883
	124	MPYMYF10	B, C	124.34	113.44	122.22	2.035	1.207	1.494	2.893
102	125	MXBYFE10	B, C	147.47	78.91	133.55	1.899	1.204	1.488	2.986
	126	MXBYFE10	B, C	146.23	79.10	134.40	1.916	1.192	1.488	2.981
103	127	NPICPO	B, C	124.82	112.74	122.44	2.035	1.215	1.491	2.905
104	128	PATYEO	B, C	124.87	114.19	120.74	2.028	1.189	1.521	2.878
	129	PATYEO	B, C	124.52	111.99	123.28	2.046	1.190	1.506	2.891
105	130	PIGVAC	B, C	124.53	111.85	123.60	1.983	1.266	1.434	2.895
106	131	PIHMOI	B, C	145.00	77.38	135.97	1.917	1.207	1.453	2.987
107	132	PIRDID	A	122.28	119.28	118.21	1.954	1.234	1.527	2.813
108	133	PIRDOJ	A	121.32	120.14	118.30	1.941	1.252	1.523	2.804
109	134	POTFIN	B, D	113.36	125.14	121.39	1.941	1.248	1.491	2.692
110	135	PRACFE	A	117.89	118.72	123.30	2.038	1.235	1.390	2.834
111	136	SATVUE	A	120.86	117.07	121.63	2.008	1.219	1.481	2.834
112	137	SATWAL	A	119.76	117.63	122.50	2.002	1.208	1.475	2.805
113	138	SATWEP	A	122.33	117.44	120.16	1.991	1.203	1.534	2.824
114	139	SAXWAP	A, C	126.22	117.23	116.48	1.954	1.235	1.532	2.862
115	140	SAZYOH	B, D	111.64	131.38	116.98	1.978	1.260	1.482	2.710
116	141	SEHZEK	B, C	123.12	117.77	118.97	2.043	1.213	1.505	2.890
	142	SEHZEK	B, C	123.27	118.29	118.42	2.035	1.207	1.508	2.880
117	143	SIFPEC	B, C	146.32	77.74	135.39	1.910	1.194	1.460	2.978
	144	SIFPEC	B, C	146.40	77.34	135.86	1.934	1.185	1.484	2.993
118	145	SIFPIG	B, C	145.94	77.31	135.76	1.905	1.202	1.465	2.978
119	146	SIHLOK	A, D	123.42	127.96	105.85	1.799	1.298	1.584	2.737
	147	SIHLOK	A, D	125.22	113.36	120.44	2.029	1.204	1.539	2.895
120	148	SIZNUK	A, C	143.14	75.96	140.01	1.895	1.198	1.434	2.943
121	149	SIZPAS	A, C	144.22	76.43	138.21	1.888	1.200	1.449	2.946
122	150	SOBPAA	B, C	130.73	107.72	121.15	1.978	1.220	1.479	2.924
123	151	SOGXOB	A	125.68	115.82	118.31	1.965	1.209	1.534	2.844
124	152	SOTYEF	A	124.25	120.61	115.06	1.939	1.211	1.522	2.806
125	153	TACFAE	B, C	143.94	61.47	128.19	2.426	1.207	1.468	3.475
126	154	TAKCUD	B	118.93	126.51	114.36	1.974	1.208	1.366	2.768
127	155	TCTAFE	B, C	145.32	76.92	137.42	1.917	1.190	1.470	2.974
128	156	TEAFEA	B, D	116.83	127.82	113.76	1.888	1.317	1.542	2.747
129	157	VAKBEO	B, C	146.06	76.61	135.86	1.907	1.226	1.465	3.003
130	158	VAKBIS	B, C	146.25	77.64	131.87	1.906	1.202	1.488	2.981
131	159	VAKDUG	A, C	128.31	115.38	116.31	1.928	1.221	1.525	2.851
132	160	VEBVUT	B, C, D	118.11	120.53	121.33	1.941	1.253	1.443	2.762

Cmpd	Frag	Refcode	Group(s)	Angles (degrees)			Distances (Å)			
				Fe-C=O	Fe-C-C	C-C=O	Fe-C	C=O	C-C	Fe...O
133	161	VEHPON	B, C	128.61	111.26	119.73	1.969	1.221	1.470	2.893
134	162	VESJOS	B	121.89	119.47	118.60	1.994	1.162	1.485	2.788
135	163	VETHEH	B, C	129.80	111.79	118.39	1.994	1.201	1.550	2.912
136	164	VETHIL	B, C	124.22	120.50	115.28	2.002	1.204	1.557	2.858
	165	VETHIL	B, C	124.52	119.82	115.66	2.008	1.202	1.561	2.866
137	166	VETHOR	B, C	130.14	110.78	119.08	1.992	1.194	1.549	2.909
138	167	VIVNET	B, D	114.41	129.73	115.85	2.002	1.252	1.479	2.766
	168	VIVNET	B, D	114.66	129.16	116.18	2.009	1.246	1.486	2.771
139	169	VIVNIX	B, D	117.63	125.74	116.61	1.979	1.245	1.494	2.784
140	170	VIVTEZ	A	120.85	122.00	116.94	1.964	1.225	1.513	2.797
141	171	VOKZAW	B, C	124.08	114.11	121.81	2.023	1.194	1.489	2.868
	172	VOKZAW	B, C	122.79	114.86	122.35	2.008	1.216	1.512	2.856
142	173	VOVWOS	A, C	126.80	113.52	119.66	1.943	1.218	1.532	2.845
143	174	VOVWUY	A, C	126.56	112.12	121.13	1.952	1.208	1.538	2.842
144	175	VOVXAF	A	120.92	118.84	120.05	1.994	1.202	1.520	2.808
145	176	VOWTUW	A	124.66	120.68	114.60	1.949	1.226	1.539	2.832
	177	VOWTUW	A	125.03	119.00	115.95	1.951	1.229	1.521	2.841
146	178	VOWVAE	A	119.93	124.94	115.11	1.966	1.204	1.569	2.771
147	179	VOZMOM	A	124.40	118.80	116.70	1.964	1.198	1.510	2.820
148	180	VULNAR	A, C	129.95	116.29	113.75	1.938	1.191	1.640	2.853
149	181	WAGKIY	B, C	144.18	77.73	137.34	1.903	1.187	1.472	2.948
150	182	WAJYOV	A	122.13	121.12	116.67	1.961	1.227	1.531	2.812
151	183	WAJYUB	A	121.96	121.99	115.97	1.954	1.221	1.572	2.800
152	184	WEDMAT	A	121.18	121.28	117.42	1.955	1.243	1.534	2.808
153	185	YAWGIM	A	120.33	121.08	118.44	1.956	1.214	1.541	2.775
154	186	YEBYOT	B, C	121.03	115.02	123.94	2.049	1.205	1.514	2.863
155	187	YIBVEK	A, C	126.80	118.33	114.87	1.942	1.232	1.531	2.856
	188	YIBVEK	A, C	126.91	118.65	114.30	1.946	1.236	1.522	2.865
156	189	YIFNIK	B, C	123.88	114.93	121.20	2.028	1.205	1.553	2.879
157	190	YISLAN	B, C	130.75	107.78	121.48	1.971	1.196	1.498	2.897
158	191	YOTMUP	A	128.09	117.75	114.15	1.928	1.192	1.534	2.824

The primary focus of this study was the compounds with a cyclopentadienyl or substituted cyclopentadienyl (eg. pentamethylcyclopentadienyl) ligand coordinated to the iron. In particular those compounds of the general formula [CpFe(L)(L′)(C(O)R)] where Cp = cyclopentadienyl or substituted cyclopentadienyl, L, L′ = CO or tertiary phosphine, R = H or an organic fragment (eg. alkyl), and the acyl was not part of a metallocycle or involved in π-coordination with a metal. These compounds, a subset of type A, designated type A′, could be further classified as follows:

A1. **Di-carbonyl compounds (i.e. $CpFe(CO)_2(C(O)R)$).** There were seven compounds of this type found in the database. Of these four had acyl ligands which were part of a bridge between two metals. The remaining three compounds had bulky R groups (See Table 3.2.2 & Figure 3.2.4). No structures of simple acyl compounds of the type $[CpFe(CO)_2(C(O)R)]$ were found.

A2. **Bis-phosphine compounds (i.e. $CpFe(PXYZ)_2(C(O)R)$).** There were only two compounds of this type in the database, $[CpFe(PMe_3)_2(C(O)C_2H_5)]$ (BITYEI) [93]and $[CpFe(PPh_2C_2H_4PPh_2)(C(O)C_2H_5)]$ (BZPEFE) [94]. Note that in the second structure the phosphine is a bidentate ligand (See Figure 3.2.5).

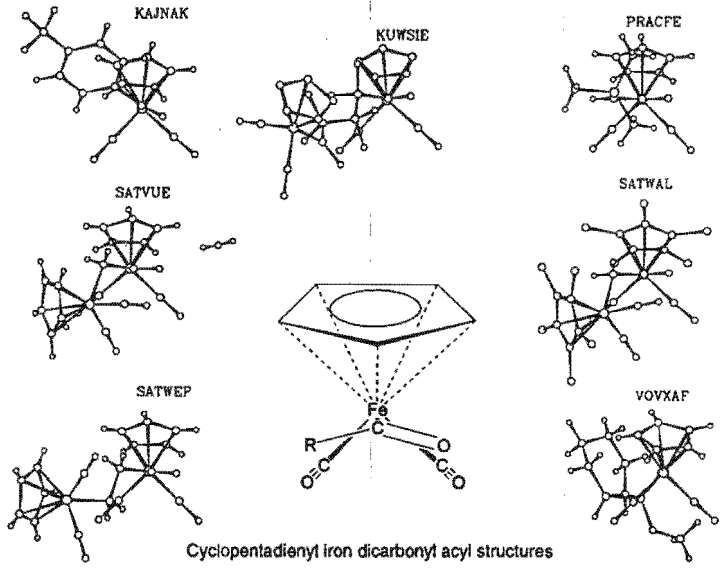

Figure 3.2.4 View of the seven $[CpFe(CO)_2C(O)R]$ acyl structures found in the Cambridge Structural Database. Structures are viewed along the C(acyl)-Fe bond.

A3. Mono-carbonyl, mono-phosphine compounds (i.e. CpFe(CO)(PXYZ)C(O)R), where X, Y, and Z are substituents (eg. phenyl). This was by far the largest group of structures with 41 different compounds located. This is probably due to the fact that these compounds are chiral and have significance in chiral syntheses [91,95]. The majority of the compounds have PPh_3 as the tertiary phosphine ligand and C_5H_5 as the cyclopentadienyl ligand (i.e. the differences are in the acyl ligand itself). 13 of the structures had R = simple alkyl. A detailed list of structural features is given in Table 3.2.2.

A4. Compounds where the acyl is part of a bridge between two metals. There were four structures of this type, all of which were also dicarbonyl compounds (i.e. of type A1).

A5. Compounds where the tertiary phosphine is very bulky (eg. $((Ph)_2PC_4H_5)W(CO)_3CH_3$. Compounds of this type had substituents on phosphorus which were much larger than phenyl. There were four structures which were in this class.

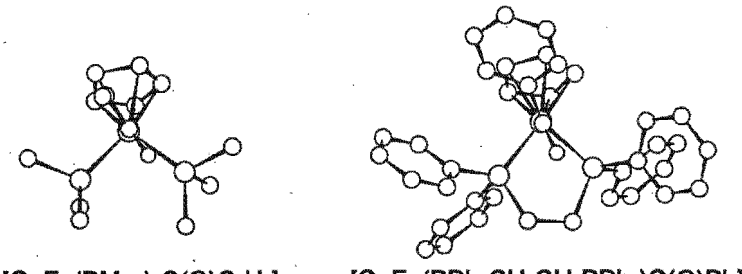

[CpFe(PMe$_3$)$_2$C(O)C$_2$H$_5$] (BITYEI)

[CpFe(PPh$_2$CH$_2$CH$_2$PPh$_2$)C(O)Ph] (BZPEFE)

Figure 3.2.5 View of the two bis-phosphine cyclopentadieyl iron acyl structures found in the Cambridge Structural Database.

A6. Compounds with a substituted cyclopentadienyl ligand (eg. pentamethylcyclopentadienyl or indenyl). There were 10 structures of this type in the database.

A7. Compounds with a bulky R group (eg. $CH_2CH_2C(CN)(CH(CH_3)_2)(3, 4\text{-}C_6H_3(OCH_3)_2)$). Structures of this type included all compounds with substituents larger than a simple unbranched alkyl, including bridged structures. There were 41 compounds of this type.

A total of 60 fragments were found involving 50 compounds of type A', [CpFe(L)(L')(C(O)R)]. Of these only one was a formyl compound (2 fragments). The formyl compound, $[(\eta^5\text{-}C_5Ph_5)Fe(CO)(PMe_3)(CHO)]$, had a structure with disorder between the CHO ligand and the CO ligand. This gave an "averaged" structure for the two ligands, making a detailed analysis of it impossible (See Figure 3.2.6).

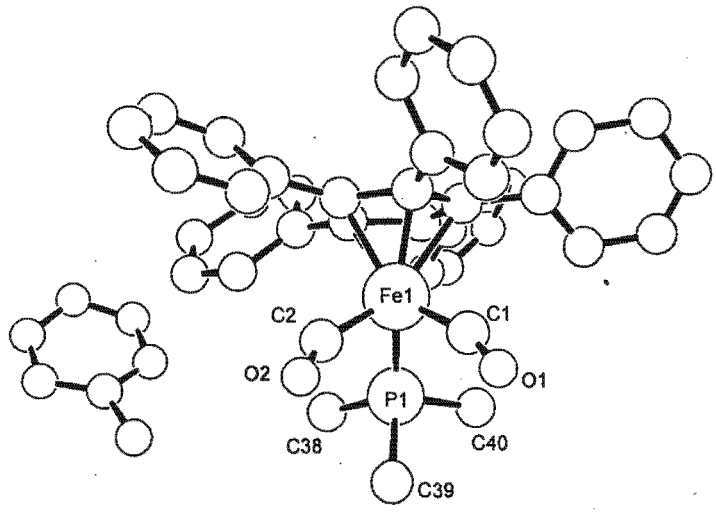

Figure 3.2.6 The structure of $[(\eta^5\text{-}C_5Ph_5)Fe(CO)(PMe_3)CHO]$ (YECHIX01) showing the average of the formyl ligand and the carbonyl.

Table 3.2 Cyclopentadienyl iron acyl structures (Type A′, i.e. [CpFe(L)(L′)(C(O)R)] where L, L′ = CO or PR″$_3$).

Entry	CSD								Torsion	Bond length (Å)				Angle
No.	Refcode	$(CO)_2$	$(PXYZ)_2$	(CO)PXYZ	XL-Phosphine	Bridged	Sub-Cp	Sub-R	X1-Fe-C=O	Fe-X1	Fe-C	C=O	C-C	Fe-C=O
1	ACMPFE			PPh_3			1-Me, 3-Ph	$-CH_3$	89.56	1.758	1.964	1.228	1.531	123.73
2	BAPYEW			-P(Ph)NHMePh			C_5H_5	$-CH_3$	158.50	1.756	1.975	1.209	1.544	124.58
3	BITYEI		PMe_3				C_5H_5	$-C_2H_5$	-148.74	1.799	1.878	1.287	1.515	126.04
4	BZPEFE		$(-CH_2PPh_2)_2$				C_5H_5	-Ph	-159.41	1.740	1.934	1.237	1.514	126.18
5	CALWAN			PPh_3			C_5H_5	-CHEtMe	60.05	1.752	1.965	1.206	1.536	122.91
6	CUXBIG			PPh_3			C_5H_5	$-CH_2CH(OH)Ph$	68.97	1.740	1.952	1.217	1.540	123.57
7	DAWDUA			PPh_3			C_5H_5	$-CH_2CH_2CH(OH)Ph$	51.92	1.743	1.956	1.215	1.514	121.65
8	DOKHOA			$P(OPh)_3$			C_5H_5	$-(C(CH_3))_2Ph$	-45.26	1.738	1.967	1.211	1.517	121.81
9	DOKHUG			$P(OPh)_3$			C_5H_5	$-(C(CH_3))_2SPh$	-64.71	1.740	1.968	1.208	1.535	122.37
	DOKHUG			$P(OPh)_3$			C_5H_5	$-(C(CH_3))_2SPh$	-58.97	1.744	1.955	1.220	1.515	122.61
10	DOKXIK			PPh_3			C_5H_5	-metholato-propionyl	91.28	1.739	1.976	1.185	1.539	125.08
11	DUHXOT			PPh_3			C_5H_5	$-transCHCHCH_3$	65.57	1.746	1.958	1.223	1.488	122.84
12	FAMNAI			PPh_3			C_5H_5	-CH2CH(NHPh)Ph	52.24	1.743	1.950	1.228	1.523	123.10
13	FEHTUH			PPh_3			C_5H_5	$-CH_2$-cyclopropyl	-72.82	1.747	1.956	1.208	1.520	123.08
14	FELFOR			PPh_3			C_5H_5	$-cisCHCHCH_3$	77.38	1.750	1.962	1.211	1.497	124.77
15	FUXHUB			$P(OPh)_3$			C_5H_5	$C(CH_2OMe)=C(Ph)Me$	-59.47	1.740	1.967	1.220	1.519	123.69
16	GADWEN01			PPh_3			C_5H_5	$-CH_3$	-75.60	1.760	1.939	1.215	1.462	124.55
17	GADWEN02			PPh_3			C_5H_5	$-CH_3$	-64.65	1.752	1.917	1.234	1.490	123.09
18	GAKJEH			PPh_3			C_5H_5		-57.58	1.747	1.952	1.228	1.546	123.08
19	GEGHEF			PMe_2Ph			C_5H_5	$-CH_3$	61.61	1.738	1.945	1.220	1.508	123.19
	GEGHEF01			PMe_2Ph			C_5H_5	$-CH_3$	61.34	1.739	1.949	1.214	1.514	123.02
20	GIBTUG			PPh_3			C_5H_5		-67.42	1.746	1.964	1.215	1.509	122.54
21	HAPSIA			PPh_3			C_5H_5		56.07	1.757	1.973	1.213	1.547	121.64
22	JAWKOH			PPh_3			C_5H_4Me	$-CH_3$	-65.66	1.747	1.920	1.219	1.512	124.32
23	JUCJEW			PPh_3			Indenyl	$-CH_3$	77.63	1.792	1.943	1.210	1.526	123.62

Entry No.	CSD Refcode	$(CO)_2$	$(PXYZ)_2$	(CO)PXYZ	XL-Phosphine	Bridged	Sub-Cp	Sub-R	Torsion X1-Fe-C=O	Bond length (Å) Fe-X1	Fe-C	C=O	C-C	Angle Fe-C=O
	JUCJEW			PPh_3			Indenyl	$-CH_3$	68.21	1.796	1.950	1.210	1.500	121.50
24	JUDNEB			PPh_3			C_5H_5	-Ph	70.74	1.737	1.952	1.217	1.556	123.35
	JUDNEB01			PPh_3			C_5H_5	-Ph	75.80	1.736	1.928	1.213	1.593	125.78
25	KAJNAK						C_5H_5	$p\text{-}C_6H_4(CF_3)$	-117.79	1.743	1.972	1.217	1.520	124.15
26	KALTOG			$P(Ph_2)(CpW(CO)_3CH_3$			C_5H_5	$-CH_3$	89.78	1.742	1.907	1.147	1.591	131.93
27	KAVVOS			PPh_2Me			C_5H_4Me	$-CH_3$	88.28	1.738	1.926	1.213	1.498	128.04
28	KEWSEK			PPh_3			C_5H_5	$CH_2CH(Ph)(OTiCl_2(Cp)_2$	-84.61	1.746	1.962	1.212	1.538	124.33
29	KITVAK			PPh_3			C_5H_5	$C_5H_5NCH_3$	80.54	1.753	1.982	1.232	1.471	118.28
30	KITVEO			PPh_2(menthyl oxy)			C_5H_5	nicotinyl	78.06	1.748	1.959	1.219	1.514	121.29
31	KUWSIE					$-C_3F_6C=O-$	C_5H_5	$-C_3F_6C(O)-(CpFe(CO)_2)$	-92.59	1.745	1.953	1.213	1.556	127.90
	KUWSIE					$-C_3F_6C=O-$	C_5H_5	$-C_3F_6C(O)-(CpFe(CO)_2)$	84.14	1.717	1.919	1.185	1.543	127.41
32	LEZVAN			PPh_3			C_5H_5	-C4H9	82.61	1.750	1.992	1.220	1.502	120.91
33	PIRDID			PPh_3			C_5H_5		-75.02	1.752	1.954	1.234	1.527	122.28
34	PIRDOJ			PPh_3			C_5H_5		61.39	1.739	1.941	1.252	1.523	121.32
35	PRACFE						C_5H_5	$-CH=P(CH_3)_3$	-86.52	1.751	2.038	1.235	1.390	117.89
36	SATVUE					$-CH_2-$	C_5H_5	$-CH_2(CpFe(CO)_2$	88.74	1.743	2.008	1.219	1.481	120.86
37	SATWAL					$-CH_2-$	Cp*	$-CH_2(Cp^*Fe(CO)_2$	-81.92	1.752	2.002	1.208	1.475	119.76
38	SATWEP					$-CH_2CH_2-$	C_5H_5	$-CH_2CH_2(CpFe(CO)_2$	-91.81	1.738	1.991	1.203	1.534	122.33
39	SOGXOB			PPh_3			C_5H_5	$-CH_2OCH_3$	73.84	1.745	1.965	1.209	1.534	125.68
40	SOTYEF			PPh_2Me			C_5H_4Me	$-CH_3$	75.61	1.733	1.939	1.211	1.522	124.25
41	VIVTEZ			PPh_3			C_5H_5	$-CH_2P(Ph)_2$	59.90	1.746	1.964	1.225	1.513	120.85
42	VOVXAF						C_5H_5	$-CH(OCH_3)C_6H_9$	41.20	1.741	1.994	1.202	1.520	120.92
43	VOWTUW			PPh_3			C_5H_5	$-C(=CH_2)(OCH_2Ph)$	83.61	1.737	1.949	1.226	1.539	124.66
	VOWTUW			PPh_3			C_5H_5	$-C(=CH_2)(OCH_2Ph)$	-68.45	1.740	1.951	1.229	1.521	125.03
44	VOWVAE			PPh_3			C_5H_5	$-CH(OCH_2Ph)(C_5H_{11})CH_3$	78.35	1.745	1.966	1.204	1.569	119.93

Entry	CSD								Torsion	Bond length (Å)				Angle
No.	**Refcode**	**$(CO)_2$**	**$(PXYZ)_2$**	**(CO)PXYZ**	**XL-Phosphine**	**Bridged**	**Sub-Cp**	**Sub-R**	**X1-Fe-C=O**	**Fe-X1**	**Fe-C**	**C=O**	**C-C**	**Fe-C=O**
45	VOZMOM			PPh_3				$-CH_3$	65.34	1.750	1.964	1.198	1.510	124.40
46	WAJYOV			PPh_3			C_5H_5	$-CH(Ph)(C(CH_3)_2OH)$	99.04	1.743	1.961	1.227	1.531	122.13
47	WAJYUB			PPh_3			C_5H_5	$-CH(Ph)(C(CH_3)(H)OH)$	71.91	1.753	1.954	1.221	1.572	121.96
48	WEDMAT			PPh_3			Cp*	$-C_2H_2Ph$	-70.46	1.767	1.955	1.243	1.534	121.18
49	YAWGIM						Indenyl	-iPr	-61.52	1.797	1.956	1.214	1.541	120.33
50	YOTMUP			$P(Ph)_2(C_5H_4PPh_2Fe(CO)_2C_5H_5Me$			C_5H_5	$-CH_3$	98.87	1.748	1.928	1.192	1.534	128.09

Note: References for these structures may be found in Appendix C.

All the structures used in this part of the study had R factors of R < 0.10, except for $[(\eta^5\text{-}C_5H_5)Fe(PMe_3)_2(C(O)CH_3)]$ (Refcode BITYEI) [93] which had R = 0.1170. It was included in the analysis as it was one of only two bis-tertiary phosphine compounds (type A2) found in the database. The iron atom in these types of structures (i.e. [CpFe(L)(L′)(C(O)R)]) is pseudo-octahedral [88], where the cyclopentadienyl ligand occupies three coordination sites. The iron to acyl-carbon bond length in all the structures found was in the range 1.799 to 2.426 Å (See Figure 3.2.7), and those structures of type A′ in the range 1.878 to 2.038 Å, which is slightly shorter than the iron alkyl bond (sp^3 hybridised, 1.852 to 2.201 Å) in cyclopentadienyl iron alkyl compounds (See section 3.1.1 above), and corresponds to an iron-carbon single bond.

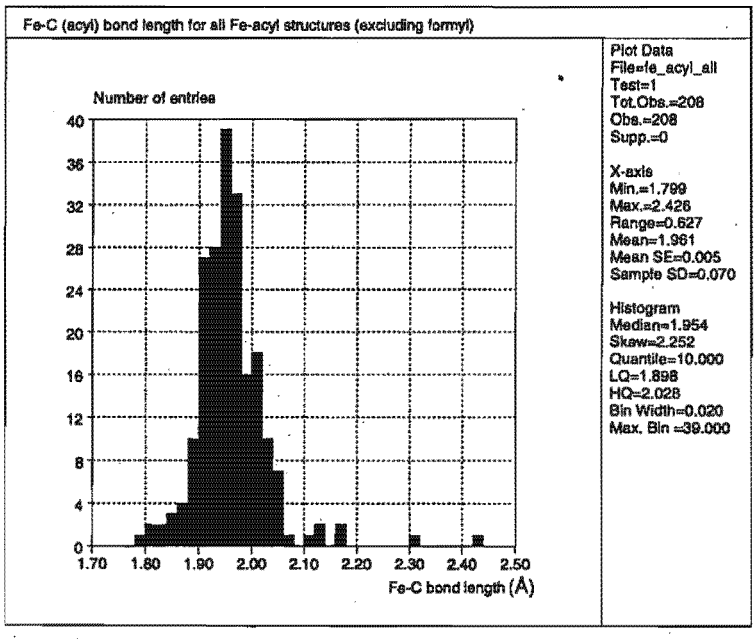

Figure 3.2.7 Histogram showing the distribution of Fe-C(acyl) bond lengths for the iron acyl compounds found in the Cambridge Structural Database.

The conformation of the acyl group, in compounds of the type $[CpFe(CO)(PR'_3)(C(O)R)]$, with respect to the other ligands around the metal has been studied in detail some years ago using van der Waals (steric) interaction calculations [88]. Conformational analysis is a standard technique for understanding product selectivity in organic chemistry, and has more recently been applied to organometallic chemistry, particularly reactions of the chiral auxiliary $CpFe(CO)(PPh_3)$ [88,96,97]. The importance of this type of reaction is exemplified by the recent

commercialization of a variety of metallocene catalysts for the production of highly ordered polymers [98,99]. It is useful in the context of type A compounds (i.e. cyclopentadienyl iron acyl compounds) to examine this area of conformation in more detail. The acyl ligand's conformation may be described by the torsion angle defined from the centroid of the cyclopentadienyl ligand to the iron atom, to the acyl carbon and finally to the acyl oxygen (ie. Cp-Fe-C=O). The acyl oxygen would be in an eclipsed position with the cyclopentadienyl ligand at a torsion angle of 0° and with the phosphine and/or carbonyl ligands at approximately ±135° (See Figure 3.2.8). As

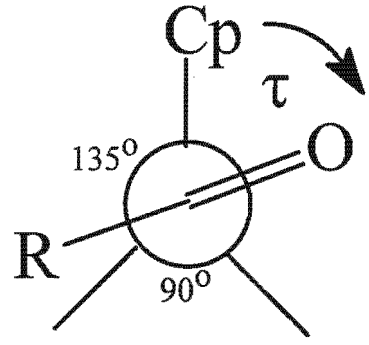

Figure 3.2.8 Torsion angle defining the conformation of the acyl ligand.

the substituent on the acyl was never observed to occur in between the cyclopentadienyl and tertiary phosphine ligands, or on the tertiary phosphine half of the molecule, torsion values between -180° to 0° are redundant. All negative torsions (caused by the presence of different enantiomers) could be converted to positive values without loss of information. The torsion angles found for these compounds are shown in Figure 3.2.9. As can be seen, all except three structures have a torsion angle between 0° and ±135° (i.e. the oxygen and carbon substituents of the acyl lie between the Cp and one of the other ligands).

The seven dicarbonyl structures which are shown in Figure 3.2.4 all adopt a conformation with a Cp-Fe-C=O torsion angle between 41° and 118° (i.e. the acyl orientated between the Cp and the carbonyl ligands). Of the seven compounds, four have acyl groups which form part of a metal-metal bridge (type A4), one has a pentamethylcyclopentadienyl ligand (type A6) and all of them have bulky R groups attached to the acyl. It appears from these seven structures and that of $[(\eta^5\text{-}C_5H_5)Fe(CO)_2(C(O)CH_3)]$ (See Section 3.2.2 for determination), that neither a bulky R group attached to the acyl (type A5), nor a metal-metal bridging acyl (type A6), nor crystal packing play a role in determining the conformation which the acyl adopts. This is in contrast to

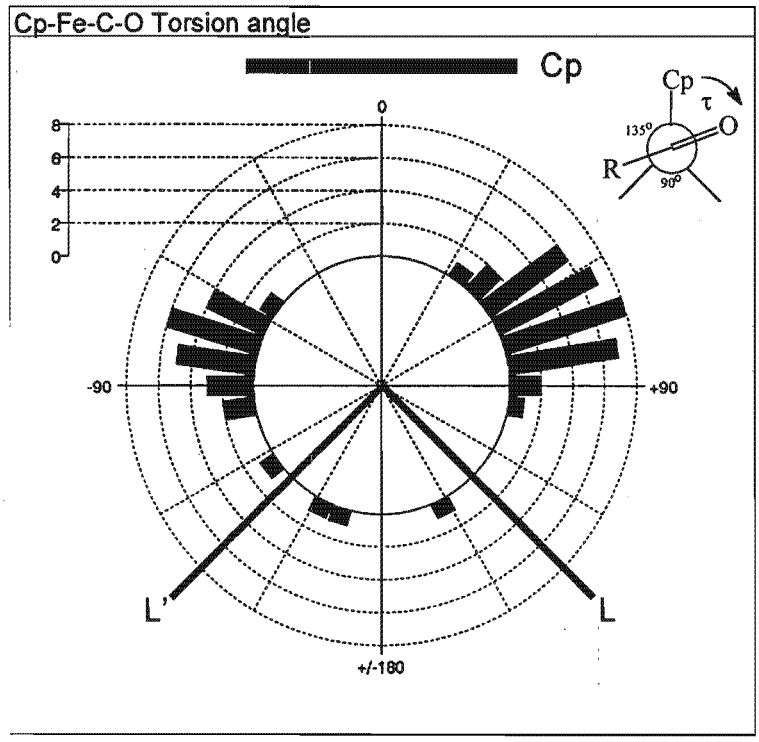

Figure 3.2.9 Polar histogram of the conformation of the acyl ligand in [CpFe(L)(L')(C(O)R)] type structures.

the alkyl compounds discussed in Section 3.1.1. It is therefore interesting to compare conformations adopted by cyclopentadienyl iron dicarbonyl acyls (sp^2 carbon) with cyclopentadienyl iron dicarbonyl alkyls (sp^3 carbon) and the factors that influence them. The arrangement in the two cases is illustrated in Figure 3.2.10. In the acyl compounds, the ideal angle between the iron, acyl carbon, and R (Fe-C-R) is 120° (sp^2) (See Figure 3.2.10), while in the alkyl compounds it is 109° (i.e. the β carbon in the alkyls is brought in closer to the iron and the other ligands). The acyl has in addition to the carbon substituent, an oxygen atom bonded with an ideal Fe-C=O angle of 120°. The oxygen of the acyl is sterically less demanding than the β carbon because the carbon-oxygen double bond is shorter than the carbon-carbon single bond and there are no substituents bonded to the oxygen. The hydrogen atoms of the α-carbon of the alkyl are smaller that the acyl oxygen and therefore less sterically demanding. The steric influences may be ordered as follows R(alkyl) > R(acyl) > O(acyl) > 2H(alkyl).

There were only two bis-tertiary phosphine compounds whose structures were found in the database (See Figure 3.2.5). In both of these, the acyl oxygen is placed between the two tertiary

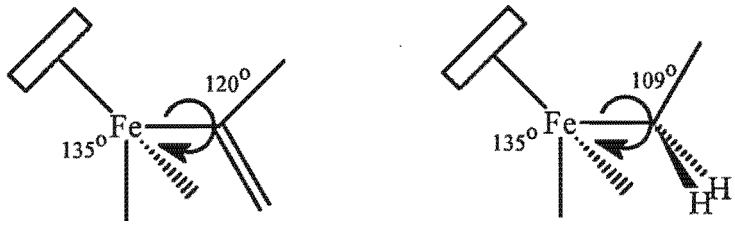

alpha-C sp^2 hybridised alpha-C sp^3 hybridised

Figure 3.2.10 Illustration of the CpFe(L)(L') fragment with sp^2 and sp^3 carbon atoms bonded to the metal.

phosphine ligands (τ = 148.7° and 154.1°). The conformation adopted by the bis-tertiary phosphine acyls was originally predicted to lie between the cyclopentadienyl and the phosphine ligand [88], however on widening the P-Fe-P angle, the predicted preferred conformation was with the acyl ligand between the two tertiary phosphines. This agreed with the observed structure

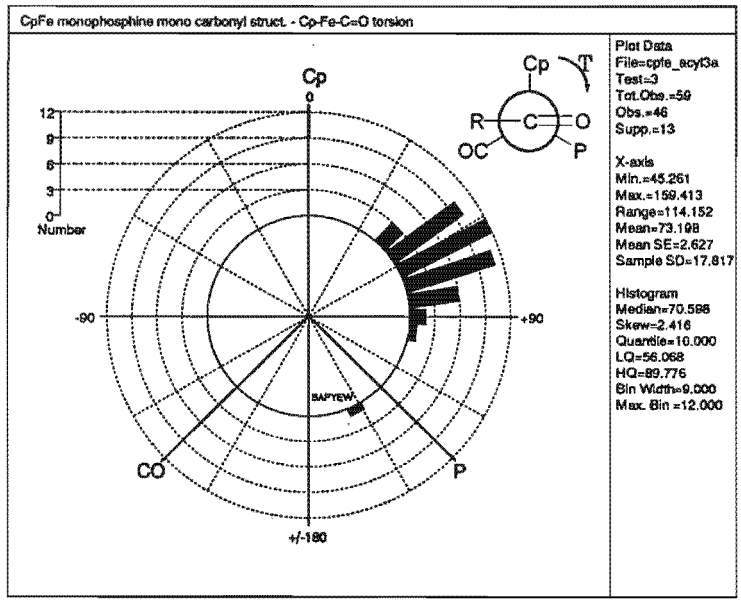

Figure 3.2.11 Polar histogram of the conformation of the acyl ligand in [CpFe(CO)(PXYZ)(C(O)R)] type structures.

$[(CpFe(PMe_3)_2C(O)C_2H_5]$ (BITYEI) where the P-Fe-P angle was 99°. However the other bis-tertiary phosphine iron acyl structure in the database, $[(CpFe(PPh_2C_2H_4PPh_2)C(O)CH_3]$ (BZPEFE),

adopts the same conformation (i.e. acyl oxygen between the two tertiary phosphines) but has a P-Fe-P angle of only 86°, suggesting that the P-Fe-P angle may not be the determining factor.

The monocarbonyl mono-tertiary phosphine iron acyl compounds, whose structures have been determined, were by far the largest type of cyclopentadienyl iron acyl structures in the database (41 compounds). All of these compounds, except for one, adopts a conformation with the acyl oxygen between the cyclopentadienyl ligand and the phosphine (45 - 100 degree torsion, See Figure 3.2.11). The exception in these types of structures (type A3) was the compound $[CpFe(CO)(PPh_2NHCPhMe)(C(O)CH_3)]$ (BAPYEW), where the acyl oxygen lies between the carbonyl and tertiary phosphine ligands ($\tau = 158.5°$). In this complex, the conformation is caused by a hydrogen bond from the NH on the tertiary phosphine to the acyl oxygen.

3.2.3. Crystal growing of $[(\eta^5\text{-}C_5H_5)Fe(CO)_2(C(O)CH_3)]$

A saturated hexane solution of $[(\eta^5\text{-}C_5H_5)Fe(CO)_2(C(O)CH_3)]$ was prepared and degassed with nitrogen. The solution was cooled to -15 °C, and suitable orange crystals were formed over two months. The solvent was syringed from the cold solution and the remaining hexane removed by blowing nitrogen over the crystals. The crystals were found to be generally rhombohedral in shape and 0.1 to 1 mm in size.

3.2.4. X-ray photography of $[(\eta^5\text{-}C_5H_5)Fe(CO)_2(C(O)CH_3)]$

A crystal (0.5 x 0.5 x 0.3 mm) was mounted in a Lindemann tube and aligned with the long edge perpendicular to the X-ray beam and parallel to the oscillation axis. Oscillation setting photographs were taken and the crystal adjusted to complete the alignment. An oscillation photograph was recorded with the large face of the crystal perpendicular to the X-ray beam (± 6°, Ni filter, 4h30 , 670 oscillations). The photograph showed a layer line corresponding to a unit cell dimension of 6.676Å.

The camera was set for a zero level Weissenberg photograph with a slit width of 2mm. The camera was allowed to oscillate by ± 100° and the photograph recorded (Ni filter, 24hrs 30min, 219 oscillations). The photograph revealed no mirror symmetry, and hence the crystal system

was deduced to be triclinic. The approximate dimensions of the remaining two unit cell dimensions (actually layer separations) were determined to be 11.420Å and 6.167Å. The unit cell volume was calculated to be 470Å^3. The number of molecules per unit cell was estimated to be two, giving a calculated density of 1.55g.cm^{-3}. A smaller crystal was used for the data collection (See Table 3.2.3).

3.2.5. Structure of [(η^5-C_5H_5)Fe(CO)$_2$(C(O)CH$_3$)]

[(η^5-C_5H_5)Fe(CO)$_2$(C(O)CH$_3$)] crystallizes in the triclinic space group $P\bar{1}$ with two molecules per unit cell. Lattice parameters were determined by least-squares fitting of the setting angles of 25 reflections $1° \geq \theta \geq 25°$ automatically centred on a CAD4 diffractometer. Intensities were collected with graphite-monochromated Mo Kα radiation, ω/2θ scan mode, scan width (0.80+0.35 tan θ)°, aperture setting (1.12 + 1.05 tan θ)mm and 4mm length, range of reflections $24.97 \geq \theta \geq 1.77°$. 1586 reflections measured all of which were unique. Three intensity control reflections (2 2 5, 3 -1 -8, 3 -4 5) monitored every 60 minutes showed a 0.6% loss in intensity; no correction was applied. Data were corrected for background, scan speed, absorption, Lorentz and polarization effects. The iron atom was located using the Patterson function. The remainder of the structure was solved using SHELX86 [77] and refined by difference Fourier methods using SHELX93 [100]. The final model included anisotropic refinement of all non-hydrogen atoms and isotropic refinement of hydrogens constrained to idealized positions with C-H = 1.00 Å. Good temperature factors and standard deviations of bond lengths and angles were obtained, and a final R of 0.0258. The data for the structure are given in Tables 3.2.3. The atomic coordinates are given in Table 3.2.4, bond lengths and angles are given in Table 3.2.5, temperature factors are given in Table 3.2.6, and coordinates and isotropic temperature factors are given in Table 3.2.7. The observed and calculated structure factors are given in Appendix B.

Table 3.2.3.

Crystal data and structure refinement for $[(\eta^5\text{-}C_5H_5)Fe(CO)_2(C(O)CH_3)]$.

Identification code	roh56	
Empirical formula	C9 H8 Fe O3	
Formula weight	220.00	
Temperature	293(2) K	
Wavelength	0.71069 Å	
Crystal system	Triclinic	
Space group	$P\bar{1}$	
Unit cell dimensions	a = 6.378(2) Å	α = 96.05(2) deg.
	b = 6.594(2) Å	β = 98.86(2) deg.
	c = 11.817(3) Å	γ = 110.53(3) deg.
Volume	453.0(2)Å^3	
Z	2	
Density (calculated)	1.613 Mg/m^3	
Absorption coefficient	1.632 mm^{-1}	
F(000)	224	
Crystal size	0.34 x 0.31 x 0.25 mm	
Theta range for data collection	1.77 to 24.97 deg.	
Index ranges	$-7 \le h \le 6, 0 \le k \le 7, -14 \le l \le 13$	
Reflections collected	1586	
Independent reflections	1586 [R(int) = 0.0000]	
Refinement method	Full-matrix least-squares on F^2	
Data / restraints / parameters	1586 / 0 / 135	
Goodness-of-fit on F^2	1.082	
Final R indices [$I > 2\sigma(I)$]	$R_1 = 0.0258$, $wR_2 = 0.0709$	
R indices (all data)	$R_1 = 0.0290$, $wR_2 = 0.0721$	
Largest diff. peak and hole	0.419 and -0.286 e.Å^{-3}	

Table 3.2.4.
Atomic coordinates (x 10^4) and equivalent isotropic displacement parameters ($Å^2$ x 10^3) with esd's in parentheses for [(η^5-C_5H_5)Fe$(CO)_2$(C(O)CH_3)]. U(eq) is defined as one third of the trace of the orthogonalized U_{ij} tensor.

	x	y	z	U(eq)
Fe(1)	2222(1)	4548(1)	2166(1)	37(1)
C(1)	2620(4)	7099(4)	3509(2)	53(1)
C(2)	385(4)	6315(4)	2828(2)	53(1)
C(3)	579(4)	6711(4)	1685(2)	54(1)
C(4)	2888(5)	7662(4)	1653(2)	58(1)
C(5)	4155(4)	7891(4)	2784(2)	56(1)
C(6)	3260(4)	3232(4)	3464(2)	44(1)
O(1)	5204(3)	3364(3)	3745(2)	62(1)
C(7)	1537(6)	2099(5)	4162(3)	65(1)
C(8)	4041(4)	3796(4)	1393(2)	47(1)
O(2)	5216(3)	3279(4)	889(2)	74(1)
C(9)	-99(4)	2096(4)	1566(2)	49(1)
O(3)	-1601(3)	489(3)	1154(2)	77(1)

Table 3.2.5.
Selected bond lengths [Å] and angles [degrees] for $[(\eta^5\text{-}C_5H_5)Fe(CO)_2(C(O)CH_3)]$ (See Figure 3.2.13 for numbering).

Fe(1)-C(8)	1.749(2)	C(1)-C(2)	1.410(4)
Fe(1)-C(9)	1.751(3)	C(2)-C(3)	1.418(4)
Fe(1)-C(6)	1.979(2)	C(3)-C(4)	1.392(4)
Fe(1)-C(5)	2.095(3)	C(4)-C(5)	1.415(4)
Fe(1)-C(2)	2.096(2)	C(6)-O(1)	1.203(3)
Fe(1)-C(1)	2.104(2)	C(6)-C(7)	1.509(4)
Fe(1)-C(3)	2.120(2)	C(8)-O(2)	1.143(3)
Fe(1)-C(4)	2.120(3)	C(9)-O(3)	1.146(3)
C(1)-C(5)	1.400(4)		
C(8)-Fe(1)-C(9)	92.66(11)	C(5)-Fe(1)-C(4)	39.22(10)
C(8)-Fe(1)-C(6)	88.65(10)	C(2)-Fe(1)-C(4)	65.59(10)
C(9)-Fe(1)-C(6)	92.01(10)	C(1)-Fe(1)-C(4)	65.49(10)
C(8)-Fe(1)-C(5)	101.32(11)	C(3)-Fe(1)-C(4)	38.34(10)
C(9)-Fe(1)-C(5)	161.26(11)	C(5)-C(1)-C(2)	107.9(2)
C(6)-Fe(1)-C(5)	100.66(10)	C(5)-C(1)-Fe(1)	70.19(14)
C(8)-Fe(1)-C(2)	161.77(11)	C(2)-C(1)-Fe(1)	70.07(14)
C(9)-Fe(1)-C(2)	97.72(11)	C(1)-C(2)-C(3)	107.3(2)
C(6)-Fe(1)-C(2)	105.85(10)	C(1)-C(2)-Fe(1)	70.68(14)
C(5)-Fe(1)-C(2)	65.66(11)	C(3)-C(2)-Fe(1)	71.25(14)
C(8)-Fe(1)-C(1)	135.65(11)	C(4)-C(3)-C(2)	108.7(2)
C(9)-Fe(1)-C(1)	131.02(11)	C(4)-C(3)-Fe(1)	70.84(14)
C(6)-Fe(1)-C(1)	83.34(9)	C(2)-C(3)-Fe(1)	69.44(13)
C(5)-Fe(1)-C(1)	38.94(10)	C(3)-C(4)-C(5)	107.5(2)
C(2)-Fe(1)-C(1)	39.25(10)	C(3)-C(4)-Fe(1)	70.82(14)
C(8)-Fe(1)-C(3)	124.62(11)	C(5)-C(4)-Fe(1)	69.45(14)
C(9)-Fe(1)-C(3)	96.82(11)	C(1)-C(5)-C(4)	108.5(2)
C(6)-Fe(1)-C(3)	144.86(10)	C(1)-C(5)-Fe(1)	70.86(14)
C(5)-Fe(1)-C(3)	64.97(11)	C(4)-C(5)-Fe(1)	71.33(14)
C(2)-Fe(1)-C(3)	39.31(10)	O(1)-C(6)-C(7)	118.9(2)
C(1)-Fe(1)-C(3)	65.29(10)	O(1)-C(6)-Fe(1)	123.1(2)
C(8)-Fe(1)-C(4)	96.20(11)	C(7)-C(6)-Fe(1)	117.9(2)
C(9)-Fe(1)-C(4)	127.40(11)	O(2)-C(8)-Fe(1)	179.2(2)
C(6)-Fe(1)-C(4)	139.79(10)	O(3)-C(9)-Fe(1)	178.7(2)

Although $[(\eta^5\text{-}C_5H_5)Fe(CO)_2(C(O)CH_3)]$ is a symmetrical molecule (i.e. it has two carbonyl ligands and an acetyl ligand, C_s symmetry), Figure 3.2.12, it crystallizes in a chiral conformation, with the O-CH_3 vector of the acetyl nearly parallel to the plane of the cyclopentadienyl ligand (See Figure 3.2.13). This is in contrast to the structure of the alkyl, $[Cp^*Fe(CO)_2(n\text{-}C_5H_{11})]$, in which the alkyl aligns itself on the mirror plane in the molecule (See Figure 3.1.1), however it is consistent with other iron acyl structures determined previously (See Section 3.2.1 above). The torsion angle from the centre of the cyclopentadienyl ring to the iron, carbon, and acyl oxygen (Cp-Fe-C(6)-O(1)) is 94°, comparing closely with those determined for other similar acyl structures (See Section 3.2.1) and the conformation predicted previously by Davies *et al* [88]. The

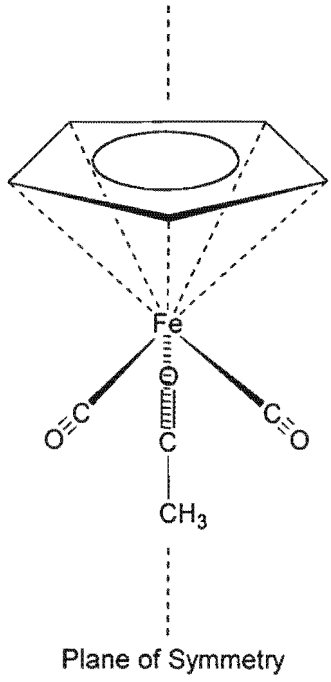

Figure 3.2.12 Molecular symmetry of $[CpFe(CO)_2(C(O)CH_3)]$.

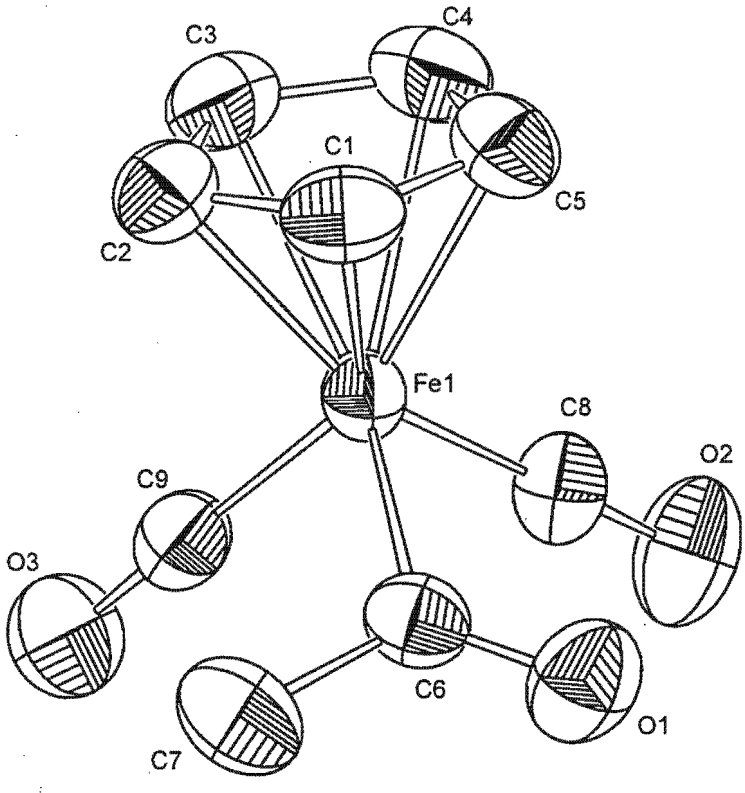

Figure 3.2.13 ORTEP plot of the molecular structure of $[(\eta^5\text{-}C_5H_5)Fe(CO)_2(C(O)CH_3)]$. Note the conformation of the acetyl group.

space group $P\bar{1}$ contains the inversion symmetry operator which allows for the mirror image of the molecule to exist within the crystal structure.

Table 3.2.6.
Anisotropic displacement parameters ($Å^2$ x 10^3) for $[(\eta^5\text{-}C_5H_5)Fe(CO)_2(C(O)CH_3)]$. The anisotropic displacement factor exponent takes the form: $-2\pi^2$ [$h^2 a^{*2} U_{11}$ + ... + 2hka*b* U_{12}]

	U_{11}	U_{22}	U_{33}	U_{23}	U_{13}	U_{12}
Fe(1)	34(1)	37(1)	40(1)	6(1)	10(1)	13(1)
C(1)	72(2)	41(1)	48(1)	3(1)	10(1)	26(1)
C(2)	55(1)	49(1)	65(2)	9(1)	22(1)	27(1)
C(3)	58(1)	50(1)	60(1)	12(1)	7(1)	30(1)
C(4)	74(2)	43(1)	61(2)	19(1)	22(1)	21(1)
C(5)	52(1)	38(1)	68(2)	6(1)	7(1)	8(1)
C(6)	53(1)	37(1)	41(1)	5(1)	10(1)	15(1)
O(1)	60(1)	78(1)	55(1)	19(1)	7(1)	35(1)
C(7)	75(2)	60(2)	58(2)	23(1)	23(1)	17(2)
C(8)	41(1)	58(1)	43(1)	9(1)	9(1)	19(1)
O(2)	61(1)	102(2)	69(1)	7(1)	27(1)	41(1)
C(9)	42(1)	46(1)	60(1)	7(1)	6(1)	20(1)
O(3)	51(1)	52(1)	105(2)	-1(1)	-11(1)	7(1)

Table 3.2.7.
Hydrogen coordinates (x 10^4) and isotropic displacement parameters ($Å^2$ x 10^3) for $[(\eta^5\text{-}C_5H_5)Fe(CO)_2(C(O)CH_3)]$.

	x	y	z	U(eq)
H(11)	3006(4)	7091(4)	4299(2)	64(8)
H(21)	-966(4)	5661(4)	3082(2)	77(9)
H(31)	-635(4)	6390(4)	1060(2)	63(8)
H(41)	3488(5)	8071(4)	1006(2)	79(10)
H(51)	5741(4)	8470(4)	3008(2)	72(9)

H(71)	365(66)	2555(65)	4087(35)	102(13)
H(72)	2167(69)	1908(67)	4853(39)	111(13)
H(73)	845(85)	676(88)	3730(45)	157(20)

The iron atom in the $[(\eta^5\text{-}C_5H_5)Fe(CO)_2(C(O)CH_3)]$ structure is octahedral with the cyclopentadienyl ring occupying three coordination sites and the carbonyls and acetyl ligands one each. The cyclopentadienyl ring adopts a conformation with one carbon eclipsing the acetyl carbon, allowing the carbonyl carbons to occupy an uneclipsed conformation (See Figure 3.2.14). No evidence for disorder in the ring was found. Thermal parameters for the methyl hydrogens (See Table 3.2.7) were 50-100% larger than those for the hydrogens of the cyclopentadienyl ring and the non-hydrogen atoms (Table 3.2.6), this is most likely due to rotational freedom of the methyl group.

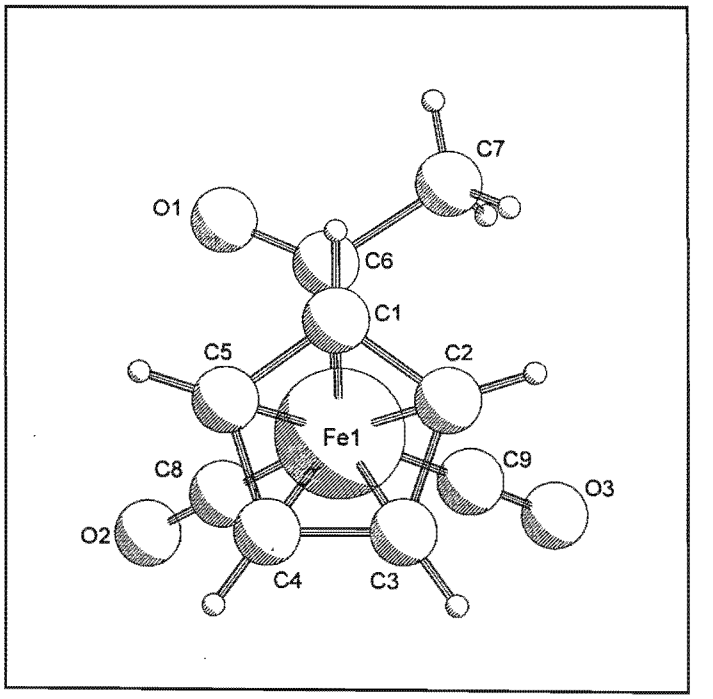

Figure 3.2.14 Molecular structure of $[CpFe(CO)_2(C(O)CH_3]$ showing the conformation of cyclopentadienyl ligand and the atom numbering.

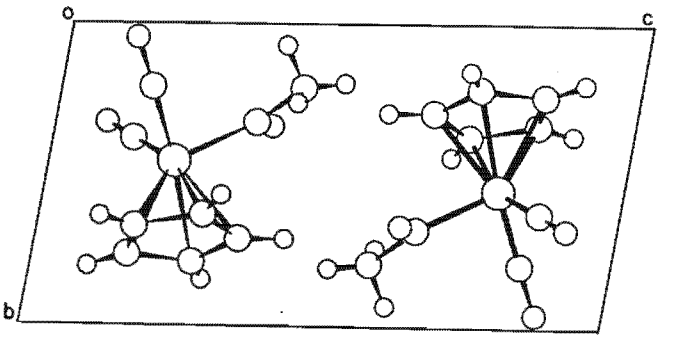

Figure 3.2.15 View of unit cell of $[CpFe(CO)_2CH_3]$, showing the two molecules related by a centre of inversion.

3.4. References

1. Dunitz, J. D.; Burgi, H.-B.; Murray-Rust, P. *Acta Cryst., Sect. B* **1978**, *34*, 1793.
2. Dunitz, J. D.; Britton, D. *J. Am. Chem. Soc.* **1982**, *103*, 2971.
3. Dunitz, J. D.; Burgi, H.-B. *Acc. Chem. Res.* **1983**, *16*, 153.
4. Dunitz, J. D.; Burgi, H.-B. *J. Am. Chem. Soc.* **1987**, *109*, 2924.
5. Dunitz, J. D.; Burgi, H.-B. *Acta Cryst.,Sect.B (Str.Sci.)* **1988**, *44*, 445.
6. McCormick, F. B.; Angelici, R. J.; Pickering, R. A.; Wagner, R. E.; Jacobson, R. A. *Inorg. Chem.* **1981**, *20*, 4108.
7. Connor, E. J. O.; Helquist, P. *J. Am. Chem. Soc.* **1982**, *104*, 1869.
8. Koch, O.; Edelmann, F.; Lubke, B.; Behrens, U. *Chem. Ber.* **1982**, *115*, 3049.
9. HIndson, K. J.; Laing, M.; Moss, J. R.; Pope, L.; Sommerville, P. *J. Organomet. Chem.* **1976**, *112*, 309.
10. Leung, T. W.; Christoph, G. G.; Gallucci, J.; Wojcicki, A. *Organometallics* **1986**, *5*, 846.
11. Ribankov, V. B.; Aslanov, L. A.; Ionov, V. M.; Eremin, S. A. *Zh. Strukt. Khim.* **1983**, *24*, 74.
12. Wright, M. E. *Organometallics* **1983**, *2*, 558.
13. Ribankov, V. B.; Aslanov, L. A.; Ionov, V. M.; Eremin, S. A. *Zh. Strukt. Khim.* **1983**, *24*, 100.
14. Yu, Y. S.; Angelici, R. J. *Organometallics* **1983**, *2*, 1018.
15. Bernal, I.; Brunner, H.; Hammer, B.; Draux, M. *Organometallics* **1983**, *2*, 1595.
16. Brunner, H.; Fisch, K.; Jones, P. G.; Salbeck, J. *Angew. Chem., Int. Ed. Engl.* **1989**, *28*, 1521.
17. Laing, M.; Moss, J. R.; Johnson, J. *J. Chem. Soc., Chem. Comm.* **1977**, 656.
18. Green, M. L. H.; Ariyaratne, J. K. P.; Bierrum, A. M.; Prout, C. K.; Swanwick, M. G. *J. Chem. Soc. A* **1969**, 1309.
19. Bennett, M. J.; Cotton, F. A.; Davison, A.; Faller, J. W.; Lippard, S. J.; Morehouse, S. M. *J. Am. Chem. Soc.* **1966**, *88*, 4371.
20. Churchill, M. R.; Chang, S. W. Y. N. *J. Am. Chem. Soc.* **1973**, *95*, 5931.
21. Kolobova, N. E.; Rozantseva, T. V.; Yu, T. S.; Batsanov, A. S.; Bakhmutov, V. I. *J. Organomet. Chem.* **1985**, *292*, 247.

22. Rosenblum, M.; Turnbull, M. M.; Foxman, B. M. *Organometallics* **1986**, *5*, 1062.

23. Turnbull, M. M.; Foxman, B. M.; Rosenblum, M. *Organometallics* **1988**, *7*, 200.

24. Reger, D. L.; Klaeren, S. A.; Lebioda, L. *Organometallics* **1986**, *5*, 1072.

25. Bruce, M. I.; Duffy, D. N.; Snow, M. R.; Tiekink, E. R. T. *J. Organomet. Chem.* **1986**, *310*, C33.

26. Orlova, T. Y.; Setkina, V. N.; Petrovskii, P. V.; Yanovskii, A. I.; Batsanov, A. S.; Yu, T. S. *J. Organomet. Chem.* **1986**, *304*, 331.

27. Orlova, T. Y.; Setkina, V. N.; Andrianov, V. G.; Struchkov, Y. T. *Izv. Akad. Nauk SSSR, Ser. Khim.* **1986**, 437.

28. Davies, S. G.; Dordor-Hedgecock, I. M.; Sutton, K. H.; Whittaker, M. *J. Am. Chem. Soc.* **1987**, *109*, 5711.

29. Davies, S. G.; Dordor-Hedgecock, I. M.; Sutton, K. H.; Whittaker, M. *J. Organomet. Chem.* **1987**, *320*, C19.

30. Stenstrom, Y.; Koziol, A. E.; Palenik, G. J.; Jones, W. M. *Organometallics* **1987**, *6*, 2079.

31. Chang, T. C. T.; Coolbaugh, T. S.; Foxman, B. M.; Rosenblum, M.; Simms, N.; Stockman, C. *Organometallics* **1987**, *6*, 2394.

32. Busetto, L.; Zanotti, V.; Albano, V. G.; Braga, D.; Monari, M. *J. Chem. Soc., Dalton Trans.* **1988**, 1067.

33. Roger, C.; Toupet, L.; Lapinte, C. *J. Chem. Soc., Chem. Comm.* **1988**, 713.

34. Lee, G.-H.; Peng, S.-M.; Lush, S.-F.; Mu, D.; Liu, R.-S. *Organometallics* **1988**, *7*, 1155.

35. Hill, D. H.; Parvez, M. A.; Sen, A. *J. Am. Chem. Soc.* **1994**, *116*, 2889.

36. Wieser, M.; Missling, C.; Robl, C.; Beck, W. *J. Organomet. Chem.* **1994**, *479*, 227.

37. Gau, H.-M.; Schei, C.-C.; Liu, L.-K.; Luh, L.-H. *J. Organomet. Chem.* **1992**, *435*, 43.

38. Stille, J. K.; Smith, C.; Anderson, O. P.; Miller, M. M. *Organometallics* **1989**, *8*, 1040.

39. Akita, M.; Kondoh, A.; Moro-oka, Y. *J. Chem. Soc. ,Dalton Trans.* **1989**, 1627.

40. Guerchais, V.; Astruc, D.; Nunn, C. M.; Cowley, A. H. *Organometallics* **1990**, *9*, 1036.

41. Furmanova, N. G.; Yu, T. S. *Koord. Khim.* **1980**, *6*, 1275.

42. Behrens, U.; Weiss, E. *J. Organomet. Chem.* **1975**, *96*, 399.

43. Gompper, R.; Bartmann, E.; Noth, H. *Chem. Ber.* **1979**, *112*, 218.

44. Malisch, W.; Zoller, J.; Schwarz, M.; Jager, V.; Arif, A. M. *Chem. Ber.* **1994**, *127*, 1243.

45. Chou, C. K.; Miles, D. L.; Bau, R.; Flood, T. C. *J. Am. Chem. Soc.* **1978**, *100*, 7271.

46. Cotton, F. A.; Schmid, G. *Inorg. Chim. Acta* **1997**, *254*, 233.

47. Wright, M. E.; Hoover, J. F.; Glass, R. S.; Day, V. W. *J. Organomet. Chem.* **1989**, *364*, 373.

48. Akita, M.; Kondoh, A.; Moro-oka, Y. *J. Chem. Soc., Dalton Trans.* **1989**, 1083.

49. Blackburn, B. K.; Bromley, L.; Davies, S. G.; Whittaker, M.; Jones, R. H. *J. Chem. Soc., Perkin Trans. 2* **1989**, 1143.

50. Pannell, K. H.; Cervantes, J.; Parkanyi, L.; Cervantes-Lee, F. *Organometallics* **1990**, *9*, 859.

51. Chu, K.-H.; Foxman, B. M.; Rosenblum, M.; Zhu, X.-Y. *Organometallics* **1990**, *9*, 3010.

52. Sterzo, C. L.; Bocelli, G. *J. Chem. Soc., Dalton Trans.* **1991**, 1881.

53. Adams, H.; Bailey, N. A.; Laskowski, J. J.; Ridgway, C.; Winter, M. J. *Mendeleev Commun.* **1991**, 99.

54. Wang, T.-F.; Juang, J.-P.; Wen, Y.-S. *J. Organomet. Chem.* **1995**, *503*, 117.

55. Meier, E. J. M.; Kozminski, W.; Linden, A.; Lustenberger, P.; Von Philipsborn, W. *Organometallics* **1996**, *15*, 2469.

56. Wright, M. E.; Day, V. W. *J. Organomet. Chem.* **1987**, *329*, 43.

57. Caballero, C.; Chavez, J. A.; Goknur, O.; Lochel, I.; Nuber, B.; Pfisterer, H.; Ziegler, M. L.; Alburquerque, P.; Eguren, L.; Korswagen, R. P. *J. Organomet. Chem.* **1989**, *371*, 329.

58. Channareddy, S.; Glaser, B.; Mayer, E. P.; Noth, H.; Helm, S. W. *Chem. Ber.* **1993**, *126*, 1119.

59. Nakazawa, H.; Yamaguchi, Y.; Mizuta, T.; Ichimura, S.; Miyoshi, K. *Organometallics* **1995**, *14*, 4635.

60. Gdanitz, R. J., *Ab Initio Prediction of Possible Molecular Crystal Structures*, in *Theoretical Aspects and Computer Modeling of the Molecular Solid State*; Gavezzotti, A., Ed.; The Molecular Solid State, Dunitz, J. D., Boldyvev, V. V., Leisernowitz, L., Oshashi, Y., Gavezzotti, A. and Whitesell, J. K., John Wiley & Sons: Chichester, 1997; Vol. 1, pp 185.

61. Boeyens, J. C. A.; Cheng, L.; Coville, N. J.; Levendis, D. C.; McIntosh, K. *J. Chem. Crystallogr.* **1998**, *28*, 185.

62. Ribankov, V. B.; Aslanov, L. A.; Ionov, V. M.; Eremin, S. A. *J. Struc. Chem.* **1983**, *24*, 230.

63. McQuillan, G. P.; Robertson, A. H. J.; McKean, D. C. *J. Chem. Soc., Dalton Trans.* **1995**, 3963.

64. Mackie, S. C.; DeGrace, S. A.; Berry, S. W. *J. Organomet. Chem.* **1998**, *560*, 63.

65. Lin, Y. C.; Calabrese, J. C.; Wreford, S. S. *J. Am. Chem. Soc.* **1983**, *105*, 1679.

66. Finch, K. P.; Moss, J. R.; Niven, M. L. *Inorg. Chim. Acta* **1989**, *166*, 181.

67. Beddoes, R. L.; Davies, E. S.; Helliwell, M.; Whiteley, M. W. *J. Organomet. Chem.* **1991**, *421*, 285.

68. Chen, J.-D.; Wu, C.-K.; Wu, I.-Y.; Huang, B.-C.; Lin, Y.-C.; Wang, Y. *J. Organomet. Chem.* **1993**, *454*, 173.

69. Gafoor, M. A.; Hutton, A. T.; Moss, J. R. *J. Organomet. Chem.* **1996**, *510*, 233.

70. Lindsay, C.; Cesarotti, E.; Adams, H.; Bailey, N. A.; White, C. *Organometallics* **1990**, *9*, 2594.

71. Rasley, B. T.; Rapta, M.; Kulawiec, R. J. *Organometallics* **1996**, *15*, 2852.

72. Lehmkuhl, H.; Bellenbaum, M.; Grundke, J.; Mauermann, H.; Kruger, C. *Chem. Ber.* **1988**, *121*, 1719.

73. Yang, J.; Yin, J.; Abboud, K. A.; Jones, W. M. *Organometallics* **1994**, *13*, 971.

74. Abboud, K. A.; Yin, J.; Jones, W. *Acta Cryst., Sect. C (Cr. Str. Comm.)* **1997**, 11.

75. Hubbard, J. L.; Morneau, A.; Burns, R. M.; Nadeau, O. W. *J. Am. Chem. Soc.* **1991**, *113*, 9180.

76. Sheldrick, G. M., *The SHELX Program*, in *Computing in Crystallography*; Shenk, H., Oltof-Hazenkamp, R., Van Konigsveld, J. and Bassi, G. C., Ed., Delft University Press: Delft, 1978, pp 34.

77. Sheldrick, G. M., in *Computing in Crystallography*; Sheldrick, G. M., Kruger, C. and Goddard, R., Ed., Oxford University Press: Oxford, 1985; Vol. 3, pp 175.

78. Moss, J. R.; Mavunkal, I.; Basca, J. *Unpublished results*, 1998.

79. Davies, S. G.; Watkins, W. C. *J. Chem. Soc., Chem. Commun.* **1994**, 491.

80. Crabtree, R. H., *Alkene Hydroformylation*, in *The Organometallic Chemistry of the Transition Metals*, 1st ed., John Wiley & Sons, Inc.: Singapore, 1988, pp 200.

81. Thomas, J. M.; Thomas, W. J., *Fischer-Tropsch Catalysis*, in *Principles and Practice of Heterogeneous Catalysis*, 1st ed., VCH Verlagsgesellschaft mbH: Weinheim, 1996, pp 524.

82. Piper, T. S.; Wilkinson, G. *J. Inorg. Nucl. Chem.* **1956**, *3*, 104.

83. King, R. B. *J. Am. Chem. Soc.* **1963**, *85*, 1918.

84. King, R. B. *J. Am. Chem. Soc.* **1968**, *90*, 1417.

85. Ingletto, G.; Tondello, E.; Di Sipio, L.; Carturan, G.; Graziani, M. *J. Organomet. Chem.* **1973**, *56*, 335.

86. Weber, L. *J. Organomet. Chem.* **1976**, *122*, 69.

87. Kuhlmann, E. J.; Alexander, J. J. *Inorg. Chim. Acta* **1979**, *34*, L193.

88. Blackburn, B. K.; Davies, S. G.; Sutton, K. H.; Whittaker, M. *Chem. Soc. Rev.* **1988**, *17*, 147.

89. Davies, S. G.; Seeman, J. I. *J. Am. Chem. Soc.* **1985**, *107*, 6522.

90. Davies, S. G.; Seeman, J. L. *J. Am. Chem. Soc.* **1985**, *107*, 6522.

91. Brown, S. L.; Davies, S. G.; Foster, D. F.; Seeman, J. I.; Warner, P. *Tetrahedron Let.* **1986**, *27*, 623.

92. Barras, J. P.; Davies, S. G.; Humphreys, V. M.; Prout, K. *J. Organomet. Chem.* **1993**, *461*, 157.

93. Alt, H. G.; Eichner, M. E.; Jansen, B. M.; Thewalt, U. *Z. Naturforsch., Teil B* **1982**, *37*, 1109.

94. Felkin, H.; Meunier, B.; Pascard, C.; Prange, T. *J. Organomet. Chem.* **1977**, *135*, 361.

95. Cook, S. J.; Costello, J. F.; Davies, S. G.; Kruk, H. T. *J. Chem. Soc., Perkin Trans. 1* , *17*, 2369.

96. Davies, S. G.; Seeman, J. I.; Williams, I. H. *Tetrahedron Let.* **1986**, *27*, 619.

97. Davies, S. G.; Smallridge, A. J. *J. Organomet. Chem.* **1990**, *397*, c13.

98. Thayer, A. M. *Chem. Eng. News* **1995**, 15.

99. Kaminsky, W. *J. Chem. Soc., Dalton Trans.* **1998**, 1413.

100. Sheldrick, G. M. *SHELX93. Program for Crystal Structure Refinement*; ; University of Götingen: Götingen, Germany, **1993**.

101. Desiraju, G. R. *Acc. Chem. Res.* **1991**, *24*, 290.

102. Steiner, T. *Cryst. Rev.* **1996**, *6*, 1.

103. Jeffrey, G. A., *Weak Hydrogen Bonds*, in *An Introduction to Hydrogen Bonding*, Oxford University Press: New York, 1997, pp 79.

Chapter 4

Quantum Mechanical Calculations on the β-Elimination Reaction of $(\eta^5\text{-}C_5H_5)M(CO)_2R$, M = Fe or Ru, R = Alkyl and Related Systems

Chapter 4

Model: A schematic description of a system, theory, or phenomenon that accounts for its known or inferred properties and may be used for further study of its characteristics

- The American Heritage Dictionary of the English Language

Quantum Mechanical Calculations on the β-Elimination Reaction of $(\eta^5\text{-}C_5H_5)M(CO)_2R$, M = Fe or Ru, R = Alkyl and Related Systems

4.1. The β-elimination reaction of $[(\eta^5\text{-}C_5H_5)Fe(CO)_2R]$

4.1.1. Introduction

β-hydride elimination and its reverse, alkene insertion, are important reaction pathways in organometallic chemistry (See also Chapter 2). Alkene insertion reactions play an important role industrially in the production of polyalkenes in both heterogenous and homogenous reactions. Recent research in this area has led to the commercialization of a number of asymmetric, single site organometallic catalysts which can be used to produce highly structured polymers with well defined structures [1]. Hydrogenation of alkenes by homogenous catalysis also occurs through an alkene insertion reaction.

The Fischer-Tropsch reaction has attracted much interest since its discovery as a route from inorganic compounds (i.e. CO and H_2) to hydrocarbons (See Chapter 1). Its commercial use, principally to produce hydrocarbon fuels, has however been limited due to the higher cost involved compared to crude oil. Efforts to separate out components from the product stream for sale as high value chemicals have been made in recent years. SASOL of South Africa, the largest commercial Fischer-Tropsch company in the world, is now the largest synthetic wax producer in the world [2], and is also selling α-olefins (1-alkenes) [3]. These are separated out of the product stream prior to reformation and refining. 1-alkenes are a high value product and it is thus desirable to increase the selectivity of the catalyst to the formation of 1-alkenes. This could be achieved by altering the reaction conditions and/or catalyst composition, and many such experiments have been performed in this manner [4], however an understanding of the mechanism may enable a more rational approach to be taken.

Fischer-Tropsch chemistry is essentially a polymerization where the monomer unit (i.e. $-CH_2-$) is not initially present. As such it obeys Schultz-Flory statistics for chain length distribution [5-

7]. Despite this constraint it is desirable to devise experiments that can help elucidate the mechanism of the reaction. An understanding of the reaction mechanism may enable a more active and selective catalyst for the formation of α-olefins to be synthesised.

It has been proposed that 1-alkene formation in the Fischer-Tropsch reaction occurs via a β-hydride elimination from an iron alkyl species [8-11]. It was decided therefore to examine this reaction by molecular modelling for a known organometallic iron alkyl compound which has been observed to produce 1-alkenes on thermal decomposition (see Figure 4.1) [12]. It has been suggested that these 1-alkenes are produced via a β-elimination reaction forming an iron alkene

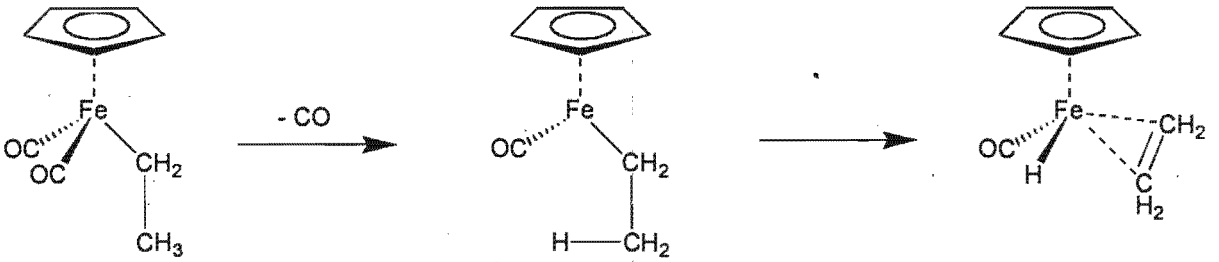

Figure 4.1 Decomposition of $[(\eta^5\text{-}C_5H_5)Fe(CO)_2CH_2CH_3]$ by loss of CO followed by β-elimination.

hydride which decomposes, releasing the 1-alkene [13]. The key iron alkene hydride has, however, never been isolated for the reaction of the dicarbonyl complex, although it has been for the bis-trimethylphosphine analogue [14,15]. It was thus of further interest in our group as a target for a molecular modelling study. The dicarbonyl complex, $[(\eta^5\text{-}C_5H_5)Fe(CO)_2CH_2CH_3]$, may be a good model for species in the Fischer-Tropsch reaction because there is an iron atom with two carbonyls and an alkyl group bonded to it - all these species may be present in a Fischer-Tropsch synthesis. The cyclopentadienyl ligand is firmly attached to the iron, and although η^5 to η^3 ring slippage is possible, evidence suggests that it does not occur in this case [13]. The cyclopentadienyl ligand may therefore be considered as a spectator ligand in the model.

The approach taken here in studying this reaction computationally, was to fully optimize structures of the reactant and product molecules and compare these with known crystal structures as a measure of their validity. The relative energies obtained from the calculation for these compounds would indicate the energy of the reaction (i.e. thermodynamic control). An estimated structure for the transition state could then be constructed and calculations performed to optimize this structure. The relative energy of this structure would then indicate the activation energy required for the reaction to proceed (i.e. kinetic control). All the energies obtained from these

calculations would be for single molecules in a vacuum at 0 K, and do not include any entropic effects (i.e. energies relate to enthalpy of the reaction), or effects of surrounding molecules (i.e. environment/solvent/etc). Full details of the computational methods employed are given in Section 4.5. The aim of the calculations was to provide further information in terms of the energetics, reaction path and hypothetical products of the system under consideration, rather than to be a full theoretical investigation of the underlying electronic structure. Obtaining the necessary accuracy for the prediction of structures (with full optimization) and energies led to the use of *ab initio* MO and DFT methods.

This investigation began by using *ab initio* molecular orbital methods (i.e. RHF) for the calculations. Deficiencies in the structures obtained and computational restraints, which restricted the extent to which improvements to the model might be made through larger basis sets and correlated methods, led to the use of density functional theory (DFT) for the bulk of the calculations presented in this thesis. A limited number of calculations have been performed at the MP2 level, however the basis sets used for geometry optimizations were necessarily small. The results of these calculations are presented below.

4.1.2. The structure of $[(\eta^5\text{-}C_5H_5)Fe(CO)_2CH_2CH_3]$ determined by DFT and MO calculations

The structure of $[(\eta^5\text{-}C_5H_5)Fe(CO)_2CH_2CH_3]$ was fully optimized by Density Functional Theory (DFT) calculations as well as *ab initio* Molecular Orbital Theory (MO) calculations, using the crystal structure of $[(\eta^5\text{-}C_5(CH_3)_5)Fe(CO)_2CH_2CH_2CH_2CH_2CH_3]$ obtained by X-ray crystallography (See Chapter 3) to build the starting model. $[(\eta^5\text{-}C_5H_5)Fe(CO)_2(CH_2CH_3)]$ was chosen to model the β-hydride elimination reaction as it is more convenient to perform calculations on than the pentamethylcyclopentadienyl analogues from a computational perspective. A singlet ground state was assumed for the calculations as $[(\eta^5\text{-}C_5R'_5)Fe(CO)_2R)]$ type compounds are known to be diamagnetic (i.e. paired electrons), evidenced by their amenability to conventional NMR spectroscopy.

Ab initio and density functional calculations gave optimized structures of the reactant, $[(\eta^5\text{-}C_5H_5)Fe(CO)_2(CH_2CH_3)]$. The DFT and RHF-MP2 structures are shown in Figure 4.2. Comparison of the calculated structures with known crystal data is given in Table 4-1.

Table 4 -1

Comparison of calculated bond lengths (Å) and angles (°) for $[(\eta^5\text{-}C_5H_5)Fe(CO)_2(CH_2CH_3)]$ with experimental data.

Bond/angle	MO-RHF	MO-RHF-MP2	DFT	Expt[a].	Expt. Ref.
$Fe\text{-}C_1$	1.93	1.94	2.13	2.06-2.20	[16-19]
$Fe\text{-}C_3$	1.89	1.58	1.76	1.72-1.79	[16-19]
$Fe\text{-}C_4$	1.89	1.58	1.76	1.67-1.86	[16-19]
$C_3\text{-}O_1$	1.19	1.28	1.2	1.14-1.19	[16-19]
$C_4\text{-}O_2$	1.19	1.28	1.2	1.15-1.19	[16-19]
$C_1\text{-}C_2$	1.59	1.59	1.55	1.51-1.55	[16-19]
$Fe\text{-}C_{Cp}$	2.30-2.35	2.05-2.08	2.22-2.23	2.07-2.26	[16-19]
$C_3\text{-}Fe\text{-}C_4$	97.5	91.4	96.5	89.2-95.0	[16-19]
$C_1\text{-}Fe\text{-}C_3$	90.4	92.0	89.4	88.0-94.2	[16-19]
$Fe\text{-}C_3\text{-}O_1$	173.7	174.4	177	177.5-178.8	[16-19]
$Fe\text{-}C_1\text{-}C_2$	121.5	117.4	118.8	113.3-119.2	[16-19]

[a]Values from X-ray structural data.

The DFT results were consistently closer to experimental results than the Hartree-Fock calculations, with all the bond lengths within the range observed in X-ray crystal structures except for the C≡O bond of the carbonyl which was 0.01 Å longer than the experimentally observed bond lengths. Bond angles all agreed very well with those observed in X-ray crystal structures.

The structure obtained from Hartree-Fock calculations was less consistent with the observed X-ray crystal structures than the structures obtained from DFT calculations. The bonds between the cyclopentadienyl ligand and the iron were slightly longer than those observed in structures from crystallographic data and predicted by the DFT calculations (See Table 4-1). The iron to carbonyl bond was overestimated by 0.1 Å, and the C-C bond of the ethyl chain by 0.04 Å. The iron to ethyl bond was underestimated by 0.13 Å. Key bond angles were generally in good agreement with those observed experimentally, the largest deviation from experimental values being 3.8° for the Fe-C≡O bond. The Hartree-Fock calculations were extended to the MP2 level

to assess the effect of electron correlation on the structure. The MP2 calculations predicted structures where the iron to carbon bond lengths were shorter than those predicted by DFT calculations. In particular the iron to alkyl carbon bond was shortened beyond the range of experimental values, as was the iron to carbonyl bond lengths which were > 0.1 Å shorter than

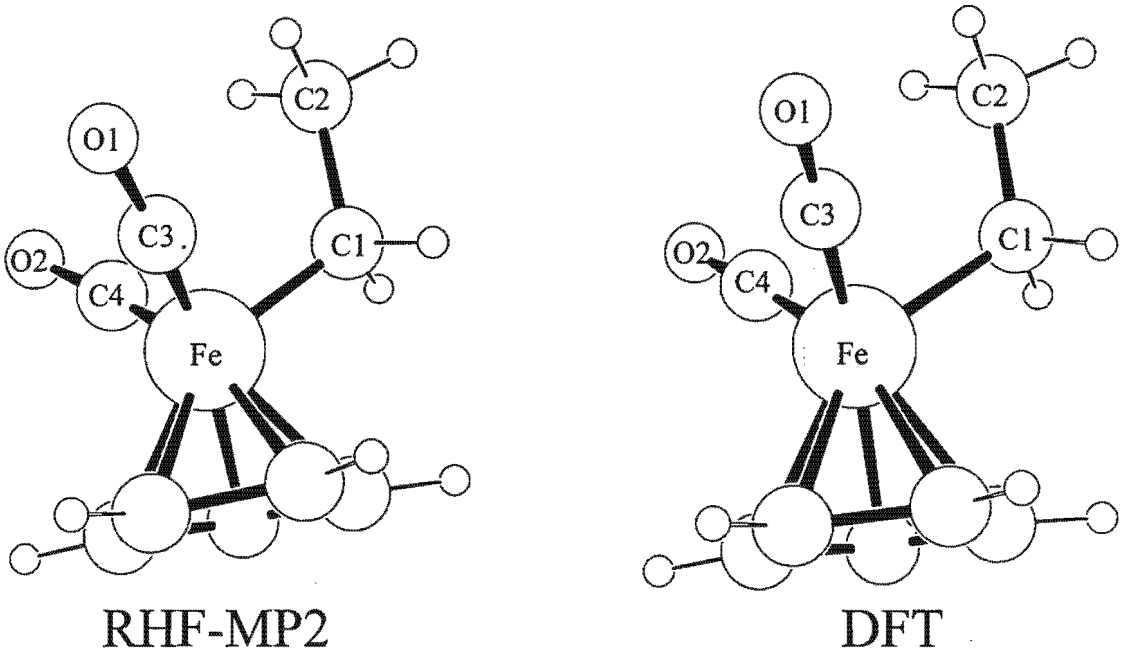

Figure 4.2 Optimized structure of $[(\eta^5\text{-}C_5H_5)Fe(CO)_2CH_2CH_3]$ determined by RHF-MP2 and DFT calculations.

the experimental values. This shortening was accompanied by an increase in the carbon to oxygen bond length of the carbonyl which is > 0.1 Å longer than the experimentally observed values.

The results indicate that DFT predicts a structure which corresponds more closely with the experimental data for approximately the same computational effort. The inclusion of correlation effects in the molecular orbital calculations (i.e. by inclusion of MP2 corrections) leads to an over correction to the bond lengths in the structure that may be due to the small size of the basis set. However, MP2 energy calculations, using a larger basis set, carried out on the DFT optimized structures, were higher in energy than equivalent calculations on the MP2 optimized structure

using a small basis set. The virial ratio[a] in both cases is in the region of -2.5, indicating that both structures are not stationary points at this level (i.e MP2 and SBK basis set).The reasonable structure predicted by Hartree-Fock calculations indicates that correlation effects on this structure are not pronounced, and could possibly be ignored for optimizations. Similar observations have been made for other transition metal complexes [21].

The structure of $[(\eta^5\text{-}C_5H_5)Fe(CO)_2(CH_2CH_3)]$ potentially possesses C_s symmetry when the ethyl group is positioned between the carbonyl groups (See Figure 4.3, conformer A), as was found in the crystal structure of $[(\eta^5\text{-}C_5(CH_3)_5)Fe(CO)_2((CH_2)_4CH_3)]$ (See Chapter 3). The molecular

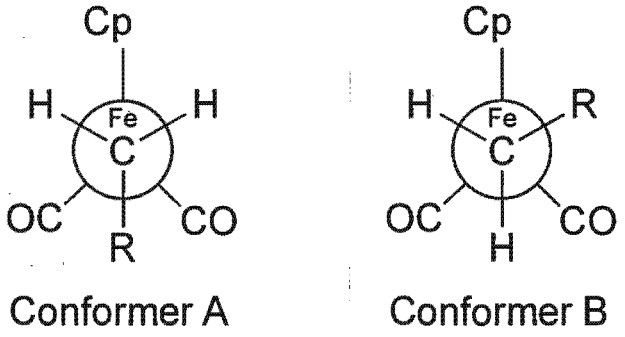

Figure 4.3 Diagram showing the two low energy conformations of $[(\eta^5\text{-}C_5H_5)Fe(CO)_2(CH_2CH_3)]$. Note that conformer B exists in a symmetrically equivalent conformation.

symmetry exhibited by the molecule in the crystal state was not found to be expressed in the space group symmetry of the crystal structure. It is therefore possible that the molecule adopts a quasi C_s symmetrical structure. Optimizations were carried out, using DFT, both with a symmetrical structure and a structure with the symmetry broken. The result was that the symmetrical structure was predicted to be 0.14 kcal.mol^{-1} lower than the quasi symmetrical structure. A frequency analysis of both structures resulted in the identification of imaginary vibrational modes. This was a general problem encountered with larger molecules in the DMol program (See Section 4.5 and Appendix D). Analysis of these modes showed that they involved the rotation of the cyclopentadienyl group in relation to the rest of the molecule, and methyl group rotation. Since the energy of ring rotation in these types of compounds is known to be small, evidenced by the equivalent NMR signals at room temperature, the lowest energy structure

[a]The virial ratio should be -2, and is a necessary (but not sufficient) condition for stationary points [20].

(i.e. the C_s structure) was taken to be the minimum energy structure of this conformer without further investigation. Furthermore the MP2 predicted structure of this conformer (i.e. conformer A), with C_s symmetry enforced, exhibited no imaginary modes after a vibrational analysis calculation. The structure is therefore characterized as a true minimum energy structure at the MP2 (MINI) level of theory.

The ethyl complex, $[(\eta^5\text{-}C_5H_5)Fe(CO)_2(CH_2CH_3)]$, may also exist in a conformation where the ethyl (alkyl) chain extends between the cyclopentadienyl ligand and one carbonyl (See Figure 4.3, conformer B). Examples of both conformers of the type A and B have been observed in crystal structures which have been determined for similar compounds (See Chapter 3). The crystallographic evidence suggests that the energy difference between these two conformations is small, as instances exist where identical molecules/groups adopt different conformations depending on the crystal environment (See Chapter 3 and [22-24]). In solution too, variable temperature infrared studies indicate the presence of two conformers of similar energy, however the authors were unable to quantify the energies involved experimentally [25]. These same authors did perform molecular mechanics (MMX) calculations on the rotational preferences of

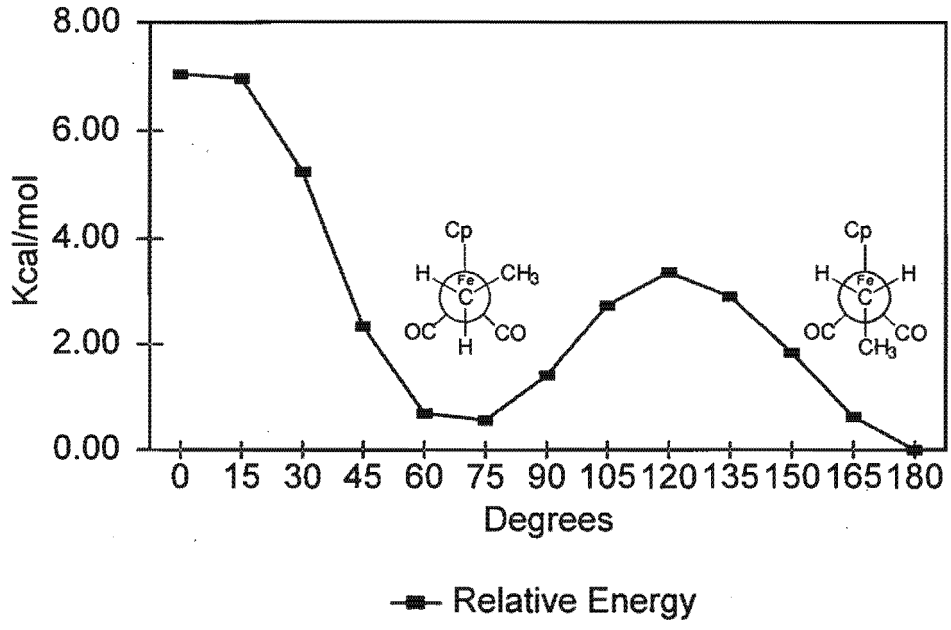

Figure 4.4 Rotational barrier of the ethyl group in $[(\eta^5\text{-}C_5H_5)Fe(CO)_2(CH_2CH_3)]$ calculated by DFT.

$[(\eta^5\text{-}C_5H_5)Fe(CO)_2(CH_2CH_3)]$. These calculations predicted a preference for the C_1 conformer, B. This conformer was calculated as being 1.1 kcal.mol^{-1} lower in energy than conformer A.

In this work a series of single point DFT calculations based on the optimized structure of conformer A were performed (See Figure 4.4). The calculations predict that the C_s structure, conformer A, is more stable than conformer B by 0.56 kcal.mol^{-1}. Optimization (without hessian) of conformer B by DFT resulted in a structure that was just 0.252 kcal.mol^{-1} higher in energy than conformer A. The eclipsing conformations of the carbonyls and the cyclopentadienyl ligands are maxima (i.e. representing the barriers to free rotation), and are predicted to be 3.36 kcal.mol^{-1} and 7.05 kcal.mol^{-1} respectively. This is greater than the 1.8 kcal.mol^{-1} and 2.8 kcal.mol^{-1} predicted by molecular mechanics (MMX) calculations [25]. Unfortunately there are no experimental data available with which to compare these predictions.

MP2 optimizations of conformers A and B predicted that the C_1 structure of conformer B was more stable than conformer A by 0.58 kcal.mol^{-1}. Although the DFT and MP2 results conflict over which conformer is more stable, the energies involved are within the limits of accuracy that are associated with these types of calculation [26,27]. Recent experimental work on related compounds [28] suggest that results previously reported results [25] may be interpreted as a slight preference for conformer B in solution.

The bond between the iron and the ethyl carbon is a single σ-type bond and remains essentially unchanged during rotation. This is evidenced by the DFT calculated difference electron density maps shown in Figure 4.5. In this figure the electron density of a particular conformation is subtracted from that of a base conformation. The resultant three dimensional contour map shows not only whether there is any change in a particular bond, but also whether changes are induced in other parts of the molecule. As can be seen no change is found in the region of the iron ethyl bond, although some very small changes are seen at the metal centre. The large contours associated with the ethyl CH_3 group are due to spacial differences between a particular conformation and the reference conformation, and are not due to changes in the bonding.

The electronic structure of the iron ethyl, $[(\eta^5\text{-}C_5H_5)Fe(CO)_2(CH_2CH_3)]$, is very similar to that of the iron methyl, $[(\eta^5\text{-}C_5H_5)Fe(CO)_2CH_3]$, which has been investigated previously by

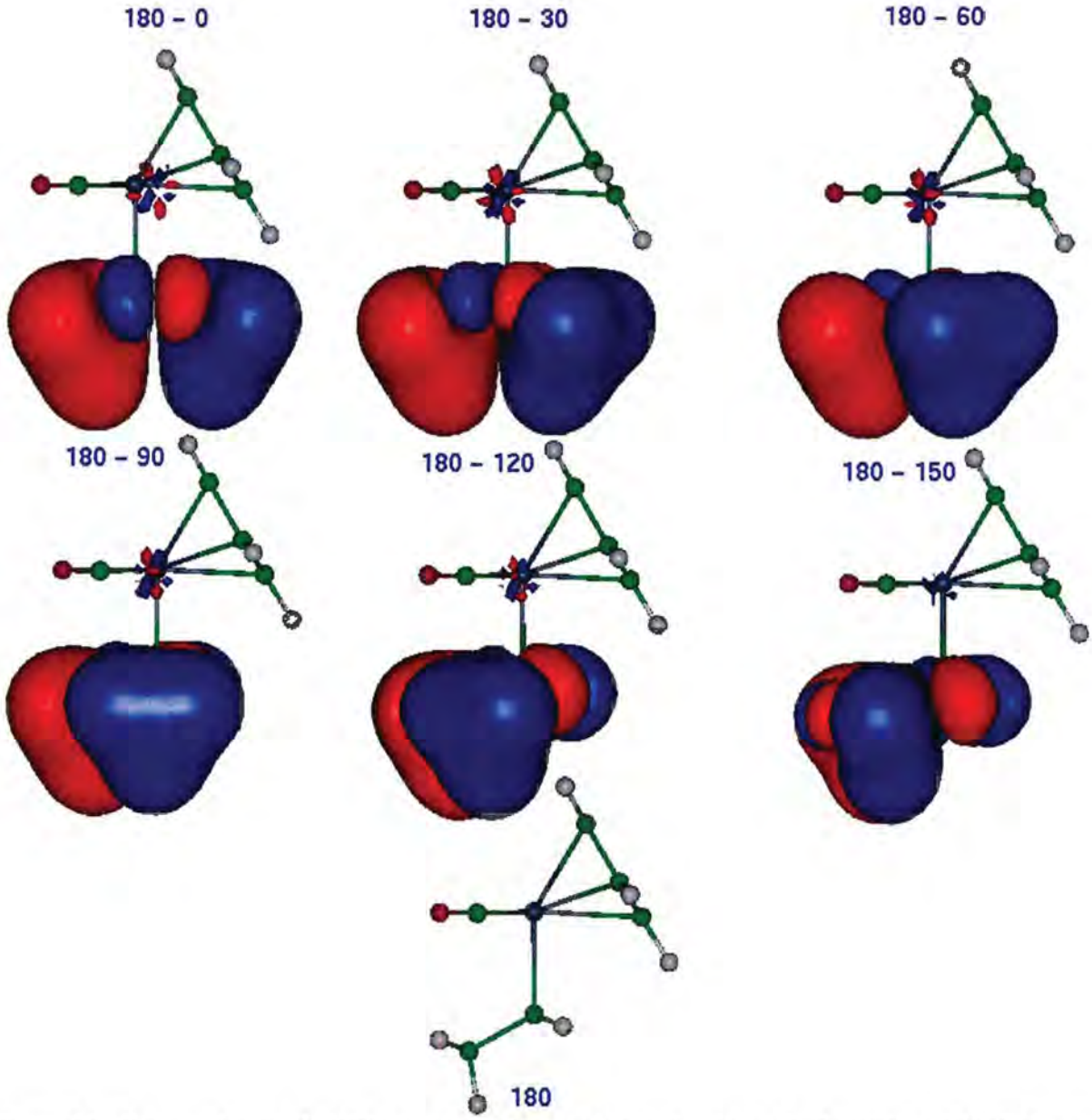

Figure 4.5 Diagram showing the DFT calculated difference electron density map for the rotation of the ethyl group in $[(\eta^5\text{-}C_5H_5)Fe(CO)_2(CH_2CH_3)]$.

photoelectron spectroscopy [29-31] and by Extended Hückel calculations [32]. Extended Hückel calculations provide a convienient tool for qualitative analysis using Hoffmann type fragment analysis. Calculations performed here on the iron ethyl, $[(\eta^5\text{-}C_5H_5)Fe(CO)_2(CH_2CH_3)]$, using C_s symmetry results in the orbital interaction diagram shown in Figure 4.6. The interaction to form the bond between the metal and the ethyl fragment involves predominantly two filled orbitals, 14a′ and 15a′, and one unfilled orbital, 16a′, on the metal fragment interacting with the 5a′ (HOMO) on the ethyl fragment. The resulting iron-ethyl bond is found in the second highest molecular orbital of the complex.

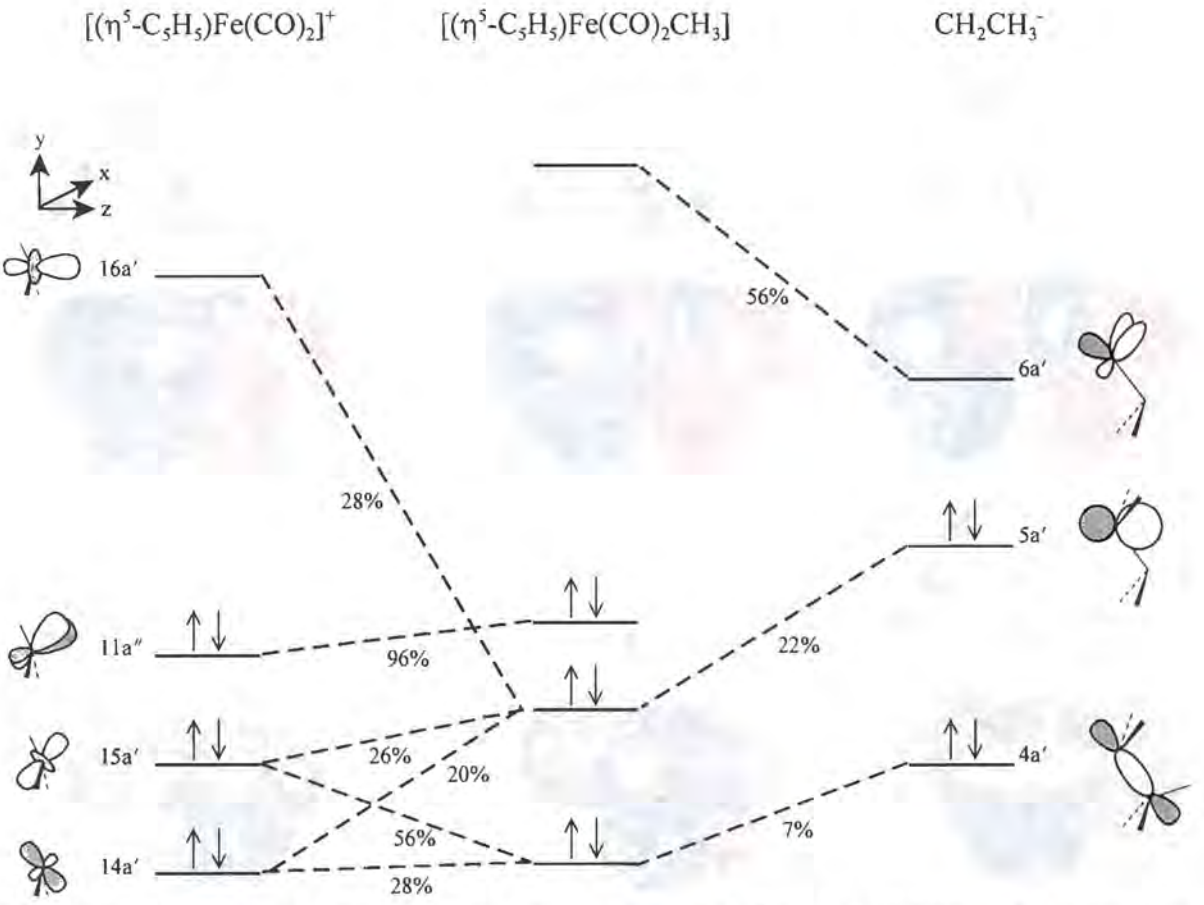

Figure 4.6 Interaction of fragment molecular orbitals of $[(\eta^5\text{-}C_5H_5)Fe(CO)]^+$ and CH_3^- to form $[(\eta^5\text{-}C_5H_5)Fe(CO)CH_3]$.

4.1.3. The structure of the alkene hydride $[(\eta^5\text{-}C_5H_5)Fe(CO)(H)(CH_2CH_2)]$ and correlation effects determined by MO, MO-MP2 and DFT calculations

The reaction scheme to form the alkene hydride involves the loss of CO and rearrangement via β-hydride elimination (See Figure 4.1). The structure for the theoretical product of β-hydride elimination, $[(\eta^5\text{-}C_5H_5)Fe(CO)(H)(CH_2CH_2)]$ which has never been isolated, was optimized using DFT, MO Hartree-Fock (RHF), and RHF-MP2 calculations using the structure of $[(\eta^5\text{-}C_5H_5)Fe(CO)_2(\eta^2\text{-}CH_2CHCH_2N(SO_2CH_3)SNH(SO_2CH_3))][PF_6]$, which has been determined previously [33], to build the starting structure for optimization. Key geometrical parameters for the predicted structures are presented in Table 4-2, and the RHF-MP2 and DFT predicted structures are shown in Figure 4.7.

Table 4 - 2

Comparison of calculated bond lengths (Å) and angles (°) for $[(\eta^5\text{-}C_5H_5)Fe(CO)(H)(CH_2CH_2)]$ with experimental data.

Bond/angle	MO-RHF	MO-RHF-MP2	DFT	Expt[a].	Expt. Ref.
$Fe\text{-}C_1$	2.72	1.93	2.13	2.02-2.32	[34-40]
$Fe\text{-}C_2$	2.71	1.95	2.14	2.02-2.32	[34-40]
$Fe\text{-}C_3$	1.83	1.58	1.74	1.74-2.00	[35,36,39,40]
$C_3\text{-}O_1$	1.19	1.28	1.20	1.11-1.18	[35,36,39,40]
$Fe\text{-}C_{Cp}$	2.20-2.30	1.99-2.14	2.14-2.17	2.06-2.12	[35]
$C_1\text{-}C_2$	1.34	1.50	1.43	1.36-1.43	[34-40]
$Fe\text{-}H_1$	1.41	1.55	1.52	1.54-1.62[b]	[41,42]

[a]Values from X-ray structural data.

[b]Neutron diffraction data.

The DFT predicted structure of $[(\eta^5\text{-}C_5H_5)Fe(CO)(H)(CH_2CH_2)]$ was in excellent agreement with experimentally observed data (See Table 4-2), with almost all the bond lengths being within the ranges observed in crystal structures. The differences observed were less than 0.1 Å from the crystal structure data. The distance from the cyclopentadienyl carbons to the iron in $[(\eta^5\text{-}C_5H_5)Fe(CO)(H)(CH_2CH_2)]$ was calculated to be 0.02 Å longer than the experimental range observed for $[(\eta^5\text{-}C_5H_4CH_3)Fe(C_2H_4)_2]$ [35], and the iron hydride bond was calculated to be 0.02 Å shorter than that observed by neutron diffraction [41,42].

The Hartree-Fock predicted structure was not in very good agreement with either the DFT calculations or crystal structure data. The method was unable to correctly describe the bonding between the iron and the ethylene in the ethylene hydride compound, $[(\eta^5\text{-}C_5H_5)Fe(CO)(H)(CH_2CH_2)]$. The iron to ethylene π bond was 0.4 Å longer than that observed in similar X-ray crystal structures. This was found to be due to the single determinant nature of the Hartree-Fock calculation, and this effect has been observed previously for transition metal metallocenes [43,44], and π bonded systems [45]. Extending the RHF calculations to the MP2 level resulted in a correction (i.e. shortening) of the iron to alkene bond length. However the MP2 calculations predicted structures where the iron to carbon bond lengths were shorter

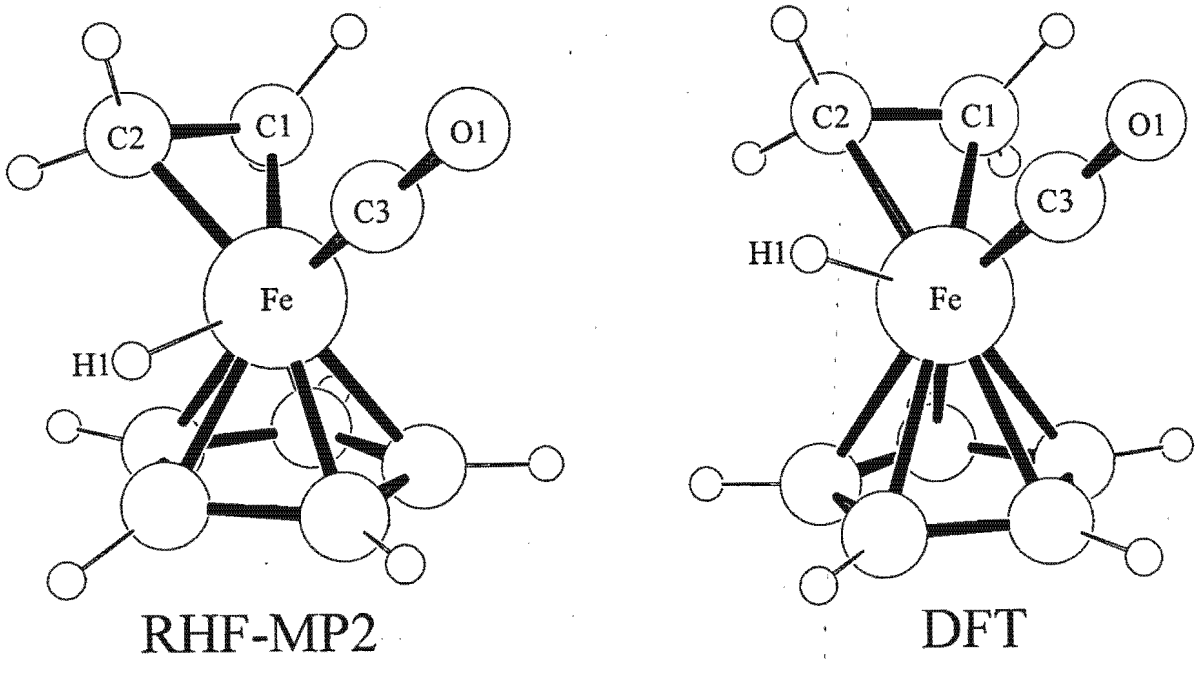

Figure 4.7 Optimized structure of $[(\eta^5\text{-}C_5H_5)Fe(CO)(H)(CH_2CH_2)]$ determined by RHF-MP2 and DFT calculations.

than those obtained by DFT calculations and experimentally observed distances from the Cambridge Crystallographic Database (CSD) [33,35-40]. The iron to carbon bonds for the coordinated alkene were > 0.1 Å shorter than the experimentally observed values in similar structures. The iron to carbonyl bond lengths were similarly effected and were > 0.1 Å shorter than the experimental values. This shortening was accompanied by an increase in the carbon to oxygen bond length of the carbonyl, which is > 0.1 Å longer than the experimentally observed values.

The structures obtained from MP2 calculations were generally in agreement with similar structures determined by X-ray crystallography (See Table 4-2), although not as good as the structures obtained from DFT calculations. In particular the position of the hydride in the MP2 determined structure of $[(\eta^5\text{-}C_5H_5)Fe(CO)(H)(CH_2CH_2)]$ may be too close to the cyclopentadienyl ring. This has the effect of distorting the usual tripod ligand arrangement typically observed in structures of the type [CpFe(L)(L')(L")], as can be seen clearly in Figure 4.7. The structural differences observed for the MP2 calculations may in part be due to the small basis set which had

to be employed to render the calculations feasible. However single point energy calculations on the DFT predicted structure using a larger basis set (SBK) [46,47] resulted in a higher energy than that obtained from larger basis set (SBK) calculations on the MP2 predicted structure, optimized using the small (MINI) basis set [48].

The alkene hydride structure, $[(\eta^5\text{-}C_5H_5)Fe(CO)(H)(CH_2CH_2)]$, was markedly less well described by RHF calculations than the ethyl structure, $[(\eta^5\text{-}C_5H_5)Fe(CO)_2(CH_2CH_3)]$. This was due to the greater effects of electron correlation in the alkene hydride structure, evidenced by a larger second order contribution to the MP2(MINI) energy (-536.19kcal.mol^{-1}) in the alkene hydride than in the monocarbonyl ethyl complex $[(\eta^5\text{-}C_5H_5)Fe(CO)(CH_2CH_3)]$ (-491.04kcal.mol^{-1}).

4.1.4. Rearrangement of $[(\eta^5\text{-}C_5H_5)Fe(CO)CH_2CH_3]$ to form alkene hydride.

Experimental evidence suggests that the loss of one carbonyl from $[(\eta^5\text{-}C_5H_5)Fe(CO)_2(CH_2CH_3)]$ would occur before proposed β-elimination to form an alkene [12,13]. The investigation of the reaction pathway therefore began by studying the monocarbonyl species, $[(\eta^5\text{-}C_5H_5)Fe(CO)(CH_2CH_3)]$. Hartree-Fock calculations identified a transition state for the reaction (i.e. the transformation of the monocarbonyl ethyl into the alkene hydride), and intrinsic reaction co-ordinate (IRC) calculations confirmed the reaction path. However further investigation by performing single point MP2 calculations at the stationary points indicated shortcomings of the structures optimized at the Hartree-Fock level. In particular the MP2 calculated total energy of the transition state was lower than that calculated for the product $[(\eta^5\text{-}C_5H_5)Fe(CO)(H)(CH_2CH_2)]$.

Density Functional investigation of the β-hydride elimination reaction of $[(\eta^5\text{-}C_5H_5)Fe(CO)_2(CH_2CH_3)]$ indicates that with one CO removed, the reaction proceeds without a barrier to form the ethylene hydride complex, $[(\eta^5\text{-}C_5H_5)Fe(CO)(H)(CH_2CH_2)]$. Optimization of the monocarbonyl, $[(\eta^5\text{-}C_5H_5)Fe(CO)(CH_2CH_3)]$ led to the product $[(\eta^5\text{-}C_5H_5)Fe(CO)(H)(CH_2CH_2)]$. The transition state for the reaction is therefore likely to lie in the region of CO loss.

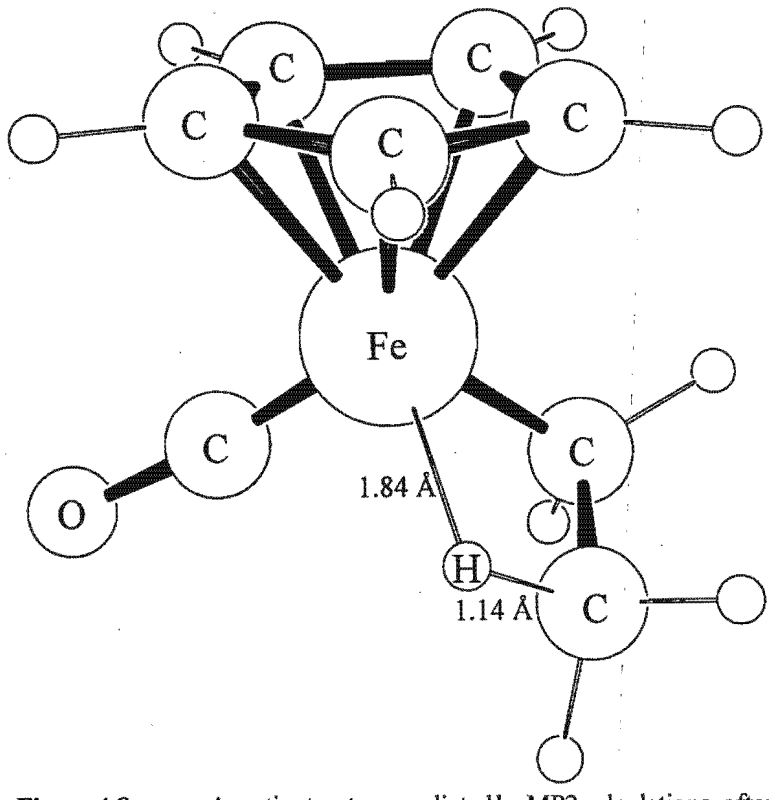

Figure 4.8 Agostic structure predicted by MP2 calculations, after the removal of a carbonyl from $[(\eta^5\text{-}C_5H_5)Fe(CO)_2(CH_2CH_3)]$.

The MP2 results for this system also predict a rearrangement of the ethyl complex, $[(\eta^5\text{-}C_5H_5)Fe(CO)_2(CH_2CH_3)]$, after CO removal. However optimization does not lead to the product structure, but an agostic type structure. This structure (See Figure 4.8) was characterized as a minimum energy structure, and is +64.24kcal.mol^{-1} above the calculated energy of the alkene hydride, $[(\eta^5\text{-}C_5H_5)Fe(CO)(H)(CH_2CH_2)]$ using the SBK basis set. The value seems rather high (it is greater than the calculated CO dissociation energy - see Section 4.1.5), with the value obtained with the MINI basis set being +19 kcal.mol^{-1} above the calculated energy of the alkene hydride. The result conflicts with the DFT results, which predicted better structures for the reactant and product, and the position of the hydride in the final alkene hydride product seems to be incorrectly predicted by the MP2 calculations (i.e. the interaction of the hydrogen with the iron may not be well described). No further investigation was therefore carried out for this species. Furthermore it has been suggested from experimental evidence that a ground state agostic structure does not exist in a similar system [15]. Recent calculations on the β-elimination reaction of the iron ethyl cation, $[FeCH_2CH_3]^+$ found that the reaction was endothermic and proceeded with a barrier [49] (i.e. a transition state), however no evidence was found for an

agostic minimum energy structure. Care should be taken however in comparing this highly coordinatively unsaturated system with the present system being studied.

The overall energy for the reaction can be predicted from the relative energies of the reactant and products. The energy difference between the reactant, $[(\eta^5\text{-}C_5H_5)Fe(CO)_2(CH_2CH_3)]$, and products of the reaction, $[(\eta^5\text{-}C_5H_5)Fe(CO)(H)(CH_2CH_2)]$ + CO, was calculated as being +35.28 kcal.mol^{-1} by DFT, and +38.80 kcal.mol^{-1} by MP2 calculations including +5.79 kcal.mol^{-1} contributed as the BSSE[b] correction to the ethyl complex. These values for the energy of the reaction are in reasonable agreement with each other, adding confidence to their representation of the actual energetics of the reaction.

4.1.5. The loss of CO in $[(\eta^5\text{-}C_5H_5)Fe(CO)_2CH_2CH_3]$ and the search for a transition state for a concerted reaction.

The calculations described above in Section 4.1.4 are strong evidence that loss of one carbonyl results in spontaneous β-elimination. What is not determined is whether the carbonyl loss is a necessary precondition to the β-elimination, or whether the reaction can occur by a concerted mechanism where the β-elimination occurs simultaneous to the loss of the carbonyl. In this case a transition state would exist, in which the carbonyl ligand is leaving, the ethyl group is rearranging to form a coordinated alkene, and a β-hydrogen from the ethyl is migrating to the metal. Several attempts to find this transition state using both DFT and MP2 methods failed. Starting structures for the optimizations were constructed both intuitively and through the use of a series of intermediate structures generated from the interpolation of appropriate Z-matrix coordinates. In these structures the iron carbonyl bond length of the leaving carbonyl was varied from 1.76 Å to 2.8 Å and also set to 5.0 Å. In many instances the carbonyl was "pulled" back onto the metal during optimization, even from relatively large distances. This could be as a result of the lack of environment (eg. solvent) and/or thermal energy in the system being studied. The imaginary vibrational mode of the optimized structures turned out to be trivial (eg. rotation of the cyclopentadienyl ring) in all cases. Transition state searching is computationally very

[b]Basis Set Superposition Error

demanding, due to the necessity of having accurate hessians at all stages during the search (i.e. prior to optimization, during optimization (recalculated every 50-60 iterations), and after optimization). This problem is exacerbated in this case due to the numerical method of hessian calculation. These factors prevented further investigation of possible transition state structures.

To estimate the activation energy for the reaction in the absence of a transition state, a number of single point calculations were performed by DFT (spin unrestricted) in which the carbonyl ligand was removed from the complex. These calculations gave a maximum energy of 56.33kcal.mol^{-1} for carbonyl loss (See Table 4-3).

Table 4-3

DFT calculated energy of $[(\eta^5\text{-}C_5H_5)Fe(CO)_2(CH_2CH_3)]$ during dissociation of one carbonyl ligand

Fe-CO distance (Å)	**Rel. Energy (kcal.mol^{-1})**
1.76	0.00
1.85	2.86
1.95	7.44
2.05	13.39
2.15	19.69
5.00	56.29
10.00	56.33
∞	54.30

The infinity distance for the iron carbonyl bond represents two calculations (i.e. $[(\eta^5\text{-}C_5H_5)Fe(CO)(CH_2CH_3)]$ and CO), in which the CO is optimized. The sum of these two energies represents not only an upper bound to the activation energy of the reaction, within this level of theory, but also the bonding energy of the CO to the iron in the complex $[(\eta^5\text{-}C_5H_5)Fe(CO)_2(CH_2CH_3)]$. The bond energy obtained from MP2 calculations was 52.74kcal.mol^{-1} including a BSSE component of 5.79kcal.mol^{-1}. Iron carbonyl bond energies have been determined experimentally, and in $Fe(CO)_5$ vary from 41kcal.mol^{-1} for the first

carbonyl dissociated to 10kcal.mol^{-1} for the last carbonyl [50]. Values for the cation $[Fe(CO)_5]^+$ vary from 36 kcal.mol^{-1} for the first carbonyl dissociated to 16 kcal.mol^{-1} for the last carbonyl [51]. The DFT and MP2 calculated values are rather higher than experimental values. This may be due to the different molecular systems studied to obtain the experimental results, and the unoptimized nature of the structures in each steps of the dissociation calculation. The DFT and MP2 results are within 2kcal.mol^{-1} of each other, indicating reasonably good agreement.

Density functional theory produced structures for both the ethyl compound and the alkene hydride that agreed very well with X-ray crystal structural data on related compounds and appears to be better than RHF for the study of this reaction. DFT calculations are also computationally less expensive than MO schemes which include correlation effects. The DFT calculations predict that the reaction is endothermic, however once the CO has been removed there is no barrier to the rearrangement to form the alkene hydride complex. This supports the findings of a UV/mass spectral study performed on these compounds [13].

4.2. Effects of changing the metal on the β-hydride elimination reaction in $[(\eta^5\text{-}C_5H_5)M(CO)_2R]$ (M = Fe, Ru).

The ruthenium analogues of the iron alkyl compounds discussed above have generally been found to be much more stable [52]. The aim of these calculations was to determine how this stability may be expressed in terms of the energies and properties found from DFT calculations. Comparison of calculations performed on metals in different transition series does introduce some problems, the most obvious of which is the increase in relativistic effects as the atoms become heavier. These could not be corrected for in the present work, and may therefore effect the results.

Structures of the ethyl compound, $[(\eta^5\text{-}C_5H_5)Ru(CO)_2(CH_2CH_3)]$, and the alkene hydride compound, $[(\eta^5\text{-}C_5H_5)Ru(CO)(H)(CH_2CH_2)]$, were optimized. The structures, which are in reasonable agreement with the literature, are shown in Figure 4.9. The ruthenium alkyl carbon bond of 2.23 Å is slightly longer than the 2.14 ± 0.07 Å observed in available X-ray structural data (See Chapter 3). Single point energy calculations predict an energy of reaction of +31.34 kcal.mol^{-1} (i.e. endothermic). This is 3 kcal.mol^{-1} less endothermic than what was

predicted in the case of iron (See Section 4.1.4). If the calculated values of the relative energy for the iron and ruthenium systems were comparable with each other, the greater stability of the ruthenium alkyl compounds may be attributable to a larger activation energy for the reaction. It is more likely however, that relativistic effects need to be accounted for in the ruthenium system.

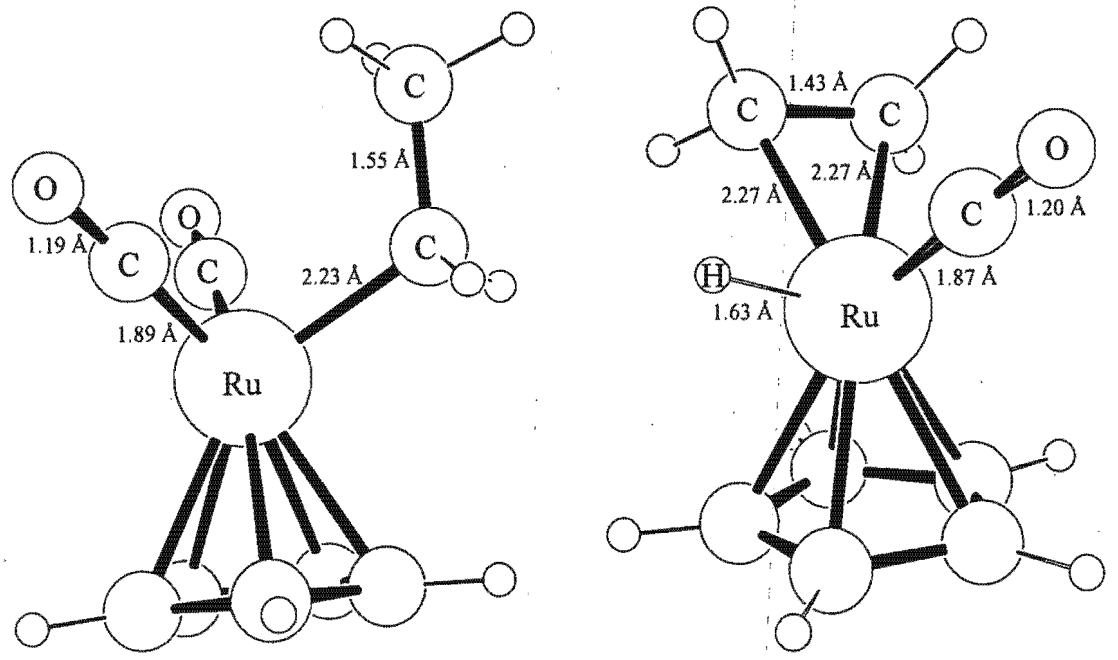

$[(\eta^5\text{-}C_5H_5)Ru(CO)_2(CH_2CH_3)]$ $[(\eta^5\text{-}C_5H_5)Ru(CO)(H)(CH_2CH_2)]$

Figure 4.8 DFT predicted structures for the ruthenium ethyl and alkene hydride complexes, with key bond lengths shown.

4.3. Effects of changing the ligands on the β-hydride elimination reaction in $[(\eta^5\text{-}C_5H_5)M(L)(L')R]$ (L, L′ = CO, PH_3).

The effect of replacing both one and two carbonyl ligands with phosphine (PH_3) ligands was examined in respect of the total energy of reaction (i.e. comparison of reactants and products). The possible reaction schemes are shown in Figure 4.10.

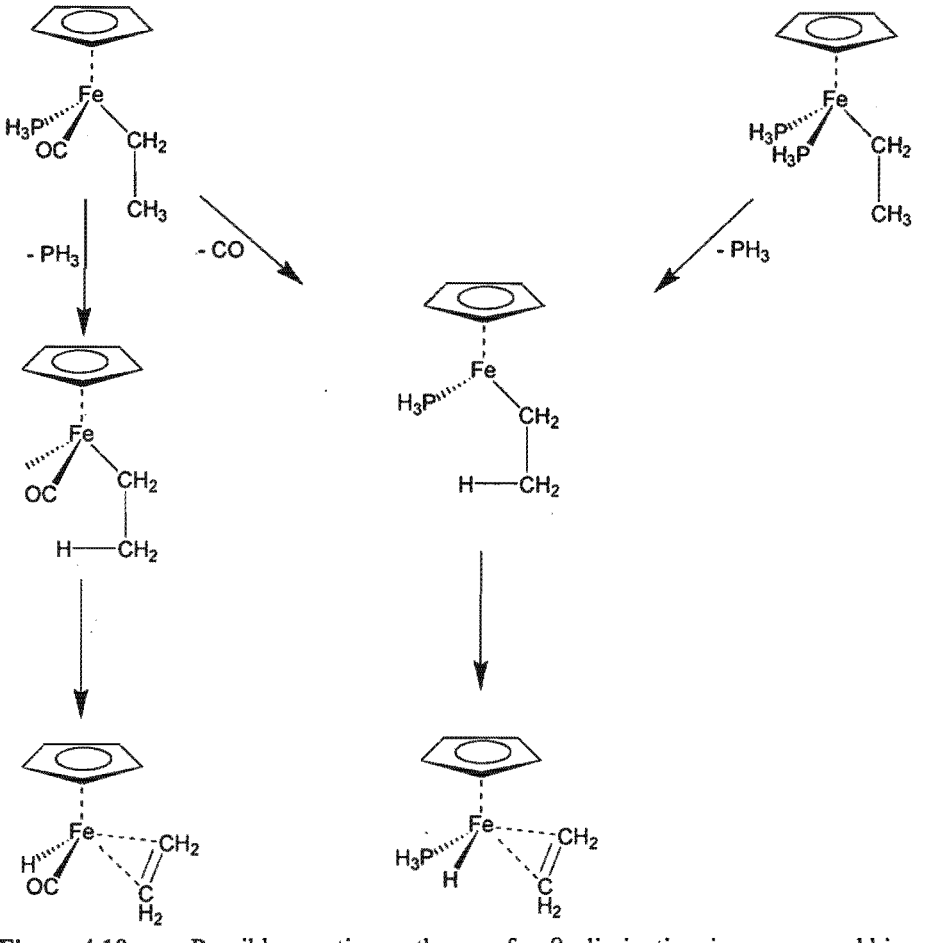

Figure 4.10 Possible reaction pathways for β-elimination in mono- and bis-substituted phosphine complexes.

The calculated energies for the three different pathways are given in the following table:

Table 4-4

DFT Calculated Reaction Energies for Phosphine Substituted β-elimination Reaction

Reaction	Reaction Energy (kcal/mol)
$[(\eta^5\text{-}C_5H_5)Fe(CO)(PH_3)(CH_2CH_3)] \rightarrow [(\eta^5\text{-}C_5H_5)Fe(CO)(H)(CH_2CH_3)]$	8.6
$[(\eta^5\text{-}C_5H_5)Fe(CO)(PH_3)(CH_2CH_3)] \rightarrow [(\eta^5\text{-}C_5H_5)Fe(PH_3)(H)(CH_2CH_3)]$	34.2
$[(\eta^5\text{-}C_5H_5)Fe(PH_3)_2(CH_2CH_3)] \rightarrow [(\eta^5\text{-}C_5H_5)Fe\ (PH_3)(H)(CH_2CH_3)]$	8.2

The results show that energy of the reaction is endothermic in all cases, and that the dominant contribution to the energy is the initial loss of the ligand. The reaction energy is most endothermic when a carbonyl ligand is lost, with the reaction energy correlating closely with the dicarbonyl system discussed previously. The loss of a phosphine ligand leads to a less endothermic reaction, which may be expected from the weaker π-acidity (i.e. weaker M-L bonding) of the phosphine. The energies of reactant and products are thus closer than for the systems involving carbonyl loss. This may, in part, explain why the alkene hydride has been observed in the tertiary phosphine system, $[(\eta^5\text{-}C_5(CH_3)_5)Fe(P(CH_3)_3)_2(CH_2CH_3)]$ [14,15], although the π-acidity of tertiary phosphines would be expected to be greater than that of phosphine (PH_3). The migration of the alkyl onto a carbonyl (See Chapter 5) is also not possible in this system, and may be a factor. There is less than 1 kcal.mol^{-1} difference in energy for the reactions involving the same leaving ligand (i.e. CO or PH_3) and different 'remaining' ligands (i.e. CO or PH_3). The reaction schemes where CO was the 'remaining' ligand were however, slightly more endothermic that the PH_3 systems.

4.4. The β-hydride abstraction reaction of $[(\eta^5\text{-}C_5H_5)Fe(CO)_2R]$.

The abstraction of a hydrogen from the β-carbon of the alkyl chain in $[(\eta^5\text{-}C_5H_5)Fe(CO)_2R]$ is well known [53]. The reaction is commonly performed using trityl salt as the hydride abstraction agent and leads to the formation of the cationic alkene complex $[(\eta^5\text{-}C_5H_5)Fe(CO)_2CH_2CHR']^+$ (See Figure 4.11). In a similar manner to the findings of the DFT calculations on the β-elimination reaction, the removal of hydride from the ethyl β-carbon of $[(\eta^5\text{-}C_5H_5)Fe(CO)_2CH_2CH_3]$ leads to spontaneous rearrangement of the molecule to form the alkene cation, $[(\eta^5\text{-}C_5H_5)Fe(CO)_2(\eta^2\text{-}CH_2CH_2)]^+$. The structure of the alkene is shown in Figure 4.12. It was found that the alkene adopts a conformation so as to minimise steric

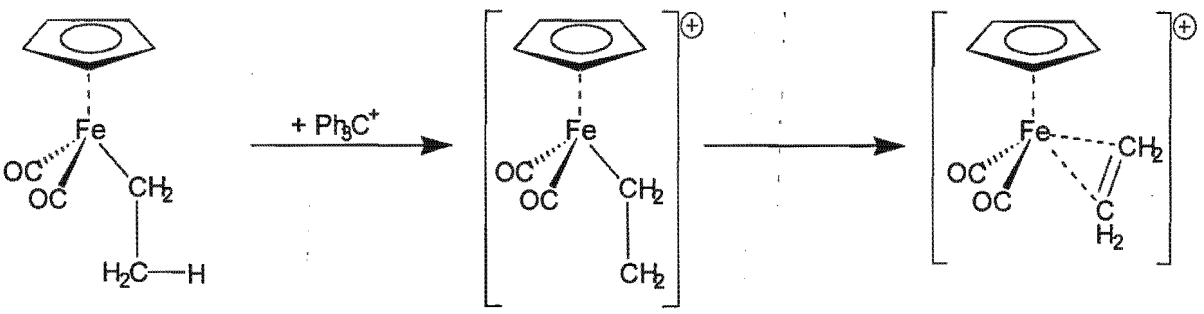

Figure 4.11 Hydride abstraction reaction of $[(\eta^5\text{-}C_5H_5)Fe(CO)_2CH_2CH_3]$ using trityl salt.

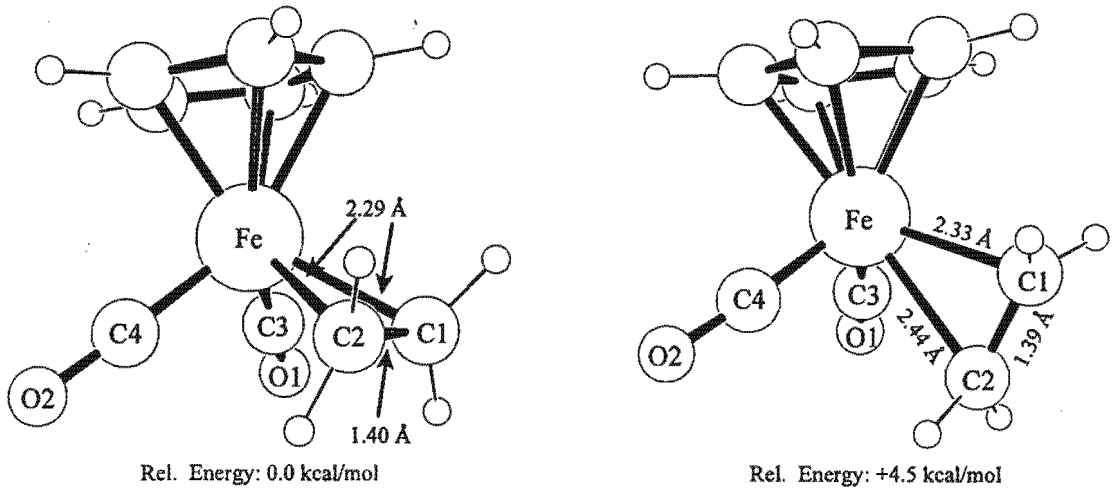

Figure 4.12 The optimized structures of $[(\eta^5\text{-}C_5H_5)Fe(CO)_2(CH_2CH_2)]^+$ showing minimum and maximum energy conformations of the alkene ligand and their relative energies.

interactions with the cyclopentadienyl ring, and the barrier to rotation of the ethylene is estimated to be +4.5 kcal.mol^{-1} from an optimization of the high energy conformer. To estimate the energy of reaction the following reaction scheme was used:

$$[(\eta^5\text{-}C_5H_5)Fe(CO)_2(CH_2CH_3)] + CH_3^+ \rightarrow [(\eta^5\text{-}C_5H_5)Fe(CO)_2(CH_2CH_2)] + CH_4$$

Calculation of the energies of the above species results in a predicted reaction energy of -117.4 kcal.mol^{-1}. This is highly exothermic, and the result may be effected by the instability of the CH_3^+ cation. If the reaction is considered as resulting in the formation of the alkene complex and a free hydride, by the following reaction,

$$[(\eta^5\text{-}C_5H_5)Fe(CO)_2(CH_2CH_3)] \rightarrow [(\eta^5\text{-}C_5H_5)Fe(CO)_2(CH_2CH_2)] + H^-$$

the energy of reaction is calculated as -92.6 kcal.mol^{-1}. This still indicates a highly exothermic reaction, and may indicate that this process (i.e. hydride abstraction) could be a energetically favourable alternative to β-elimination in the formation of 1-alkenes in the Fischer-Tropsch process. The β-elimination reaction requires a vacant coordination site, while the β-hydride abstraction may require a hydride abstraction agent. The large energies involved in the formation of the hydride however, should be investigated further.

4.5. Computational Details

The density functional theory (DFT) calculations were performed using the DMol program [54]. The BLYP functional was employed which incorporates Becke's exchange functional (B88) [55] and Lee, Yang, and Parr's correlation functional (LYP) [56]. All calculations included non-local gradient corrections. A fine numerical grid was employed throughout for all calculations. Geometry optimizations were performed in Cartesian space using a double numeric basis set (DN). Single point energy calculations were performed with a double numeric plus polarization basis set (DNP). The DNP basis set is approximately equivalent to the 6-31G** in a gaussian type orbital (GTO) scheme.

The nature of optimized stationary points was examined by second derivative (Hessian) calculations, and vibrational analysis. These calculations were performed numerically by finite difference as DMol is not able to compute these analytically. Hessians were calculated prior to transition state searching, and were updated during optimization, and recalculated after fifty-sixty iterations and at optimized stationary points. All Hessian calculations were performed on structures with no enforced symmetry (i.e. C_1).

All structures examined by DFT were optimized and checked by vibrational analysis, unless otherwise stated. Many minimum energy structures that were optimized, showed imaginary vibrational modes. Repeated re-optimizations failed to eliminate these. Further analysis showed that some of these modes involved trivial rotations of groups within the molecule, while others were low frequency and of small intensity and could consequently be rejected [57]. The vibrational modes treated in this way are shown in Appendix D. A further source of this problem may be from the numerical nature of the calculation (i.e. using a grid).

The basis sets employed in DMol are numerical in nature and are therefore able to give extremely accurate descriptions of the atomic orbitals of the constituent atoms. One result of this is that basis set superposition error is largely eliminated [58,59], and indeed DMol has no provision for its calculation. DMol energies, of the systems under study, were therefore used without applying any BSSE type corrections.

Two types of molecular orbital calculations were used to examine the molecular systems described in this Chapter and in Chapter 5, namely Restricted Hartree-Fock (RHF), and RHF followed by Møller-Plesset second order correction (MP2) calculation. The MINI basis set [48] was employed for geometry optimizations. The MINI bases are three gaussian expansions of each atomic orbital. The exponents and contraction coefficients are optimized for each element, and s and p exponents are not constrained to be equal. As a result these bases give much lower energies than STO-3G does. The Stevens-Basch-Krauss (SBK) relativistic effective core potentials (ECPs) and corresponding basis sets were used for single point energy calculations [46,47]. The basis sets consist of a -31G split for non-metals and a -311G split for first row transition metals. Geometry optimizations were carried out in the same manner as described above for the DMol calculations. RHF Hessians were calculated analytically and MP2 Hessians numerically. No problems were encountered with imaginary vibrational modes in minimum energy structures. Counterpoise corrections were made for basis set superposition error (BSSE) where appropriate, and are explicitly given in the text. The method used was that described by Tomasi *et al* [60] and incorporated in GAMESS [61] as part of the Morokuma energy decomposition calculation [62].

Zero point vibrational energy was not included in the calculation of relative energies. The quantity has been excluded by other authors, who estimate it to be <2 kcal.mol^{-1} in similar systems [45].

The DMol [54] calculations were carried out on a 64MB, 100MHz R4000 Indigo II Silicon Graphics computer in the Department of Chemistry at the University of Cape Town, a 512MB, 250MHz 4 processor R4400 Challenge XL Silicon Graphics computer at Silicon Graphics (South Africa), a 256MB, 150MHz 4 processor Onyx Silicon Graphics computer at Visual Creations, Cape Town, and two 64 MB, 180Mhz R5000 O_2 Silicon Graphics computer at the Royal Institution, London. All machines were running IRIX 5.2 or later. The DFT calculations presented in this study used more than 430 days of CPU time.

The Restricted Hartree-Fock (RHF) and Møller-Plesset second order correction (MP2) molecular orbital calculations were out carried using GAMESS [63] on a 96 MB,100MHz HP9000 computer running HP-UX or a 64MB, 100MHz R4000 Indigo II Silicon Graphics computer

running IRIX 5.2 at the University of Cape Town. PC-GAMESS version 5.1, build number 1519 [63,64] was used on a 128MB, 266MHz Pentium II running MS-Windows NT 4.0 (Service pack 3) (774 MIPS, 305 MFLOPS) or a 64MB, 166MHz Pentium running Windows 95 (396 MIPS, 190 MFLOPS).

4.6. Summary

DFT and Hartree-Fock + MP2 calculations were shown to adequately describe the structure of $[(\eta^5\text{-}C_5H_5)Fe(CO)_2R]$ compounds, with DFT producing slightly better results. The small energies between the two conformations was confirmed by calculations on $[(\eta^5\text{-}C_5H_5)Fe(CO)_2CH_2CH_3]$, in which the calculated energy difference between the two conformations is predicted to be less than 0.5 $kcal.mol^{-1}$.

The β-elimination reaction of the ethyl compound, $[(\eta^5\text{-}C_5H_5)Fe(CO)_2CH_2CH_3]$, was examined theoretically and found to occur spontaneously after the loss of one of the carbonyl ligands from the complex. A transition state for the reaction could not be found however. The overall reaction was calculated to be endothermic by about +35$kcal.mol^{-1}$, with the two methods used, DFT and MP2, differing by approximately 3$kcal.mol^{-1}$. DFT was found to give better structures than MP2, although the basis set used for the MP2 calculations was necessarily small. RHF calculations failed to give a reasonable structure for the product alkene hydride complex, $[(\eta^5\text{-}C_5H_5)Fe(CO)(H)(CH_2CH_2)]$ due to electron correlation effects, although the other structures predicted were closer to experimentally determined values. The β-hydride abstraction reaction was predicted by DFT to be highly exothermic (-117 $kcal.mol^{-1}$), and may be an alternative route to alkene formation in these complexes. The reaction may depend heavily on the presence of a suitable abstraction agent however, and this aspect requires further investigation.

4.7. References

1. Kaminsky, W. *J. Chem. Soc., Dalton Trans.* **1998**, 1413.
2. "SASOL Annual Report," Sasol Limited, **1997**.
3. Waddacor, M. *Chem. Proc. SA* **1994**, 2.
4. Anderson, R. B. *The Fischer-Tropsch Synthesis*; First ed.; Academic Press, Inc.: Orlando, 1984.
5. Jacobs, P. A.; Nijs, H. H. *J. Catalysis* **1980**, *65*, 328.
6. Yang, Y.; Pen, S.; Zhong, B. *Cat. Let.* **1992**, 351.
7. Kuipers, E. W.; Vinkenburg, I. H.; Oosterbeek, H. *J. Catalysis* **1995**, *152*, 137.
8. Brady, R. C.; Pettit, R. *J. Am. Chem. Soc.* **1980**, *102*, 6181.
9. Rofer-DePoorter, C. K. *Chem. Rev.* **1981**, *81*, 447.
10. Herrmann, W. A. *Angew. Chem. Int. Ed. Engl.* **1982**, *21*, 117.
11. Thomas, J. M.; Thomas, W. J., *Fischer-Tropsch Catalysis*, in *Principles and Practice of Heterogeneous Catalysis*, 1st ed., VCH Verlagsgesellschaft mbH: Weinheim, 1996, pp 524.
12. Culbertson, E. C.; Reger, D. L. *J. Am. Chem. Soc.* **1976**, *98*, 2789.
13. Barnhart, T. M.; Bartz, J. A.; Crim, F. F.; Galloway, D. B.; Glenewinkel-Meyer, T.; Huey, L. G.; McMahon, R. J. *J. Am. Chem. Soc.* **1993**, *115*, 8389.
14. Green, M. L. H.; Wong, L.-L. *J. Chem. Soc., Chem. Commun.* **1984**, 1442.
15. Green, M. L. H.; Wong, L.-L. *J. Chem. Soc., Dalton Trans.* **1987**, 411.
16. Green, M. L. H.; Ariyaratne, J. K. P.; Bierrum, A. M.; Prout, C. K.; Swanwick, M. G. *J. Chem. Soc. A* **1969**, 1309.
17. HIndson, K. J.; Laing, M.; Moss, J. R.; Pope, L.; Sommerville, P. *J. Organomet. Chem.* **1976**, *112*, 309.
18. Ribankov, V. B.; Aslanov, L. A.; Ionov, V. M.; Eremin, S. A. *Zh. Strukt. Khim.* **1983**, *24*, 100.
19. Chang, T. C. T.; Coolbaugh, T. S.; Foxman, B. M.; Rosenblum, M.; Simms, N.; Stockman, C. *Organometallics* **1987**, *6*, 2394.
20. Lowe, J. P., *Appendix 8 - The Virial Theorem for Atoms and Molecules*, in *Quantum Chemistry*, Second ed., Academic Press, Inc.: San Diego, 1993, pp 638.
21. Schmidt, M. W.; Gordon, M. S.; Rioux, F. *Organometallics* **1997**, *16*, 158.
22. Ribankov, V. B.; Aslanov, L. A.; Ionov, V. M.; Eremin, S. A. *Zh. Strukt. Khim.* **1983**, *24*, 74.
23. Ribankov, V. B.; Aslanov, L. A.; Ionov, V. M.; Eremin, S. A. *J. Struc. Chem.* **1983**, *24*, 230.

24. Gau, H.-M.; Schei, C.-C.; Liu, L.-K.; Luh, L.-H. *J. Organomet. Chem.* **1992**, *435*, 43.
25. Baird, M. C.; Mackie, S. C. *Organometallics* **1992**, *11*, 3712.
26. Pople, J. A.; Curtiss, L. A.; Raghavachari, K. *J. Chem. Phys.* **1993**, *98*, 1293.
27. Allinger, N. L.; Labanowski, J.; Sakakibara, K. *J. Phys. Chem.* **1995**, *99*, 9603.
28. Mackie, S. C.; DeGrace, S. A.; Berry, S. W. *J. Organomet. Chem.* **1998**, *560*, 63.
29. Symon, D. A.; Waddington, T. C. *J. Chem. Soc., Dalton Trans.* **1975**, 2140.
30. Green, J. C.; Jackson, S. E. *J. Chem. Soc., Dalton Trans.* **1976**, 1698.
31. Fenske, R. F.; Lichtenberger, D. L. *J. Am. Chem. Soc.* **1976**, *98*, 50.
32. Hoffmann, R.; Lichtenberger, D. L.; Schilling, B. E. R. *J. Am. Chem. Soc.* **1979**, *101*, 585.
33. Hu, Y.-R.; Leung, T. W.; Su, S.-C. H.; Wojcicki, A. *Organometallics* **1985**, *4*, 1001.
34. Rosenblum, M.; Stockman, C.; Foxman, B. M.; Chang, T. C. T. *J. Am. Chem. Soc.* **1981**, *103*, 7361.
35. Zenneck, U.; Frank, W. *Angew. Chem. Int. Ed. Engl.* **1986**, *25*, 831.
36. Hoberg, H.; Jenni, K.; Angermund, K.; Kruger, C. *Angew. Chem. Int. Ed. Engl.* **1987**, *26*, 153.
37. Luxmoore, A. R.; Truter, R. *Acta Cryst.* **1962**, *15*, 1117.
38. Linder, E.; Schaus, E.; Hiller, W.; Fawzi, R. *Chem. Ber.* **1985**, *118*, 3915.
39. Brookhart, M.; Chandler, W. A.; Pfister, A. C.; Santini, C. C.; White, P. S. *Organometallics* **1992**, *11*, 1263.
40. Meier-Brocks, F.; Albrecht, R.; Weiss, E. *J. Organomet. Chem.* **1992**, *439*, 65.
41. Koetzle, T. F.; Emge, T. J.; Gibbins, S. G.; Ho, D. M.; Chiang, M. Y.; Bau, R. *Inorg. Chem.* **1984**, *23*, 2823.
42. Koetzle, T. F.; Ricci, J. S.; Bautista, M. T.; Hofstede, T. M.; Morris, R. H.; Sawyer, J. F. *J. Am. Chem. Soc.* **1989**, *111*, 8823.
43. Almlöf, J.; Ammeter, J. H.; Faegri, K.; Luthi, H. P. *J. Phys. Chem.* **1982**, *77*, 2002.
44. Almlöf, J.; Park, C. *J. Chem. Phys.* **1991**, *95*, 1829.
45. Guest, M. F.; Hall, M. B.; Lin, Z.; Sherwood, P. *J. Organomet. Chem.* **1994**, *478*, 197.
46. Basch, H.; Krauss, M.; Stevens, W. J. *J. Phys. Chem.* **1984**, *81*, 6026.
47. Basch, H.; Jasien, P. G.; Krauss, M.; Stevens, W. J. *Can. J. Chem.* **1992**, *70*, 612.
48. Huzinaga, S.; Andzelm, J.; Kłobukowski, M.; Radzio-Andzelm, E.; Sakai, Y.; Tatewaki, H. *Gaussian Basis Sets for Molecular Calculations*; Elsevier: Amsterdam, 1984.
49. Fiedler, A.; Schroder, D.; Schwarz, H.; Zummack, W. *Inorg. Chim. Acta* **1997**, *259*, 227.
50. Squires, R. R.; Sunderlin, L. S.; Wang, D. *J. Am. Chem. Soc.* **1993**, *115*, 12060.
51. Armentrout, P. B. *Acc. Chem. Res.* **1995**, *28*, 430.
52. Emeran, A.; Gafoor, M. A.; Goslett, J. K. I.; Liao, Y.; Moss, J. R.; Pimble, L. *J. Organomet. Chem.* **1991**, *405*, 237.

53. Green, M. L. H.; Nagy, P. L. I. *J. Organomet. Chem.* **1963**, *1*, 58.
54. *DMol*; *V. 4.0.0*; Molecular Simulations Inc.: San Diego, **1996**.
55. Becke, A. D. *J. Chem. Phys.* **1988**, *88*, 2547.
56. Lee, C.; Yang, W.; Parr, R. G. *Physical Review B* **1988**, *37*, 785.
57. Clark, T., Personal Communication.
58. Klamt, A.; Schuurmann, G. *J. Chem. Soc., Perkin Trans. 2* **1993**, *2*, 799.
59. Wimmer, E., Personal Communication.
60. Cammi, R.; Bonaccorsi, R.; Tomasi, J. *Theo. Chim. Acta.* **1985**, *68*, 271.
61. Gordon, M. S.; Chen, W. *J. Phys. Chem.* **1996**, *100*, 14316.
62. Morokuma, K.; Kitaura, K. *Int. J. Quantum Chem.* **1976**, *10*, 325.
63. Baldridge, K. K.; Boatz, J. A.; Dupis, M.; Elbert, S. T.; Gordon, M. S.; Jensen, J. H.; Koseki, S.; Matsunaga, N.; Montgomery, J. A.; Nguyen, K. A.; Schmidt, M. W.; Su, S. J.; Windus, T. L. *J. Computational Chem.* **1993**, *14*, 1347.
64. Granovsky, A. A. *PC GAMESS*; *V. 5.1*: Moscow, **1998**.

Chapter 5

Quantum Mechanical Calculations of the Alkyl Migration Reaction of $[(\eta^5\text{-}C_5H_5)M(CO)_2R]$, M = Fe or Ru, R = Alkyl and Related Systems

Chapter 5

Quantum Mechanical Calculations of the Alkyl Migration Reaction of $[(\eta^5\text{-}C_5H_5)M(CO)_2R]$, M = Fe or Ru, R = Alkyl and Related Systems

5.1. Introduction

The alkyl migration reaction is of fundamental importance in organometallic chemistry. It is involved in the industrially significant hydroformylation and carbonylation reactions. As a consequence much research effort has been expended investigating the reaction (See Chapter 2). In this Chapter the results of a high level theoretical investigation of the alkyl migration reaction of $[(\eta^5\text{-}C_5H_5)Fe(CO)(L)R]$ will be presented (See Figure 5.1). The aims of this investigation were to apply density functional theory (DFT) and Restricted Hartree-Fock (RHF) with Møller-Plesset

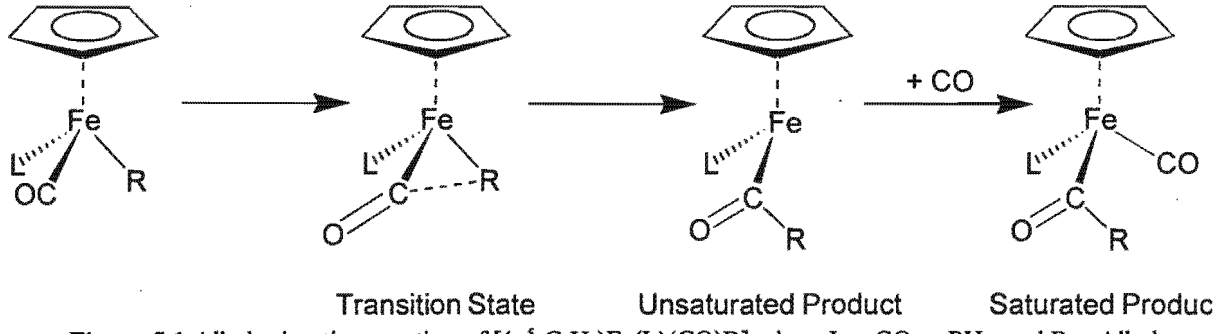

Figure 5.1 Alkyl migration reaction of $[(\eta^5\text{-}C_5H_5)Fe(L)(CO)R]$ where L = CO or PH_3, and R = Alkyl.

second order corrections (MP2) to the system and compare the results with experiment and previous theoretical work performed at a lower level [1,2]. Of particular interest was correspondence between the theoretically predicted structure of the acetyl product of the reaction

$$[(\eta^5\text{-}C_5H_5)Fe(CO)_2CH_3] + CO \rightarrow [(\eta^5\text{-}C_5H_5)Fe(CO)_2C(O)CH_3]$$

and the structure determined by X-ray crystallography and presented in Chapter 3 of this thesis; and information on the chain length dependence of the rate of reaction, which has recently been investigated within our research group [3,4]. Investigation of the literature also revealed inconsistencies concerning the conformational preferences of the acetyl ligand in $[(\eta^5\text{-}C_5H_5)Fe(CO)_2C(O)CH_3]$ [2,5,6]. The solid state conformation of the acetyl ligand has been

reported in Chapter 3 of this thesis, and is discussed further here in relation to the theoretical predictions.

Finally the experimental and theoretical data available for this reaction enable the methods used here (i.e. DFT and MP2) to be assessed for accuracy and in terms of other methods. The computational methods employed in this investigation are described in Chapter 4. The predicted relative energies calculated here are for isolated molecules at 0K, and relate to the enthalpy of reaction and do not include contributions to the entropy.

5.2. The alkyl migration reaction of $[(\eta^5\text{-}C_5H_5)Fe(CO)_2CH_3]$

The methyl complex $[(\eta^5\text{-}C_5H_5)Fe(CO)_2CH_3]$ was chosen as the base on which all other variations of the reaction (i.e. differing alkyl chain length, ligand substitution, and metal substitution) are based, as it the simplest member of this type of compound and is thus computationally less demanding than other molecules with longer chain lengths etc. The structure of the reaction product, $[(\eta^5\text{-}C_5H_5)Fe(CO)_2C(O)CH_3]$, was also experimentally determined (See Chapter 3), and provides a reliable structure with which to compare theoretically predicted structures.

5.2.1. The structure of $[(\eta^5\text{-}C_5H_5)Fe(CO)_2CH_3]$ determined by DFT and MP2.

The structure of $[(\eta^5\text{-}C_5H_5)Fe(CO)_2CH_3]$ is very similar to that of the ethyl complex, $[(\eta^5\text{-}C_5H_5)Fe(CO)_2CH_2CH_3]$ reported in Chapter 4, and is therefore not discussed in detail here. Comparison of bond lengths with experimental values are given in Table 5-1, and the structure is shown in Figure 5.2. As was found for the iron ethyl complex, $[(\eta^5\text{-}C_5H_5)Fe(CO)_2CH_2CH_3]$, in Chapter 4, the DFT method predicted geometries which were closer to experimentally observed data than results obtained from MP2 calculations (No Hartree-Fock level calculations were performed on this system). The DFT results are also better than the partial optimization results reported for the PRDDO[a] method [2].

---

[a]Partial Retention of Diatomic Differential Overlap method [7,8].

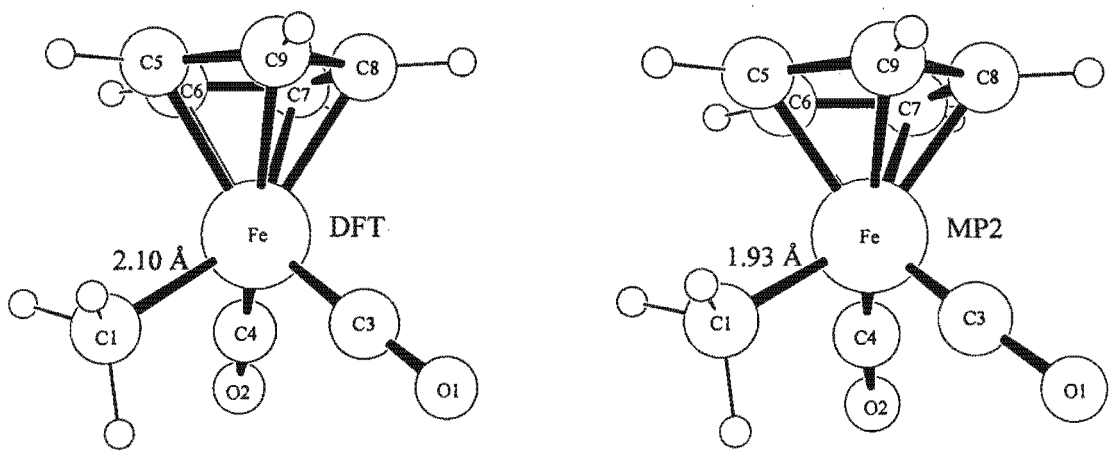

Figure 5.2 DFT and MP2 predicted structures for $[(\eta^5\text{-}C_5H_5)Fe(CO)_2CH_3]$, showing atom numbering.

The conformation of the cyclopentadienyl ring was investigated by DFT and MP2. The two symmetrical (C_s) structures were optimized and are shown in Figure 5.3 for the DFT calculations. It was found that the conformer with one of the cyclopentadienyl carbons eclipsing the methyl carbon was more stable than the other conformer by 1.15 kcal.mol^{-1} by DFT (DN basis set) and 3.14 kcal.mol^{-1} by MP2 (SBK basis set). MP2 vibrational analysis calculations confirmed a minimum energy structure for the conformer with one of the cyclopentadienyl carbons eclipsing

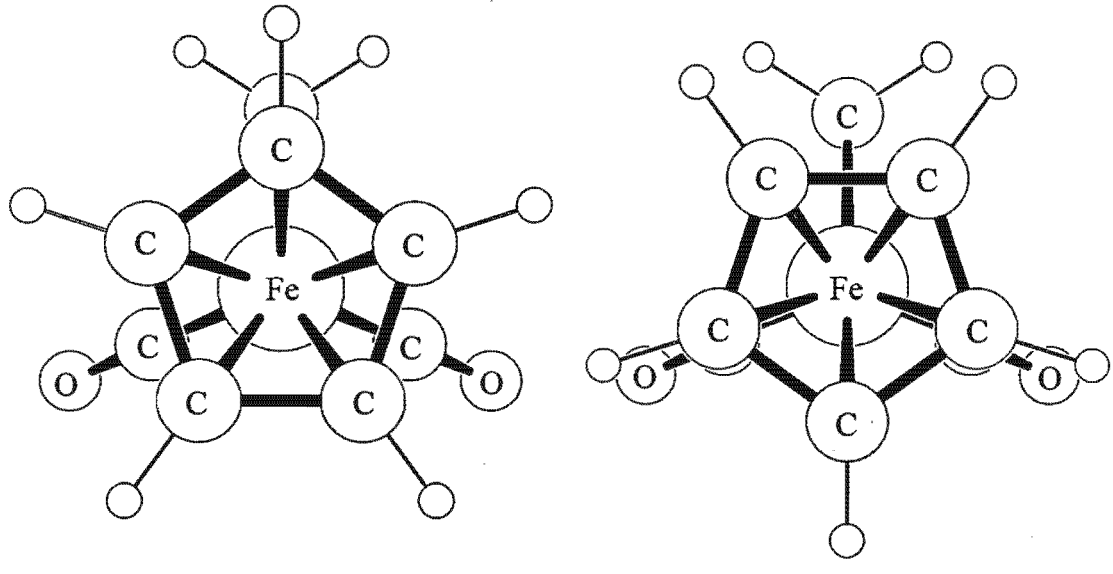

Figure 5.3 Diagram showing the two symmetric conformations of the cyclopentadienyl ring in $[(\eta^5\text{-}C_5H_5)Fe(CO)_2CH_3]$.

the methyl carbon, and gave a transition state structure for the second conformer, with the imaginary vibration corresponding to rotation of the cyclopentadienyl ring. These results are in agreement with the crystal structure of $[(\eta^5\text{-}C_5(CH_3)_5)Fe(CO)_2(CH_2)_4CH_3]$ reported in Chapter 3.

Table 5 -1

Comparison of calculated bond lengths (Å) and angles (°) for $[(\eta^5\text{-}C_5H_5)Fe(CO)_2CH_3]$ with experimental data.

Bond/angle	MO-RHF-MP2	DFT	PRDDO[a]	Expt[b].	Expt. Ref.
$Fe\text{-}C_1$	1.93	2.10	1.96	2.06-2.20	[9-12]
$Fe\text{-}C_3$	1.59	1.76	1.87	1.72-1.79	[9-12]
$Fe\text{-}C_4$	1.59	1.76	1.87	1.67-1.86	[9-12]
$C_3\text{-}O_1$	1.28	1.19	---	1.14-1.19	[9-12]
$C_4\text{-}O_2$	1.28	1.19	Fixed	1.15-1.19	[9-12]
$Fe\text{-}C_{Cp}$	2.05-2.07	2.21-2.23	2.07	2.07-2.26	[9-12]
$C_3\text{-}Fe\text{-}C_4$	91.4	95.6	91.3	89.2-95.0	[9-12]
$C_1\text{-}Fe\text{-}C_3$	91.1	89.6	87.8	88.0-94.2	[9-12]
$Fe\text{-}C_3\text{-}O_1$	175.4	178.4	Fixed	177.5-178.8	[9-12]

[a]Values from reference [2].

[b]Values from X-ray structural data.

5.2.2. The structure of the intermediate $[(\eta^5\text{-}C_5H_5)Fe(CO)C(O)CH_3]$ determined by DFT

The product of the alkyl migration reaction of $[(\eta^5\text{-}C_5H_5)Fe(CO)_2CH_3]$ is the unsaturated intermediate $[(\eta^5\text{-}C_5H_5)Fe(CO)C(O)CH_3]$. The structure of this intermediate was predicted by DFT calculation, and is shown in Figure 5.4. The unsaturated nature of the complex leads to the adoption of an η^2-acetyl group. This is evidenced by a decrease in the Fe-C1-O1 angle to 86°, a Fe-O1 distance of 2.18 Å, and an increased C1-O1 bond length of 1.29 Å. The existence of an η^2-acetyl structure was also predicted as a possibility by Marynick *et al* using PRDDO

calculations [2], and although this type of interaction has not been observed in cyclopentadienyl iron structures, it has been observed for other iron acyl complexes (See Chapter 3). The values of angles and distances are generally in agreement with those observed in X-ray crystal structures. The energy of this intermediate relative to the reactant methyl complex, $[(\eta^5\text{-}C_5H_5)Fe(CO)_2CH_3]$, is +14.8kcal.mol^{-1}.

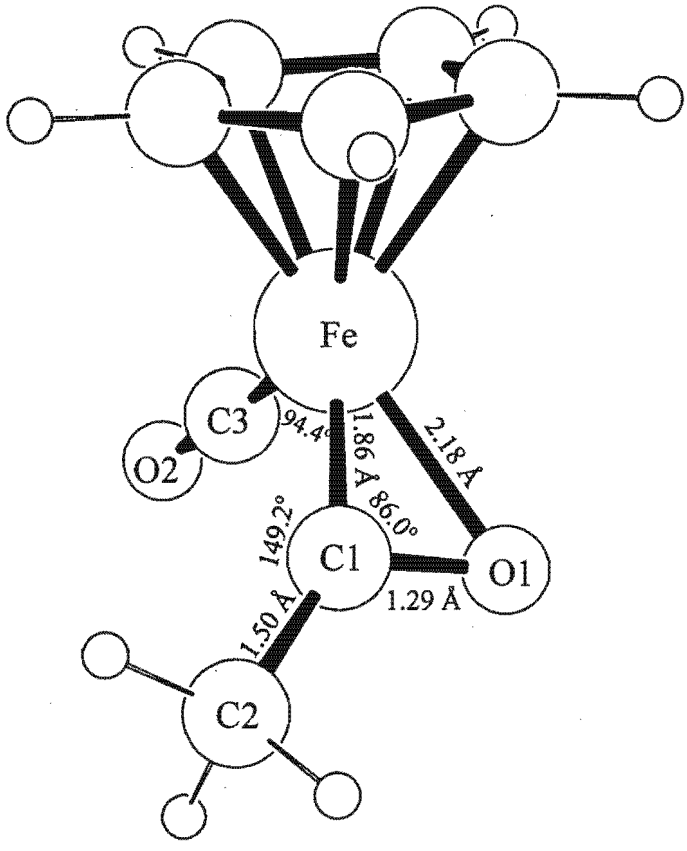

Figure 5.4 The DFT calculated structure of the intermediate product of methyl migration in $[(\eta^5\text{-}C_5H_5)Fe(CO)_2CH_3]$.

5.2.3. The structure of $[(\eta^5\text{-}C_5H_5)Fe(CO)_2C(O)CH_3]$ determined by DFT and MP2

The final product of alkyl migration of $[(\eta^5\text{-}C_5H_5)Fe(CO)_2CH_3]$ with CO as the incoming ligand is $[(\eta^5\text{-}C_5H_5)Fe(CO)_2(C(O)CH_3)]$. The X-ray crystal and molecular structure for this compound has been determined, and is reported in Chapter 3. The results of DFT and MP2 predicted structures of $[(\eta^5\text{-}C_5H_5)Fe(CO)_2(C(O)CH_3)]$ are given in Table 5-2 and Figure 5.5. The X-ray crystal structure of $[(\eta^5\text{-}C_5H_5)Fe(CO)_2(C(O)CH_3)]$ reported in Chapter 3, provides a more

rigorous set of geometrical parameters, with which to compare theoretically predicted structures, than was possible for previous theoretically predicted structures reported in this thesis (i.e. in Chapter 4). The previous structures could only be compared with similar experimentally

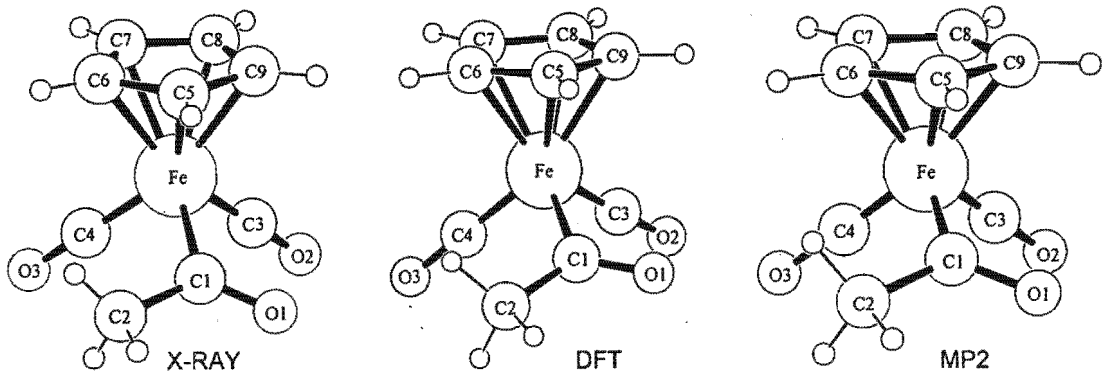

Figure 5.5 The structure of the acetyl complex $[(\eta^5\text{-}C_5H_5)Fe(CO)_2(C(O)CH_3)]$, determined by X-ray diffraction, DFT, and MP2 methods.

determined structures, and not the exact structure being studied. The results of the calculations shown in Table 5-2 indicate that DFT predicts bond lengths to within 0.05 Å of the experimental values for the carbonyl and acetyl ligands. The distances from the iron to the cyclopentadienyl carbon however, show systematic errors of between 0.12 Å and 0.15 Å too long. The MP2 calculations predicted a structure where the bond lengths from the iron to the cyclopentadienyl carbons were within 0.05 Å of the experimental values. The bond lengths between the iron and carbonyls, and iron and acetyl ligand were predicted to be 0.11 Å to 0.17 Å shorter than those observed in the X-ray crystal structure. The bond lengths within the carbonyl and acetyl ligands (i.e. C≡O, C-C, and C=O) were predicted by MP2 to be between 0.09 and 0.14 Å longer that the experimentally observed bond lengths. Predicted bond angles were generally closer to experimental values for DFT than for MP2. The iron to cyclopentadienyl bond length error in the DFT predicted structure, although not large, was unexpected. The basis sets employed in the calculation were of good quality, and it may therefore be that the error is due to the functional (BLYP) used.

The bond lengths reported for the acetyl complex, $[(\eta^5\text{-}C_5H_5)Fe(CO)_2(C(O)CH_3)]$, by the PRDDO method [2], compare well with those determined here experimentally, although neither of the conformations considered by these authors corresponds to the crystallographically observed

conformation. The minimum energy conformations predicted by DFT and MP2, as well as that observed in the crystal structure of $[(\eta^5\text{-}C_5H_5)Fe(CO)_2(C(O)CH_3)]$ are shown in Figure 5.6. The conformations shown are all qualitatively the same, with the MP2 result being closer than the DFT result to the crystallographically observed torsion angle, $C_5\text{-}Fe\text{-}C_1\text{-}C_2$. Non-bonded interactions involving the acetyl oxygen were observed in the crystal structure (See Chapter 3) and may effect the value of the torsion angle observed.

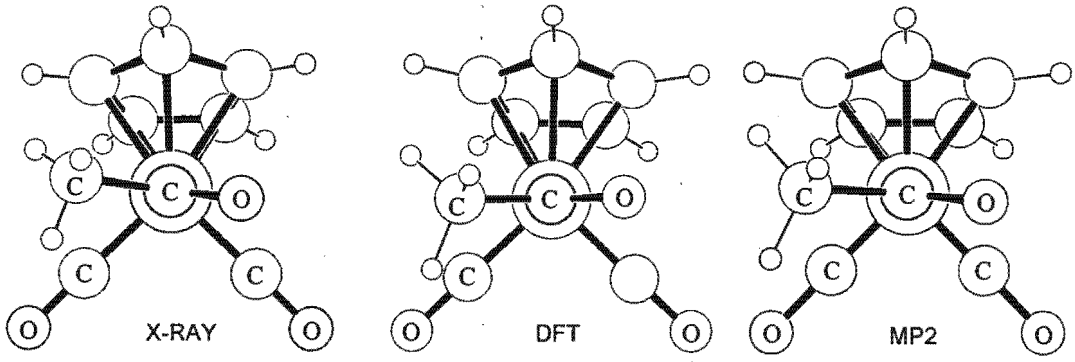

Figure 5.6 Diagram showing the conformation of the acetyl ligand, as determined by X-ray crystallography, DFT, and MP2.

Table 5 -2

Comparison of calculated bond lengths (Å) and angles (°) for $[(\eta^5\text{-}C_5H_5)Fe(CO)_2(C(O)CH_3)]$ with experimental data.

Bond/angle	MO-RHF-MP2	DFT	PRDDO[a]	Experimental[b]
$Fe\text{-}C_1$	1.87	2.02	1.97	1.979(2)
$C_1\text{-}C_2$	1.62	1.54	1.53/1.55	1.509(4)
$C_1\text{-}O_1$	1.31	1.25	1.23	1.203(3)
$Fe\text{-}C_3$	1.59	1.77	1.92/1.86	1.749(2)
$Fe\text{-}C_4$	1.58	1.76	---	1.751(3)
$C_3\text{-}O_2$	1.28	1.19	Fixed	1.143(3)
$C_4\text{-}O_3$	1.28	1.20	Fixed	1.146(3)
$Fe\text{-}C_5$	2.06	2.25	---	2.104(2)
$Fe\text{-}C_6$	2.05	2.23	2.06	2.096(2)
$Fe\text{-}C_7$	2.08	2.26	---	2.120(2)
$Fe\text{-}C_8$	2.07	2.24	---	2.120(3)
$Fe\text{-}C_9$	2.05	2.22	---	2.095(3)

C_3-Fe-C_4	89.3	93.6	---	92.66(11)
C_1-Fe-C_3	93.6	90.9	90.6	88.65(10)
Fe-C_3-O_1	175.4	177.6	Fixed	179.2(2)
Fe-C_1-C_2	118.8	119.4	124.3/125.2	117.9(2)
C_5-Fe-C_1-C_2	86.4	90.9	0/180	79.05

[a]Values from reference [2]. Two values indicate values for different conformers.

[b]Values from X-ray crystal structure of $[(\eta^5\text{-}C_5H_5)Fe(CO)_2(C(O)CH_3)]$ reported in Chapter 3.

The conformational preferences of the acetyl ligand was investigated by DFT by performing a series of single point calculations at different C_5-Fe-C_1-C_2 torsion angles using the structure determined above (0° torsion corresponds to the acetyl oxygen and cyclopentadienyl ligands being in an eclipsed conformation) . The results of these calculations are shown in Figure 5.7. The minimum energy conformation predicted is that found in the crystal structure of the complex

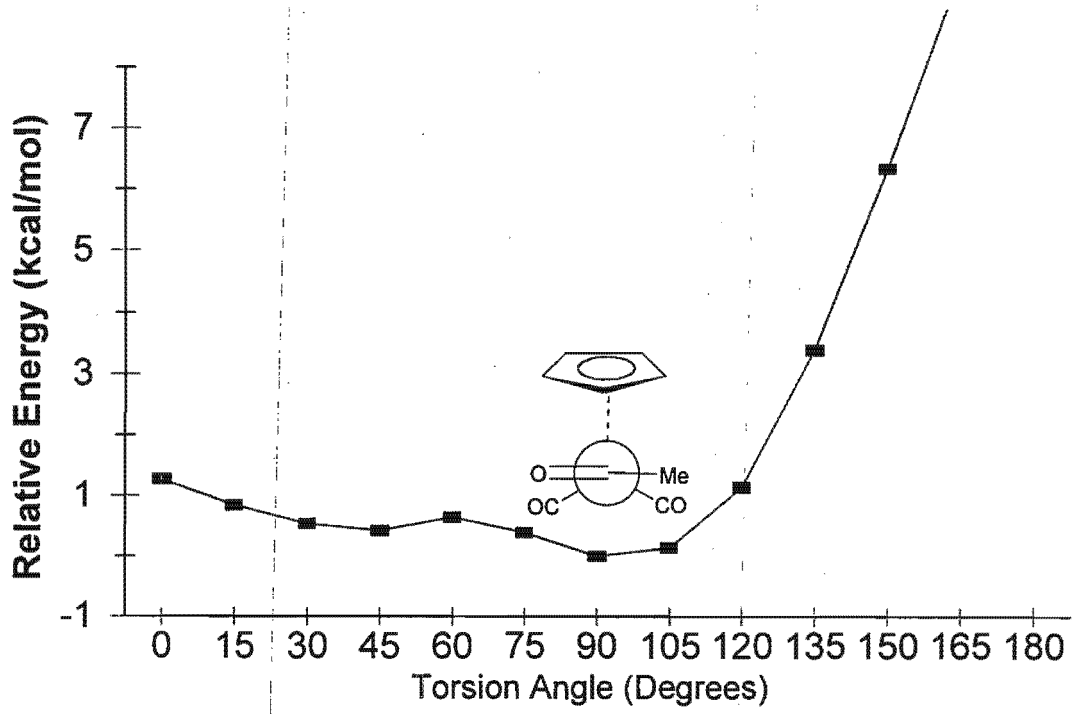

Figure 5.7 The DFT calculated rotational preferences of the acetyl ligand in $[(\eta^5\text{-}C_5H_5)Fe(CO)_2C(O)CH_3]$.

and has been previously predicted by Van der Waals interactions [5] and molecular mechanics (MMX) calculations [6,13]. The dominant factor in the determination of the conformation is the

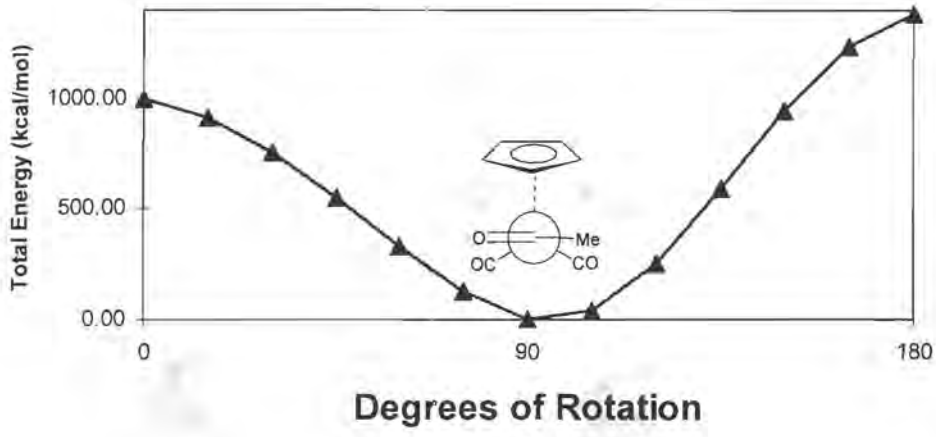

Figure 5.8 The classical nuclear-nuclear repulsion energy for the rotation of the acetyl ligand in $[(\eta^5\text{-}C_5H_5)Fe(CO)_2C(O)CH_3]$.

classical nuclear-nuclear repulsion energy which is shown in Figure 5.8. The two conformations utilized by Marynick *et al* in their PRDDO investigation of this system were found here to be maximum energy conformations, and these were confirmed as transition state structures, representing the barrier to rotation, by DFT calculations. This illustrates the danger of utilizing incompletely or partially optimized structures.

The bonding between the iron and the acetyl group consists formally of a single bond. A difference electron density map calculated during acetyl rotation (See Figure 5.9) shows that there is no change in the electron density in the region of the iron-acetyl bond (i.e. the bond order does not change) during acetyl rotation. This shows that there is no significant η^2 type interaction of the acetyl with the iron.

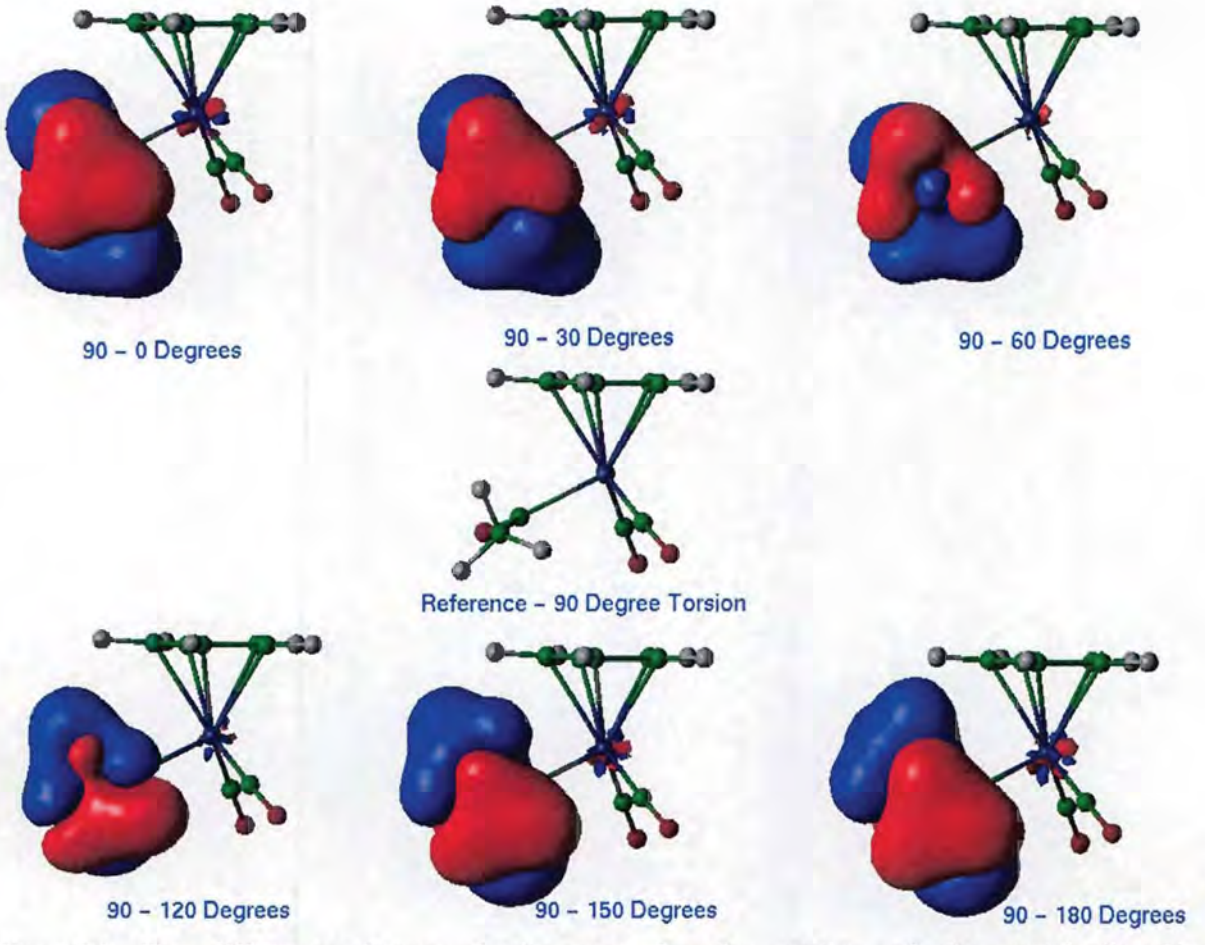

Figure 5.9 The difference electron density map for the rotation of the acetyl ligand in $[(\eta^5\text{-}C_5H_5)Fe(CO)_2C(O)CH_3]$. Note that the density shown on the acetyl ligand itself is due to the spacial changes of the group and not bonding changes.

5.2.4. The structure of the transition state for the methyl migration reaction of $[(\eta^5\text{-}C_5H_5)Fe(CO)_2CH_3]$ determined by DFT

The structure of the transition state for the methyl migration reaction was determined by DFT calculations (See Figure 5.10). The structure was fully optimized, and the stationary point located was investigated by vibrational analysis. Two imaginary vibrational modes were found, and despite repeated re-optimization the second mode reappeared in the vibrational analysis (See comments on minimum energy structures in DMol in Chapter 4). The imaginary vibrational modes appeared at 110.8i and 40.6i cm^{-1} and had intensities of 1.86 and 1.15 $km.mol^{-1}$ respectively (See Figure 5.11). Both modes appear to be contaminated with rotational modes of the cyclopentadienyl ring, however the mode at 110.8i cm^{-1} seems most likely to include the

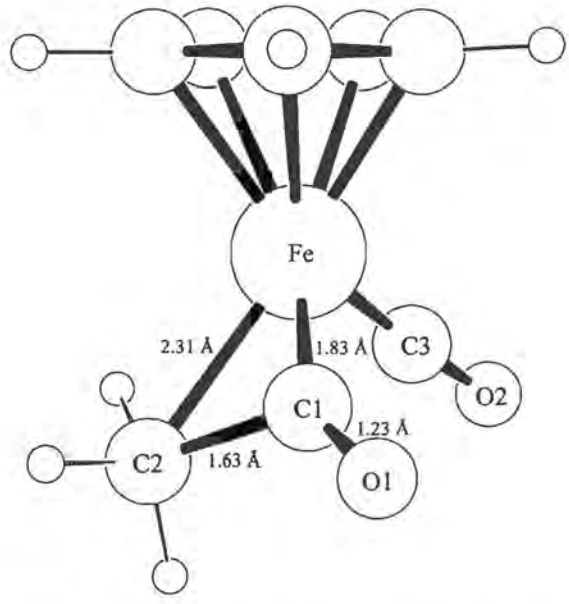

Figure 5.10 The transition state structure for the methyl migration reaction, determined by DFT.

substantial part of 'reaction' component. It is also higher frequency (absolute value) and intensity. Unfortunately DMol is not able to perform intrinsic reaction coordinate calculations, which would have verified or rejected the structure as the transition state of the reaction. Further evidence that the structure obtained is a reasonable transition state structure for the reaction is the similarity of the structure to that reported by Marynick *et al* (un-optimized) [2], the similarity of this structure to the structure obtained for the ruthenium system (See Section 5.3), which did have only one imaginary vibrational mode, and that the gradient of the energy is near zero (i.e. it is a stationary point on the PES).

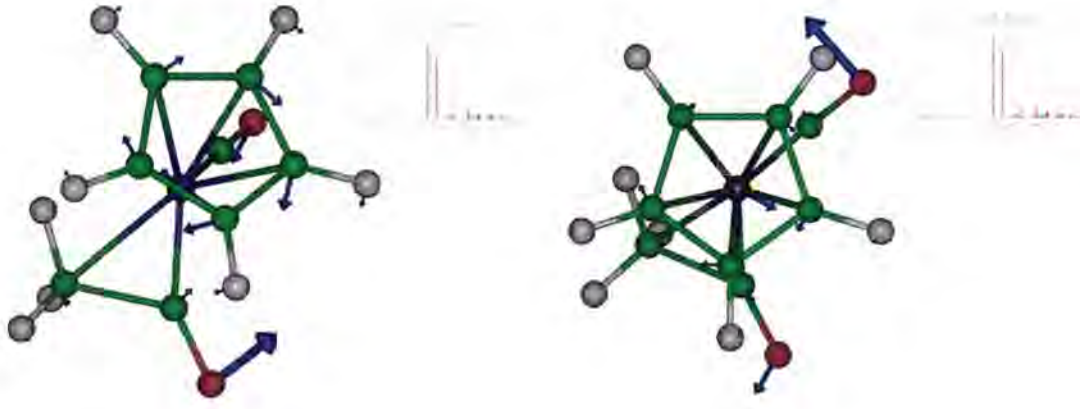

Figure 5.11 Illustration of the imaginary vibrational modes for the transition state of the methyl migration reaction. Note that only one direction of each vibration is shown.

Table 5-3		
Bond lengths (Å) and bond angles (°) for the calculated transition structure for the methyl migration reaction of		
Bond/angle	**DFT**	**PRDDO**
$Fe\text{-}C_1$	1.83	1.83
$C_1\text{-}C_2$	1.63	1.82
$C_1\text{-}O_1$	1.23	1.18
$Fe\text{-}C_2$	2.31	2.14
$Fe\text{-}C_3$	1.76	1.87
$C_3\text{-}O_2$	1.20	Fixed
$Fe\text{-}C_{Cp}$	2.13-2.23	2.05
$Fe\text{-}C_1\text{-}O_1$	150.10	178.00
$Fe\text{-}C_1\text{-}C_2$	83.90	70.00
$C_3\text{-}Fe\text{-}C_1$	93.10	88.00
$C_3\text{-}Fe\text{-}C_2$	96.30	88.80
$C_1\text{-}Fe\text{-}C_2$	44.30	56.60

The energy of the transition state (activation energy) is predicted to be +19.9 kcal.mol^{-1} above the energy of the methyl compound. This agrees well with the PRDDO result. The structure of the transition state has several differences however. The forming C1-C1 bond is shorter than in the PRDDO structure, and the forming acetyl C1=O1 double bond, from the carbonyl triple bond, is longer and the Fe-C1-O1 angle is 150° compared with 178° in PRDDO. These data suggest that the transition state occurs later along the reaction co-ordinate than was previously thought [2].

5.3. Effects of the metal on the alkyl migration reaction in $[(\eta^5\text{-}C_5H_5)M(CO)_2R]$ (M = Fe, Ru)

The effect of changing the metal from iron to ruthenium was tested by optimizing structures for the ruthenium methyl, $[(\eta^5\text{-}C_5H_5)Ru(CO)_2(CH_3)]$, the transition state,

$[(\eta^5\text{-}C_5H_5)Ru(CO)(C(O)CH_3)]$ (TS), the co-ordinatively unsaturated product, $[(\eta^5\text{-}C_5H_5)Ru(CO)(C(O)CH_3)]$ (no hessian), and the saturated acetyl product, $[(\eta^5\text{-}C_5H_5)Ru(CO)_2(C(O)CH_3)]$. The resulting energies are given in the following table.

Table 5-4

Comparison of reaction energies (kcal.mol^{-1}) for the methyl migration for the iron and ruthenium systems

	Iron	Ruthenium
Activation Energy	19.900	21.811
Reaction Energy (Unsaturated Product)	14.798	21.596
Reaction Energy (Saturated Product)	-17.946	-17.456

The above table shows that the reaction energies are rather similar, except for the energy of the unsaturated ruthenium acetyl intermediate which is more than 6kcal.mol^{-1} higher in relative energy than the corresponding iron compound. Although the activation energy and relative

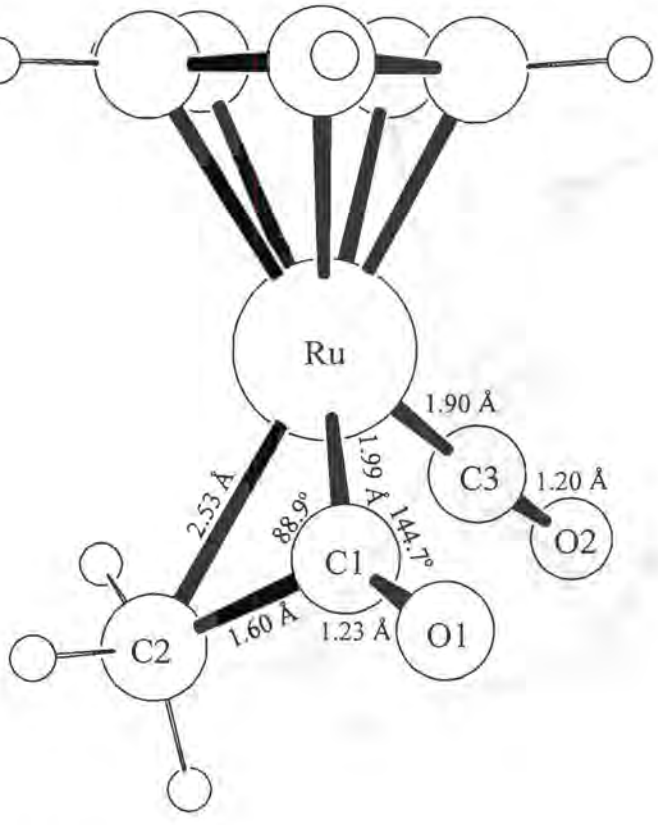

Figure 5.12 The DFT predicted transition state structure for the methyl migration reaction of $[(\eta^5\text{-}C_5H_5)Ru(CO)_2CH_3]$.

energy of the products indicates that the ruthenium system would undergo reaction more slowly and is less favourable, the energy differences may not be large enough to account for the observed slower reaction rate (more than 1000 times slower) [4], and highlights the difficulty of direct comparisons of calculations performed on metals in different transition series without consideration of relativistic effects. Recent studies on other transition metal systems, taking account of relativistic effects as a perturbation applied to the energy, have shown these effects to be important and have produced energies in close agreement with experimental energies [14].

The transition state structure for the reaction (See Figure 5.12) is similar to that obtained for the iron system. The carbon - carbon bond distance (i.e. C1-C2) is shorter than in the iron structure, and the Ru-C1-O1 angle is smaller. This may be indicative of a slightly later transition state for the ruthenium system than for the iron system. The transition state structure exhibited one imaginary vibrational mode, verifying the nature of the stationary point (See Figure 5.13). The mode indicates the reaction path, however there is also a contribution from a rotation of the cyclopentadienyl ring.

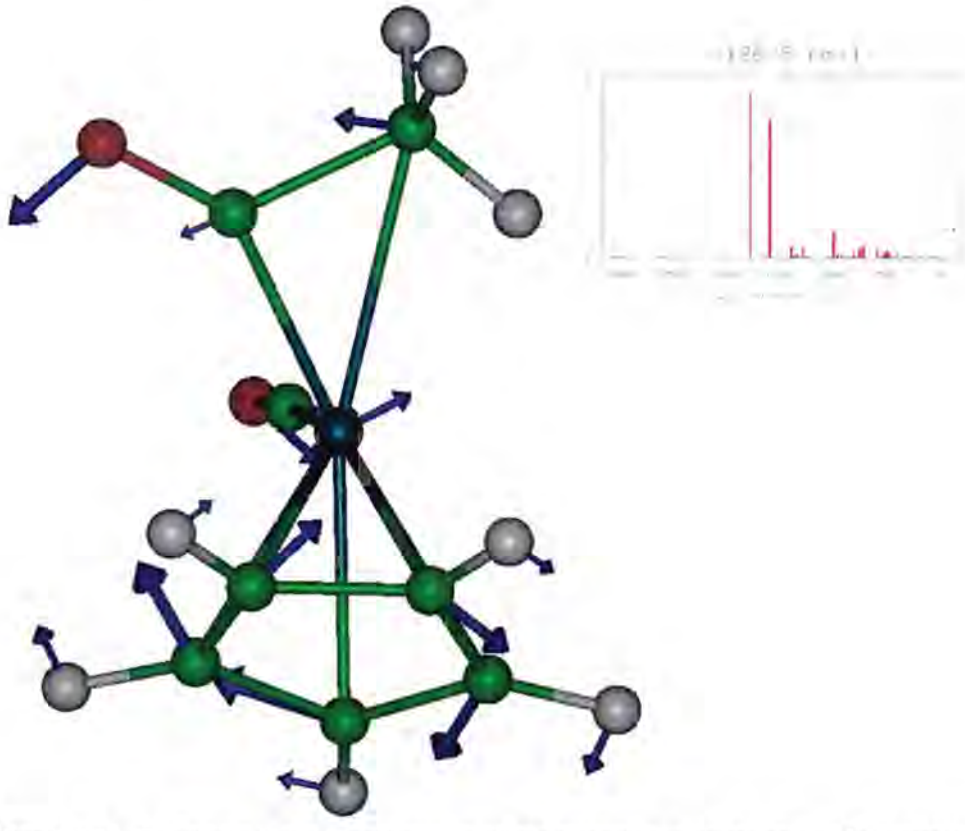

Figure 5.13 The single imaginary vibration of the transition state structure of the methyl migration reaction of $[(\eta^5\text{-}C_5H_5)Ru(CO)_2CH_3]$.

5.4. Effects of ligand substitution on the alkyl migration reaction in $[(\eta^5\text{-}C_5H_5)Fe(CO)(L)R]$ (L = CO, PH_3)

The effect of replacing one of the carbonyl ligands with phosphine (PH_3), and of using phosphine as the incoming ligand was examined by DFT calculations. The transition state was not considered, and therefore only the effect on the total reaction energy (i.e. thermodynamics) is presented.

Table 5-5

Comparison of reaction energies for phosphine substituted methyl migration reaction.

	$(CO)_2 \rightarrow (CO)_2$	$(CO)_2 \rightarrow (CO)(PH_3)$	$(CO)(PH_3) \rightarrow (CO)(PH_3)$	$(CO)(PH_3) \rightarrow (PH_3)_2$
Reaction Energy (Unsaturated)	14.798	14.798	21.728[a]	21.728[a]
Reaction Energy (Saturated)	-17.946	2.265	-20.737	11.968

[a]This intermediate was not fully optimized.

The results suggest a strong thermodynamic preference for CO as the incoming ligand, with the relative energy of the mono-phosphine intermediate higher than the activation energy for the dicarbonyl reaction. Similarly to the findings in the investigation of the relative energies in the β-elimination reaction discussed in Chapter 4, differences in energy were influenced by the replacement of a CO ligand by a PH_3 ligand. This indicates the relatively weaker binding energy of the PH_3 ligand, and would be expected to be less marked for the tertiary phosphines.

5.5. Effects of the alkyl chain length on the DFT predicted energy in the alkyl migration reaction

The effect of changing the alkyl chain length has been observed to alter the rate of alkyl migration (See Chapter 2). DFT calculation were performed on structures with alkyl chain

lengths up to four carbons long for the alkyl (i.e. up to n-butyl) to investigate theoretically the experimental observations. The theoretical model used here does not account for contributions to the entropy, which may be expected to increase with the increasing length of the alkyl chain. The quantity of interest is the activation energy (i.e. the energy of the transition state) as this relates directly to the rate of reaction. It was not possible to optimize the structures for each alkyl chain length, so the structures were constructed using the optimized structures obtained for the methyl migration above. The ethyl and propionyl structures however, were optimized. The results of theses calculations are summarized in the table below.

Table 5-6

The effect of changing the alkyl chain length on the energies ($kcal.mol^{-1}$) in the alkyl migration reaction

	Methyl	**Ethyl**	**n-Propyl**	**n-Butyl**
Activation Energy	19.900	19.364	18.469	20.110
Relative Reaction Rate[a]	1.0	1.7	4.2	0.8
Reaction Energy (Unsaturated Product)	14.798	13.796	13.115	13.979
Reaction Energy (Saturated Product)	-17.946	-20.382	-19.372	-18.446

[a]Rate of reaction $\propto e^{-\Delta E_a}$ from the Eyring equation, where ΔE_a is the activation energy.

The activation energy decreases from methyl to ethyl to n-propyl, and then increases for n-butyl. This is in agreement with experimentally observed results [4]. The difference between the methyl and ethyl activation energies is $0.536 kcal.mol^{-1}$ lower for the ethyl, which is smaller than the $1 kcal.mol^{-1}$ obtained by the partially optimized PRDDO calculations [2].

5.6. Effects of different functionals on the DFT predicted energy in the alkyl migration reaction.

The DFT calculations presented thus far have been performed using the BLYP functional [15,16]. In order to assess the sensitivity to the relative energies calculated, a series of calculations were performed on the BLYP predicted structures for the methyl migration reaction of $[(\eta^5\text{-}C_5H_5)Fe(CO)_2(CH_3)]$ using the BPW [15,17] and BVWN [15,18] functionals. The results are shown in Table 5-7.

Table 5-7

Comparison of Binding Energies (kcal.mol^{-1}) and Reaction Energies from Different Functionals for the Methyl Migration.

	BLYP	BPW	BVWN
$[(\eta^5\text{-}C_5H_5)Fe(CO)_2(CH_3)]$	-2125.411	-2174.824	-2079.142
$[(\eta^5\text{-}C_5H_5)Fe(CO)(C(O)CH_3)]$ (TS)	-2105.511	-2157.636	-2058.367
$[(\eta^5\text{-}C_5H_5)Fe(CO)(C(O)CH_3)]$	-2110.613	-2160.422	-2064.227
$[(\eta^5\text{-}C_5H_5)Fe(CO)_2(C(O)CH_3)]$	-2407.064	-2464.200	-2349.988
[CO]	-263.707	-267.444	-259.530
Activation Energy	19.900	17.188	20.775
Reaction Energy (Unsaturated Product)	14.798	14.402	14.915
Reaction Energy (Saturated Product)	-17.946	-21.932	-11.316

The activation energies for the reaction are within 3.6 kcal.mol^{-1} of each other, while the reaction energies for the unsaturated product are within 0.6 kcal.mol^{-1} of each other. The total reaction energies are within 4 kcal.mol^{-1} for the BLYP and BPW functionals, however the BVWN predicts a total reaction energy that is more than 6 kcal.mol^{-1} less exothermic than the BLYP functional and more than 10 kcal.mol^{-1} less exothermic than the BPW functional and is thus a reasonable functional to have been used in this study. The BLYP functional gives results that are close to observed experimental and other theoretically predicted values [2], and to the results obtained with the BPW functional. Prediction of stationary point structures was not tested for

other functionals, however the structures predicted using the BLYP functional are in reasonable agreement with experimental results for the compounds studied, although there may be small errors in the description of the iron cyclopentadienyl interaction.

5.7. Summary

The alkyl migration reaction for $[(\eta^5\text{-}C_5H_5)Fe(CO)_2CH_3]$ was investigated theoretically by DFT and MP2 methods. The structure predicted the calculations corresponds to the conformation observed by X-ray crystallography to be the lowest energy conformation. A second, local, minimum energy conformer was observed, which did not correspond to that previously reported for molecular mechanics calculations. The second minimum reported by other methods was characterized here as a maximum energy conformation by both DFT and MP2 methods. Comparison of the calculated structures, with the structures found by X-ray crystallography showed the DFT method yields better results, however a small systematic error was observed for the iron to cyclopentadienyl bond distance. The cause of this may be due to the choice of the functional used in the calculations.

The activation energy of the methyl migration reaction was found to be +19.9 kcal.mol^{-1} which compares favourably with experimental values. The effect of increasing the length of the alkyl chain was found to decrease the activation energy for the ethyl and n-propyl systems, after which the activation energy increased for the n-butyl system. This is broadly in line with the experimentally reported rates, which relate to the activation energy. The predicted relative rate for ethyl migration was not as high as expected however, and the predicted rate for n-butyl migration was lower than expected. The predicted relative rate for n-propyl migration was close to the experimentally observed value. A number of possible causes for the differences observed between experiment and theoretical predictions exist. These include entropic effects, the approximate (i.e. unoptimized) nature of the longer alkyl chain length structures, possible solvent/environmental effects, and effects of zero point vibrational energy. The results obtained for methyl migration in the analogous ruthenium system do not reflect the experimentally observed rate relative to the iron system. This is most likely due to relativistic effects which were not accounted for in the calculation. The effect of using different functionals on the predicted relative energies for the methyl migration in the iron system was also investigated. The

calculated energies were generally of comparable magnitude, except for the total energy of reaction calculated using the BVWN functional which predicted a much less exothermic reaction than the other two functionals tested. The cause of this difference was not identified.

5.8. References

1. Berke, H.; Hoffmann, R. *J. Am. Chem. Soc.* **1978**, *100*, 7224.
2. Rogers, J. R.; Kwon, O.; Marynick, D. S. *Organometallics* **1991**, *10*, 2816.
3. Moss, J. R.; Andersen, J.-A. M. *Organometallics* **1994**, *13*, 5013.
4. Moss, J. R.; Andersen, J.-A. M.; George, R. *J. Organomet. Chem.* **1995**, *505*, 131.
5. Blackburn, B. K.; Davies, S. G.; Sutton, K. H.; Whittaker, M. *Chem. Soc. Rev.* **1988**, *17*, 147.
6. Baird, M. C.; Mackie, S. C. *Organometallics* **1992**, *11*, 3712.
7. Halgren, T. A.; Lipscomb, W. N. *J. Chem. Phys.* **1973**, *58*, 1569.
8. Marynick, D. S.; Lipscomb, W. N. *Proc. Natl. Acad. Sci. USA* **1982**, *79*, 1341.
9. Green, M. L. H.; Ariyaratne, J. K. P.; Bierrum, A. M.; Prout, C. K.; Swanwick, M. G. *J. Chem. Soc. A* **1969**, 1309.
10. HIndson, K. J.; Laing, M.; Moss, J. R.; Pope, L.; Sommerville, P. *J. Organomet. Chem.* **1976**, *112*, 309.
11. Ribankov, V. B.; Aslanov, L. A.; Ionov, V. M.; Eremin, S. A. *Zh. Strukt. Khim.* **1983**, *24*, 100.
12. Chang, T. C. T.; Coolbaugh, T. S.; Foxman, B. M.; Rosenblum, M.; Simms, N.; Stockman, C. *Organometallics* **1987**, *6*, 2394.
13. Baird, M. C.; Mackie, S. C.; Park, Y.; Shurvell, H. F. *Organometallics* **1991**, *10*, 2993.
14. Ziegler, T.; Deng, L.; Han, Y. *J. Am. Chem. Soc.* **1997**, *119*, 5939.
15. Becke, A. D. *J. Chem. Phys.* **1988**, *88*, 2547.
16. Lee, C.; Yang, W.; Parr, R. G. *Physical Review B* **1988**, *37*, 785.
17. Perdew, J. P.; Wang, Y. *Phys. Rev. B* **1992**, *45*, 13244.
18. Vosko, S. J.; Wilk, L.; Nusair, M. *Can. J. Phys.* **1980**, *58*, 1200.

Chapter 6

Conclusions

Aspects of the chemistry of $[(\eta^5\text{-}C_5R'_5)Fe(CO)_2R]$ and related compounds have been investigated here using three major techniques: synthesis and reactivity, crystallography, and molecular modelling. These investigations have resulted in the isolation of a new series of iron alkyl compounds which are more stable and therefore easier to work with than their cyclopentadienyl analogues. The compounds have been fully characterized by microanalysis, infrared spectroscopy, ^1H NMR and ^{13}C NMR spectroscopy, and mass spectrometry. Furthermore the reactions of these compounds may be of relevance to catalytic reactions and be models for iron alkyl species on the catalyst surface (eg. iron alkyl species in the Fischer-Tropsch reaction). The increased stability of the compounds over their cyclopentadienyl analogues was instrumental in enabling an X-ray crystal structure of one member of the series, having a n-pentyl alkyl chain, to be solved. This structure is the first simple mononuclear dicarbonyl iron alkyl of this type to be reported, and shows the alkyl chain to be in an extended conformation between the two carbonyl ligands. An investigation of similar structures from the Cambridge Structural Database (CSD), indicated that a second conformation at the iron centre was possible for the alkyl chain. In this conformation the alkyl chain lies between the cyclopentadienyl ligand and a carbonyl ligand. The data suggested that the energy differences between these two conformations may be rather small, with the conformation of the alkyl group being determined by crystal packing effects. The small energies between the two conformations was confirmed by theoretical calculations on $[(\eta^5\text{-}C_5H_5)Fe(CO)_2CH_2CH_3]$, in which the calculated energy difference between the two conformations is predicted to be less than 0.5 kcal.mol^{-1}. The available structural data, including the structure of $[(\eta^5\text{-}C_5(CH_3)_5)Fe(CO)_2(n\text{-}C_5H_{11})]$ determined here and the structure of $[(\eta^5\text{-}C_5(CH_3)_5)Fe(CO)_2]_2[\mu\text{-}C_4H_8]$, recently determined within our research group, suggests that the steric bulk of the pentamethylcyclopentadienyl ligand induces a conformational preference where the alkyl chain lies between the two carbonyl ligands.

The β-elimination reaction of the ethyl compound, $[(\eta^5\text{-}C_5H_5)Fe(CO)_2CH_2CH_3]$, was examined theoretically and found to occur spontaneously after the loss of one of the carbonyl ligands from the complex. A transition state for the reaction could not be found however. The overall reaction

was calculated to be endothermic by about +35kcal.mol^{-1}, with the two methods used, DFT and MP2, differing by approximately 3kcal.mol^{-1}. DFT was found to give better structures than MP2, although the basis set used for the MP2 calculations was necessarily small. RHF calculations failed to give a reasonable structure for the product alkene hydride complex, $[(\eta^5\text{-}C_5H_5)Fe(CO)(H)(CH_2CH_2)]$ due to electron correlation effects, although the other structures predicted were closer to experimentally determined values. The β-hydride abstraction reaction was predicted by DFT to be highly exothermic (-117 kcal.mol^{-1}), and may be an alternative route to alkene formation in these complexes. The reaction may depend heavily on the presence of a suitable abstraction agent however, and this aspect requires further investigation.

The alkyl migration reaction for $[(\eta^5\text{-}C_5H_5)Fe(CO)_2CH_3]$ was investigated theoretically. The acetyl product of the reaction, $[(\eta^5\text{-}C_5H_5)Fe(CO)_2C(O)CH_3]$ was synthesized by known methods and a crystal structure of this fundamental acyl compound obtained. The crystal structure shows unequivocally the conformation adopted by the acetyl group, and clarifies some conflicting data in the literature. The crystal structure exhibits intermolecular C-H····O hydrogen bonding that may be responsible for the layered structure observed in the crystal packing. Theoretical investigation of the structure by DFT and MP2, predicted the conformation observed by X-ray crystallography to be the lowest energy conformation. A second, local, minimum energy conformer was observed, which did not correspond to that previously reported for molecular mechanics calculations. The second minimum reported by other methods was characterized here as a maximum energy conformation by DFT and MP2 calculations. Comparison of the calculated structures, with the structures found by X-ray crystallography showed the DFT method yields better results, however a small systematic error was observed for the iron to cyclopentadienyl bond distance. The cause of this may be due to the choice of the functional used in the calculations.

The activation energy of the methyl migration reaction was found to be +19.9 kcal.mol^{-1} which compares favourably with experimental values. The effect of increasing the length of the alkyl chain was found to decrease the activation energy for the ethyl and n-propyl systems, after which the activation energy increased for the n-butyl system. This is broadly in line with the

experimentally reported rates, which relate to the activation energy. The predicted relative rate for ethyl migration was not as high as expected however, and the predicted rate for n-butyl migration was lower than expected. The predicted relative rate for n-propyl migration was close to the experimentally observed value. A number of possible causes for the differences observed between experiment and theoretical predictions exist. These include entropic effects, the approximate (i.e. unoptimized) nature of the longer alkyl chain length structures, possible solvent/environmental effects, and effects of zero point vibrational energy. The results obtained for methyl migration in the analogous ruthenium system do not reflect the experimentally observed rate relative to the iron system. This is most likely due to relativistic effects which were not accounted for in the calculation. The effect of using different functionals on the predicted relative energies for the methyl migration in the iron system was also investigated. The calculated energies were generally of comparable magnitude, except for the total energy of reaction calculated using the BVWN functional which predicted a much less exothermic reaction than the other two functionals tested. The cause of this difference was not identified.

The work presented here represents a multifaceted approach to the study of catalytically significant iron alkyls and their reactions. The combination of synthesis, structural studies and molecular modelling has provided a new series of relatively stable complexes, and structural data on representative complexes of the systems under study. These data enabled the theoretical predictions to be validated and assessed in a number of ways, and transformations of the complexes to be investigated. Limitations in the methods could be identified from differences between theoretical predictions and experimental data. Further increases in computational power and development of the methods employed should render these types of investigation more common place in organometallic chemistry in future.

Appendix A

Observed and Calculated Structure Factors for $[(\eta^5\text{-}C_5(CH_3)_5)Fe(CO)_2(CH_2)_4CH_3]$

H	K	L	FO	FC	H	K	L	FO	FC	H	K	L	FO	FC	H	K	L	FO	FC	H	K	L	FO	FC
2	0	0	44	-44	5	5	0	16	17	3	10	0	14	-15	3	17	0	20	21	-5	2	1	31	28
4	0	0	122	-118	6	5	0	6	-3	5	10	0	14	18	4	17	0	15	-15	-4	2	1	38	-32
6	0	0	47	42	7	5	0	7	7	6	10	0	7	13	0	18	0	15	16	-3	2	1	21	22
8	0	0	9	9	8	5	0	20	-20	1	11	0	27	-26	1	18	0	25	25	0	2	1	64	-64
2	1	0	123	-128	9	5	0	20	-17	2	11	0	54	-58	1	19	0	11	10	1	2	1	24	25
3	1	0	58	-57	0	6	0	26	-24	3	11	0	7	8	2	19	0	12	-11	2	2	1	29	27
4	1	0	64	59	1	6	0	52	-53	4	11	0	14	16	-9	0	1	12	-8	3	2	1	84	82
5	1	0	39	34	2	6	0	37	42	5	11	0	6	-6	-7	0	1	40	27	4	2	1	9	8
6	1	0	26	24	3	6	0	6	-4	6	11	0	6	9	-5	0	1	15	11	5	2	1	41	-39
7	1	0	19	17	4	6	0	7	-6	0	12	0	41	-42	-3	0	1	42	-40	6	2	1	24	-26
8	1	0	20	-16	5	6	0	38	36	2	12	0	7	5	1	0	1	5	-5	7	2	1	5	-9
9	1	0	6	-5	6	6	0	5	-7	3	12	0	10	10	3	0	1	123	-118	8	2	1	9	-7
0	2	0	106	-112	7	6	0	25	-29	4	12	0	17	21	5	0	1	46	40	9	2	1	15	12
2	2	0	11	-13	1	7	0	35	36	6	12	0	18	-32	7	0	1	31	30	-9	3	1	15	-10
3	2	0	45	44	3	7	0	35	52	2	13	0	23	22	9	0	1	10	-9	-8	3	1	8	-6
4	2	0	60	59	4	7	0	23	-22	3	13	0	9	-6	-9	1	1	15	8	-7	3	1	7	-4
5	2	0	37	31	5	7	0	16	-28	4	13	0	18	-18	-8	1	1	11	6	-6	3	1	47	-38
6	2	0	19	-17	9	7	0	18	17	6	13	0	8	-9	-7	1	1	19	-18	-5	3	1	40	38
7	2	0	11	-10	0	8	0	13	-15	0	14	0	31	28	-6	1	1	9	8	-4	3	1	17	16
9	2	0	6	-2	1	8	0	79	82	2	14	0	10	-10	-5	1	1	46	-41	-3	3	1	61	-68
5	3	0	32	-32	2	8	0	15	15	3	14	0	13	13	-3	1	1	99	100	-2	3	1	24	29
6	3	0	13	-12	4	8	0	14	13	4	14	0	14	-15	0	1	1	49	49	-1	3	1	51	-53
7	3	0	27	-24	5	8	0	22	-21	5	14	0	7	-9	1	1	1	143	-146	0	3	1	52	-52
8	3	0	18	17	7	8	0	9	20	6	14	0	16	18	2	1	1	5	-4	1	3	1	67	66
9	3	0	16	13	8	8	0	8	9	1	15	0	11	11	3	1	1	24	23	2	3	1	38	37
0	4	0	72	-75	1	9	0	42	44	2	15	0	28	-27	4	1	1	42	35	3	3	1	8	7
2	4	0	12	-12	2	9	0	59	59	4	15	0	14	12	5	1	1	7	8	4	3	1	10	-8
5	4	0	25	-27	3	9	0	29	-37	6	15	0	8	9	6	1	1	8	9	5	3	1	49	-43
7	4	0	20	22	4	9	0	15	-15	0	16	0	32	-29	7	1	1	30	-28	6	3	1	30	-32
8	4	0	8	-5	5	9	0	13	13	1	16	0	5	-6	9	1	1	8	6	7	3	1	16	15
1	5	0	51	-52	8	9	0	6	7	2	16	0	25	24	-9	2	1	9	6	9	3	1	5	-3
2	5	0	11	-15	0	10	0	23	21	4	16	0	17	16	-8	2	1	8	4	-9	4	1	9	-5
3	5	0	15	-18	1	10	0	27	-32	1	17	0	15	-14	-7	2	1	30	-22	-8	4	1	20	-16
4	5	0	42	40	2	10	0	32	-30	2	17	0	27	26	-6	2	1	20	-18	-7	4	1	11	10

H	K	L	FO	FC	H	K	L	FO	FC	H	K	L	FO	FC	H	K	L	FO	FC	H	K	L	FO	FC
-6	4	1	29	24	0	6	1	5	3	-4	9	1	28	-42	-7	12	1	8	-18	5	15	1	13	12
-5	4	1	24	-20	1	6	1	36	35	-3	9	1	26	-26	-5	12	1	12	13	6	15	1	8	11
-4	4	1	5	8	2	6	1	15	-13	-2	9	1	30	32	-3	12	1	22	23	-5	16	1	6	7
-3	4	1	21	-21	3	6	1	15	14	-1	9	1	35	-35	-2	12	1	13	13	-3	16	1	30	26
-2	4	1	37	-40	4	6	1	56	51	0	9	1	71	70	-1	12	1	46	-48	-2	16	1	8	7
-1	4	1	9	9	5	6	1	21	-19	1	9	1	57	57	1	12	1	18	-17	-1	16	1	24	-24
0	4	1	7	7	8	6	1	8	-10	2	9	1	56	-56	2	12	1	5	-6	0	16	1	11	-10
1	4	1	31	-30	9	6	1	5	6	3	9	1	21	-19	3	12	1	22	20	1	16	1	6	5
2	4	1	21	-20	-8	7	1	9	-7	4	9	1	13	12	5	12	1	30	-24	3	16	1	28	27
3	4	1	53	-51	-5	7	1	5	21	5	9	1	27	-24	6	12	1	6	8	5	16	1	8	-7
4	4	1	33	-33	-4	7	1	20	44	6	9	1	9	29	-5	13	1	19	19	-4	17	1	9	11
5	4	1	14	14	-3	7	1	8	7	-6	10	1	6	-16	-3	13	1	12	-11	-3	17	1	25	-24
6	4	1	26	35	-2	7	1	6	-6	-5	10	1	22	-28	-2	13	1	22	-23	-1	17	1	6	-6
8	4	1	6	7	-1	7	1	19	-18	-4	10	1	11	-13	-1	13	1	7	6	0	17	1	15	-15
9	4	1	12	-11	0	7	1	47	-48	-3	10	1	36	-34	1	13	1	23	23	1	17	1	24	23
-9	5	1	10	7	1	7	1	43	41	-2	10	1	17	19	3	13	1	13	-11	2	17	1	23	22
-7	5	1	7	-4	2	7	1	64	66	-1	10	1	75	75	5	13	1	10	-9	3	17	1	15	-15
-6	5	1	25	24	3	7	1	10	-10	0	10	1	35	-35	6	13	1	6	-6	-2	18	1	29	-28
-5	5	1	13	-16	4	7	1	14	-15	2	10	1	21	-21	7	13	1	10	16	-1	18	1	15	16
-3	5	1	24	27	5	7	1	6	-4	3	10	1	31	-29	-5	14	1	6	-7	0	18	1	8	8
-2	5	1	12	-12	8	7	1	16	22	4	10	1	26	24	-3	14	1	20	-19	1	18	1	7	-7
-1	5	1	61	60	-8	8	1	16	-15	5	10	1	27	22	-2	14	1	15	12	2	18	1	6	7
0	5	1	37	-34	-6	8	1	6	20	6	10	1	6	-16	-1	14	1	25	23	3	18	1	17	-16
1	5	1	22	-24	-4	8	1	10	14	-5	11	1	25	-31	0	14	1	7	9	0	19	1	8	11
2	5	1	31	-31	-3	8	1	10	10	-4	11	1	8	9	2	14	1	8	8	1	19	1	10	-9
3	5	1	6	8	-2	8	1	63	-65	-3	11	1	25	27	3	14	1	21	-18	-8	0	2	38	23
5	5	1	14	13	-1	8	1	6	6	-2	11	1	13	-13	5	14	1	19	14	-6	0	2	16	-15
6	5	1	11	16	0	8	1	73	73	0	11	1	11	-9	-5	15	1	13	-11	-4	0	2	88	-80
8	5	1	19	-20	2	8	1	27	26	1	11	1	62	-62	-3	15	1	15	15	0	0	2	33	32
-8	6	1	28	25	3	8	1	22	19	2	11	1	14	-13	-1	15	1	12	11	4	0	2	85	77
-6	6	1	5	-7	4	8	1	58	-54	3	11	1	28	24	0	15	1	14	13	6	0	2	29	27
-3	6	1	12	14	5	8	1	16	17	4	11	1	7	-6	1	15	1	33	-32	8	0	2	28	-28
-2	6	1	32	39	8	8	1	6	9	5	11	1	27	22	2	15	1	7	6	-9	1	2	6	3
-1	6	1	42	-40	-5	9	1	5	7	7	11	1	8	-15	3	15	1	29	25	-6	1	2	45	-33

H	K	L	FO	FC	H	K	L	FO	FC	H	K	L	FO	FC	H	K	L	FO	FC	H	K	L	FO	FC
-5	1	2	28	-26	5	3	2	33	-29	-5	6	2	5	-19	1	8	2	11	13	-1	11	2	27	-28
-4	1	2	24	26	6	3	2	15	18	-4	6	2	8	8	2	8	2	10	10	0	11	2	24	-24
0	1	2	172	-177	-9	4	2	15	-11	-3	6	2	67	61	3	8	2	53	-51	1	11	2	24	24
1	1	2	56	-55	-8	4	2	17	13	-2	6	2	9	-9	4	8	2	19	-17	2	11	2	12	12
3	1	2	34	-32	-7	4	2	6	5	-1	6	2	17	15	5	8	2	13	12	3	11	2	6	6
4	1	2	57	51	-6	4	2	14	13	0	6	2	18	-17	7	8	2	10	18	4	11	2	10	8
5	1	2	26	21	-5	4	2	6	11	1	6	2	16	-18	8	8	2	6	7	5	11	2	27	-23
6	1	2	36	-37	-2	4	2	9	11	2	6	2	15	16	-6	9	2	11	10	6	11	2	16	-25
7	1	2	5	2	-1	4	2	79	74	3	6	2	64	61	-5	9	2	15	-14	-7	12	2	6	4
8	1	2	7	-8	0	4	2	15	15	7	6	2	8	-13	-3	9	2	10	-10	-5	12	2	14	12
-9	2	2	8	6	1	4	2	96	93	8	6	2	5	9	-2	9	2	36	-33	-4	12	2	22	22
-8	2	2	25	-17	2	4	2	30	-30	9	6	2	14	15	-1	9	2	22	23	-3	12	2	15	-13
-7	2	2	18	-14	3	4	2	50	-49	-8	7	2	12	9	0	9	2	12	-10	-2	12	2	44	-42
-6	2	2	6	3	4	4	2	13	12	-7	7	2	29	-23	1	9	2	20	-19	0	12	2	10	-10
-5	2	2	11	-11	5	4	2	7	-4	-6	7	2	11	-9	2	9	2	20	-17	1	12	2	7	6
0	2	2	9	-9	6	4	2	6	-2	-5	7	2	20	18	5	9	2	25	22	2	12	2	44	41
1	2	2	91	-90	7	4	2	7	9	-2	7	2	23	21	-7	10	2	5	-10	3	12	2	15	-13
2	2	2	63	63	8	4	2	15	-16	-1	7	2	63	-62	-5	10	2	17	-16	4	12	2	16	-13
3	2	2	19	18	9	4	2	11	-10	0	7	2	4	4	-4	10	2	13	-11	5	12	2	10	9
4	2	2	53	-50	-7	5	2	28	22	1	7	2	66	66	-3	10	2	19	19	6	12	2	7	-9
6	2	2	11	-12	-6	5	2	7	-4	2	7	2	19	20	-2	10	2	35	34	7	12	2	5	8
7	2	2	17	-16	-3	5	2	4	3	3	7	2	24	24	-1	10	2	22	-22	-6	13	2	25	22
8	2	2	21	21	-2	5	2	39	33	4	7	2	7	6	0	10	2	7	7	-4	13	2	19	-18
9	2	2	7	5	-1	5	2	72	71	5	7	2	32	-31	1	10	2	18	-16	-3	13	2	6	-7
-8	3	2	14	-10	0	5	2	63	-62	6	7	2	5	-8	2	10	2	39	-39	-2	13	2	16	-14
-7	3	2	6	-4	1	5	2	68	-67	7	7	2	11	17	3	10	2	23	19	0	13	2	53	54
-6	3	2	29	21	2	5	2	12	10	8	7	2	6	6	4	10	2	9	8	4	13	2	25	-22
-5	3	2	28	33	3	5	2	28	-26	9	7	2	8	7	5	10	2	17	-15	6	13	2	18	23
-1	3	2	51	-54	4	5	2	42	41	-8	8	2	7	-5	7	10	2	8	-13	-6	14	2	8	-7
0	3	2	20	19	5	5	2	42	38	-7	8	2	18	14	-7	11	2	7	-9	-5	14	2	10	8
1	3	2	21	19	7	5	2	15	-17	-5	8	2	17	15	-6	11	2	27	-25	-4	14	2	22	-19
2	3	2	30	-30	-9	6	2	25	16	-4	8	2	20	15	-5	11	2	23	22	-2	14	2	36	35
3	3	2	12	12	-8	6	2	13	-9	-3	8	2	45	-41	-4	11	2	12	10	0	14	2	7	6
4	3	2	38	-37	-7	6	2	9	-6	-2	8	2	5	5	-2	11	2	20	21	2	14	2	47	-43

H	K	L	FO	FC	H	K	L	FO	FC	H	K	L	FO	FC	H	K	L	FO	FC	H	K	L	FO	FC
4	14	2	17	14	-5	0	3	50	-45	7	2	3	30	29	2	5	3	72	-69	-6	8	3	6	21
5	14	2	13	11	-3	0	3	5	-5	-9	3	3	16	-12	3	5	3	51	51	-4	8	3	46	-44
6	14	2	9	12	-1	0	3	66	63	-8	3	3	11	-7	4	5	3	54	50	-2	8	3	5	-5
-6	15	2	12	-10	1	0	3	17	19	-7	3	3	30	20	5	5	3	8	7	-1	8	3	5	2
-4	15	2	9	7	3	0	3	14	15	-6	3	3	16	21	7	5	3	8	-13	0	8	3	73	73
-2	15	2	19	19	7	0	3	33	-32	-1	3	3	58	56	8	5	3	7	-8	1	8	3	11	-10
-1	15	2	9	9	9	0	3	6	5	0	3	3	30	30	9	5	3	7	7	2	8	3	39	-39
0	15	2	26	-25	-9	1	3	15	12	1	3	3	16	-15	-8	6	3	10	-8	3	8	3	25	-24
2	15	2	6	6	-7	1	3	33	-21	2	3	3	84	79	-7	6	3	8	9	4	8	3	17	-16
3	15	2	9	-7	-5	1	3	26	-23	3	3	3	66	-65	-4	6	3	21	57	6	8	3	16	30
4	15	2	17	17	-4	1	3	7	-9	4	3	3	14	-14	-3	6	3	14	-17	-6	9	3	24	-20
5	15	2	5	6	-1	1	3	26	24	5	3	3	46	43	-2	6	3	11	-9	-5	9	3	11	-7
-4	16	2	8	7	0	1	3	10	10	6	3	3	6	7	-1	6	3	12	-11	-4	9	3	25	-21
-3	16	2	12	10	1	1	3	74	71	8	3	3	8	7	0	6	3	83	-81	-3	9	3	32	-31
-2	16	2	22	-21	2	1	3	48	-45	9	3	3	15	-15	1	6	3	24	23	-2	9	3	35	35
1	16	2	12	-12	3	1	3	18	16	-9	4	3	10	5	2	6	3	48	50	-1	9	3	21	22
2	16	2	28	27	4	1	3	6	-6	-6	4	3	16	20	3	6	3	20	19	0	9	3	25	-25
3	16	2	12	12	5	1	3	61	-57	-5	4	3	8	-16	4	6	3	30	28	2	9	3	15	-13
-4	17	2	11	-10	6	1	3	13	12	-1	4	3	12	12	6	6	3	11	-20	3	9	3	22	-22
-3	17	2	10	9	7	1	3	13	-11	0	4	3	99	96	7	6	3	5	-7	4	9	3	44	40
-2	17	2	14	-13	8	1	3	7	-6	1	4	3	49	-47	8	6	3	10	11	8	9	3	6	-11
-1	17	2	14	-14	9	1	3	17	16	2	4	3	84	-84	-8	7	3	17	-12	-6	10	3	18	-15
0	17	2	20	21	-9	2	3	17	-9	3	4	3	21	19	-7	7	3	6	-8	-5	10	3	16	-16
1	17	2	11	11	-8	2	3	6	-4	4	4	3	31	-30	-6	7	3	5	16	-4	10	3	22	24
2	17	2	8	-7	-7	2	3	18	-13	5	4	3	15	14	-3	7	3	18	15	-3	10	3	7	8
4	17	2	17	-17	-6	2	3	5	7	6	4	3	22	27	-2	7	3	47	-48	-2	10	3	5	-5
-3	18	2	20	-20	-5	2	3	47	54	7	4	3	10	-10	-1	7	3	35	35	0	10	3	24	-25
-2	18	2	12	13	-1	2	3	64	-63	-9	5	3	12	8	0	7	3	47	45	1	10	3	39	-38
1	18	2	14	13	1	2	3	75	73	-8	5	3	24	16	1	7	3	18	18	2	10	3	25	25
2	18	2	12	-11	2	2	3	8	-7	-7	5	3	5	-6	2	7	3	25	24	3	10	3	27	27
3	18	2	16	-17	3	2	3	33	-31	-6	5	3	11	-21	3	7	3	7	6	4	10	3	16	-14
-1	19	2	20	19	4	2	3	8	-7	-1	5	3	47	-45	4	7	3	50	-48	5	10	3	30	25
1	19	2	16	-14	5	2	3	30	-27	0	5	3	53	-51	5	7	3	6	-5	6	10	3	14	-23
-9	0	3	14	8	6	2	3	5	-2	1	5	3	19	-18	8	7	3	10	12	8	10	3	5	8

H	K	L	FO	FC	H	K	L	FO	FC	H	K	L	FO	FC	H	K	L	FO	FC	H	K	L	FO	FC
-7	11	3	16	-13	-1	14	3	17	17	-6	0	4	21	-18	0	3	4	12	12	-7	6	4	11	-22
-6	11	3	14	12	0	14	3	8	8	-4	0	4	11	-9	1	3	4	89	89	-5	6	4	11	34
-5	11	3	12	9	1	14	3	39	-38	-2	0	4	51	50	2	3	4	32	-31	-2	6	4	19	-18
-4	11	3	22	20	2	14	3	10	9	0	0	4	127	-124	3	3	4	21	-21	-1	6	4	91	-84
-3	11	3	32	33	3	14	3	7	7	2	0	4	9	9	4	3	4	15	14	0	6	4	33	30
-2	11	3	11	-10	4	14	3	9	8	4	0	4	43	43	5	3	4	22	-19	1	6	4	44	44
-1	11	3	50	-51	5	14	3	15	15	6	0	4	22	-21	7	3	4	9	8	2	6	4	19	-17
0	11	3	6	7	-4	15	3	10	-7	-8	1	4	23	-15	8	3	4	17	-18	3	6	4	50	49
1	11	3	25	-25	-3	15	3	24	21	-7	1	4	6	2	-8	4	4	12	7	5	6	4	40	-38
2	11	3	11	9	-1	15	3	25	-24	-6	1	4	8	-7	-7	4	4	12	10	7	6	4	8	6
3	11	3	30	30	0	15	3	6	-6	-5	1	4	15	-15	-6	4	4	10	-17	-7	7	4	7	17
4	11	3	27	-25	3	15	3	18	17	-2	1	4	23	-25	-2	4	4	7	10	-5	7	4	8	24
5	11	3	22	-20	4	15	3	8	7	-1	1	4	19	18	-1	4	4	53	52	-4	7	4	5	10
-7	12	3	6	-3	5	15	3	9	-9	0	1	4	12	-11	0	4	4	53	-53	-3	7	4	57	-66
-6	12	3	6	4	-4	16	3	10	8	1	1	4	35	-31	1	4	4	14	-13	-2	7	4	6	-3
-5	12	3	24	21	-3	16	3	10	-11	2	1	4	42	41	2	4	4	28	27	-1	7	4	8	9
-4	12	3	10	-7	-1	16	3	10	-9	4	1	4	65	-62	3	4	4	37	-35	1	7	4	42	42
-3	12	3	17	-16	0	16	3	9	-9	5	1	4	6	4	4	4	4	43	41	2	7	4	10	10
1	12	3	41	40	1	16	3	22	22	6	1	4	14	-11	5	4	4	43	40	3	7	4	63	-59
2	12	3	9	-7	2	16	3	12	10	8	1	4	26	28	6	4	4	23	-28	4	7	4	6	-6
3	12	3	16	-16	3	16	3	13	-11	-8	2	4	18	-13	9	4	4	10	-7	6	7	4	7	-13
4	12	3	9	9	4	16	3	5	-4	-6	2	4	22	18	-9	5	4	20	11	7	7	4	21	24
5	12	3	17	-15	5	16	3	10	-8	-2	2	4	9	-11	-7	5	4	10	-14	-7	8	4	6	14
7	12	3	9	16	-4	17	3	15	13	-1	2	4	111	-109	-6	5	4	8	-21	-4	8	4	7	-7
-7	13	3	16	10	-3	17	3	16	-15	0	2	4	13	13	-2	5	4	13	15	-3	8	4	29	-26
-3	13	3	16	-15	-2	17	3	21	-20	1	2	4	82	81	-1	5	4	28	-26	-2	8	4	15	-14
-2	13	3	7	8	2	17	3	9	9	3	2	4	8	8	0	5	4	18	-16	-1	8	4	51	52
-1	13	3	40	37	3	17	3	16	-15	4	2	4	36	-34	1	5	4	73	-73	0	8	4	30	28
1	13	3	6	6	4	17	3	11	-10	5	2	4	32	-28	3	5	4	50	49	1	8	4	20	-20
3	13	3	25	-23	-3	18	3	7	6	6	2	4	23	23	5	5	4	14	12	2	8	4	18	-16
5	13	3	21	19	-2	18	3	7	-5	-9	3	4	8	-5	6	5	4	6	4	3	8	4	17	-17
-5	14	3	26	-20	0	18	3	7	6	-8	3	4	20	13	7	5	4	19	-21	4	8	4	17	-17
-3	14	3	15	13	2	18	3	16	-15	-2	3	4	8	10	8	5	4	8	9	5	8	4	15	13
-2	14	3	6	6	-8	0	4	21	16	-1	3	4	29	30	9	5	4	9	8	6	8	4	8	15

H	K	L	FO	FC	H	K	L	FO	FC	H	K	L	FO	FC	H	K	L	FO	FC	H	K	L	FO	FC
-6	9	4	6	12	-6	12	4	27	22	1	15	4	5	-6	2	1	5	12	12	-6	4	5	9	-20
-5	9	4	11	-14	-5	12	4	26	-23	2	15	4	32	31	3	1	5	8	-7	-4	4	5	5	-15
-4	9	4	13	-12	-4	12	4	13	-10	3	15	4	9	7	4	1	5	29	-27	-2	4	5	51	51
-3	9	4	39	37	-3	12	4	14	12	4	15	4	11	-11	6	1	5	12	12	-1	4	5	38	-36
-2	9	4	9	10	-2	12	4	23	-22	-2	16	4	19	-18	7	1	5	21	20	1	4	5	20	-20
1	9	4	32	-32	-1	12	4	30	28	-1	16	4	15	-14	-9	2	5	18	-12	2	4	5	44	-42
2	9	4	21	-21	0	12	4	27	30	0	16	4	14	13	-8	2	5	11	-6	3	4	5	54	53
3	9	4	32	32	1	12	4	29	-28	1	16	4	13	13	-7	2	5	23	16	4	4	5	45	42
4	9	4	8	7	3	12	4	21	-21	4	16	4	6	-4	-6	2	5	10	-8	5	4	5	29	-27
7	9	4	10	-13	4	12	4	25	-24	-4	17	4	12	-10	-2	2	5	23	-26	6	4	5	8	-8
-7	10	4	9	-9	5	12	4	24	24	-3	17	4	14	-12	-1	2	5	35	35	7	4	5	17	-18
-6	10	4	12	-13	6	12	4	18	26	0	17	4	9	8	0	2	5	12	12	8	4	5	20	-18
-5	10	4	25	24	-4	13	4	27	-23	1	17	4	17	16	2	2	5	7	-7	-8	5	5	9	-10
-4	10	4	9	-8	-3	13	4	11	9	2	17	4	6	-5	3	2	5	42	-40	-6	5	5	10	-25
-2	10	4	23	25	-2	13	4	33	31	3	17	4	11	-8	4	2	5	22	-22	-2	5	5	10	-11
-1	10	4	31	-33	-1	13	4	13	-12	-1	18	4	23	20	5	2	5	33	32	0	5	5	50	-49
0	10	4	8	-9	0	13	4	7	8	1	18	4	16	-16	6	2	5	6	7	1	5	5	7	8
1	10	4	24	25	1	13	4	13	-13	-9	0	5	20	15	8	2	5	9	9	2	5	5	42	39
2	10	4	19	21	2	13	4	44	-43	-7	0	5	8	-6	9	2	5	17	-16	3	5	5	13	-12
3	10	4	20	18	3	13	4	10	10	-5	0	5	30	-23	-9	3	5	13	7	4	5	5	34	33
5	10	4	33	-30	4	13	4	21	20	-3	0	5	35	38	-7	3	5	10	8	6	5	5	43	-45
6	10	4	10	-18	5	13	4	9	8	-1	0	5	26	-26	-6	3	5	13	19	-8	6	5	12	-13
-7	11	4	10	7	6	13	4	10	13	1	0	5	38	35	-5	3	5	21	-32	-6	6	5	8	21
-6	11	4	11	-9	-6	14	4	21	-15	3	0	5	27	31	-2	3	5	19	-21	-5	6	5	7	18
-5	11	4	13	12	-2	14	4	26	23	5	0	5	23	-22	-1	3	5	14	14	-4	6	5	7	15
-3	11	4	25	-24	0	14	4	27	-25	9	0	5	9	10	1	3	5	47	-47	-2	6	5	60	-58
-2	11	4	17	-17	3	14	4	8	-7	-7	1	5	18	-13	2	3	5	45	-45	0	6	5	24	23
0	11	4	9	-10	4	14	4	17	16	-5	1	5	24	27	3	3	5	9	-8	1	6	5	20	-23
1	11	4	29	28	6	14	4	10	-13	-4	1	5	7	-5	5	3	5	41	38	2	6	5	55	55
2	11	4	33	33	-5	15	4	10	-4	-3	1	5	11	-13	6	3	5	24	22	3	6	5	7	8
3	11	4	18	-18	-4	15	4	21	16	-2	1	5	24	22	7	3	5	25	-22	4	6	5	50	-48
5	11	4	7	-7	-3	15	4	16	12	-1	1	5	73	-73	-9	4	5	16	10	5	6	5	14	13
7	11	4	8	14	-2	15	4	26	-24	0	1	5	15	15	-8	4	5	19	13	6	6	5	9	-10
-7	12	4	6	3	0	15	4	6	-5	1	1	5	68	69	-7	4	5	15	-16	8	6	5	15	17

H	K	L	FO	FC	H	K	L	FO	FC	H	K	L	FO	FC	H	K	L	FO	FC	H	K	L	FO	FC
-6	7	5	5	18	-3	10	5	34	32	1	13	5	16	-15	8	0	6	19	18	0	3	6	34	-35
-4	7	5	24	-42	-2	10	5	41	-41	2	13	5	13	12	-8	1	6	16	-11	1	3	6	11	-12
-3	7	5	20	-23	-1	10	5	42	-41	3	13	5	10	10	-6	1	6	11	10	2	3	6	17	-17
-2	7	5	9	-9	0	10	5	10	11	5	13	5	21	20	-4	1	6	16	-16	4	3	6	39	38
-1	7	5	5	1	1	10	5	16	-15	-3	14	5	20	18	-3	1	6	14	14	5	3	6	27	25
0	7	5	98	96	2	10	5	41	40	-2	14	5	10	-10	-2	1	6	41	-43	6	3	6	25	-24
1	7	5	7	9	3	10	5	22	22	-1	14	5	13	-11	-1	1	6	15	-16	8	3	6	5	-5
2	7	5	39	-40	4	10	5	27	-26	3	14	5	17	15	0	1	6	76	75	-8	4	6	13	-11
3	7	5	21	20	5	10	5	10	-10	4	14	5	7	5	1	1	6	27	27	-7	4	6	6	-6
4	7	5	22	-21	-7	11	5	10	-9	5	14	5	18	-17	2	1	6	10	11	-6	4	6	7	-15
6	7	5	22	26	-5	11	5	16	18	-5	15	5	21	16	3	1	6	8	-6	-5	4	6	10	-16
-4	8	5	13	-16	-4	11	5	25	-22	-4	15	5	12	7	4	1	6	45	-43	-4	4	6	12	21
-3	8	5	12	-14	-2	11	5	13	10	-1	15	5	18	-18	6	1	6	9	8	-3	4	6	19	28
-2	8	5	62	60	0	11	5	17	18	0	15	5	8	-8	-9	2	6	10	-5	-2	4	6	7	-5
-1	8	5	38	36	1	11	5	26	26	1	15	5	27	27	-8	2	6	13	10	-1	4	6	19	-17
0	8	5	31	-30	3	11	5	22	-22	3	15	5	17	-15	-5	2	6	10	12	0	4	6	20	-20
1	8	5	18	19	4	11	5	16	-15	5	15	5	13	-12	-4	2	6	32	-40	1	4	6	38	-39
2	8	5	31	-30	5	11	5	20	-18	-4	16	5	10	5	-2	2	6	44	43	2	4	6	23	22
3	8	5	30	-30	7	11	5	10	14	-3	16	5	24	-21	-1	2	6	12	-9	3	4	6	42	43
4	8	5	31	30	-7	12	5	15	10	-2	16	5	21	-16	0	2	6	32	34	4	4	6	20	-19
7	8	5	7	10	-6	12	5	9	-7	-1	16	5	12	12	2	2	6	46	-47	5	4	6	18	15
-6	9	5	9	-14	-3	12	5	22	-23	0	16	5	8	9	3	2	6	31	-31	6	4	6	16	-14
-4	9	5	29	32	-2	12	5	18	16	2	16	5	14	14	4	2	6	9	9	7	4	6	24	-22
-2	9	5	7	6	-1	12	5	13	13	3	16	5	11	-9	5	2	6	5	-3	8	4	6	18	18
-1	9	5	19	21	0	12	5	9	-9	4	16	5	14	-12	6	2	6	14	11	-7	5	6	16	-20
0	9	5	70	-67	1	12	5	13	13	0	17	5	20	18	7	2	6	8	7	-5	5	6	14	27
1	9	5	40	-41	2	12	5	26	-25	2	17	5	19	-18	8	2	6	20	-19	-3	5	6	10	13
2	9	5	31	33	3	12	5	22	-23	-8	0	6	13	-9	-8	3	6	14	10	-2	5	6	16	-15
3	9	5	14	14	4	12	5	12	13	-6	0	6	10	-8	-7	3	6	12	9	-1	5	6	54	-55
4	9	5	20	21	5	12	5	15	13	-4	0	6	52	53	-6	3	6	19	-19	0	5	6	27	26
5	9	5	8	9	-5	13	5	27	-21	-2	0	6	12	-14	-5	3	6	10	-16	1	5	6	24	26
6	9	5	14	-17	-4	13	5	7	7	0	0	6	50	-50	-3	3	6	24	-31	2	5	6	23	-22
-6	10	5	13	16	-3	13	5	6	2	2	0	6	36	36	-2	3	6	18	18	3	5	6	34	33
-4	10	5	7	9	0	13	5	16	-16	4	0	6	11	-9	-1	3	6	10	11	4	5	6	15	-13

H	K	L	FO	FC	H	K	L	FO	FC	H	K	L	FO	FC	H	K	L	FO	FC	H	K	L	FO	FC
5	5	6	57	-55	3	8	6	27	28	-5	12	6	7	-4	-2	16	6	8	7	1	2	7	62	-65
6	5	6	22	20	6	8	6	12	14	-4	12	6	23	-22	0	16	6	9	9	2	2	7	15	-15
7	5	6	5	2	7	8	6	11	-11	-3	12	6	27	24	1	16	6	24	23	4	2	7	10	-12
-7	6	6	6	9	-7	9	6	6	-6	-2	12	6	8	5	2	16	6	15	-14	5	2	7	33	32
-5	6	6	15	31	-4	9	6	10	-8	1	12	6	32	-33	3	16	6	15	-14	7	2	7	21	-19
-3	6	6	25	-38	-3	9	6	8	8	2	12	6	26	-25	-1	17	6	22	21	-8	3	7	12	7
-2	6	6	29	-26	-2	9	6	23	23	3	12	6	14	15	0	17	6	9	-10	-7	3	7	18	-16
0	6	6	13	-13	-1	9	6	34	-34	4	12	6	7	6	1	17	6	11	-11	-5	3	7	9	-10
1	6	6	60	62	0	9	6	18	-17	5	12	6	10	10	-7	0	7	7	-4	-4	3	7	8	-12
2	6	6	8	6	1	9	6	13	12	6	12	6	11	10	-5	0	7	10	13	-3	3	7	32	35
3	6	6	44	-42	3	9	6	23	22	-6	13	6	24	-19	-3	0	7	10	-9	-2	3	7	21	20
4	6	6	21	20	5	9	6	7	-5	-4	13	6	7	4	-1	0	7	27	-28	-1	3	7	48	-46
5	6	6	7	-6	6	9	6	7	-7	-3	13	6	6	4	1	0	7	7	9	1	3	7	23	-24
6	6	6	6	-9	-3	10	6	39	-37	-2	13	6	31	31	3	0	7	11	11	2	3	7	10	-10
7	6	6	31	30	-2	10	6	10	-8	-1	13	6	20	-19	7	0	7	12	10	3	3	7	39	39
-7	7	6	8	13	0	10	6	5	-4	0	13	6	20	-20	-7	1	7	18	14	4	3	7	12	12
-4	7	6	8	-14	1	10	6	34	33	4	13	6	33	32	-6	1	7	8	-7	5	3	7	33	-33
-3	7	6	11	-12	2	10	6	19	19	6	13	6	20	-20	-5	1	7	8	7	6	3	7	11	-10
-2	7	6	7	-7	3	10	6	11	-11	-4	14	6	27	21	-3	1	7	42	-44	7	3	7	11	-10
-1	7	6	72	69	4	10	6	6	-5	-3	14	6	12	10	-2	1	7	15	15	-6	4	7	23	-27
0	7	6	36	36	5	10	6	16	-17	-2	14	6	17	-15	-1	1	7	11	11	-5	4	7	24	29
1	7	6	32	-33	7	10	6	9	8	0	14	6	11	-12	0	1	7	7	-7	-4	4	7	19	28
2	7	6	28	29	-7	11	6	9	6	2	14	6	39	38	2	1	7	10	-10	-3	4	7	13	-17
3	7	6	32	-33	-6	11	6	15	17	3	14	6	7	6	3	1	7	49	-48	-2	4	7	19	16
4	7	6	15	-17	-5	11	6	25	-23	4	14	6	17	-16	4	1	7	6	6	-1	4	7	36	-37
5	7	6	31	32	-3	11	6	5	3	-4	15	6	8	6	5	1	7	13	13	0	4	7	51	-49
6	7	6	6	5	-2	11	6	25	-26	-2	15	6	19	-18	7	1	7	14	13	1	4	7	51	50
-5	8	6	7	-15	-1	11	6	41	40	-1	15	6	14	-12	-7	2	7	19	12	2	4	7	49	47
-4	8	6	9	-10	1	11	6	16	-16	0	15	6	17	16	-5	2	7	32	-33	4	4	7	26	25
-3	8	6	34	40	2	11	6	9	-10	1	15	6	9	8	-4	2	7	12	-13	5	4	7	31	-29
-2	8	6	23	22	3	11	6	36	-37	3	15	6	19	19	-3	2	7	14	14	6	4	7	39	-36
0	8	6	28	28	5	11	6	17	18	4	15	6	12	-11	-2	2	7	25	-23	7	4	7	10	10
1	8	6	45	-46	6	11	6	15	16	-4	16	6	10	-7	-1	2	7	52	54	8	4	7	6	5
2	8	6	26	-27	-6	12	6	13	10	-3	16	6	19	-15	0	2	7	17	-16	-8	5	7	17	-11

H	K	L	FO	FC	H	K	L	FO	FC	H	K	L	FO	FC	H	K	L	FO	FC	H	K	L	FO	FC
-6	5	7	7	9	-4	8	7	10	16	2	11	7	14	-14	1	16	7	17	-16	8	2	8	10	-10
-5	5	7	6	11	-1	8	7	14	15	3	11	7	19	-21	2	16	7	13	-12	-8	3	8	13	-11
-4	5	7	15	22	0	8	7	49	-48	4	11	7	16	16	-1	17	7	11	-11	-6	3	8	8	-6
-2	5	7	65	-63	1	8	7	14	-15	-6	12	7	9	-6	-8	0	8	15	-10	-4	3	8	24	26
-1	5	7	17	14	2	8	7	16	18	-5	12	7	21	-18	-6	0	8	21	17	-3	3	8	33	32
0	5	7	16	18	4	8	7	17	18	-4	12	7	12	11	-4	0	8	13	-12	-2	3	8	21	-21
1	5	7	8	7	5	8	7	6	7	-2	12	7	11	11	-2	0	8	41	-40	-1	3	8	7	-7
2	5	7	58	61	6	8	7	17	-16	-1	12	7	13	13	0	0	8	53	53	0	3	8	27	-27
3	5	7	6	-6	-7	9	7	6	-6	0	12	7	13	-14	2	0	8	12	-12	1	3	8	38	-41
4	5	7	47	-46	-6	9	7	7	8	1	12	7	16	-15	4	0	8	58	-57	2	3	8	29	29
5	5	7	13	13	-4	9	7	12	15	2	12	7	6	6	6	0	8	11	9	3	3	8	22	21
7	5	7	11	10	-2	9	7	34	-32	3	12	7	9	8	8	0	8	12	11	4	3	8	17	-17
8	5	7	16	17	-1	9	7	16	-14	5	12	7	17	16	-8	1	8	14	10	5	3	8	12	13
-7	6	7	7	-5	1	9	7	14	-14	6	12	7	8	-9	-6	1	8	11	10	6	3	8	14	-12
-6	6	7	10	15	2	9	7	25	26	-3	13	7	30	27	-4	1	8	48	-46	7	3	8	6	-6
-4	6	7	12	-19	4	9	7	20	-19	-1	13	7	16	-14	-3	1	8	14	-11	8	3	8	10	10
0	6	7	63	63	7	9	7	6	-3	1	13	7	10	-11	-1	1	8	8	-6	-8	4	8	8	-5
2	6	7	18	-17	-6	10	7	8	7	3	13	7	32	32	0	1	8	34	35	-7	4	8	13	-9
4	6	7	13	-12	-5	10	7	15	20	5	13	7	6	-6	1	1	8	9	8	-6	4	8	15	15
6	6	7	28	27	-4	10	7	18	-22	-5	14	7	19	14	2	1	8	43	-45	-5	4	8	11	11
7	6	7	6	5	-2	10	7	10	-9	-4	14	7	9	6	3	1	8	7	-7	-3	4	8	16	16
-8	7	7	10	9	-1	10	7	15	-16	-1	14	7	19	-18	6	1	8	27	24	-2	4	8	22	-23
-6	7	7	7	-12	0	10	7	24	23	1	14	7	23	24	8	1	8	17	-16	-1	4	8	43	-42
-4	7	7	10	-13	1	10	7	22	21	3	14	7	6	-6	-8	2	8	14	8	0	4	8	35	34
-2	7	7	42	42	2	10	7	16	-17	4	14	7	7	8	-6	2	8	22	-16	1	4	8	6	-5
-1	7	7	17	14	3	10	7	8	-7	-3	15	7	20	-18	-5	2	8	15	-12	2	4	8	18	18
0	7	7	16	-15	4	10	7	17	-19	-2	15	7	6	-4	-3	2	8	18	-20	3	4	8	28	28
1	7	7	15	13	5	10	7	20	-21	-1	15	7	20	20	-2	2	8	31	30	4	4	8	24	-23
2	7	7	43	-43	6	10	7	10	10	1	15	7	13	11	-1	2	8	35	33	5	4	8	20	-20
3	7	7	13	-12	-4	11	7	13	-11	2	15	7	9	7	0	2	8	31	-30	6	4	8	14	14
4	7	7	34	33	-3	11	7	30	-29	3	15	7	18	-18	2	2	8	8	-7	-8	5	8	10	9
5	7	7	6	5	-2	11	7	15	13	4	15	7	11	-10	3	2	8	35	-36	-5	5	8	17	20
6	7	7	15	14	-1	11	7	14	13	-1	16	7	7	6	4	2	8	41	41	-4	5	8	11	-14
-6	8	7	8	-11	1	11	7	17	16	0	16	7	20	20	6	2	8	14	-13	-3	5	8	21	-24

H	K	L	FO	FC	H	K	L	FO	FC	H	K	L	FO	FC	H	K	L	FO	FC	H	K	L	FO	FC
-2	5	8	11	11	5	8	8	19	-18	-2	12	8	38	34	3	0	9	63	-65	2	3	9	25	25
0	5	8	18	18	6	8	8	9	-8	-1	12	8	11	-12	5	0	9	12	12	3	3	9	15	13
1	5	8	54	56	-7	9	8	5	-5	0	12	8	16	-17	7	0	9	21	21	4	3	9	20	22
2	5	8	9	-8	-5	9	8	8	12	2	12	8	9	-9	-7	1	9	14	9	5	3	9	35	-35
3	5	8	20	-20	-3	9	8	15	-13	3	12	8	12	12	-5	1	9	26	-21	6	3	9	17	-16
4	5	8	10	10	-2	9	8	8	-9	4	12	8	25	26	-4	1	9	10	-9	7	3	9	7	7
5	5	8	8	-8	-1	9	8	11	-9	5	12	8	10	-11	-2	1	9	18	-18	-7	4	9	12	11
6	5	8	6	4	1	9	8	12	12	-4	13	8	28	24	-1	1	9	42	41	-4	4	9	8	8
7	5	8	16	17	3	9	8	18	-19	-2	13	8	14	-13	0	1	9	12	12	-3	4	9	8	-8
-7	6	8	14	14	4	9	8	16	-16	-1	13	8	9	10	1	1	9	42	-44	-2	4	9	29	-27
-2	6	8	15	16	6	9	8	11	-9	0	13	8	23	-24	2	1	9	16	-15	-1	4	9	23	23
-1	6	8	54	53	-6	10	8	9	10	2	13	8	39	40	3	1	9	8	-8	0	4	9	11	-12
0	6	8	11	-9	-4	10	8	11	12	4	13	8	5	6	5	1	9	24	22	1	4	9	34	36
1	6	8	18	-18	-3	10	8	19	-17	-4	14	8	7	-9	7	1	9	11	-9	2	4	9	30	32
2	6	8	12	-12	-2	10	8	24	-22	-2	14	8	28	-26	-7	2	9	17	-13	3	4	9	10	-11
3	6	8	15	-15	-1	10	8	10	8	-1	14	8	6	-5	-5	2	9	9	-8	4	4	9	10	-9
5	6	8	37	37	0	10	8	5	-4	0	14	8	23	24	-4	2	9	10	-9	7	4	9	12	12
-6	7	8	7	4	1	10	8	14	-15	1	14	8	9	8	-3	2	9	34	32	-6	5	9	18	16
-5	7	8	17	-25	2	10	8	7	7	2	14	8	9	11	-2	2	9	25	23	-5	5	9	13	-16
-3	7	8	16	16	3	10	8	20	-20	3	14	8	17	18	-1	2	9	12	-12	-4	5	9	10	-10
1	7	8	35	-36	5	10	8	16	16	4	14	8	20	-20	1	2	9	18	-18	-3	5	9	13	12
3	7	8	17	16	-5	11	8	9	-9	-3	15	8	14	-12	2	2	9	18	-20	-1	5	9	27	28
4	7	8	17	17	-4	11	8	15	-15	-2	15	8	18	18	3	2	9	37	38	0	5	9	29	29
6	7	8	10	9	-3	11	8	14	12	0	15	8	17	18	5	2	9	11	-12	1	5	9	22	-21
7	7	8	22	-22	-2	11	8	6	6	1	15	8	6	6	7	2	9	14	-15	3	5	9	11	-11
-7	8	8	11	-10	-1	11	8	9	10	2	15	8	20	-21	-7	3	9	9	-4	4	5	9	13	-13
-6	8	8	10	-11	0	11	8	13	11	3	15	8	12	-13	-6	3	9	17	-13	5	5	9	10	10
-4	8	8	8	-11	1	11	8	8	-9	-1	16	8	9	9	-5	3	9	25	25	6	5	9	23	22
-3	8	8	14	14	2	11	8	31	-30	0	16	8	20	-20	-4	3	9	21	19	-4	6	9	15	-16
-2	8	8	5	5	3	11	8	23	22	-7	0	9	18	12	-3	3	9	13	-14	-3	6	9	8	9
-1	8	8	20	-20	4	11	8	6	-6	-5	0	9	19	16	-2	3	9	26	26	-2	6	9	26	25
0	8	8	9	-10	6	11	8	10	9	-3	0	9	58	-54	-1	3	9	29	-29	-1	6	9	20	-19
1	8	8	15	15	-4	12	8	8	7	-1	0	9	15	15	0	3	9	30	-32	1	6	9	12	-13
3	8	8	11	11	-3	12	8	9	7	1	0	9	7	-7	1	3	9	31	30	2	6	9	26	-27

H	K	L	FO	FC	H	K	L	FO	FC	H	K	L	FO	FC	H	K	L	FO	FC	H	K	L	FO	FC
4	6	9	28	28	-1	10	9	25	26	6	0	10	22	21	5	3	10	14	-14	3	7	10	9	9
5	6	9	6	5	1	10	9	23	21	-6	1	10	21	-14	-6	4	10	11	7	5	7	10	25	-24
-6	7	9	14	-14	2	10	9	14	-14	-5	1	10	8	-5	-5	4	10	9	11	-6	8	10	7	-3
-4	7	9	6	3	3	10	9	21	-21	-3	1	10	15	-14	-4	4	10	11	-12	-5	8	10	14	17
-2	7	9	7	8	4	10	9	20	20	-2	1	10	53	49	-3	4	10	10	-9	-3	8	10	14	-11
-1	7	9	19	-19	-5	11	9	18	-18	-1	1	10	29	30	0	4	10	24	25	-1	8	10	10	-9
0	7	9	38	-38	-2	11	9	6	6	0	1	10	45	-48	1	4	10	15	14	0	8	10	12	-13
1	7	9	18	19	-1	11	9	27	24	1	1	10	21	-24	3	4	10	9	-8	1	8	10	26	27
2	7	9	7	7	0	11	9	9	10	2	1	10	17	-17	4	4	10	5	-4	3	8	10	26	-26
3	7	9	8	8	1	11	9	30	-31	3	1	10	14	-16	5	4	10	11	-12	4	8	10	8	-7
4	7	9	5	3	2	11	9	8	8	4	1	10	45	45	6	4	10	12	11	-4	9	10	11	7
6	7	9	18	-17	5	11	9	24	24	-5	2	10	17	-13	-7	5	10	14	11	-3	9	10	21	-19
-4	8	9	27	26	-3	12	9	27	24	-4	2	10	29	25	-3	5	10	6	-7	-2	9	10	22	-18
-2	8	9	25	-25	-2	12	9	12	11	-3	2	10	22	21	-2	5	10	16	16	-1	9	10	16	15
-1	8	9	7	-7	-1	12	9	14	-15	-2	2	10	14	-13	-1	5	10	6	7	0	9	10	19	19
0	8	9	7	9	1	12	9	22	-21	-1	2	10	10	10	0	5	10	22	-22	1	9	10	15	-16
1	8	9	6	-4	2	12	9	8	-8	0	2	10	33	-32	1	5	10	13	15	2	9	10	7	7
2	8	9	21	20	3	12	9	31	32	1	2	10	29	-32	2	5	10	7	-9	3	9	10	17	-16
4	8	9	30	-30	-1	13	9	17	-16	2	2	10	24	25	3	5	10	9	-10	4	9	10	8	-6
-6	9	9	15	13	1	13	9	10	10	3	2	10	24	25	4	5	10	13	13	5	9	10	15	15
-5	9	9	12	13	3	13	9	12	12	4	2	10	10	10	5	5	10	22	22	-5	10	10	7	-6
-4	9	9	9	-8	4	13	9	6	6	5	2	10	8	9	-6	6	10	7	-4	-4	10	10	14	-11
-2	9	9	17	-15	-3	14	9	21	-16	6	2	10	17	-16	-5	6	10	20	-22	-3	10	10	14	12
-1	9	9	18	-18	-1	14	9	13	13	7	2	10	7	-8	-4	6	10	14	14	-2	10	10	13	13
0	9	9	23	24	1	14	9	14	15	-7	3	10	7	-5	-1	6	10	9	12	-1	10	10	9	8
1	9	9	24	25	3	14	9	18	-16	-6	3	10	14	10	0	6	10	14	-13	0	10	10	17	15
2	9	9	26	-29	-1	15	9	19	18	-5	3	10	8	5	1	6	10	20	-20	1	10	10	9	-10
3	9	9	9	-8	1	15	9	18	-18	-3	3	10	18	19	2	6	10	15	17	2	10	10	27	-29
4	9	9	15	-15	-6	0	10	11	8	-2	3	10	7	-7	3	6	10	13	13	3	10	10	7	8
5	9	9	18	-16	-4	0	10	56	-46	-1	3	10	20	-21	-3	7	10	21	21	5	10	10	8	8
6	9	9	21	21	-2	0	10	8	9	1	3	10	6	5	-2	7	10	12	-13	-2	11	10	28	25
-4	10	9	16	-15	0	0	10	53	53	2	3	10	25	25	-1	7	10	31	-29	0	11	10	13	-14
-3	10	9	26	-23	2	0	10	58	-62	3	3	10	20	21	1	7	10	10	10	2	11	10	12	-11
-2	10	9	6	4	4	0	10	6	-4	4	3	10	21	-21	2	7	10	5	-5	3	11	10	19	19

H	K	L	FO	FC	H	K	L	FO	FC	H	K	L	FO	FC	H	K	L	FO	FC	H	K	L	FO	FC
4	11	10	17	16	3	2	11	20	21	-4	7	11	21	20	-6	0	12	15	-9	-1	4	12	11	12
-4	12	10	20	16	5	2	11	23	-24	-2	7	11	15	-13	-2	0	12	36	34	0	4	12	6	-6
-2	12	10	7	-7	6	2	11	6	-6	0	7	11	6	-7	0	0	12	27	-28	3	4	12	12	-13
0	12	10	14	-13	-5	3	11	9	8	1	7	11	8	-8	2	0	12	28	-28	4	4	12	9	10
2	12	10	28	28	-4	3	11	13	10	2	7	11	19	20	4	0	12	32	35	5	4	12	14	14
-2	13	10	23	-22	-3	3	11	19	-18	4	7	11	17	-18	-5	1	12	8	-6	-5	5	12	18	-17
0	13	10	7	7	-2	3	11	11	-12	-4	8	11	13	-11	-4	1	12	28	22	-4	5	12	8	8
2	13	10	17	17	-1	3	11	10	10	-2	8	11	14	-14	-2	1	12	5	-6	-3	5	12	5	3
-1	14	10	6	-8	1	3	11	25	27	-1	8	11	11	-10	-1	1	12	7	7	-2	5	12	9	8
0	14	10	15	15	2	3	11	17	18	0	8	11	42	42	0	1	12	34	-33	-1	5	12	9	10
1	14	10	5	-5	3	3	11	15	-15	2	8	11	13	-13	1	1	12	12	-14	0	5	12	10	-10
-5	0	11	23	-15	4	3	11	16	-16	4	8	11	17	-18	2	1	12	19	22	1	5	12	18	-19
-3	0	11	10	12	-6	4	11	21	16	-4	9	11	18	-17	4	1	12	9	9	2	5	12	6	6
-1	0	11	47	45	-5	4	11	10	-9	-3	9	11	14	-11	5	1	12	13	12	3	5	12	11	11
1	0	11	34	-39	-2	4	11	13	-15	-2	9	11	24	23	-5	2	12	8	5	5	5	12	7	9
3	0	11	22	-22	-1	4	11	16	16	-1	9	11	20	18	-4	2	12	9	7	-3	6	12	17	17
5	0	11	14	13	0	4	11	8	8	1	9	11	21	22	-2	2	12	24	-22	-1	6	12	23	-22
-5	1	11	10	-7	2	4	11	13	-14	2	9	11	25	-26	-1	2	12	12	-13	3	6	12	19	19
-4	1	11	5	-3	3	4	11	8	-10	3	9	11	13	-13	0	2	12	11	11	-3	7	12	9	-8
-3	1	11	40	35	4	4	11	15	-15	4	9	11	13	14	2	2	12	15	17	-1	7	12	12	-13
-2	1	11	6	7	5	4	11	14	14	-4	10	11	12	11	3	2	12	15	16	0	7	12	9	-10
-1	1	11	8	-8	6	4	11	21	21	-2	10	11	8	6	4	2	12	21	-21	1	7	12	21	22
0	1	11	8	-9	-4	5	11	17	-16	-1	10	11	22	22	5	2	12	8	-8	3	7	12	8	-7
1	1	11	22	-22	-2	5	11	8	6	0	10	11	14	-14	-5	3	12	14	11	-3	8	12	18	-17
2	1	11	10	-11	-1	5	11	10	-11	1	10	11	24	-25	-4	3	12	14	-12	-1	8	12	21	20
3	1	11	29	31	1	5	11	9	-12	4	10	11	14	14	-3	3	12	10	-8	2	8	12	6	6
4	1	11	8	9	2	5	11	14	-15	-3	11	11	24	22	0	3	12	19	19	3	8	12	22	-23
-6	2	11	7	-5	3	5	11	11	13	-2	11	11	6	-6	1	3	12	20	21	-3	9	12	17	16
-5	2	11	21	17	4	5	11	18	17	-1	11	11	17	-18	2	3	12	9	-10	-1	9	12	8	8
-3	2	11	7	-7	-6	6	11	14	-13	1	11	11	19	-18	3	3	12	11	-12	0	9	12	11	10
-2	2	11	19	17	-1	6	11	10	-9	3	11	11	25	25	5	3	12	16	-16	1	9	12	22	-22
-1	2	11	38	-36	0	6	11	21	-22	-1	12	11	9	-9	-4	4	12	8	-7	2	9	12	8	-8
1	2	11	25	28	1	6	11	12	13	1	12	11	10	11	-3	4	12	14	-14	-3	10	12	9	9
2	2	11	17	19	4	6	11	9	9	2	12	11	6	5	-2	4	12	6	5	-2	10	12	12	11

H	K	L	FO	FC	H	K	L	FO	FC	H	K	L	FO	FC	H	K	L	FO	FC	H	K	L	FO	FC
-1	10	12	15	-14	1	2	13	12	12	3	4	13	10	13	-1	9	13	8	9	2	2	14	10	-10
-1	11	12	11	-11	2	2	13	11	12	4	4	13	6	7	0	9	13	25	-26	-3	3	14	13	-11
0	11	12	8	-7	3	2	13	17	-17	-4	5	13	9	6	0	0	14	23	-25	-1	3	14	18	19
1	11	12	16	15	-2	3	13	15	-15	-2	5	13	15	14	2	0	14	18	19	1	3	14	11	12
-5	0	13	15	-10	-1	3	13	17	16	-1	5	13	6	-6	-3	1	14	8	6	2	3	14	7	-7
-3	0	13	14	14	0	3	13	13	13	0	5	13	19	-21	-2	1	14	13	-12	-1	4	14	11	9
1	0	13	10	-8	1	3	13	14	-14	-2	6	13	16	-14	-1	1	14	15	-16	1	4	14	17	-17
3	0	13	17	18	4	3	13	13	-13	0	6	13	9	-11	0	1	14	14	14	-2	5	14	8	-7
-5	1	13	8	5	-4	4	13	16	-13	2	6	13	22	23	2	1	14	6	6	-1	5	14	14	-13
-3	1	13	5	1	-3	4	13	9	7	-2	7	13	14	-13	-3	2	14	7	-7	1	5	14	11	-12
-1	1	13	19	-19	-2	4	13	16	15	0	7	13	27	28	-1	2	14	11	-11	-1	6	14	17	-16
1	1	13	16	17	0	4	13	10	10	-2	8	13	16	16	0	2	14	10	10	0	6	14	6	6
3	1	13	6	8	1	4	13	7	-8	0	8	13	9	11	1	2	14	17	19	1	6	14	20	22
-3	2	13	16	-14	2	4	13	21	-23	2	8	13	23	-23										

Appendix B

Observed and Calculated Structure Factors for $[(\eta^5\text{-}C_5H_5)Fe(CO)_2C(O)CH_3]$

H	K	L	FO	FC	θ
1	0	0	0	1	0
2	0	0	15	15	180
3	0	0	19	19	180
4	0	0	24	24	0
5	0	0	13	13	0
6	0	0	3	3	180
-7	1	0	7	7	0
-6	1	0	12	12	0
-5	1	0	17	18	180
-4	1	0	31	31	180
-3	1	0	4	3	180
-2	1	0	26	25	0
-1	1	0	7	7	0
0	1	0	67	64	180
1	1	0	10	10	0
2	1	0	11	11	0
3	1	0	17	17	0
4	1	0	14	15	180
5	1	0	4	4	180
6	1	0	3	3	0
-7	2	0	4	4	180
-6	2	0	14	13	180
-5	2	0	17	17	0
-4	2	0	16	16	0
-3	2	0	5	4	180
-2	2	0	36	34	180
-1	2	0	10	9	180
0	2	0	13	13	180
1	2	0	39	38	0
2	2	0	30	30	180
3	2	0	26	26	180
4	2	0	2	2	180
5	2	0	8	8	0
-7	3	0	2	2	180
-6	3	0	14	14	0
-5	3	0	2	2	180
-4	3	0	14	14	180
-3	3	0	17	16	180
-2	3	0	23	23	0
-1	3	0	18	17	0
0	3	0	5	4	0
1	3	0	32	32	180
2	3	0	23	22	0
3	3	0	15	15	0
4	3	0	0	0	0
5	3	0	14	13	180
-7	4	0	1	0	0
-6	4	0	10	10	180
-5	4	0	7	7	180
-4	4	0	23	23	0
-3	4	0	12	11	0
-2	4	0	43	42	180
-1	4	0	24	23	180
0	4	0	10	10	0
1	4	0	26	26	0
2	4	0	0	0	0
3	4	0	13	13	180
4	4	0	4	4	180
-7	5	0	4	4	0
-6	5	0	10	10	0
-5	5	0	19	19	0
-4	5	0	15	14	180
-3	5	0	7	7	180
-2	5	0	17	16	0
-1	5	0	15	15	0
0	5	0	0	0	0
1	5	0	8	8	180
2	5	0	2	2	180
3	5	0	8	8	0
-6	6	0	6	6	180
-5	6	0	10	10	180
-4	6	0	7	7	0
-3	6	0	10	10	0
-2	6	0	2	1	0
-1	6	0	15	15	180
0	6	0	1	1	0
1	6	0	10	10	0
2	6	0	5	5	0
-5	7	0	4	4	0
-4	7	0	0	0	0
-3	7	0	14	13	180
-2	7	0	6	6	180
-1	7	0	8	8	0
0	7	0	2	2	180
0	-7	1	9	9	0
1	-7	1	2	2	180
2	-7	1	11	11	180
3	-7	1	4	3	180
4	-7	1	8	8	0
5	-7	1	4	4	0
-2	-6	1	11	11	0
-1	-6	1	5	4	0
0	-6	1	13	13	180
1	-6	1	3	3	180
2	-6	1	8	8	0
3	-6	1	7	7	0
4	-6	1	11	11	180
5	-6	1	5	5	180
6	-6	1	1	2	0
-3	-5	1	2	2	0
-2	-5	1	11	11	180
-1	-5	1	5	5	0
0	-5	1	18	17	0
1	-5	1	17	16	0
2	-5	1	13	13	180
3	-5	1	14	14	180
4	-5	1	16	15	0
5	-5	1	17	17	0
6	-5	1	1	1	180
7	-5	1	7	6	180
-4	-4	1	11	11	180
-3	-4	1	4	4	180
-2	-4	1	14	13	0
-1	-4	1	4	4	0
0	-4	1	14	14	180
1	-4	1	35	34	180
2	-4	1	18	17	0
3	-4	1	18	17	0
4	-4	1	2	2	180
5	-4	1	19	18	180
6	-4	1	7	6	0
7	-4	1	7	8	0
-5	-3	1	1	1	0
-4	-3	1	12	13	0
-3	-3	1	1	0	180
-2	-3	1	21	22	180
-1	-3	1	24	24	180
0	-3	1	32	31	0
1	-3	1	18	18	0
2	-3	1	22	21	180
3	-3	1	38	37	180
4	-3	1	19	19	180
5	-3	1	17	17	0
6	-3	1	3	3	180
7	-3	1	6	7	180
-6	-2	1	10	10	0
-5	-2	1	5	5	0
-4	-2	1	19	19	180
-3	-2	1	16	16	180
-2	-2	1	14	13	0
-1	-2	1	52	52	0
0	-2	1	4	4	180
1	-2	1	24	22	0
2	-2	1	16	17	180
3	-2	1	27	26	0
4	-2	1	11	11	0
5	-2	1	13	13	180
6	-2	1	8	8	180
7	-2	1	6	7	0
-6	-1	1	5	5	180
-5	-1	1	10	10	180
-4	-1	1	15	14	0
-3	-1	1	11	12	0
-2	-1	1	7	8	180
-1	-1	1	47	46	180
0	-1	1	10	9	0
1	-1	1	43	41	0
2	-1	1	12	12	0
3	-1	1	41	40	180
4	-1	1	13	13	180
5	-1	1	13	13	0
6	-1	1	19	20	0
7	-1	1	4	4	180
-7	0	1	5	5	180
-6	0	1	11	11	0
-5	0	1	19	19	0
-4	0	1	2	3	180
-3	0	1	28	28	180
-2	0	1	3	2	0
-1	0	1	83	84	0
0	0	1	16	17	0
1	0	1	70	70	180
2	0	1	2	2	0
3	0	1	19	19	0
4	0	1	8	9	0
5	0	1	8	8	180
6	0	1	11	12	180
-7	1	1	5	5	0
-6	1	1	11	12	180
-5	1	1	15	15	180
-4	1	1	0	0	0
-3	1	1	39	38	0
-2	1	1	30	28	180
-1	1	1	54	52	180
0	1	1	16	16	180
1	1	1	69	68	0
2	1	1	23	23	0
3	1	1	6	6	180
4	1	1	15	15	180
5	1	1	1	0	180
6	1	1	8	8	0
-7	2	1	7	7	180
-6	2	1	4	4	0
-5	2	1	19	19	0
-4	2	1	3	3	180
-3	2	1	47	45	180
-2	2	1	30	29	180
-1	2	1	48	45	180

H	K	L	FO	FC	θ
0	2	1	40	38	0
1	2	1	22	22	180
2	2	1	27	27	180
3	2	1	0	1	180
4	2	1	8	9	0
5	2	1	1	1	180
-7	3	1	9	9	0
-6	3	1	7	7	0
-5	3	1	12	13	180
-4	3	1	4	4	0
-3	3	1	21	21	0
-2	3	1	33	31	0
-1	3	1	3	3	180
0	3	1	33	32	180
1	3	1	16	17	0
2	3	1	30	30	0
3	3	1	3	3	180
4	3	1	17	18	180
5	3	1	3	4	180
-7	4	1	10	10	180
-6	4	1	8	8	180
-5	4	1	18	17	0
-4	4	1	15	14	0
-3	4	1	17	17	180
-2	4	1	26	25	180
-1	4	1	25	25	0
0	4	1	17	17	0
1	4	1	[illegible]	8	0
2	4	1	1[illegible]	13	180
3	4	1	2	2	0
4	4	1	11	11	0
-7	5	1	9	8	0
-6	5	1	5	5	0
-5	5	1	11	11	180
-4	5	1	13	13	180
-3	5	1	16	16	0
-2	5	1	9	9	0
-1	5	1	15	15	180
0	5	1	13	13	180
1	5	1	9	9	180
2	5	1	10	11	0
3	5	1	5	5	0
-6	6	1	5	5	180
-5	6	1	5	5	0
-4	6	1	14	14	0
-3	6	1	0	2	0
-2	6	1	11	12	180
-1	6	1	5	5	180
0	6	1	9	8	0
1	6	1	5	5	0
2	6	1	3	3	180
-5	7	1	1	1	180
-4	7	1	12	12	180
-3	7	1	7	7	180
-2	7	1	11	11	0
-1	7	1	2	2	0
0	7	1	9	9	180
0	-7	2	1	1	0
1	-7	2	9	8	180
2	-7	2	5	4	180
3	-7	2	8	7	0
4	-7	2	8	7	0
5	-7	2	2	2	180
-2	-6	2	4	4	0
-1	-6	2	14	13	180
0	-6	2	2	2	180
1	-6	2	15	15	0
2	-6	2	8	9	0
3	-6	2	9	8	180
4	-6	2	10	9	180
5	-6	2	7	7	0
6	-6	2	9	9	0
-3	-5	2	13	12	180
-2	-5	2	6	6	180
-1	-5	2	19	18	0
0	-5	2	11	11	0
1	-5	2	13	12	180
2	-5	2	16	15	180
3	-5	2	7	7	0
4	-5	2	11	11	0
5	-5	2	5	5	180
6	-5	2	8	8	180
-4	-4	2	2	2	180
-3	-4	2	6	6	0
-2	-4	2	1	1	0
-1	-4	2	11	11	180
0	-4	2	17	17	180
1	-4	2	20	19	0
2	-4	2	19	18	0
3	-4	2	9	8	180
4	-4	2	23	23	180
5	-4	2	0	0	180
6	-4	2	12	12	0
7	-4	2	3	3	0
-5	-3	2	11	11	0
-4	-3	2	0	1	180
-3	-3	2	14	14	180
-2	-3	2	20	19	180
-1	-3	2	9	9	0
0	-3	2	38	36	0
1	-3	2	17	16	180
2	-3	2	35	33	180
3	-3	2	21	20	180
4	-3	2	20	19	0
5	-3	2	5	5	0
6	-3	2	10	10	180
7	-3	2	3	3	180
-6	-2	2	6	6	0
-5	-2	2	9	9	180
-4	-2	2	7	7	180
-3	-2	2	19	19	0
-2	-2	2	30	30	0
-1	-2	2	8	8	180
0	-2	2	23	23	180
1	-2	2	6	6	0
2	-2	2	39	38	0
3	-2	2	17	17	0
4	-2	2	22	23	180
5	-2	2	15	15	180
6	-2	2	8	8	0
7	-2	2	7	7	0
-6	-1	2	9	9	180
-5	-1	2	14	14	0
-4	-1	2	24	24	0
-3	-1	2	18	18	180
-2	-1	2	41	40	180
-1	-1	2	11	11	180
0	-1	2	52	52	0
1	-1	2	46	45	0
2	-1	2	12	12	180
3	-1	2	4	5	180
4	-1	2	13	12	0
5	-1	2	21	21	0
6	-1	2	4	4	180
-7	0	2	3	3	0
-6	0	2	12	13	0
-5	0	2	6	6	180
-4	0	2	22	22	180
-3	0	2	7	7	180
-2	0	2	16	16	0
-1	0	2	17	17	180
0	0	2	67	71	180
1	0	2	9	9	180
2	0	2	33	33	0
3	0	2	6	7	0
4	0	2	12	12	180
5	0	2	19	20	180
6	0	2	2	2	0
-7	1	2	6	6	180
-6	1	2	10	10	180
-5	1	2	2	2	0
-4	1	2	30	29	0
-3	1	2	6	6	0
-2	1	2	51	50	180
-1	1	2	6	5	180
0	1	2	40	42	0
1	1	2	38	39	0
2	1	2	16	16	180
3	1	2	18	19	180
4	1	2	4	4	180
5	1	2	5	5	0
6	1	2	3	2	0
-7	2	2	4	3	0
-6	2	2	7	7	0
-5	2	2	5	5	0
-4	2	2	29	29	180
-3	2	2	9	9	180
-2	2	2	11	11	0
-1	2	2	24	24	0
0	2	2	14	15	180
1	2	2	38	38	180
2	2	2	14	13	0
3	2	2	24	23	0
4	2	2	3	3	0
5	2	2	8	8	180
-7	3	2	1	1	0
-6	3	2	9	10	180
-5	3	2	4	4	180
-4	3	2	27	27	0
-3	3	2	26	26	0
-2	3	2	6	6	180
-1	3	2	51	51	180
0	3	2	2	1	180
1	3	2	27	28	0
2	3	2	3	3	0
3	3	2	17	17	180
4	3	2	1	2	180
5	3	2	6	6	0
-7	4	2	4	4	180
-6	4	2	12	12	0
-5	4	2	12	13	0
-4	4	2	5	5	180
-3	4	2	14	14	180
-2	4	2	24	23	0
-1	4	2	21	21	0
0	4	2	0	0	180
1	4	2	11	11	180
2	4	2	0	0	180
3	4	2	17	17	0
4	4	2	3	3	0
-7	5	2	3	2	0
-6	5	2	12	13	180
-5	5	2	13	13	180
-4	5	2	4	4	0
-3	5	2	11	11	0
-2	5	2	15	15	180
-1	5	2	14	13	180

H	K	L	FO	FC	θ
0	5	2	10	10	180
1	5	2	8	8	0
2	5	2	8	9	0
3	5	2	3	3	180
-6	6	2	5	5	0
-5	6	2	9	8	0
-4	6	2	0	0	180
-3	6	2	11	11	180
-2	6	2	5	5	180
-1	6	2	9	8	0
0	6	2	3	3	0
1	6	2	8	8	180
-5	7	2	8	8	180
-4	7	2	3	3	180
-3	7	2	15	15	0
-2	7	2	10	10	0
-1	7	2	8	8	180
0	-7	3	4	5	180
1	-7	3	3	2	180
2	-7	3	8	8	0
3	-7	3	8	8	0
4	-7	3	2	2	180
5	-7	3	9	9	180
-2	-6	3	10	11	180
-1	-6	3	6	6	180
0	-6	3	18	19	0
1	-6	3	8	7	0
2	-6	3	8	8	180
3	-6	3	15	14	180
4	-6	3	4	4	0
5	-6	3	12	12	0
6	-6	3	1	0	180
-3	-5	3	6	6	180
-2	-5	3	13	12	0
-1	-5	3	11	11	0
0	-5	3	19	19	180
1	-5	3	8	8	180
2	-5	3	5	5	0
3	-5	3	12	12	0
4	-5	3	8	8	180
5	-5	3	9	9	180
6	-5	3	4	4	180
-4	-4	3	10	9	0
-3	-4	3	1	1	0
-2	-4	3	9	9	180
-1	-4	3	21	22	180
0	-4	3	12	11	0
1	-4	3	19	18	0
2	-4	3	3	2	180
3	-4	3	23	23	180
4	-4	3	5	5	180
5	-4	3	7	7	0
6	-4	3	6	6	0
-5	-3	3	4	4	0
-4	-3	3	3	4	180
-3	-3	3	10	10	180
-2	-3	3	0	0	0
-1	-3	3	22	23	0
0	-3	3	3	3	0
1	-3	3	30	29	180
2	-3	3	5	5	0
3	-3	3	30	29	0
4	-3	3	11	10	0
5	-3	3	15	15	180
6	-3	3	7	7	180
7	-3	3	7	6	0
-6	-2	3	7	7	180
-5	-2	3	5	5	180
-4	-2	3	12	12	0
-3	-2	3	27	27	0
-2	-2	3	24	24	180
-1	-2	3	24	23	180
0	-2	3	15	15	180
1	-2	3	77	77	0
2	-2	3	12	12	0
3	-2	3	18	18	180
4	-2	3	23	22	180
5	-2	3	10	10	0
6	-2	3	9	9	0
-6	-1	3	6	6	0
-5	-1	3	19	19	0
-4	-1	3	14	13	180
-3	-1	3	30	31	180
-2	-1	3	17	16	0
-1	-1	3	14	14	0
0	-1	3	45	46	0
1	-1	3	39	39	180
2	-1	3	7	6	0
3	-1	3	8	8	0
4	-1	3	22	22	0
5	-1	3	8	8	180
6	-1	3	11	11	180
-7	0	3	3	4	0
-6	0	3	4	4	180
-5	0	3	25	25	180
-4	0	3	8	8	0
-3	0	3	18	18	0
-2	0	3	8	8	0
-1	0	3	58	57	180
0	0	3	30	31	180
1	0	3	8	8	0
2	0	3	26	27	0
3	0	3	5	6	180
4	0	3	20	20	180
5	0	3	1	0	180
6	0	3	8	9	0
-7	1	3	6	6	180
-6	1	3	4	4	180
-5	1	3	22	22	0
-4	1	3	11	11	0
-3	1	3	14	14	180
-2	1	3	37	35	180
-1	1	3	36	36	0
0	1	3	17	17	180
1	1	3	8	8	180
2	1	3	39	39	180
3	1	3	12	12	0
4	1	3	7	7	0
5	1	3	1	2	0
6	1	3	10	10	180
-7	2	3	8	8	0
-6	2	3	3	4	0
-5	2	3	13	13	180
-4	2	3	7	7	180
-3	2	3	38	38	0
-2	2	3	38	36	0
-1	2	3	24	25	180
0	2	3	26	26	180
1	2	3	9	9	0
2	2	3	41	42	0
3	2	3	4	4	0
4	2	3	5	5	180
5	2	3	8	8	180
-7	3	3	13	13	180
-6	3	3	1	1	180
-5	3	3	8	8	0
-4	3	3	22	22	0
-3	3	3	18	18	180
-2	3	3	29	29	180
-1	3	3	2	1	180
0	3	3	28	29	0
1	3	3	1	0	180
2	3	3	15	15	180
3	3	3	2	1	180
4	3	3	12	12	0
-7	4	3	12	12	0
-6	4	3	2	2	0
-5	4	3	4	4	180
-4	4	3	20	20	180
-3	4	3	15	15	0
-2	4	3	21	21	0
-1	4	3	3	3	0
0	4	3	24	25	180
1	4	3	9	9	180
2	4	3	9	9	0
3	4	3	6	6	0
-7	5	3	8	8	180
-6	5	3	11	11	180
-5	5	3	2	2	0
-4	5	3	12	12	0
-3	5	3	2	2	180
-2	5	3	7	7	180
-1	5	3	6	6	180
0	5	3	9	9	0
1	5	3	6	6	0
2	5	3	5	5	180
-6	6	3	9	9	0
-5	6	3	6	6	180
-4	6	3	9	9	180
-3	6	3	7	7	180
-2	6	3	11	10	0
-1	6	3	4	4	0
0	6	3	10	10	180
1	6	3	10	10	180
-5	7	3	2	2	0
-4	7	3	11	11	0
-3	7	3	10	10	0
-2	7	3	8	8	180
-1	7	3	3	2	180
0	-7	4	1	1	180
1	-7	4	7	7	0
2	-7	4	10	10	0
3	-7	4	1	2	180
4	-7	4	9	9	180
-2	-6	4	8	9	180
-1	-6	4	11	12	0
0	-6	4	3	3	0
1	-6	4	10	10	180
2	-6	4	14	14	180
3	-6	4	4	4	0
4	-6	4	10	10	0
5	-6	4	1	1	180
-3	-5	4	12	11	0
-2	-5	4	6	6	0
-1	-5	4	18	18	180
0	-5	4	12	12	180
1	-5	4	11	11	0
2	-5	4	15	15	0
3	-5	4	6	7	180
4	-5	4	10	10	180
5	-5	4	10	10	180
6	-5	4	6	6	0
-4	-4	4	5	5	0
-3	-4	4	11	11	180
-2	-4	4	11	11	180
-1	-4	4	3	3	180
0	-4	4	32	32	0

H	K	L	FO	FC	θ
1	-4	4	4	4	180
2	-4	4	5	6	180
3	-4	4	7	7	180
4	-4	4	9	9	0
5	-4	4	8	8	0
6	-4	4	8	8	180
-5	-3	4	5	5	180
-4	-3	4	6	6	180
-3	-3	4	5	5	0
-2	-3	4	17	16	0
-1	-3	4	14	13	0
0	-3	4	46	46	180
1	-3	4	10	9	0
2	-3	4	26	26	0
3	-3	4	23	23	0
4	-3	4	22	21	180
5	-3	4	6	6	180
6	-3	4	5	5	0
-6	-2	4	8	8	180
-5	-2	4	7	7	0
-4	-2	4	19	19	0
-3	-2	4	2	2	180
-2	-2	4	25	26	180
-1	-2	4	4	4	180
0	-2	4	37	38	0
1	-2	4	19	19	0
2	-2	4	30	30	180
3	-2	4	11	11	180
4	-2	4	19	18	0
5	-2	4	8	7	0
6	-2	4	0	0	0
-6	-1	4	10	10	0
-5	-1	4	13	13	180
-4	-1	4	18	18	180
-3	-1	4	9	8	0
-2	-1	4	29	30	0
-1	-1	4	24	22	180
0	-1	4	29	30	180
1	-1	4	47	49	180
2	-1	4	29	29	0
3	-1	4	14	15	0
4	-1	4	2	2	180
5	-1	4	18	18	180
6	-1	4	3	3	180
-7	0	4	4	4	180
-6	0	4	13	13	180
-5	0	4	4	4	0
-4	0	4	21	21	0
-3	0	4	13	13	0
-2	0	4	43	42	180
-1	0	4	21	21	180
0	0	4	25	26	180
1	0	4	43	44	0
2	0	4	7	7	180
3	0	4	14	14	180
4	0	4	4	4	180
5	0	4	13	13	0
6	0	4	1	1	180
-7	1	4	3	3	0
-6	1	4	8	8	0
-5	1	4	15	16	0
-4	1	4	24	24	180
-3	1	4	18	18	180
-2	1	4	35	35	0
-1	1	4	20	20	0
0	1	4	8	9	180
1	1	4	37	38	180
2	1	4	7	7	0
3	1	4	23	23	0
4	1	4	4	5	0
5	1	4	9	9	180
-7	2	4	1	1	0
-6	2	4	7	7	180
-5	2	4	18	19	180
-4	2	4	33	31	0
-3	2	4	24	24	0
-2	2	4	3	3	180
-1	2	4	32	32	180
0	2	4	22	22	0
1	2	4	17	17	0
2	2	4	5	5	0
3	2	4	12	12	180
4	2	4	3	3	180
5	2	4	6	6	0
-7	3	4	3	4	180
-6	3	4	8	8	0
-5	3	4	7	7	0
-4	3	4	14	13	180
-3	3	4	16	17	180
-2	3	4	7	7	0
-1	3	4	39	39	0
0	3	4	12	13	180
1	3	4	15	15	180
2	3	4	11	11	180
3	3	4	16	15	0
4	3	4	8	8	0
-7	4	4	5	4	0
-6	4	4	12	12	180
-5	4	4	9	9	180
-4	4	4	6	6	180
-3	4	4	22	22	0
-2	4	4	0	0	180
-1	4	4	24	24	180
0	4	4	15	15	180
1	4	4	5	5	0
2	4	4	6	7	0
3	4	4	8	8	180
-6	5	4	6	7	0
-5	5	4	9	9	0
-4	5	4	4	4	0
-3	5	4	13	14	180
-2	5	4	3	3	180
-1	5	4	10	11	0
0	5	4	12	12	0
1	5	4	11	10	180
2	5	4	8	8	180
-6	6	4	2	2	180
-5	6	4	10	10	180
-4	6	4	1	3	180
-3	6	4	9	8	0
-2	6	4	9	9	0
-1	6	4	5	4	180
0	6	4	6	6	180
1	6	4	4	4	0
-4	7	4	1	2	0
-3	7	4	7	7	180
-2	7	4	5	5	180
0	-7	5	5	6	0
1	-7	5	9	9	0
2	-7	5	2	2	180
3	-7	5	8	8	180
4	-7	5	1	1	180
-2	-6	5	5	4	0
-1	-6	5	4	4	0
0	-6	5	10	10	180
1	-6	5	9	8	180
2	-6	5	5	5	0
3	-6	5	11	12	0
4	-6	5	1	0	180
5	-6	5	11	12	180
-3	-5	5	6	5	0
-2	-5	5	11	11	180
-1	-5	5	12	12	180
0	-5	5	8	8	0
1	-5	5	11	11	0
2	-5	5	5	5	180
3	-5	5	12	13	180
4	-5	5	7	8	180
5	-5	5	5	4	0
6	-5	5	5	6	0
-4	-4	5	7	7	180
-3	-4	5	3	3	180
-2	-4	5	8	8	0
-1	-4	5	24	24	0
0	-4	5	2	1	0
1	-4	5	14	14	180
2	-4	5	1	1	0
3	-4	5	15	15	0
4	-4	5	13	13	0
5	-4	5	5	5	180
6	-4	5	10	11	180
-5	-3	5	7	7	180
-4	-3	5	4	3	0
-3	-3	5	18	18	0
-2	-3	5	3	3	0
-1	-3	5	35	34	180
0	-3	5	18	18	180
1	-3	5	29	29	0
2	-3	5	19	20	0
3	-3	5	13	13	180
4	-3	5	7	7	180
5	-3	5	7	7	0
6	-3	5	9	10	0
-6	-2	5	3	3	0
-5	-2	5	12	13	0
-4	-2	5	1	1	0
-3	-2	5	25	24	180
-2	-2	5	2	2	180
-1	-2	5	11	12	0
0	-2	5	11	12	0
1	-2	5	46	46	180
2	-2	5	13	13	180
3	-2	5	22	22	0
4	-2	5	9	9	0
5	-2	5	4	4	180
6	-2	5	10	10	180
-6	-1	5	4	4	180
-5	-1	5	18	18	180
-4	-1	5	4	4	0
-3	-1	5	21	22	0
-2	-1	5	2	1	180
-1	-1	5	14	15	180
0	-1	5	29	31	180
1	-1	5	20	20	0
2	-1	5	19	21	0
3	-1	5	4	4	180
4	-1	5	16	16	180
5	-1	5	4	4	180
6	-1	5	5	5	0
-7	0	5	7	7	180
-6	0	5	1	1	0
-5	0	5	13	13	0
-4	0	5	2	2	0
-3	0	5	15	17	180
-2	0	5	15	15	180
-1	0	5	17	17	0
0	0	5	18	20	0

H	K	L	FO	FC	θ	H	K	L	FO	FC	θ	H	K	L	FO	FC	θ
1	0	5	3	3	0	1	-7	6	6	7	180	-5	0	6	3	2	0
2	0	5	36	36	180	2	-7	6	8	9	180	-4	0	6	12	12	180
3	0	5	1	1	180	3	-7	6	3	3	180	-3	0	6	8	9	180
4	0	5	22	21	0	-2	-6	6	7	7	0	-2	0	6	17	18	0
5	0	5	2	2	0	-1	-6	6	3	4	180	-1	0	6	35	36	0
-7	1	5	10	10	0	0	-6	6	8	8	180	0	0	6	3	4	180
-6	1	5	6	6	0	1	-6	6	4	4	0	1	0	6	24	25	180
-5	1	5	12	12	180	2	-6	6	12	12	0	2	0	6	12	12	180
-4	1	5	19	19	180	3	-6	6	4	4	0	3	0	6	32	32	0
-3	1	5	34	33	0	4	-6	6	10	10	180	4	0	6	5	5	0
-2	1	5	45	45	0	5	-6	6	2	2	180	5	0	6	5	5	180
-1	1	5	8	9	180	-3	-5	6	7	7	180	-7	1	6	4	4	0
0	1	5	24	26	180	-2	-5	6	8	8	180	-6	1	6	10	10	180
1	1	5	13	12	180	-1	-5	6	3	3	0	-5	1	6	9	9	180
2	1	5	31	31	0	0	-5	6	8	8	0	-4	1	6	11	10	0
3	1	5	7	7	0	1	-5	6	1	2	180	-3	1	6	29	29	0
4	1	5	8	8	180	2	-5	6	12	12	180	-2	1	6	20	20	180
5	1	5	2	2	180	3	-5	6	1	0	0	-1	1	6	24	25	180
-7	2	5	10	10	180	4	-5	6	9	9	0	0	1	6	8	8	180
-6	2	5	10	10	180	5	-5	6	10	9	0	1	1	6	26	26	0
-5	2	5	11	10	0	-4	-4	6	5	4	180	2	1	6	8	8	0
-4	2	5	24	24	0	-3	-4	6	9	9	0	3	1	6	17	17	180
-3	2	5	17	16	180	-2	-4	6	16	16	0	4	1	6	2	2	180
-2	2	5	21	22	180	-1	-4	6	1	2	180	5	1	6	8	7	0
-1	2	5	17	17	0	0	-4	6	18	18	180	-7	2	6	8	8	180
0	2	5	17	18	0	1	-4	6	7	7	180	-6	2	6	13	13	0
1	2	5	5	5	180	2	-4	6	18	18	0	-5	2	6	11	11	0
2	2	5	15	15	180	3	-4	6	10	10	0	-4	2	6	10	10	180
3	2	5	5	5	180	4	-4	6	3	3	180	-3	2	6	31	31	180
4	2	5	8	9	0	5	-4	6	15	15	180	-2	2	6	17	17	0
-7	3	5	8	8	0	6	-4	6	3	3	0	-1	2	6	22	24	0
-6	3	5	4	5	0	-5	-3	6	1	2	0	0	2	6	5	5	0
-5	3	5	9	9	180	-4	-3	6	11	11	0	1	2	6	17	18	180
-4	3	5	19	18	180	-3	-3	6	1	1	0	2	2	6	9	9	180
-3	3	5	1	1	0	-2	-3	6	24	24	180	3	2	6	3	2	0
-2	3	5	24	25	0	-1	-3	6	4	4	180	4	2	6	9	9	0
-1	3	5	5	5	180	0	-3	6	22	23	0	-7	3	6	7	7	0
0	3	5	18	18	180	1	-3	6	22	22	0	-6	3	6	10	10	180
1	3	5	9	8	180	2	-3	6	17	18	180	-5	3	6	13	13	180
2	3	5	4	4	0	3	-3	6	7	7	180	-4	3	6	6	6	180
3	3	5	10	10	0	4	-3	6	7	7	0	-3	3	6	16	17	0
4	3	5	4	4	180	5	-3	6	11	11	0	-2	3	6	1	1	180
-7	4	5	5	5	180	6	-3	6	2	2	180	-1	3	6	13	13	180
-6	4	5	7	7	180	-6	-2	6	5	5	0	0	3	6	5	5	180
-5	4	5	1	1	180	-5	-2	6	1	1	180	1	3	6	3	3	0
-4	4	5	11	11	0	-4	-2	6	23	24	180	2	3	6	5	6	0
-3	4	5	5	5	0	-3	-2	6	5	6	180	3	3	6	3	3	180
-2	4	5	20	20	180	-2	-2	6	20	20	0	-6	4	6	1	1	0
-1	4	5	8	8	180	-1	-2	6	8	9	0	-5	4	6	12	12	0
0	4	5	14	14	0	0	-2	6	33	33	180	-4	4	6	4	4	0
1	4	5	9	9	0	1	-2	6	33	34	180	-3	4	6	15	14	180
2	4	5	9	9	180	2	-2	6	14	14	0	-2	4	6	11	11	180
3	4	5	8	8	180	3	-2	6	9	9	0	-1	4	6	17	17	0
-6	5	5	11	11	0	4	-2	6	5	4	180	0	4	6	12	12	0
-5	5	5	1	0	180	5	-2	6	7	7	180	1	4	6	7	8	180
-4	5	5	13	12	180	6	-2	6	4	4	180	2	4	6	11	11	180
-3	5	5	8	8	180	-6	-1	6	8	8	180	-6	5	6	4	4	0
-2	5	5	14	14	0	-5	-1	6	1	2	180	-5	5	6	12	12	180
-1	5	5	16	16	0	-4	-1	6	22	22	0	-4	5	6	2	2	180
0	5	5	10	10	180	-3	-1	6	8	8	0	-3	5	6	10	10	0
1	5	5	9	9	180	-2	-1	6	1	1	0	-2	5	6	17	16	0
2	5	5	2	2	0	-1	-1	6	19	19	180	-1	5	6	10	10	180
-5	6	5	1	1	0	0	-1	6	18	19	0	0	5	6	8	8	180
-4	6	5	8	8	0	1	-1	6	9	10	0	1	5	6	7	7	0
-3	6	5	7	8	0	2	-1	6	7	7	180	-5	6	6	9	9	0
-2	6	5	3	3	180	3	-1	6	20	20	180	-4	6	6	3	2	0
-1	6	5	5	6	180	4	-1	6	0	1	0	-3	6	6	5	5	180
0	6	5	6	6	0	5	-1	6	7	7	0	-2	6	6	9	10	180
0	-7	6	6	6	0	-6	0	6	8	8	0	-1	6	6	4	5	0

H	K	L	FO	FC	θ
1	-7	7	9	9	180
2	-7	7	0	0	0
3	-7	7	6	6	0
-1	-6	7	5	5	180
0	-6	7	1	1	180
1	-6	7	12	12	0
2	-6	7	3	3	0
3	-6	7	8	8	180
4	-6	7	5	5	180
-3	-5	7	8	8	180
-2	-5	7	5	5	0
-1	-5	7	8	8	0
0	-5	7	9	9	0
1	-5	7	14	14	180
2	-5	7	3	3	0
3	-5	7	11	11	0
4	-5	7	13	13	0
5	-5	7	4	3	180
-4	-4	7	4	4	0
-3	-4	7	9	10	0
-2	-4	7	3	3	180
-1	-4	7	15	15	180
0	-4	7	10	9	180
1	-4	7	10	11	0
2	-4	7	3	3	0
3	-4	7	7	7	180
4	-4	7	14	13	180
5	-4	7	5	5	0
-5	-3	7	8	8	0
-4	-3	7	2	1	180
-3	-3	7	11	12	180
-2	-3	7	0	0	180
-1	-3	7	27	27	0
0	-3	7	4	4	0
1	-3	7	12	13	180
2	-3	7	25	25	180
3	-3	7	9	9	0
4	-3	7	9	9	0
5	-3	7	1	1	180
-5	-2	7	13	13	180
-4	-2	7	6	6	180
-3	-2	7	16	16	0
-2	-2	7	13	15	0
-1	-2	7	27	27	180
0	-2	7	14	15	180
1	-2	7	0	1	0
2	-2	7	24	25	0
3	-2	7	8	8	180
4	-2	7	2	1	180
5	-2	7	4	4	180
-6	-1	7	3	2	0
-5	-1	7	11	12	0
-4	-1	7	12	12	0
-3	-1	7	15	14	180
-2	-1	7	19	20	180
-1	-1	7	13	13	0
0	-1	7	16	16	0
1	-1	7	6	6	180
2	-1	7	24	25	180
3	-1	7	0	0	180
4	-1	7	9	9	0
5	-1	7	6	7	0
-6	0	7	1	0	0
-5	0	7	3	2	180
-4	0	7	16	16	180
-3	0	7	17	18	0
-2	0	7	25	25	0
-1	0	7	13	13	0
0	0	7	19	19	180
1	0	7	2	2	0
2	0	7	21	21	0
3	0	7	9	9	0
4	0	7	12	12	180
5	0	7	2	2	180
-6	1	7	7	7	180
-5	1	7	1	1	0
-4	1	7	14	13	0
-3	1	7	20	20	180
-2	1	7	19	19	180
-1	1	7	8	7	180
0	1	7	34	35	0
1	1	7	1	1	0
2	1	7	17	17	180
3	1	7	12	12	180
4	1	7	11	11	0
-7	2	7	6	6	0
-6	2	7	13	13	0
-5	2	7	13	12	180
-4	2	7	15	15	180
-3	2	7	1	0	0
-2	2	7	19	20	0
-1	2	7	3	3	0
0	2	7	21	21	180
1	2	7	10	10	180
2	2	7	1	1	180
3	2	7	8	8	0
4	2	7	5	5	180
-7	3	7	3	3	180
-6	3	7	13	13	180
-5	3	7	8	9	0
-4	3	7	9	9	0
-3	3	7	11	12	0
-2	3	7	18	19	180
-1	3	7	0	0	0
0	3	7	6	6	0
1	3	7	12	12	0
2	3	7	1	1	180
3	3	7	11	11	180
-6	4	7	10	11	0
-5	4	7	3	3	0
-4	4	7	11	11	180
-3	4	7	13	14	180
-2	4	7	13	13	0
-1	4	7	9	10	0
0	4	7	2	2	180
1	4	7	10	10	180
2	4	7	4	4	0
-6	5	7	6	6	180
-5	5	7	4	4	180
-4	5	7	12	12	0
-3	5	7	8	8	0
-2	5	7	7	8	180
-1	5	7	10	11	180
0	5	7	9	9	0
1	5	7	8	8	0
-4	6	7	7	7	180
-3	6	7	6	6	180
-2	6	7	1	1	0
-1	6	7	8	8	0
-1	-6	8	1	0	180
0	-6	8	9	9	0
1	-6	8	3	2	0
2	-6	8	10	10	180
3	-6	8	7	7	180
4	-6	8	6	6	0
-3	-5	8	4	4	0
-2	-5	8	11	11	0
-1	-5	8	8	8	0
0	-5	8	10	10	180
1	-5	8	8	8	180
2	-5	8	13	13	0
3	-5	8	9	9	0
4	-5	8	5	4	180
-4	-4	8	8	8	0
-3	-4	8	1	2	180
-2	-4	8	16	16	180
-1	-4	8	4	4	180
0	-4	8	5	5	0
1	-4	8	7	8	0
2	-4	8	11	11	180
3	-4	8	8	8	180
4	-4	8	5	5	0
5	-4	8	9	10	0
-5	-3	8	2	1	0
-4	-3	8	11	11	180
-3	-3	8	4	3	180
-2	-3	8	16	16	0
-1	-3	8	2	2	180
0	-3	8	8	8	180
1	-3	8	22	22	180
2	-3	8	2	2	0
3	-3	8	8	8	0
4	-3	8	2	2	180
5	-3	8	10	10	180
-5	-2	8	4	5	180
-4	-2	8	14	14	0
-3	-2	8	9	9	0
-2	-2	8	11	11	180
-1	-2	8	8	8	180
0	-2	8	16	17	0
1	-2	8	23	24	0
2	-2	8	1	0	0
3	-2	8	12	12	180
4	-2	8	3	3	180
5	-2	8	8	8	0
-6	-1	8	6	6	0
-5	-1	8	6	6	0
-4	-1	8	15	15	180
-3	-1	8	18	19	180
-2	-1	8	8	7	0
-1	-1	8	32	34	0
0	-1	8	10	10	180
1	-1	8	11	12	180
2	-1	8	8	8	180
3	-1	8	15	15	0
4	-1	8	7	7	0
5	-1	8	2	2	180
-6	0	8	8	8	180
-5	0	8	5	5	180
-4	0	8	6	6	0
-3	0	8	23	23	0
-2	0	8	1	1	180
-1	0	8	24	25	180
0	0	8	3	3	0
1	0	8	10	10	0
2	0	8	6	7	0
3	0	8	18	18	180
4	0	8	5	5	180
-6	1	8	7	7	0
-5	1	8	5	5	0
-4	1	8	2	2	180
-3	1	8	21	21	180
-2	1	8	0	0	180
-1	1	8	21	21	0
0	1	8	12	12	0
1	1	8	16	16	180
2	1	8	8	8	180

H	K	L	FO	FC	θ
3	1	8	8	7	0
4	1	8	5	5	0
-6	2	8	7	7	180
-5	2	8	10	11	180
-4	2	8	2	2	180
-3	2	8	10	9	0
-2	2	8	1	1	180
-1	2	8	18	18	180
0	2	8	13	13	180
1	2	8	10	11	0
2	2	8	7	7	0
3	2	8	3	2	180
-6	3	8	5	5	0
-5	3	8	16	17	0
-4	3	8	5	4	0
-3	3	8	10	10	180
-2	3	8	7	7	180
-1	3	8	10	11	0
0	3	8	15	15	0
1	3	8	1	1	180
2	3	8	10	10	180
-6	4	8	4	4	0
-5	4	8	14	14	180
-4	4	8	5	5	180
-3	4	8	9	9	0
-2	4	8	12	12	0
-1	4	8	2	3	180
0	4	8	8	8	180
1	4	8	4	4	0
-5	5	8	8	8	0
-4	5	8	5	5	0
-3	5	8	7	7	180
-2	5	8	11	12	180
-1	5	8	3	3	0
0	5	8	6	6	0
0	-6	9	3	3	0
1	-6	9	8	9	180
2	-6	9	6	6	180
3	-6	9	8	8	0
-2	-5	9	2	2	0
-1	-5	9	10	9	180
0	-5	9	10	11	180
1	-5	9	11	11	0
2	-5	9	7	7	0
3	-5	9	10	10	180
4	-5	9	7	7	180
-3	-4	9	12	12	180
-2	-4	9	3	3	180
-1	-4	9	11	12	0
0	-4	9	10	10	0
1	-4	9	6	6	180
2	-4	9	10	10	180
3	-4	9	3	3	0
4	-4	9	9	8	0
-4	-3	9	5	5	180
-3	-3	9	10	10	0
-2	-3	9	1	2	0
-1	-3	9	6	6	180
0	-3	9	8	8	180
1	-3	9	3	3	180
2	-3	9	10	10	0
3	-3	9	1	0	180
4	-3	9	10	10	180
-5	-2	9	8	8	0
-4	-2	9	10	10	0
-3	-2	9	6	6	180
-2	-2	9	7	7	180
-1	-2	9	10	11	0
0	-2	9	19	19	0
1	-2	9	1	1	0
2	-2	9	16	16	180
3	-2	9	7	7	180
4	-2	9	9	9	0
-5	-1	9	7	7	180
-4	-1	9	12	13	180
-3	-1	9	6	6	0
-2	-1	9	25	25	0
-1	-1	9	8	8	180
0	-1	9	14	15	180
1	-1	9	2	3	0
2	-1	9	15	15	0
3	-1	9	10	10	0
4	-1	9	5	6	180
-6	0	9	6	6	180
-5	0	9	6	6	0
-4	0	9	10	10	0
-3	0	9	6	6	180
-2	0	9	32	32	180
-1	0	9	2	2	180
0	0	9	11	11	0
1	0	9	4	4	0
2	0	9	12	12	180
3	0	9	9	9	180
4	0	9	2	2	0
-6	1	9	10	10	0
-5	1	9	3	3	180
-4	1	9	8	8	180
-3	1	9	5	5	180
-2	1	9	16	16	0
-1	1	9	11	11	0
0	1	9	12	12	180
1	1	9	8	7	180
2	1	9	6	6	0
3	1	9	3	3	0
-6	2	9	11	10	180
-5	2	9	1	1	0
-4	2	9	7	7	0
-3	2	9	6	7	0
-2	2	9	10	10	180
-1	2	9	12	12	180
0	2	9	16	15	0
1	2	9	13	12	0
2	2	9	1	1	180
3	2	9	8	7	180
-6	3	9	10	10	0
-5	3	9	4	3	0
-4	3	9	11	11	180
-3	3	9	6	6	180
-2	3	9	6	6	0
-1	3	9	11	11	0
0	3	9	5	5	180
1	3	9	10	11	180
2	3	9	1	0	0
-5	4	9	4	4	180
-4	4	9	14	14	0
-3	4	9	7	7	0
-2	4	9	1	2	180
-1	4	9	9	9	180
0	4	9	1	1	0
1	4	9	10	9	0
-4	5	9	7	8	180
-3	5	9	8	8	180
-2	5	9	1	0	180
-1	5	9	5	5	0
1	-6	10	5	5	180
-2	-5	10	7	7	180
-1	-5	10	7	8	180
0	-5	10	10	9	0
1	-5	10	6	6	0
2	-5	10	10	10	180
3	-5	10	10	10	180
-3	-4	10	2	2	180
-2	-4	10	10	10	0
-1	-4	10	9	10	0
0	-4	10	9	9	180
1	-4	10	7	7	180
2	-4	10	1	1	180
3	-4	10	10	10	0
4	-4	10	4	3	180
-4	-3	10	8	8	0
-3	-3	10	7	6	0
-2	-3	10	7	7	180
-1	-3	10	6	6	180
0	-3	10	1	1	0
1	-3	10	12	12	0
2	-3	10	8	9	0
3	-3	10	10	10	180
4	-3	10	1	1	0
-5	-2	10	5	5	0
-4	-2	10	4	3	180
-3	-2	10	14	13	180
-2	-2	10	3	3	0
-1	-2	10	9	10	0
0	-2	10	4	4	0
1	-2	10	14	15	180
2	-2	10	6	6	180
3	-2	10	8	8	0
4	-2	10	5	6	0
-5	-1	10	6	6	180
-4	-1	10	2	2	0
-3	-1	10	18	19	0
-2	-1	10	8	7	180
-1	-1	10	15	15	180
0	-1	10	2	2	0
1	-1	10	17	16	0
2	-1	10	4	4	0
3	-1	10	6	6	180
4	-1	10	10	10	180
-5	0	10	7	7	0
-4	0	10	6	6	180
-3	0	10	20	20	180
-2	0	10	0	1	180
-1	0	10	14	14	0
0	0	10	4	4	0
1	0	10	9	9	180
2	0	10	5	5	180
3	0	10	1	1	0
-6	1	10	1	0	0
-5	1	10	10	10	180
-4	1	10	3	3	0
-3	1	10	7	7	0
-2	1	10	12	13	0
-1	1	10	16	16	180
0	1	10	11	11	180
1	1	10	4	4	0
2	1	10	6	6	0
3	1	10	1	1	180
-6	2	10	1	1	180
-5	2	10	13	13	0
-4	2	10	6	6	0
-3	2	10	0	0	0
-2	2	10	15	15	180
-1	2	10	14	14	0
0	2	10	13	13	0
1	2	10	1	1	180
2	2	10	6	6	180
-5	3	10	10	10	180

H	K	L	FO	FC	θ
-4	3	10	7	7	180
-3	3	10	6	5	0
-2	3	10	7	7	0
-1	3	10	5	6	180
0	3	10	11	11	180
1	3	10	2	2	0
-5	4	10	7	7	0
-4	4	10	6	6	0
-3	4	10	7	7	180
-2	4	10	5	5	180
-1	4	10	4	4	180
0	4	10	8	7	0
-1	-5	11	7	6	0
0	-5	11	5	5	0
1	-5	11	5	5	180
2	-5	11	8	8	180
-2	-4	11	6	6	0
-1	-4	11	7	7	180
0	-4	11	6	6	180
1	-4	11	3	3	0
2	-4	11	9	9	0
3	-4	11	1	1	180
-3	-3	11	7	7	180
-2	-3	11	6	6	180
-1	-3	11	1	1	0
0	-3	11	14	14	0
1	-3	11	5	5	0
2	-3	11	6	6	180
3	-3	11	5	5	180
-4	-2	11	8	8	180
-3	-2	11	1	1	0
-2	-2	11	9	9	0
-1	-2	11	5	5	0
0	-2	11	16	16	180
1	-2	11	3	3	180
2	-2	11	6	6	0
3	-2	11	9	8	0
-5	-1	11	5	5	0
-4	-1	11	8	8	0
-3	-1	11	1	1	0
-2	-1	11	17	17	180
-1	-1	11	1	1	180
0	-1	11	9	9	0
1	-1	11	0	1	0
2	-1	11	7	6	180
3	-1	11	10	10	180
-5	0	11	3	3	180
-4	0	11	7	7	180
-3	0	11	1	1	180
-2	0	11	15	15	0
-1	0	11	1	1	180
0	0	11	5	5	180
1	0	11	6	6	180
2	0	11	5	5	0
3	0	11	6	6	0
-5	1	11	1	0	180
-4	1	11	9	8	0
-3	1	11	6	5	0
-2	1	11	10	10	180
-1	1	11	12	12	180
0	1	11	5	4	0
1	1	11	11	11	0
2	1	11	1	1	180
-5	2	11	8	8	0
-4	2	11	8	7	180
-3	2	11	9	8	180
-2	2	11	5	5	0
-1	2	11	15	15	0
0	2	11	5	5	180
1	2	11	8	8	180
-5	3	11	9	8	180
-4	3	11	8	8	0
-3	3	11	7	6	0
-2	3	11	1	1	180
-1	3	11	10	10	180
0	3	11	1	2	0
-3	4	11	5	5	180
-2	4	11	3	3	180
-1	-4	12	7	7	180
0	-4	12	5	5	0
1	-4	12	6	6	0
2	-4	12	2	2	0
-3	-3	12	7	6	180
-2	-3	12	1	2	0
-1	-3	12	10	10	0
0	-3	12	1	0	0
1	-3	12	8	8	180
2	-3	12	4	5	180
-3	-2	12	8	7	0
-2	-2	12	2	2	0
-1	-2	12	13	14	180
0	-2	12	7	7	180
1	-2	12	9	9	0
2	-2	12	6	6	0
-4	-1	12	1	1	180
-3	-1	12	10	10	180
-2	-1	12	5	5	180
-1	-1	12	8	8	0
0	-1	12	5	5	0
1	-1	12	7	6	180
2	-1	12	6	6	180
-4	0	12	1	1	0
-3	0	12	9	8	0
-2	0	12	4	4	0
-1	0	12	4	4	180
0	0	12	6	6	180
1	0	12	4	4	0
2	0	12	6	6	0
-4	1	12	3	3	0
-3	1	12	5	5	180
-2	1	12	7	6	180
-1	1	12	5	5	0
0	1	12	11	11	0
1	1	12	1	1	180
-4	2	12	8	8	180
-3	2	12	6	5	0
-2	2	12	10	10	0
-1	2	12	5	5	180
0	2	12	11	10	180
-3	3	12	4	4	180
-2	3	12	7	7	180
-1	3	12	1	0	180
-1	-3	13	1	1	180
0	-3	13	8	8	180
1	-3	13	1	2	180
-3	-2	13	1	0	180
-2	-2	13	9	8	180
-1	-2	13	6	6	180
0	-2	13	9	9	0
1	-2	13	4	4	0
-3	-1	13	1	1	180
-2	-1	13	7	6	0
-1	-1	13	9	9	0
0	-1	13	6	6	180
1	-1	13	7	6	180
-3	0	13	3	3	0
-2	0	13	0	1	180
-1	0	13	8	8	180
0	0	13	1	2	0
1	0	13	7	7	0
-3	1	13	3	4	180
-2	1	13	2	2	0
-1	1	13	8	7	0
0	1	13	1	1	180
-2	2	13	5	5	180
-1	-1	14	5	5	180

Appendix C

References for Iron Acyl Complexes from the Cambridge Structural Database (CSD)

No.	Refcode[a]	Ref. No.	Reference
1	ACFENA	[1]	Ginsburg, R. E.; Berg, J. M.; Rothrock, R. K.; Collman, J. P.; Hodgson, K. O.; Dahl, L. F. *J. Am. Chem. Soc.* **1979**, *101*, 7218.
2	ACMPFE	[2]	Attig, T. G.; Teller, R. G.; Wu, S. M.; Bau, R.; Wojcicki, A. *J. Am. Chem. Soc.* **1979**, *101*, 619.
3	APZBFE	[3]	Cotton, F. A.; Frenz, B. A.; Shaver, A. *Inorg. Chim. Acta* **1973**, *7*, 161.
4	BAPYEW	[4]	Korp, J. D.; Bernal, I. *J. Organomet. Chem.* **1981**, *220*, 355.
5	BIRBIN	[5]	Annis, G. D.; Ley, S. V.; Self, C. R.; Silvaramakrishnan, R.; Williams, D. J. *J. Chem. Soc. ,Perkin Trans. 1* **1982**, 1355.
6	BITYEI	[6]	Alt, H. G.; Eichner, M. E.; Jansen, B. M.; Thewalt, U. *Z. Naturforsch. ,Teil B* **1982**, *37*, 1109.
7	BOPPAX10	[7]	Yu, Y. F.; Gallucci, J.; Wojcicki, A. *J. Am. Chem. Soc.* **1983**, *105*, 4826.
8	BOWBUK	[8]	Wong, W. K.; Wilkinson, G.; Galas, A. M. R.; Thornton-Pett, M. A.; Hursthouse, M. B. *Polyhedron* **1982**, *1*, 842.
9	BYFELI	[1]	Ginsburg, R. E.; Berg, J. M.; Rothrock, R. K.; Collman, J. P.; Hodgson, K. O.; Dahl, L. F. *J. Am. Chem. Soc.* **1979**, *101*, 7218.
10	BZPEFE	[9]	Felkin, H.; Meunier, B.; Pascard, C.; Prange, T. *J. Organomet. Chem.* **1977**, *135*, 361.
11	CALWAN	[10]	Baird, G. J.; Bandy, J. A.; Davies, S. G.; Prout, K. *J. Chem. Soc. ,Chem. Comm.* **1983**, 1202.
12	CECBUH	[11]	Sellmann, D.; Lanzrath, G.; Huttner, G.; Zsolnai, L.; Kruger, C.; Claus, K. H. *Z. Naturforsch. ,Teil B* **1983**, *38*, 961.
13	CEZYIP	[12]	Gambino, O.; Gervasio, G.; Rossetti, R.; Stanghellini, P. L. *Inorg. Chim. Acta* **1984**, *84*, 51.
14	CFMTPI	[13]	Guerchais, J. E.; Floch-Perennou, F. L.; Petillon, F. Y.; Keith, A. N.; Manojlovic-Muir, L.; Muir, K. W.; Sharp, D. W. A. *J. Chem. Soc. ,Chem. Comm.* **1979**, 410.
15	CIYPIJ	[14]	Rosen, R. P.; Hoke, J. B.; Whittle, R. R.; Geoffroy, G. L.; Hutchinson, J. P.; Zubieta, J. A. *Organometallics* **1984**, *3*, 846.
16	CORTAE10	[15]	Casey, C. P.; Miles, W. H.; Fagan, P. J.; Haller, K. J. *Organometallics* **1985**, *4*, 559.
17	CUBGIP	[16]	Casey, C. P.; Meszaros, M. W.; Neumann, S. M.; Cesa, I. G.; Haller, K. J. *Organometallics* **1985**, *4*, 143.
18	CUXBIG	[17]	Liebeskind, L. S.; Welker, M. E. *Tetrahedron Lett.* **1984**, *25*, 4341.
19	CYPFEP	[18]	Herbstein, F. H.; Kaftory, M. *Acta Crystallogr. ,Sect. B* **1977**, *33*, 3318.
20	DAJNAD10	[19]	Jeffery, J. C.; Lawrence-Smith, J. G. *J. Chem. Soc. ,Dalton Trans.* **1990**, 1063.

[a] The CSD Refcode is the unique identification given to each structural entry in the database.

21	DAJNEH	[20]	Jeffery, J. C.; Lawrence-Smith, J. G. *J. Chem. Soc. ,Chem. Comm.* **1985**, 275.
22	DAWDUA	[21]	Brown, S. L.; Davies, S. G.; Warner, P.; Jones, R. H.; Prout, K. *J. Chem. Soc. ,Chem. Comm.* **1985**, 1446.
23	DCHPFE10	[22]	Vuuren, P. J. v.; Fletterick, R. J.; Meinwald, J.; Hughes, R. E. *J. Am. Chem. Soc.* **1971**, *93*, 4394.
24	DEFCPO	[23]	Aime, S.; Milone, L.; Sappa, E.; Tiripicchio, A.; Lanfredi, A. M. M. *J. Chem. Soc. ,Dalton Trans.* **1979**, 1664.
25	DFMCFE10	[24]	Davidson, J. L.; Green, M.; Stone, F. G. A.; Welch, A. J. *J. Chem. Soc., Dalton Trans.* **1976**, 2044.
26	DIWSUX	[25]	Targos, T. S.; Geoffroy, G. L.; Rheingold, A. L. *J. Organomet. Chem.* **1986**, *299*, 223.
27	DOKHOA	[26]	Reger, D. L.; Mintz, E.; Lebioda, L. *J. Am. Chem. Soc.* **1986**, *108*, 1940.
28	DOKHUG	[26]	Reger, D. L.; Mintz, E.; Lebioda, L. *J. Am. Chem. Soc.* **1986**, *108*, 1940.
29	DOKXIK	[27]	Davies, S. G.; Dordor-Hedgecock, I. M.; Sutton, K. H.; Walker, J. C.; Bourne, C.; Jones, R. H.; Prout, K. *J. Chem. Soc. ,Chem. Comm.* **1986**, 607.
30	DORBUH10	[28]	Lenhert, P. G.; Lukehart, C. M.; Sacksteder, L. A. *Acta Crystallogr. ,Sect. C (Cr. Str. Comm.)* **1987**, *43*, 653.
31	DORCAO10	[29]	Lenhert, P. G.; Lukehart, C. M.; Sacksteder, L. A. *Acta Crystallogr. ,Sect. C (Cr. Str. Comm.)* **1986**, *42*, 958.
32	DORHAT	[30]	Newlands, M. J.; Mackay, M. F. *Acta Crystallogr. ,Sect. C (Cr. Str. Comm.)* **1986**, *42*, 677.
33	DUHFUH	[31]	McNamara, W. F.; Duesler, E. N.; Paine, R. T. *Organometallics* **1986**, *5*, 1747.
34	DUHXOT	[32]	Davies, S. G.; Dordor-Hedgecock, I. M.; Sutton, K. H.; Walker, J. C.; Jones, R. H.; Prout, K. *Tetrahedron* **1986**, *42*, 5123.
35	DUZBIJ	[33]	Birk, R.; Berke, H.; Huttner, G.; Zsolnai, L. *J. Organomet. Chem.* **1986**, *309*, C18.
36	EMOPFC	[34]	Cotton, F. A.; Jamerson, J. D.; Stults, B. R. *Inorg. Chim. Acta* **1976**, *17*, 235.
37	FAMNAI	[35]	Liebeskind, L. S.; Welker, M. E.; Fengl, R. W. *J. Am. Chem. Soc.* **1986**, *108*, 6328.
38	FCPENO	[36]	Hoffmann, K.; Weiss, E. *J. Organomet. Chem.* **1977**, *128*, 399.
39	FEBNAB	[37]	Bonnesen, P. V.; Baker, A. T.; Hersh, W. H. *J. Am. Chem. Soc.* **1986**, *108*, 8304.
40	FEBNEF	[37]	Bonnesen, P. V.; Baker, A. T.; Hersh, W. H. *J. Am. Chem. Soc.* **1986**, *108*, 8304.
41	FECPCC10	[38]	Mitsudo, T. A.; Watanabe, H.; Sasaki, T.; Takegami, Y.; Watanabe, Y.; Kafuku, K.; Nakatsu, K. *Organometallics* **1989**, *8*, 368.

42	FEHTUH	[39]	Pannell, K. H.; Kapoor, R. N.; Wells, M.; Giasolli, T.; Parkanyi, L. *Organometallics* **1987**, *6*, 663.
43	FELFOR	[40]	Davies, S. G.; Easton, R. C. J.; Sutton, K. H.; Walker, J. C.; Jones, R. H. *J. Chem. Soc. ,Perkin Trans. 1* **1987**, 489.
44	FEYBAM	[41]	Fontaine, X. L. R.; Jacobsen, G. B.; Shaw, B. L.; Thornton-Pett, M. *J. Chem. Soc. ,Chem. Comm.* **1987**, 662.
45	FICBOI	[42]	Chen, J.; Lei, G.; Pan, Z.; Zhang, S.; Tang, Y. *J. Chem. Soc. ,Chem. Comm.* **1987**, 1273.
46	FISBIS10	[43]	Denise, B.; Navarre, D.; Rudler, H.; Daran, J. C. *J. Organomet. Chem.* **1989**, *375*, 273.
47	FIZMIK	[44]	Ashby, M. T.; Enemark, J. H. *Organometallics* **1987**, *6*, 1318.
48	FIZPOT	[45]	Ashby, M. T.; Enemark, J. H. *Organometallics* **1987**, *6*, 1323.
49	FOBDOP	[46]	Sielisch, T.; Behrens, U. *J. Organomet. Chem.* **1987**, *322*, 203.
50	FOCTUM	[47]	Hoke, J. B.; Dewan, J. C.; Seyferth, D. *Organometallics* **1987**, *6*, 1816.
51	FOHGIS	[48]	Butler, I. R.; Cullen, W. R.; Rettig, S. J. *Organometallics* **1987**, *6*, 872.
52	FORTOV	[49]	Kisch, H.; Kruger, C.; Marcolin, H. E.; Trautwein, A. X. *Z. Naturforsch., Teil B* **1987**, *42*, 1435.
53	FUWMEP	[50]	Heppert, J. A.; Thomas-Miller, M. E.; Swepston, P. N.; Extine, M. W. *J. Chem. Soc. ,Chem. Comm.* **1988**, 280.
54	FUXGUA	[51]	Cardaci, G.; Bellachioma, G.; Zanazzi, P. *Organometallics* **1988**, *7*, 172.
55	FUXHUB	[52]	Reger, D. L.; Klaeren, S. A.; Babin, J. E.; Adams, R. D. *Organometallics* **1988**, *7*, 181.
56	GACWIQ	[53]	Hogarth, G.; Knox, S. A. R.; Lloyd, B. R.; Macpherson, K. A.; Morton, D. A. V.; Orpen, A. G. *J. Chem. Soc. ,Chem. Comm.* **1988**, 360.
57	GADWEN01	[54]	Marsh, R. E. *Inorg. Chim. Acta* **1989**, *157*, 1.
58	GADWEN02	[55]	Liu, H. Y.; Koh, L. L.; Eriks, K.; Giering, W. P.; Prock, A. *Acta Crystallogr. ,Sect. C (Cr. Str. Comm.)* **1990**, *46*, 51.
59	GAKJEH	[56]	Capon, R. J.; MacLeod, J. K.; Coote, S. J.; Davies, S. G.; Gravatt, G. L.; Dordor-Hedgecock, I. M.; Whittaker, M. *Tetrahedron* **1988**, *44*, 1637.
60	GARHOW	[57]	Hermes, A. R.; Girolami, G. S. *Organometallics* **1988**, *7*, 394.
61	GATZAC	[58]	Fontaine, X. L. R.; Jacobsen, G. B.; Shaw, B. L.; Thornton-Pett, M. *J. Chem. Soc. ,Dalton Trans.* **1988**, 1185.
62	GEGHEF	[59]	Herndon, J. W.; Chao, W.; Ammon, H. L. *J. Org. Chem.* **1988**, *53*, 2873.
63	GEJFAC	[60]	Birk, R.; Berke, H.; Huttner, G.; Zsolnai, L. *Chem. Ber.* **1988**, *121*, 471.
64	GIBTUG	[61]	Lee, G.-H.; Peng, S.-M.; Lush, S.-F.; Liu, R.-S. *J. Organomet. Chem.* **1988**, *349*, 219.
65	GIKDIN	[62]	Garcia, M. E.; Jeffery, J. C.; Sherwood, P.; Stone, F. G. A. *J. Chem. Soc., Dalton Trans.* **1988**, 2431.

66	HAPSIA	[63]	Brunner, H.; Forster, S.; Nuber, B. *Organometallics* **1993**, *12*, 3819.
67	HEMCOR	[64]	Askham, F. R.; Carroll, K. M.; Briggs, P. M.; Rheingold, A. L.; Haggerty, B. S. *Organometallics* **1994**, *13*, 2139.
68	HXCPFE10	[65]	Churchill, M. R.; Chang, S. W. Y. *Inorg. Chem.* **1975**, *14*, 1680.
69	JALKEM	[66]	Muller, F.; Han, I. M.; Koten, G. V.; Vrieze, K.; Heijdenrijk, D.; Mechelen, J. V.; Stam, C. H. *Inorg. Chim. Acta* **1989**, *158*, 99.
70	JAWKOH	[55]	Liu, H. Y.; Koh, L. L.; Eriks, K.; Giering, W. P.; Prock, A. *Acta Crystallogr. ,Sect. C (Cr. Str. Comm.)* **1990**, *46*, 51.
71	JUCJEW	[67]	Davies, S. G.; Holland, K. S.; Sutton, K. H.; McNally, J. P. *Isr. J. Chem.* **1991**, *31*, 25.
72	JUDNEB	[68]	Krajewski, J. W.; Gluzinski, P.; Zamojski, A.; Mishnyov, A.; Kemme, A.; Zhong-Wu, G. *J. Crystallogr. Spectrosc. Res.* **1992**, *22*, 213.
73	JUDNEB01	[69]	Baker, T. M.; Bodwell, G. J.; Davies, S. G.; Edwards, A. J.; Metzler, M. R. *Tetrahedron* **1993**, *49*, 5635.
74	JUZHIV	[70]	Akita, M.; Sugimoto, S.; Terada, M.; Moro-oka, Y. *J. Organomet. Chem.* **1993**, *447*, 103.
75	KAJLOW	[71]	Seyferth, D.; Ruschke, D. P.; Davis, W. M.; Cowie, M.; Hunter, A. D. *Organometallics* **1989**, *8*, 836.
76	KAJLOW10	[72]	Seyferth, D.; Ruschke, D. P.; Davis, W. M. *Organometallics* **1994**, *13*, 4695.
77	KAJNAK	[73]	Jiabi, C.; Jianguo, Y.; Guixin, L.; Yongyin, W.; Guangda, L. *J. Chem. Soc., Dalton Trans.* **1989**, 635.
78	KAJYID	[74]	Suades, J.; Dahan, F.; Mathieu, R. *Organometallics* **1989**, *8*, 842.
79	KALTOG	[75]	Stille, J. K.; Smith, C.; Anderson, O. P.; Miller, M. M. *Organometallics* **1989**, *8*, 1040.
80	KAVVOS	[76]	Liu, H. Y.; Rahman, M. M.; Lip Lin, K.; Eriks, K.; Giering, W. P.; Prock, A. *Acta Crystallogr. ,Sect. C (Cr. Str. Comm.)* **1989**, *45*, 1683.
81	KAXFOE	[77]	Paquette, L. A.; Doherty, G. A. O.; Miller, B. L.; Rogers, R. D.; Rheingold, A. L.; Geib, S. L. *Organometallics* **1989**, *8*, 2167.
82	KAXYAJ	[78]	Hitchcock, P. B.; Madden, T. J.; Nixon, J. F. *J. Chem. Soc. ,Chem. Comm.* **1989**, 1660.
83	KEDSER	[79]	Buchholz, D.; Huttner, G.; Imhof, W.; Zsolnai, L.; Gunauer, D. *J. Organomet. Chem.* **1990**, *381*, 79.
84	KEDSIV	[79]	Buchholz, D.; Huttner, G.; Imhof, W.; Zsolnai, L.; Gunauer, D. *J. Organomet. Chem.* **1990**, *381*, 79.
85	KEDSOB	[79]	Buchholz, D.; Huttner, G.; Imhof, W.; Zsolnai, L.; Gunauer, D. *J. Organomet. Chem.* **1990**, *381*, 79.
86	KETFEA	[80]	Herrmann, W. A.; Gimeno, J.; Weichmann, J.; Ziegler, M. L.; Balbach, B. *J. Organomet. Chem.* **1981**, *213*, C26.

87	KETFEA11	[81]	Bkouche-Waksman, I.; Junior, J. S. R.; Koetzle, T. F.; Weichmann, J.; Herrmann, W. A. *Inorg. Chem.* **1985**, *24*, 1492.
88	KEWSEK	[82]	Berno, P.; Floriani, C.; Chiesi-Villa, A.; Guastini, C. *Organometallics* **1990**, *9*, 1995.
89	KEWSIO	[82]	Berno, P.; Floriani, C.; Chiesi-Villa, A.; Guastini, C. *Organometallics* **1990**, *9*, 1995.
90	KINFOC	[83]	Gunale, A. S.; Jensen, M. P.; Stern, C. L.; Shriver, D. F. *J. Am. Chem. Soc.* **1991**, *113*, 1458.
91	KISZAN	[84]	Weber, L.; Nolte, U.; Stammler, H. G.; Neumann, B. *Chem. Ber.* **1991**, *124*, 989.
92	KITVAK	[85]	Davies, S. G.; Edwards, A. J.; Skerlj, R. T.; Sutton, K. H.; Whittaker, M. *J. Chem. Soc. ,Perkin Trans. 1* **1991**, 1027.
93	KITVEO	[85]	Davies, S. G.; Edwards, A. J.; Skerlj, R. T.; Sutton, K. H.; Whittaker, M. *J. Chem. Soc. ,Perkin Trans. 1* **1991**, 1027.
94	KOJDES	[86]	Aumann, R.; Trentmann, B.; Kruger, C.; Lutz, F. *Chem. Ber.* **1991**, *124*, 2595.
95	KUCGIY	[87]	Jaiwook, P.; Sunhwa, K.; Dongmok, W.; Kimoon, K. *Organometallics* **1992**, *11*, 1738.
96	KUCTEH	[88]	Choi, N.; Kabe, Y.; Ando, W. *Organometallics* **1992**, *11*, 1506.
97	KUWSIE	[89]	Archer, S. J.; Harvey, G. A.; Moss, J. R.; Crouch, A. M. *Inorg. Chim. Acta* **1992**, *201*, 43.
98	LAGHAC	[90]	Imhof, W.; Eber, B.; Huttner, G.; Emmerich, C. *J. Organomet. Chem.* **1993**, *447*, 21.
99	LAGHEG	[90]	Imhof, W.; Eber, B.; Huttner, G.; Emmerich, C. *J. Organomet. Chem.* **1993**, *447*, 21.
100	LAJPUH	[91]	Wu, I.-Y.; Tseng, T.-W.; Chen, C.-T.; Cheng, M.-C.; Lin, Y.-C.; Wang, Y. *Inorg. Chem.* **1993**, *32*, 1539.
101	LEXYUI	[92]	Balch, A. L.; Olmstead, M. M.; Safari, N.; Claire, T. N. S. *Inorg. Chem.* **1994**, *33*, 2815.
102	LEZVAN	[93]	Liu, L.-K.; Luh, L.-S. *Organometallics* **1994**, *13*, 2816.
103	MAFOTR	[94]	Dettlaf, G.; Behrens, U.; Eicher, T.; Weiss, E. *J. Organomet. Chem.* **1978**, *152*, 197.
104	MPYMYF10	[95]	Pettersen, R. C.; Levenson, R. A. *Acta Crystallogr. ,Sect. B* **1976**, *32*, 723.
105	MXBYFE10	[38]	Mitsudo, T. A.; Watanabe, H.; Sasaki, T.; Takegami, Y.; Watanabe, Y.; Kafuku, K.; Nakatsu, K. *Organometallics* **1989**, *8*, 368.
106	NPICPO	[96]	Cotton, F. A.; Troup, J. M.; Billups, W. E.; Lin, L. P.; Smith, C. V. *J. Organomet. Chem.* **1975**, *102*, 345.
107	PATYEO	[97]	Cheng, M.-H.; Shu, H.-G.; Lee, G.-H.; Peng, S.-M.; Liu, R.-S. *Organometallics* **1993**, *12*, 108.

108	PIGVAC	[98]	Alvarez-Toledano, C.; Cano, A. C.; Toscamo, R. A.; Parlier, A.; Rudler, H. *Bull. Soc. Chim. Fr.* **1993**, *130*, 601.
109	PIHMOI	[99]	Hitchcock, P. B.; Madden, T. J.; Nixon, J. F. *J. Organomet. Chem.* **1993**, *463*, 155.
110	PIRDID	[100]	Case-Green, S. C.; Costello, J. F.; Davies, S. G.; Heaton, N.; Hedgecock, C. J. R.; Humphreys, V. M.; Metzler, M. R.; Prime, J. C. *J. Chem. Soc. ,Perkin Trans. 1* **1994**, 933.
111	PIRDOJ	[100]	Case-Green, S. C.; Costello, J. F.; Davies, S. G.; Heaton, N.; Hedgecock, C. J. R.; Humphreys, V. M.; Metzler, M. R.; Prime, J. C. *J. Chem. Soc. ,Perkin Trans. 1* **1994**, 933.
112	POTFIN	[101]	Jeannin, S.; Jeannin, Y.; Robert, F.; Rosenberger, C. *J. Organomet. Chem.* **1994**, *480*, 111.
113	PRACFE	[102]	Blau, H.; Malisch, W.; Voran, S.; Blank, K.; Kruger, C. *J. Organomet. Chem.* **1980**, *202*, C33.
114	SATVUE	[103]	Akita, M.; Kondoh, A.; Moro-oka, Y. *J. Chem. Soc. ,Dalton Trans.* **1989**, 1083.
115	SATWAL	[103]	Akita, M.; Kondoh, A.; Moro-oka, Y. *J. Chem. Soc. ,Dalton Trans.* **1989**, 1083.
116	SATWEP	[103]	Akita, M.; Kondoh, A.; Moro-oka, Y. *J. Chem. Soc. ,Dalton Trans.* **1989**, 1083.
117	SAXWAP	[104]	Weber, L.; Frebel, M.; Boese, R. *New J. Chem. (Nouv. J. Chim.)* **1989**, *13*, 303.
118	SAZYOH	[105]	Song, L.; Wang, R.; Hu, Q.; Wang, H. *Jiegou Huaxue(J. Struct. Chem.)* **1989**, *8*, 115.
119	SEHZEK	[106]	Mayr, A. J.; Pannell, K. H.; Carrasco-Flores, B.; Cervantes-Lee, F. *Organometallics* **1989**, *8*, 2961.
120	SIFPEC	[107]	Shuchart, C. E.; Young, G. H.; Wojcicki, A.; Calligaris, M.; Nardin, G. *Organometallics* **1990**, *9*, 2417.
121	SIFPIG	[107]	Shuchart, C. E.; Young, G. H.; Wojcicki, A.; Calligaris, M.; Nardin, G. *Organometallics* **1990**, *9*, 2417.
122	SIHLOK	[108]	Brunner, H.; Eder, R.; Hammer, B.; Klement, U. *J. Organomet. Chem.* **1990**, *394*, 555.
123	SIZNUK	[109]	Wong, A.; Pawlick, R. V.; Thomas, C. G.; Leon, D. R.; Ling-Kang, L. *Organometallics* **1991**, *10*, 530.
124	SIZPAS	[109]	Wong, A.; Pawlick, R. V.; Thomas, C. G.; Leon, D. R.; Ling-Kang, L. *Organometallics* **1991**, *10*, 530.
125	SOBPAA	[110]	Mirkin, C. A.; Kuang-Lieh, L.; Snead, T. E.; Young, B. A.; Geoffroy, G. L.; Rheingold, A. L.; Haggerty, B. S. *J. Am. Chem. Soc.* **1991**, *113*, 3800.
126	SOGXOB	[111]	Krajewski, J. W.; Gluzinski, P.; Zamojski, A.; Mishnyov, A.; Kemme, A.; Guo, Z.-W. *J. Crystallogr. Spectrosc. Res.* **1991**, *21*, 271.
127	SOTYEF	[112]	Liu, H. Y.; Eriks, K.; Giering, W. P.; Prock, A. *Acta Crystallogr. ,Sect. C (Cr. Str. Comm.)* **1992**, *48*, 433.

128	TACFAE	[113]	Song, J.-S.; Han, S.-H.; Nguyen, S. T.; Geoffroy, G. L.; Rheingold, A. L. *Organometallics* **1990**, *9*, 2386.
129	TAKCUD	[114]	Lee, S. S.; Knobler, C. B.; Hawthorne, M. F. *Organometallics* **1991**, *10*, 1054.
130	TCTAFE	[115]	Dettlaf, G.; Behrens, U.; Weiss, E. *Chem. Ber.* **1978**, *111*, 3019.
131	TEAFEA	[116]	Wong, W. K.; Wilkinson, G.; Galas, A. M. R.; Hursthouse, M. B.; Thornton-Pett, M. *J. Chem. Soc. ,Chem. Comm.* **1981**, 189.
132	VAKBEO	[117]	Valeri, T.; Meier, F.; Weiss, E. *Chem. Ber.* **1988**, *121*, 1093.
133	VAKBIS	[117]	Valeri, T.; Meier, F.; Weiss, E. *Chem. Ber.* **1988**, *121*, 1093.
134	VAKDUG	[118]	Kergoat, R.; Kubicki, M. M.; Lima, L. C. G. d.; Scordia, H.; Guerchais, J. E.; Haridon, P. L. *J. Organomet. Chem.* **1989**, *367*, 143.
135	VEBVUT	[119]	Fassler, T.; Huttner, G. *J. Organomet. Chem.* **1989**, *376*, 367.
136	VEHPON	[120]	Fassler, T.; Huttner, G.; Gunauer, D.; Fiedler, S.; Eber, B. *J. Organomet. Chem.* **1990**, *381*, 409.
137	VESJOS	[121]	Mitsudo, T.; Ishihara, A.; Suzuki, T.; Watanabe, Y.; Masuda, H. *Organometallics* **1990**, *9*, 1357.
138	VETHEH	[122]	Karel, K. J.; Tulip, T. H.; Ittel, S. D. *Organometallics* **1990**, *9*, 1276.
139	VETHIL	[122]	Karel, K. J.; Tulip, T. H.; Ittel, S. D. *Organometallics* **1990**, *9*, 1276.
140	VETHOR	[122]	Karel, K. J.; Tulip, T. H.; Ittel, S. D. *Organometallics* **1990**, *9*, 1276.
141	VIVNET	[123]	Daqiang, X.; Kaesz, H. D.; Khan, S. I. *Inorg. Chem.* **1991**, *30*, 1341.
142	VIVNIX	[123]	Daqiang, X.; Kaesz, H. D.; Khan, S. I. *Inorg. Chem.* **1991**, *30*, 1341.
143	VIVTEZ	[124]	Berno, P.; Braunstein, P.; Floriano, C.; Chiesi-Villa, A.; Guastini, C. *Inorg. Chem.* **1991**, *30*, 1407.
144	VOKZAW	[125]	Cheng, M.-H.; Lee, G.-H.; Peng, S.-M.; Liu, R.-S. *Organometallics* **1991**, *10*, 3600.
145	VOVWOS	[126]	Crowther, D. J.; Zhang, Z.; Palenik, G. J.; Jones, W. M. *Organometallics* **1992**, *11*, 622.
146	VOVWUY	[126]	Crowther, D. J.; Zhang, Z.; Palenik, G. J.; Jones, W. M. *Organometallics* **1992**, *11*, 622.
147	VOVXAF	[126]	Crowther, D. J.; Zhang, Z.; Palenik, G. J.; Jones, W. M. *Organometallics* **1992**, *11*, 622.
148	VOWTUW	[127]	Stolz, F.; Strazewski, P.; Tamm, C.; Neuberger, M.; Zehnder, M. *Angew. Chem. ,Int. Ed. Engl.* **1992**, *31*, 193.
149	VOWVAE	[127]	Stolz, F.; Strazewski, P.; Tamm, C.; Neuberger, M.; Zehnder, M. *Angew. Chem. ,Int. Ed. Engl.* **1992**, *31*, 193.
150	VOZMOM	[128]	Colletti, S. J.; Halterman, R. L. *Organometallics* **1992**, *11*, 980.
151	VULNAR	[129]	Weber, L.; Buchwald, S.; Lentz, D.; Preugschat, D.; Stammler, H. G.; Neumann, B. *Organometallics* **1992**, *11*, 2351.

152	WAGKIY	[130]	Kraakman, M. J. A.; Koning, T. C. d.; Lange, P. P. M. d.; Vrieze, K.; Kooijman, H.; Spek, A. L. *Inorg. Chim. Acta* **1993**, *203*, 145.
153	WAJYOV	[131]	Guo, Z.-W.; Zamojski, A.; Krajewski, J. W.; Gluzinski, P. *J. Crystallogr. Spectrosc. Res.* **1993**, *23*, 209.
154	WAJYUB	[131]	Guo, Z.-W.; Zamojski, A.; Krajewski, J. W.; Gluzinski, P. *J. Crystallogr. Spectrosc. Res.* **1993**, *23*, 209.
155	WEDMAT	[132]	Barras, J. P.; Davies, S. G.; Metzler, M. R.; Edwards, A. J.; Humphreys, V. M.; Prout, K. *J. Organomet. Chem.* **1993**, *461*, 157.
156	YAWGIM	[133]	Ambrosi, L.; Bassetti, M.; Buttiglieri, P.; Mannina, L.; Monti, D.; Bocelli, G. *J. Organomet. Chem.* **1993**, *455*, 167.
157	YEBYOT	[134]	Nami, C.; Ando, W. *Organometallics* **1994**, *13*, 741.
158	YIBVEK	[135]	Weber, L.; Kaminski, O.; Stammler, H. G.; Neumann, B.; Boese, R. *Z. Naturforsch. ,Teil B* **1994**, *49*, 1693.
159	YIFNIK	[136]	Wang, J. L.; Ueng, C. H.; Cheng, S. J.; Yeh, M. C. P. *Organometallics* **1994**, *13*, 4453.
160	YISLAN	[137]	Knox, S. A. R.; Morton, D. A. V.; Orpen, A. G.; Turner, M. L. *Inorg. Chim. Acta* **1994**, *220*, 201.
161	YOTMUP	[138]	Luh, L. S.; Liu, L. K. *Organometallics* **1995**, *14*, 1514.

Appendix D

Imaginary Vibrational Modes of DFT Optimized Minimum Energy Structures

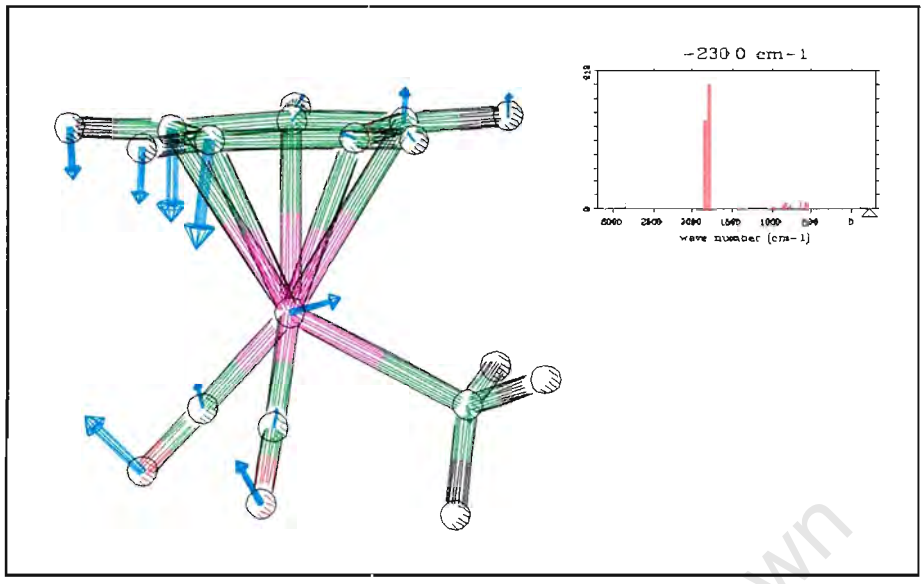

Figure 1 Imaginary vibrational mode (1) of $[(\eta^5\text{-}C_5H_5)Fe(CO)_2(CH_3)]$. The mode involves the 'rocking' of the cyclopentadienyl ligand with the carbonyl ligands.

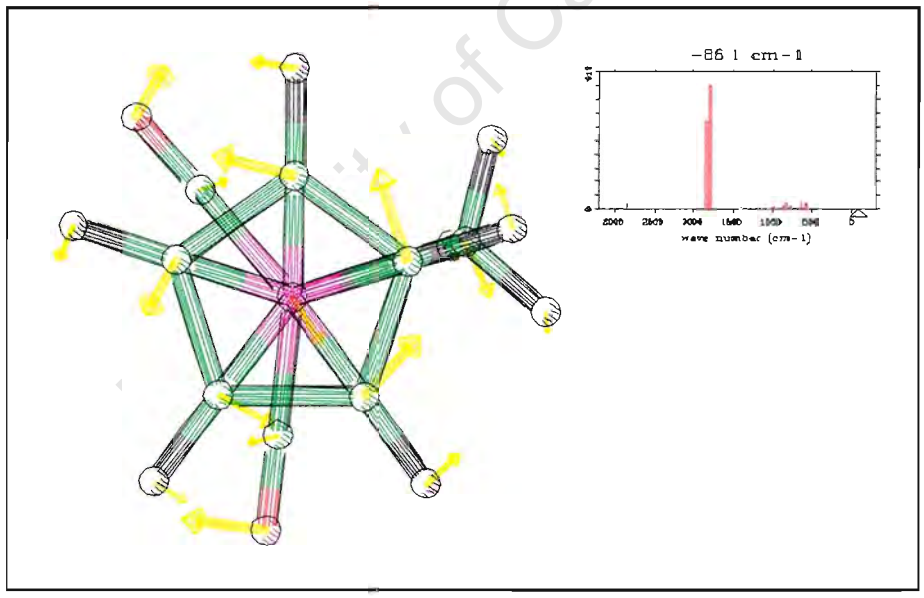

Figure 2 Imaginary vibrational mode (2) of $[(\eta^5\text{-}C_5H_5)Fe(CO)_2(CH_3)]$. The mode involves the trivial rotation of the cyclopentadienyl ligand with the counter-rotation of the carbonyl and methyl groups.

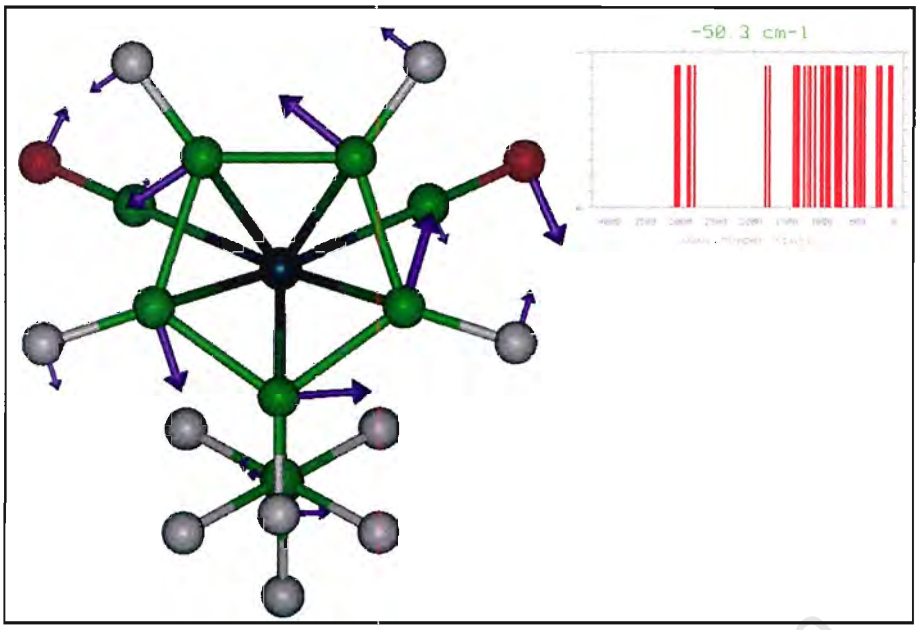

Figure 3 Imaginary vibrational mode (1) of $[(\eta^5\text{-}C_5H_5)Fe(CO)_2CH_2CH_3]$. The mode involves the trivial rotation of the cyclopentadienyl ligand.

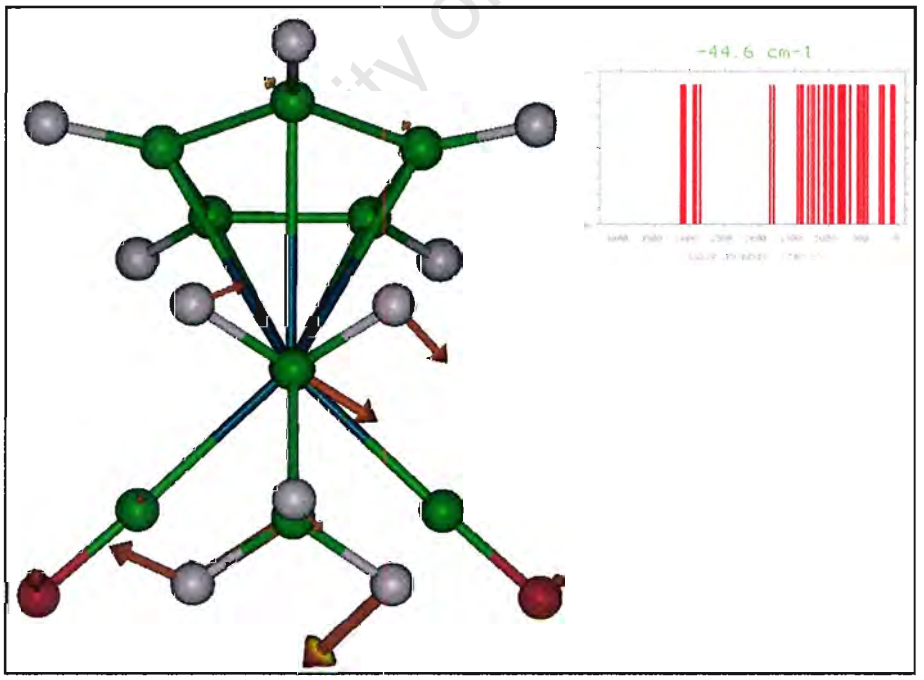

Figure 4 Imaginary vibrational mode (2) of $[(\eta^5\text{-}C_5H_5)Fe(CO)_2CH_2CH_3]$. The mode involves the trivial rotation of the carbonyl and ethyl ligands.

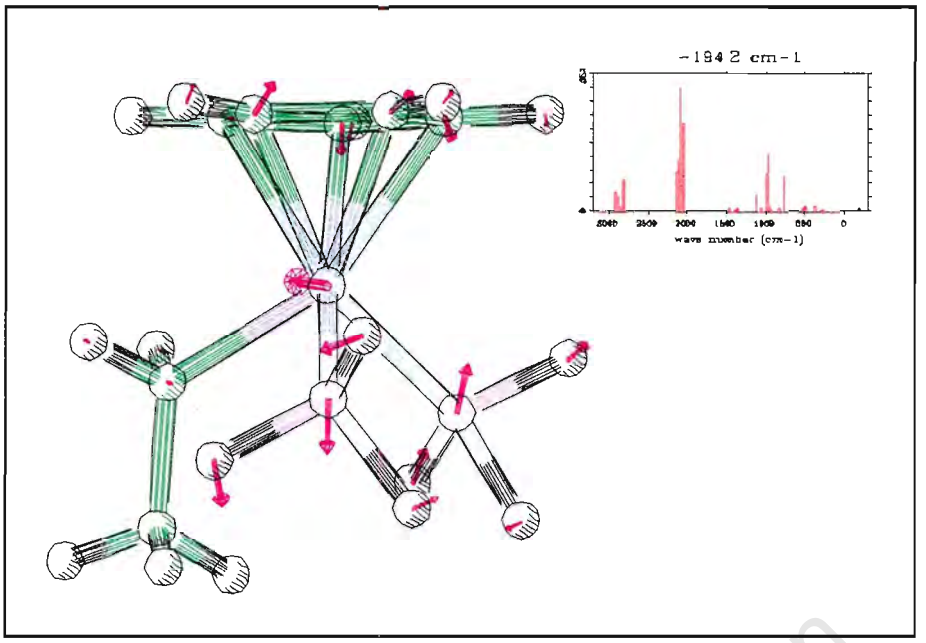

Figure 5 Imaginary vibrational mode (1) of $[(\eta^5\text{-}C_5H_5)Fe(PH_3)_2CH_2CH_3]$. The mode involves the 'rocking' of the cyclopentadienyl ligand and the phosphine groups.

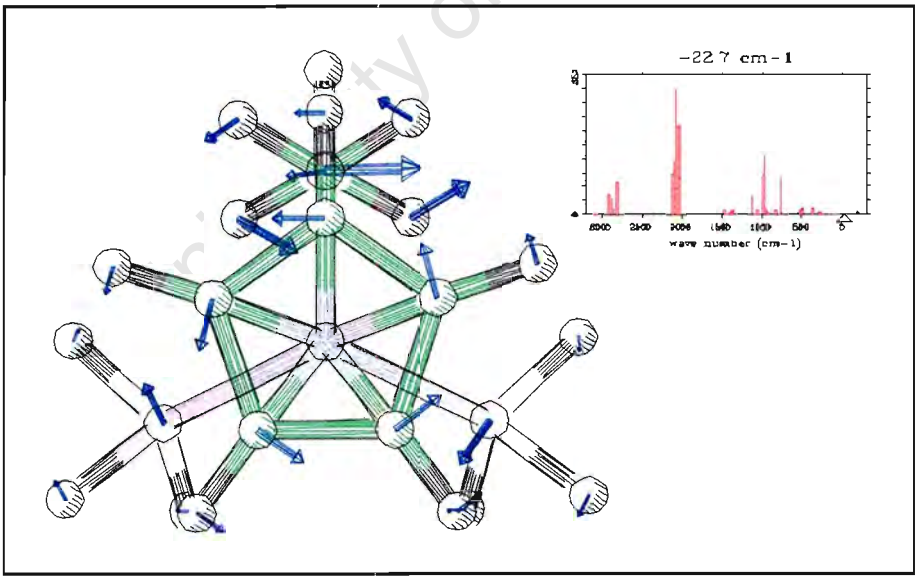

Figure 6 Imaginary vibrational mode (2) of $[(\eta^5\text{-}C_5H_5)Fe(PH_3)_2CH_2CH_3]$. The mode involves the trivial rotation of the cyclopentadienyl ligand, and counter rotation of the other groups.

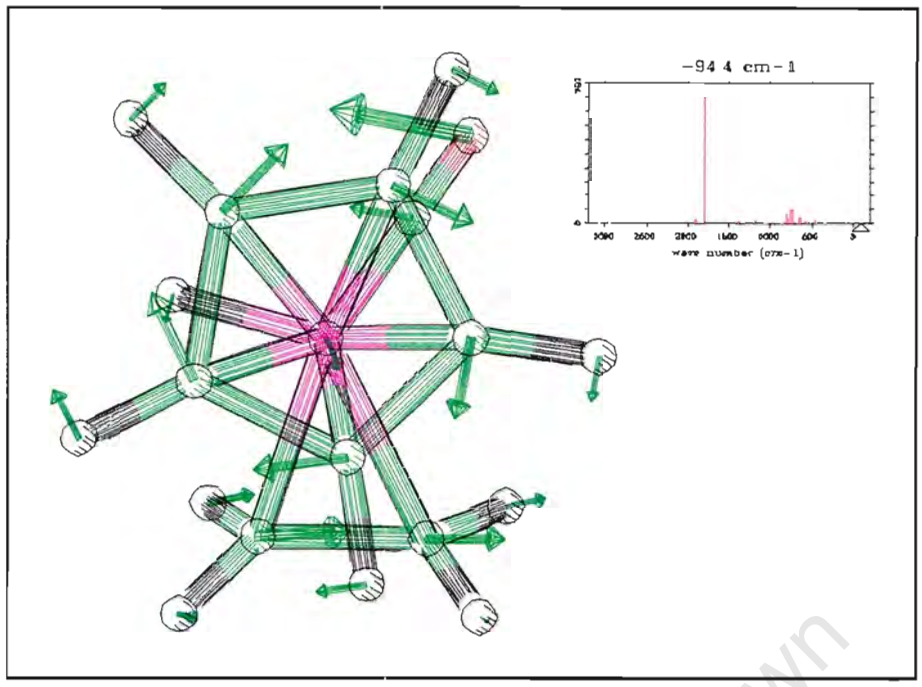

Figure 7 Imaginary vibrational mode of $[(\eta^5\text{-}C_5H_5)Fe(CO)(H)(CH_2CH_2)]$. The mode involves the trivial rotation of the cyclopentadienyl ligand, and counter rotation of the ethylene and carbonyl groups.

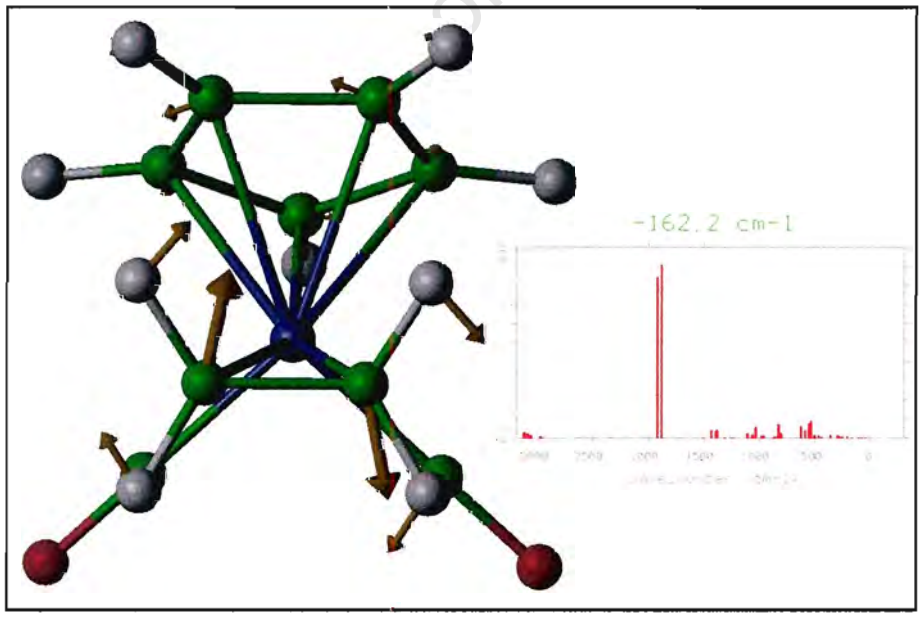

Figure 8 Imaginary vibrational mode (1) of $[(\eta^5\text{-}C_5H_5)Fe(CO)_2(CH_2CH_2)]^+$. The mode involves the rotation of the ethylene and lesser rotation of the cyclopentadienyl ligand.

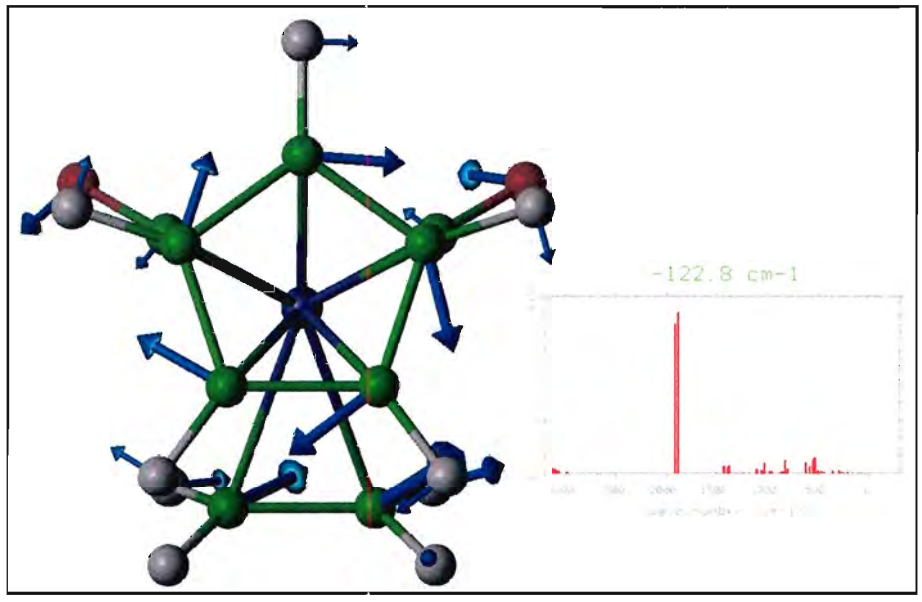

Figure 9 Imaginary vibrational mode (2) of $[(\eta^5\text{-}C_5H_5)Fe(CO)_2(CH_2CH_2)]^+$. The mode involves the rotation of the cyclopentadienyl ligand and counter rotation of the other ligands.

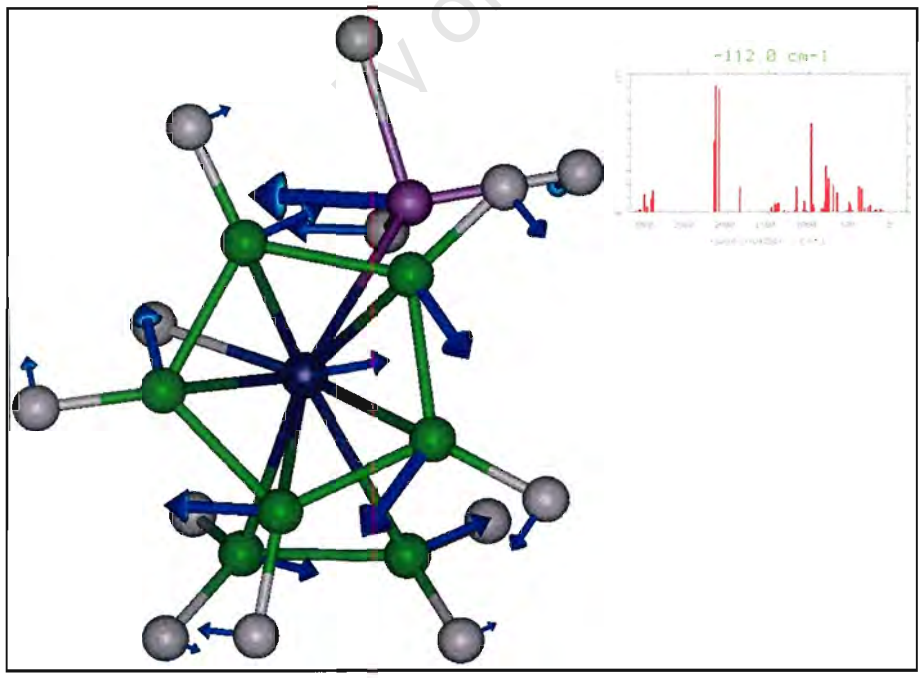

Figure 10 Imaginary vibrational mode of $[(\eta^5\text{-}C_5H_5)Fe(PH_3)(H)(CH_2CH_2)]$. The mode involves the rotation of the cyclopentadienyl ligand and counter-rotation of the other ligands.

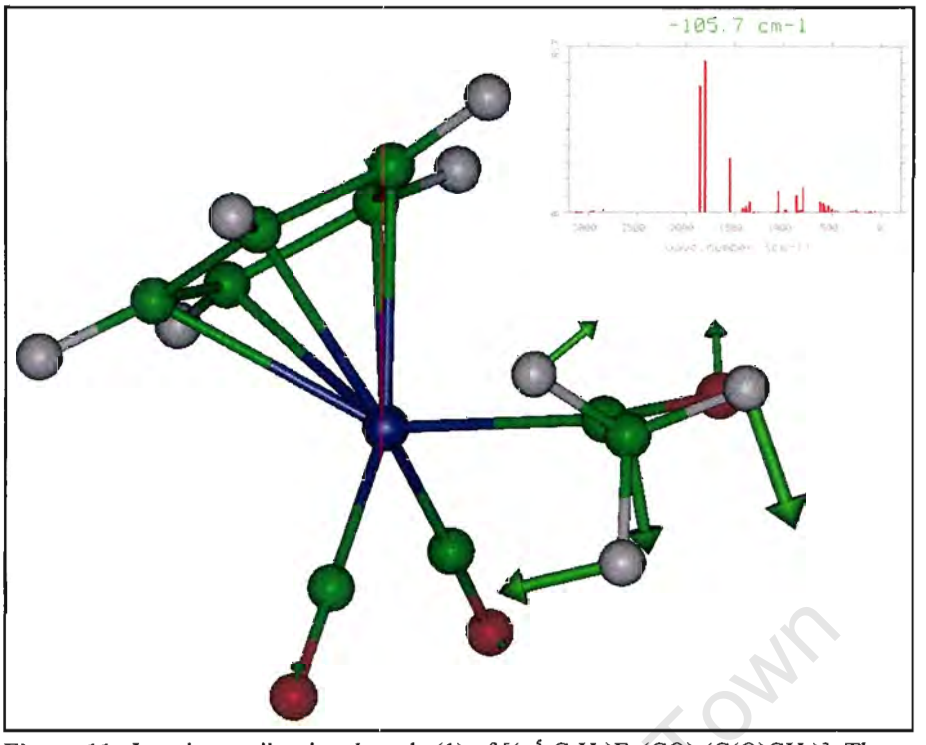

Figure 11 Imaginary vibrational mode (1) of $[(\eta^5\text{-}C_5H_5)Fe(CO)_2(C(O)CH_3)]$. The mode involves the trivial rotation of the acetyl methyl group.

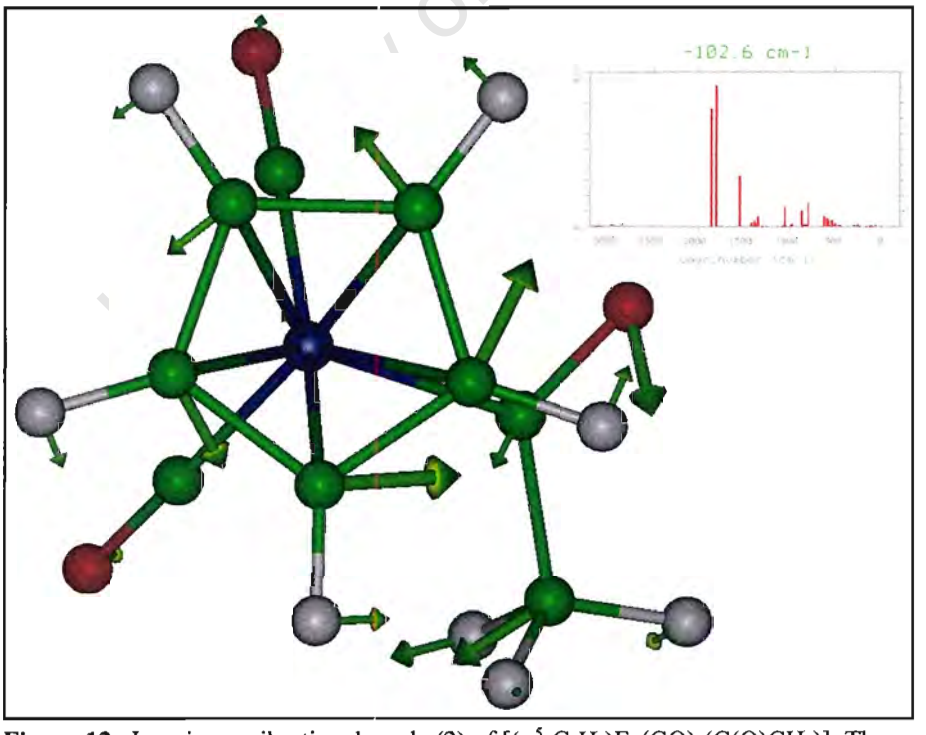

Figure 12 Imaginary vibrational mode (2) of $[(\eta^5\text{-}C_5H_5)Fe(CO)_2(C(O)CH_3)]$. The mode involves the rotation of the cyclopentadienyl ligand.

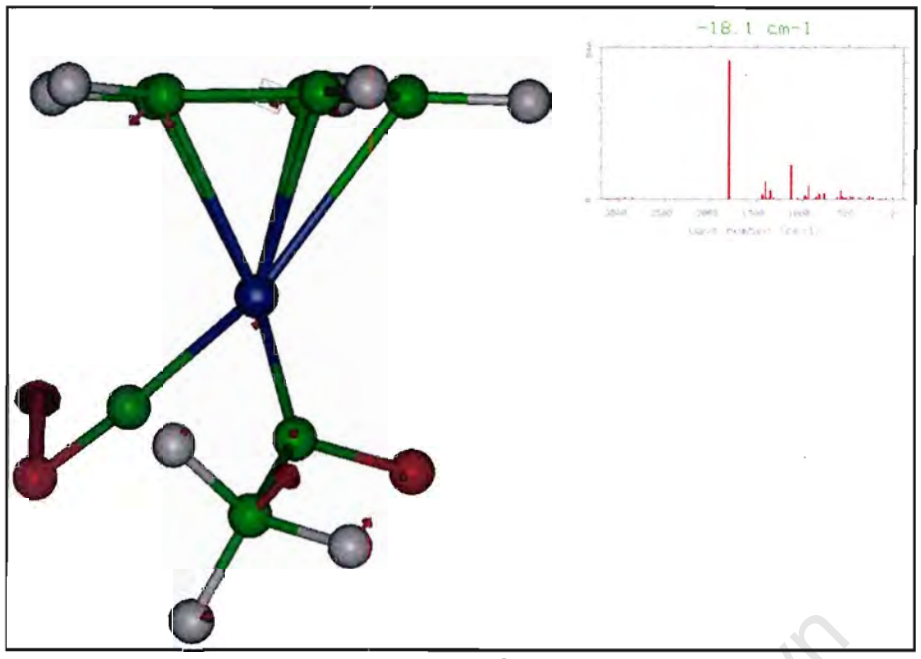

Figure 13 Imaginary vibrational mode of $[(\eta^5\text{-}C_5H_5)Fe(CO)(C(O)CH_3)]$. The mode involves a 'bending' motion of the acetyl methyl and carbonyl oxygen.

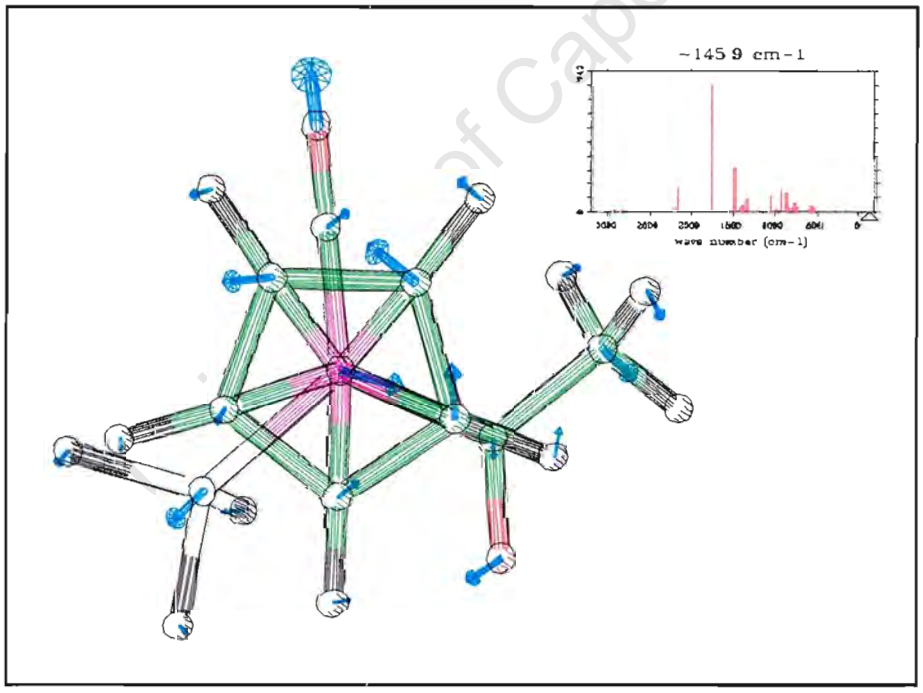

Figure 14 Imaginary vibrational mode (1) of $[(\eta^5\text{-}C_5H_5)Fe(CO)(PH_3)(C(O)CH_3)]$. The mode involves minor rotation of the cyclopentadienyl ligand with a 'bending' of the carbonyl, phosphine, and acetyl ligands.

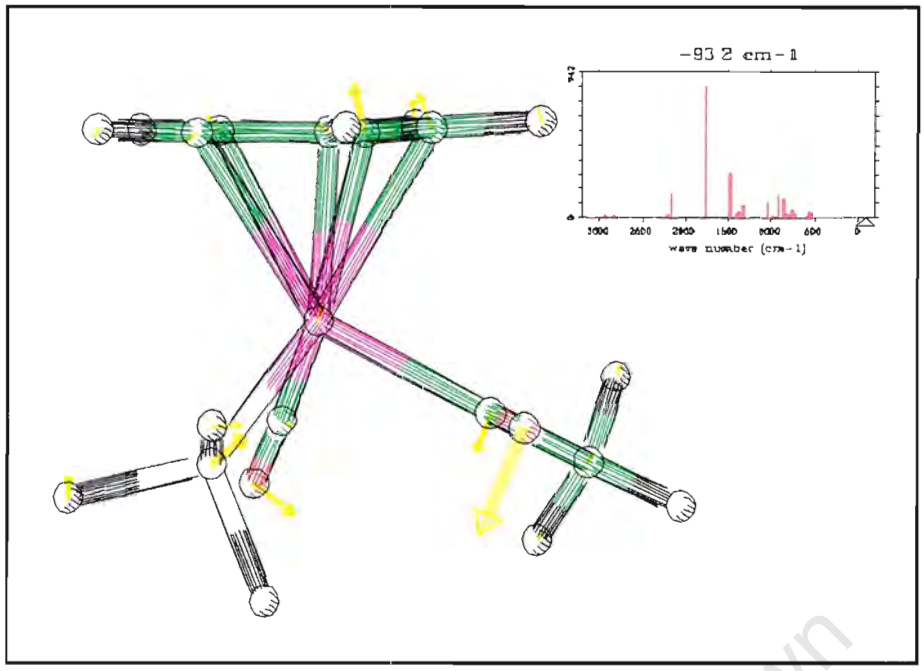

Figure 15 Imaginary vibrational mode (2) of $[(\eta^5\text{-}C_5H_5)Fe(CO)(PH_3)(C(O)CH_3)]$. The mode involves 'rocking' of the cyclopentadienyl ligand and a 'twist' of the carbonyl, phosphine, and acetyl ligands.

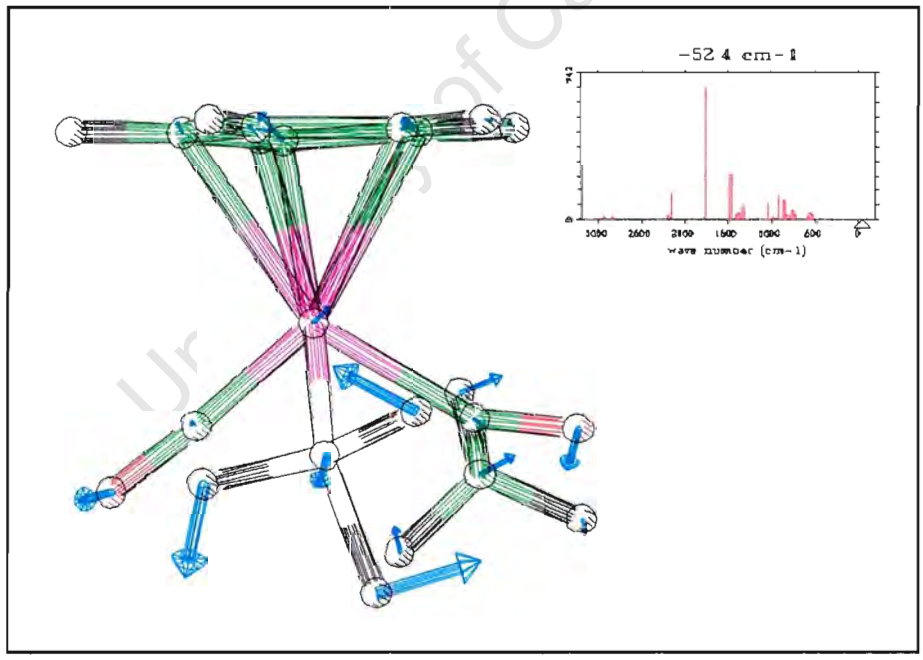

Figure 16 Imaginary vibrational mode (3) of $[(\eta^5\text{-}C_5H_5)Fe(CO)(PH_3)(C(O)CH_3)]$. The mode involves rotation of the phosphine ligand and a minor rotation of the acetyl methyl ligand.

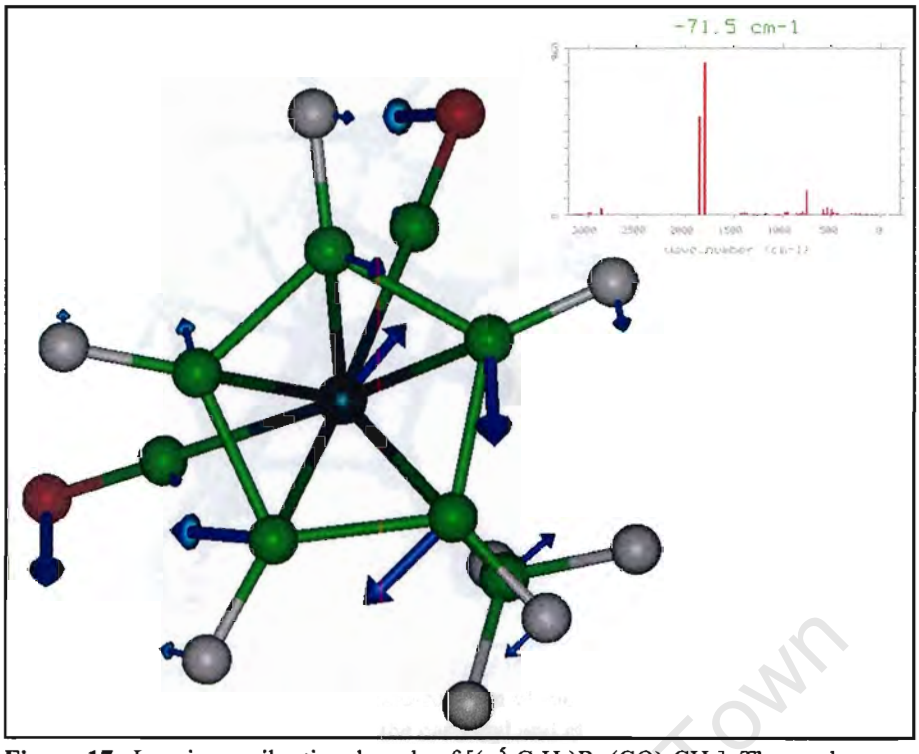

Figure 17 Imaginary vibrational mode of $[(\eta^5\text{-}C_5H_5)Ru(CO)_2CH_3]$. The mode involves the rotation of the cyclopentadienyl ligand.

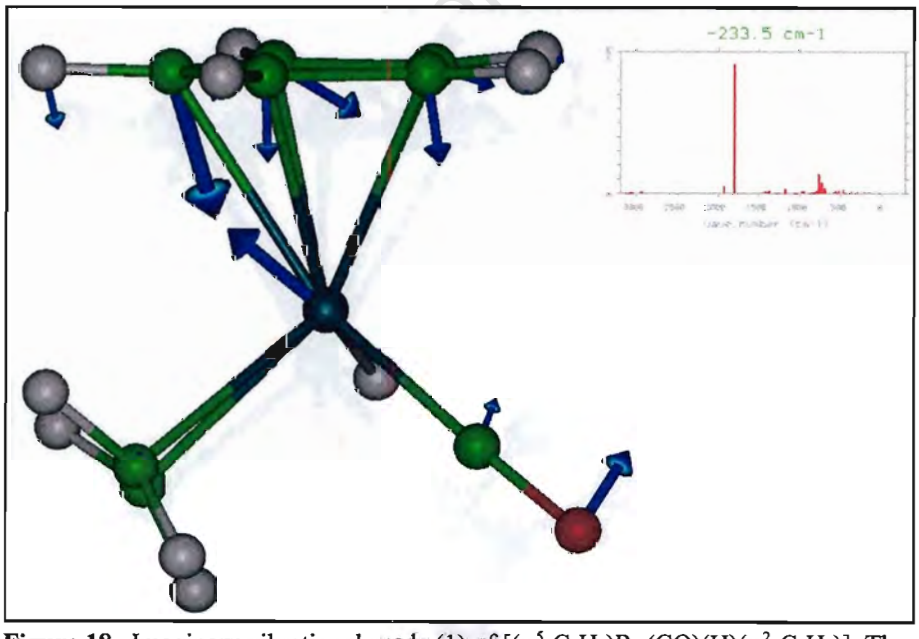

Figure 18 Imaginary vibrational mode (1) of $[(\eta^5\text{-}C_5H_5)Ru(CO)(H)(\eta^2\text{-}C_2H_4)]$. The mode involves the 'rocking' of the cyclopentadienyl ligand.